www.pattern-recognition-in-physics.net

Pattern Recognition in Physics

Special Issue | 2013

Pattern in solar variability, their planetary origin and terrestrial impacts

Editors: N.-A. Mörner, R. Tattersall, and J.-E. Solheim

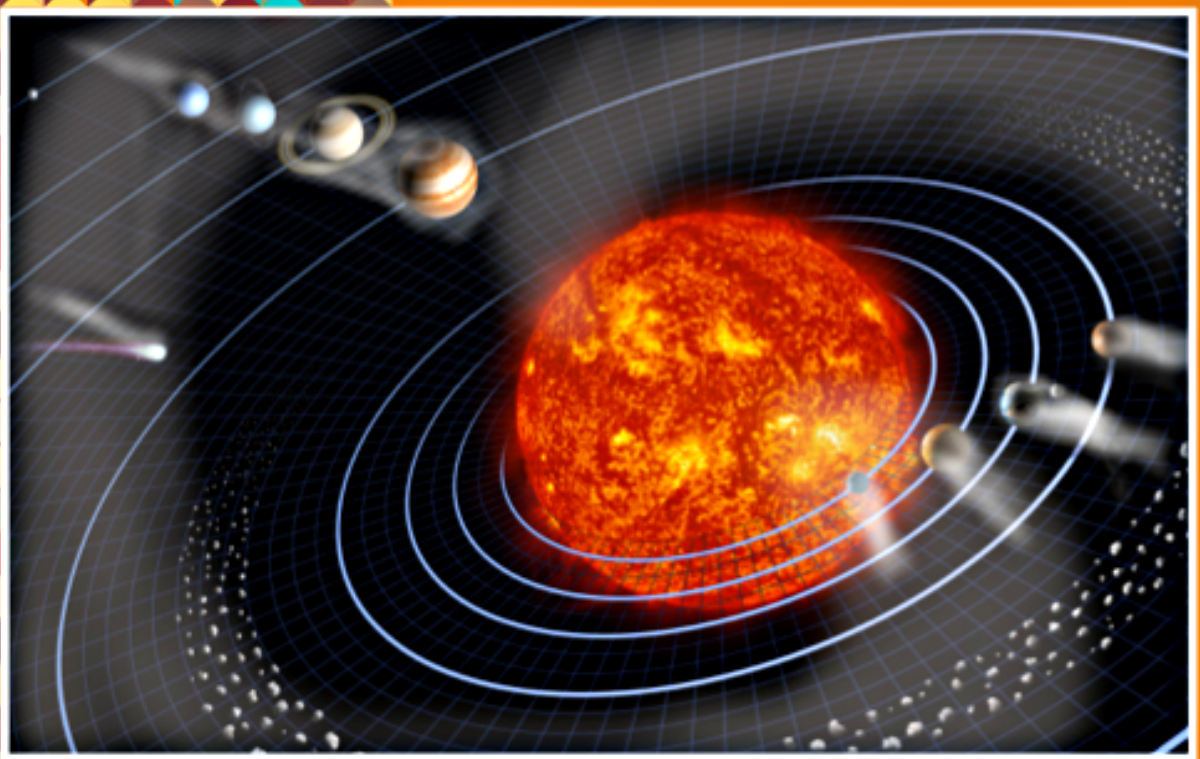

Copernicus Publications
The Innovative Open Access Publisher

Contents

The Sun's activity constantly varies in characteristic cyclic patterns. With new material and new analyses, we reinforce the old proposal that the driving forces are to be found the planetary beat on the Sun and the Sun's motions around the center of mass. This is a Special Issue published on Pattern Recognition in Physics where various aspects of the Planetary–Solar–Terrestrial interaction are highlighted in 12 independent papers. The Special Issue ends with General Conclusions co-authored by 19 prominent specialists on solar-terrestrial interaction and terrestrial climate. They conclude that the driving factor of solar variability must emerge from gravitational and inertial effects on the Sun from the planets and their satellites. By this, an old hypothesis seems elevated into a firm theory, maybe even a new paradigm.

Part I

Preface: Pattern in solar variability, their planetary origin and terrestrial impacts.

Mörner, N.-A., Tattersall, R., and Solheim, J.-E.: Pattern Recogn. Phys., 1, 203-204, doi:10.5194/prp-1-203-2013, 2013.

Pattern Recogn. Phys., 1, 203–204, 2013
www.pattern-recogn-phys.net/1/203/2013/
doi:10.5194/prp-1-203-2013

Pattern Recognition in Physics
Open Access

Preface: Pattern in solar variability, their planetary origin and terrestrial impacts

N.-A. Mörner[1], R. Tattersall[2], and J.-E. Solheim[3]

[1]Paleogeophysics & Geodynamics, Stockholm, Sweden
[2]Tallbloke, Leeds, UK
[3]Departments of Physics & Technology, Tromsø, Norway

Correspondence to: N.-A. Mörner (morner@pog.nu)

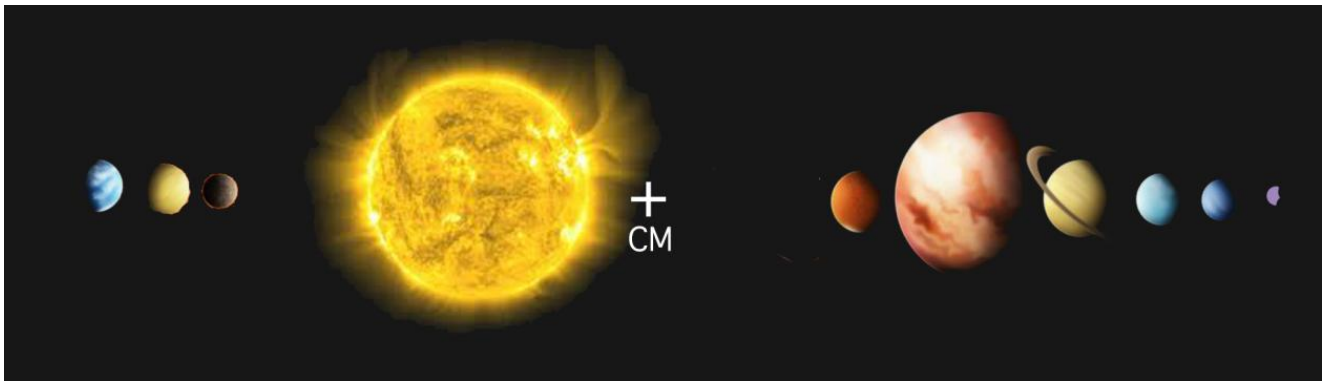

The idea that planetary effects may modulate or even control solar variability is old which was investigated by Rudolf Wolf from 1859 until his death in 1893. Many further efforts to measure and explain the possible mechanisms for planetary solar effects have been made by researchers at frequent intervals over the years. Despite this it has remained a hypothesis which is favoured by some and neglected or rebutted by others.

Today we are in a stronger position to address the question, with accurate data, computer aided methods and new insights. Therefore, we think the time is right for a broader and more extensive investigation into the question of "the possible planetary modulation of solar variability".

In this special issue of *Pattern Recognition in Physics*, we present a new, multi-component input to the question, with the aim of elevating the hypothesis to the status of a theory. We hope this work will lead to better understanding and prediction of solar and terrestrial variation, strengthening the scientific value and policy relevance of a promising new paradigm.

We consolidate this process with a collection of 12 independent papers:

1. "The complex planetary synchronization structure of the solar system"

   In this paper Nicola Scafetta reviews the "harmony" of the solar system from Kepler's basic concepts forward through time. It serves as an ideal introduction to the special issue. He ends by reviewing his own contribution to this question.

2. "The Hum: log-normal distribution of planetary–solar resonance"

   Roger Tattersall describes "the Hum" or the celestial sounds of orbital resonance. He demonstrates "the existence of strong correlations between orbital dynamics and solar variation" due to interactions between the power-law-based forces of gravity and magnetism and the interactions between both the Sun and planets as well as between the planets themselves.

Published by Copernicus Publications.

3. "Energy transfer in the solar system"

   In this paper, Hans Jelbring addresses the energy transfer in the solar system. He notes that "the reversible transfer of energy between the orbit of Moon and Earth's rotational energy is crucial to the creation of the 13.6-day and 27.3-day periods in both solar variables and Earth bound climate variables".

4. "Planetary beat and solar–terrestrial responses"

   Nils-Axel Mörner reviews the planetary–solar interaction, the dual responses in solar activity (irradiance and solar wind), the multiple terrestrial changes induced, and the likelihood that we will soon be facing a new grand solar minimum with Little Ice Age climatic conditions.

5. "Signals from the planets, via the Sun to the Earth"

   By analysing terrestrial climatic and climatic-related variables, Jan-Erik Solheim is able to show that the observed variations must lead their origin in solar variations driven by the "stable periodic oscillations" of the planetary motions.

6. "Apparent relations between planetary spin, orbit, and solar differential rotation"

   In this paper, Roger Tattersall analyses the relations between changes in the Earth's rate of rotation (LOD) and the spatio-temporal disposition of the planetary masses in the solar system, indicating an underlying physical coupling between the celestial bodies.

7. "Venus–Earth–Jupiter spin–orbit coupling model"

   Ian Wilson presents a spin–orbital coupling model and demonstrates that it "produces net tangential torques that act upon the outer convective layers of the Sun with periodicities that match many of the long-term cycles" observed in terrestrial records of cosmogenic nuclides.

8. "Celestial commensurabilities: some special cases"

   Hans Jelbring shows that planetary commensurability implies that "all celestial bodies in our solar system interact energetically". Therefore, there must exist a physical process capable of transferring energy between celestial bodies (orbital energy) as well as between orbital energy and rotational energy.

9. "Responses of the basic cycle of 178.7 and 2402 yr in solar–terrestrial phenomena during Holocene"

   Ivanka Charvatova and Pavel Hejda address the solar inertial motions (SIM). They demonstrate that it is "a very noticeable" phenomenon, and identify it throughout the Holocene, well manifested in the well-known 179 yr cycle and a long-term regular cycle of 2402 years. They report a close correlation between SIM and solar–terrestrial interaction and changes in terrestrial climate.

10. "Multiscale comparative spectral analysis of satellite total solar irradiance measurements from 2003 to 2013 reveals a planetary modulation of solar activity and its nonlinear dependence on the 11 yr solar cycle"

    Nicola Scafetta and Richard Willson use a multiscale dynamical spectral analysis technique to study different solar irradiance data. "The observed periodicities are found highly coherent with the spring, orbital and synodic periods of Mercury, Venus, Earth and Jupiter", indicating a planetary forcing on the Sun.

11. "The sunspot cycle length modulated by planets?"

    Jan-Erik Solheim addresses the relation between sunspot cycle length variations, climate and solar variability. The solar cycle length decreased during deep solar minima of the past millennium, and this is "expected to re-occur in the first part of this century". In conclusion, he finds "a strong argument for an external forcing" upon the Sun by Venus, Earth, Jupiter and Saturn.

12. "A mathematical model of the sunspot cycle for the past 1000 yr"

    Rick Salvador formulates a mathematical model of the sunspot cycles and applies it on the records of the last millennium. The model can be used "to forecast future solar cycles quantitatively for 30 yr and directionally for 100 yr", indicating "a solar minimum and quiet Sun for the next 30 to 100 yr".

We end this Special Issue of PRP with a collective paper, co-authored by 19 persons:

13. "General conclusions regarding the planetary–solar–terrestrial interaction"

    Here all authors plus nine other prominent scientists join in the general conclusion that, indeed, the planetary beat affects the Sun and, by that, a number of terrestrial variables. This implies that the old hypothesis is now elevated to a firm theory, maybe even a new paradigm. A second implication of the material presented is that we are facing a new grand solar minimum, around 2030–2040, with severe climatic conditions as were the case during previous solar minima.

We hope you enjoy our efforts

Stockholm, Leeds and Baerum in October 2013

Part II

The complex planetary synchronization structure of the solar system. Scafetta, N.: Pattern Recogn. Phys., 1, 1-19, doi:10.5194/prp-2-1-2014 , 2014.

Pattern Recogn. Phys., 2, 1–19, 2014
www.pattern-recogn-phys.net/2/1/2014/
doi:10.5194/prp-2-1-2014

Pattern Recognition in Physics
Open Access

The complex planetary synchronization structure of the solar system

N. Scafetta

Active Cavity Radiometer Irradiance Monitor (ACRIM) Lab, Coronado, CA 92118, USA

Duke University, Durham, NC 27708, USA

Correspondence to: N. Scafetta (nicola.scafetta@gmail.com)

Received: 12 December 2013 – Revised: 19 December 2013 – Accepted: 28 December 2013 – Published: 15 January 2014

Abstract. The complex planetary synchronization structure of the solar system, which since Pythagoras of Samos (ca. 570–495 BC) is known as the *music of the spheres*, is briefly reviewed from the Renaissance up to contemporary research. Copernicus' heliocentric model from 1543 suggested that the planets of our solar system form a kind of mutually ordered and quasi-synchronized system. From 1596 to 1619 Kepler formulated preliminary mathematical relations of approximate commensurabilities among the planets, which were later reformulated in the Titius–Bode rule (1766–1772), which successfully predicted the orbital position of Ceres and Uranus. Following the discovery of the ~ 11 yr sunspot cycle, in 1859 Wolf suggested that the observed solar variability could be approximately synchronized with the orbital movements of Venus, Earth, Jupiter and Saturn. Modern research has further confirmed that (1) the planetary orbital periods can be approximately deduced from a simple system of resonant frequencies; (2) the solar system oscillates with a specific set of gravitational frequencies, and many of them (e.g., within the range between 3 yr and 100 yr) can be approximately constructed as harmonics of a base period of ~ 178.38 yr; and (3) solar and climate records are also characterized by planetary harmonics from the monthly to the millennial timescales. This short review concludes with an emphasis on the contribution of the author's research on the empirical evidences and physical modeling of both solar and climate variability based on astronomical harmonics. The general conclusion is that the solar system works as a resonator characterized by a specific harmonic planetary structure that also synchronizes the Sun's activity and the Earth's climate. The special issue *Pattern in solar variability, their planetary origin and terrestrial impacts* (Mörner et al., 2013) further develops the ideas about the planetary–solar–terrestrial interaction with the personal contribution of 10 authors.

1 Introduction

In 1543 the *De revolutionibus orbium coelestium (On the Revolutions of the Heavenly Spheres)* was published. As opposed to Ptolemy's geocentric model that had been widely accepted since antiquity, Copernicus (1543) proposed a heliocentric model for the solar system: the planets, including the Earth, orbit the Sun and their orbital periods increase with the planetary distance from the Sun. Copernicus also argued that the planets form a kind of mutually ordered system. The physical properties of the planets' orbits, such as their distances from the Sun and their periods, did not appear to be randomly distributed. They appeared to obey a certain law of nature.

A typical synchronization that could be more easily highlighted by the heliocentric system was, for example, the 8 : 13 Earth–Venus orbital resonance. Every 8 yr the Earth–Venus orbital configuration approximately repeats because the Earth revolves 8 times and Venus ~ 13 times, as can be easily calculated using their sidereal orbital periods: $P_{\mathrm{Ea}} = 365.256$ days and $P_{\mathrm{Ve}} = 224.701$ days. Figure 1a demonstrates this orbital regularity by showing the relative positions of Earth and Venus on 1 January from 2012 to 2020.

However, Venus presents a more subtle and remarkable synchronization with Earth. The rotation period of Venus on its own axis is 243.021 days (that is, almost exactly two-thirds of the Earth's annual period) and is retrograde. It is

Published by Copernicus Publications.

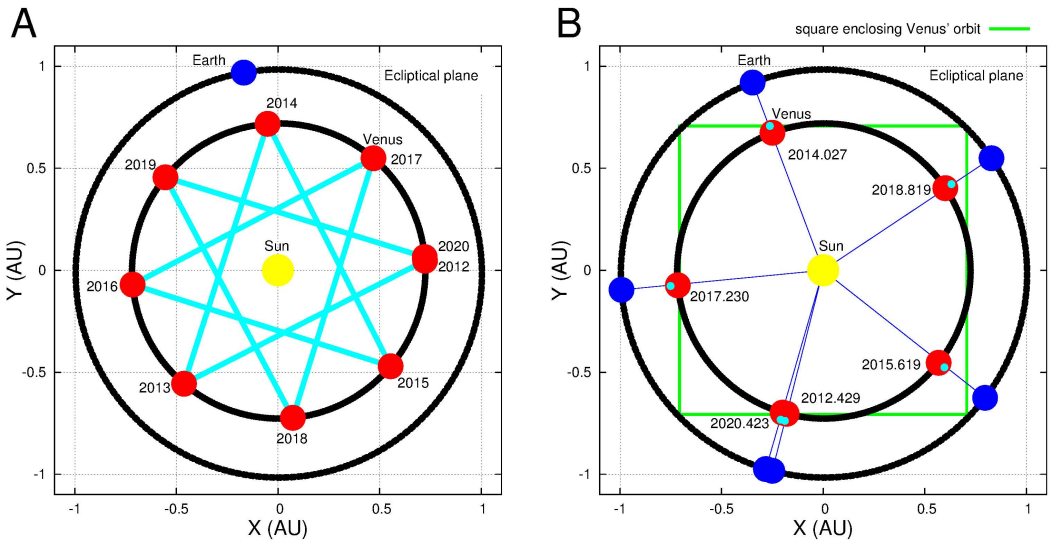

Figure 1. **(A)** Earth and Venus' orbits and their positions on 1 January for the years 2012 to 2020 in Copernicus' heliocentric system. The figure shows that every 8 yr the Venus–Earth configuration approximately repeats forming eight-point star pattern. **(B)** Earth–Venus inferior conjunctions from 2012 to 2020. The figure shows a five-point star pattern. Note that at every conjunction, the same side of Venus (represented by a small cyan circle) faces Earth. The orbits and the coordinates (in astronomical units) of the planets were determined using the JPL's HORIZONS Ephemeris system (http://ssd.jpl.nasa.gov/horizons.cgi).

easy to calculate that at every inferior conjunction (that is, every time the Sun, Venus and Earth line up), the same side of Venus faces Earth (Goldreich and Peale, 1966a; Jelbring, 2013); the Venus–Earth synodic period is 583.924 days and there are five inferior conjunctions in 8 yr. In fact, as Fig. 1b shows, in one synodic period Earth revolves 1.59867 times around the Sun, while Venus rotates on its own axis 2.40277 times in the opposite direction. The sum of the fractional part of the two numbers is almost exactly 1 (~ 1.00144). Thus, not only is Earth almost synchronized with Venus in a 8 : 13 orbital resonance and in a 8 : 5 synodic resonance but, despite the large distance separating the two planets, it seems to have also synchronized Venus' rotation. It is unlikely that this phenomenon is just a coincidence.

Earth always sees the same face of the Moon. The lunar rotation has been synchronized with Earth by tidal torque. At least 34 moons of the solar system (e.g., the Galilean moons of Jupiter) are rotationally synchronized with their planet (http://en.wikipedia.org/wiki/Synchronous_rotation). Charon and Pluto are also gravitationally locked and keep the same face toward each other. Mercury's rotation period (58.646 days) is exactly 2/3 of its orbital period (87.969 days) (Goldreich and Peale, 1966b; Jelbring, 2013). The synchronization of Mercury's rotation with its orbital period may be due to the combined effect of the strong tidal torque by the Sun and to Mercury's eccentricity (~ 0.2), which implies that at perihelion Mercury is about 2/3 of its aphelion distance from the Sun: 0.307 AU versus 0.467 AU. It is also well known that the three inner moons of Jupiter – Ganymede, Europa and Io – participate in a 1 : 2 : 4 orbital resonance. However, the synchronous rotation of Venus with the Earth's orbit is surprising, given the large distance between the two planets. In fact, the theoretical tidal elongation caused by the Earth's gravity on Venus is just a fraction of millimeter. At the inferior conjunction the tidal elongation caused by Earth on Venus is maximum and is about $3m_{\mathrm{Ea}}R_{\mathrm{Ve}}^4/2m_{\mathrm{Ve}}d_{\mathrm{VE}}^3 = 0.035$ mm, where $m_{\mathrm{Ea}} = 1$ and $m_{\mathrm{Ve}} = 0.815$ are the masses of Earth and Venus in Earth's mass unit, $R_{\mathrm{Ve}} = 6051.8$ km is the radius of Venus and $d_{\mathrm{VE}} = 41.4 \times 10^6$ km is the average distance between Earth and Venus at the inferior conjunction.

Numerous other examples of strong commensurabilities among the planets of the solar system have been found, and some of them will be discussed in this paper (cf. Jelbring, 2013; Tattersall, 2013). Furthermore, the 27.3 days sidereal orbital period of the Moon around Earth appears well synchronized with the 27.3 days period of the Carrington rotation of the Sun, as seen from the Earth, which determines a main electromagnetic oscillation of the heliospheric current sheet in a Parker spiral. The collective synchronization among all celestial bodies in our solar system indicates that they interact energetically with each other and have reached a quasi-synchronized dynamical state.

Indeed, the bodies of the solar system interact with each other gravitationally and electromagnetically, and their orbits and rotations are periodic oscillators. As discovered by Christian Huygens in the 17th century, entrainment or synchronization between coupled oscillators requires very little energy exchange if enough time is allowed. Huygens patented the first pendulum clock and first noted that, if hung on the same wall, after a while, pendulum clocks synchronize

to each other due to the weak physical coupling induced by small harmonic vibrations propagating in the wall (Pikovsky, 2001). Note that the solar system is about 5 billion years old, is not part of a stellar binary system, and in its history has not experienced particularly disrupting events such as collisions with other solar systems. Therefore, a certain degree of harmonic synchronization among its components should be expected.

Newtonian mechanics calculates that the theoretical tidal elongation induced by the gravity of the planets inside the Sun is just a fraction of millimeter (Scafetta, 2012c). Therefore, tidal forcing appears too small to effect the Sun. However, as discussed above, the magnitude of the tidal elongation induced by the Earth's gravity on Venus is also a fraction of millimeter. Thus, if the Earth's gravity or some other planetary mechanism has synchronized the rotation of Venus with Earth, the planets could have synchronized the internal dynamics of the Sun, and therefore they could be modulating solar activity. It seems simply unlikely that in a solar system where everything appears more or less synchronized with everything else, only the Sun should not be synchronized in some complex way with planetary motion.

Thus, the Earth's climate could be modulated by a complex harmonic forcing consisting of (1) lunar tidal oscillations acting mostly in the ocean; (2) planetary-induced solar luminosity and electromagnetic oscillations modulating mostly the cloud cover, and therefore the Earth's albedo; and (3) a gravitational synchronization with the Moon and other planets of the solar system modulating, for example, the Earth's orbital trajectory and its length of day (cf. Mörner, 2013).

From Kepler's basic concepts forward through time, this paper briefly summarizes some of the results that have further suggested the existence of a complex synchronization structure permeating the entire solar system whose physical origin is still not fully understood. A number of empirical studies have shown that a complex synchronized planetary harmonic order may characterize not only the solar planetary system but also the Sun's activity and the Earth's climate, fully confirming Kepler's vision about the existence of a harmony of the world. Preliminary physical mechanisms are being proposed as well.

This brief review is not fully comprehensive of all the results. It simply introduces a general reader to this fascinating issue. The next sections review general results found in the scientific literature showing and discussing (1) the ordered structure of the planetary system; (2) the likely planetary origin of the variability of the Sun's activity; and (3) the synchronization of the Earth's climate with lunar, planetary and solar harmonics.

2 Kepler's vision of a cosmographic mystery

About half of a century after Copernicus, Kepler corrected and extended the heliocentric model. Kepler found that (1) the orbit of every planet is an ellipse (instead of Copernicus' perfect cycles) with the Sun at one of the two foci (instead of being in the center of the cycle), (2) a line joining a planet and the Sun sweeps out equal areas during equal intervals of time, and (3) the square of the orbital period of a planet is proportional to the cube of the semi-major axis of its orbit. If the orbital period, T, is measured in years and the semi-major axis, a, is measured in astronomical units (AU, the average Sun–Earth distance), Kepler's third law takes the simple form of $T^2 = a^3$. The first two laws were published in 1609 (Kepler, 1609), while the third law was published in 1619 (Kepler, 1619). Kepler's three laws of planetary motion were later formally demonstrated by Newton (1687) using calculus and his law of universal gravitation stating that a planet is attracted by the Sun with a force directly proportional to the product of the two masses and inversely proportional to the square of the Sun–planet distance.

However, Kepler did more than just proposing his three laws of planetary motion. Since the publication of the *Mysterium Cosmographicum* (*The Cosmographic Mystery*) Kepler (1596) noted the existence of a "marvelous proportion of the celestial spheres" referring to the "number, magnitude, and periodic motions of the heavens". Kepler found specific distance relationships between the six planets known at that time (Mercury, Venus, Earth, Mars, Jupiter and Saturn). These relationships could be understood in terms of the five Platonic solids enclosed within each other, with the outer solid being a sphere that represented the orbit of Saturn (see Fig. 2a and b).

Some of these geometrical relations are easy to notice. For example, the ratio between the Earth's orbital radius (a = 1 AU) and Venus' orbital radius (a = 0.72 AU) is approximately equal to the ratio between the diagonal and the side of a square ($\sqrt{2} \approx 1.41$). Thus, Venus' orbit is approximately enclosed within a square enclosed within the Earth's orbit (see Fig. 1b). Analogously, the ratio between Saturn's orbital radius (a = 9.6 AU) and Jupiter's orbital radius (a = 5.2 AU) is approximately equivalent to the ratio between the diagonal and the side of a cube ($\sqrt{3} \approx 1.73$). Thus, Jupiter's orbit is approximately enclosed within a cube enclosed within Saturn's orbital sphere (see Fig. 2a).

Kepler also highlighted the existence of a 5 : 2 Jupiter–Saturn resonance, which had been, however, well known since antiquity (Ma'Sar, 9th century; Temple, 1998): every ~ 60 yr the Jupiter–Saturn configuration approximately repeats because Jupiter revolves ~ 5 times and Saturn ~ 2 times. Figure 2c shows Kepler's original diagram of the great conjunctions of Saturn and Jupiter, which occur every ~ 20 yr, from 1583 to 1723. Every three conjunctions (a *trigon*) Jupiter and Saturn meet approximately at the same location of the zodiac, which happens every ~ 60 yr. The

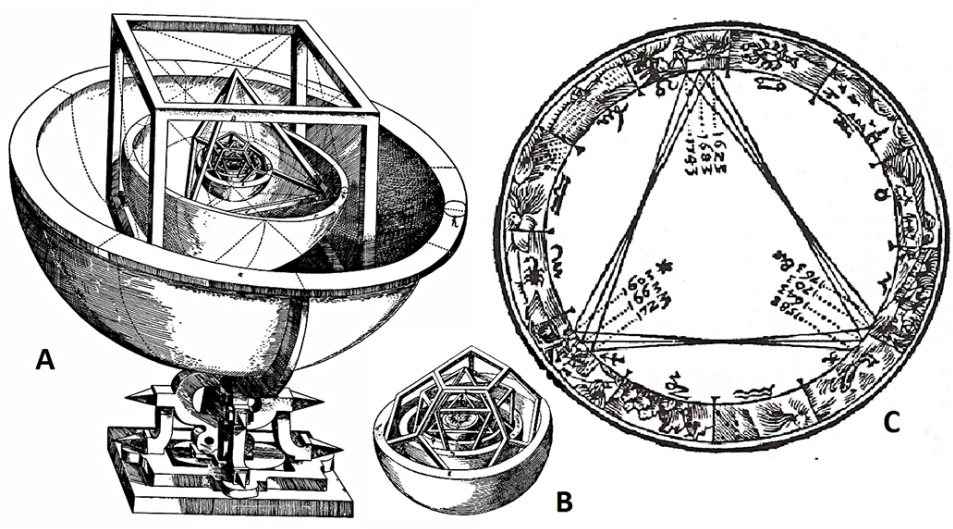

Figure 2. **(A)** Encapsulated Platonic solid model of the solar planetary system (Kepler, 1596). **(B)** Detailed view of the inner sphere. **(C)** A series of great conjunctions of Jupiter and Saturn from 1583 to 1723 by Kepler (1606). The figure demonstrates that every **(A)** 60 yr the Jupiter–Saturn configuration approximately repeats. Every ~ 20 yr a Jupiter–Saturn conjunction occurs. (Figures are adapted from http://en.wikipedia.org.)

trigon slightly rotates and the configuration repeats every 800–1000 yr.

The discovery of a geometrical relationship among the semi-major axes of the planets and the relationship between the planets' orbital semi-major axis and their orbital period (the third law of planetary motion) convinced Kepler (1619) that the planetary orbits are mutually synchronized as though the solar system formed a kind of *celestial choir*. The great advantage of the heliocentric model was mostly to make it far easier to see this ordered structure.

Kepler also conjectured that celestial harmonics could permeate the entire solar system, including the Earth's climate (Kepler, 1601, 1606, 1619). However, modern physics would require that for the planets to modulate the Earth's climate, they first need to modulate the Sun's activity. In fact, the Sun is the most likely place where the weak planetary harmonics could be energetically amplified by a large factor. This issue will be discussed in Sects. 7 and 8.

3 The planetary rhythm of the Titius–Bode rule

Titius (1766) and later Bode (1772) noted that the semi-major axes a_n of the planets of the solar system are function of the planetary sequence number n. Adding 4 to the series 0, 3, 6, 12, 24, 48, 96, 192 and 384 and dividing the result by 10 gives a series that approximately reproduces the semi-major axis length of the planets in astronomical units (1 AU = Sun–Earth average distance). The Titius–Bode rule for the orbital semi-major axis length, a_n, is a power-law equation that can be written as

$$a_n = 0.4 + 0.3 \times 2^n, \quad (1)$$

Table 1. Predictions of the Titius–Bode rule against the observations. The semi-major axes a are measured in astronomical units. The observed semi-major axes are from http://nssdc.gsfc.nasa.gov/planetary/factsheet/.

Planet	n	Titius–Bode rule a_n (AU)	Observations a (AU)	Percent error
Mercury	$-\infty$	0.40	0.387	(3.3 %)
Venus	0	0.70	0.723	(3.18 %)
Earth	1	1.00	1.00	(0 %)
Mars	2	1.60	1.524	(5.0 %)
Ceres	3	2.80	2.77	(1.1 %)
Jupiter	4	5.20	5.204	(0.1 %)
Saturn	5	10.00	9.582	(4.4 %)
Uranus	6	19.60	19.201	(2.1 %)
Neptune	?	?	30.047	?
Pluto	7	38.80	39.482	(1.7 %)

with $n = -\infty$, 0, 1, 2, 3, 4, 5, 6, 7, where $n = -\infty$ refers to Mercury, $n = 0$ to Venus, $n = 1$ to Earth, etc. As Table 1 shows, the Titius–Bode empirical rule successfully predicts the orbital semi-major axis length for all the planets and dwarf planets except for Neptune.

When the Titius–Bode rule was proposed (1766–1772) the dwarf planet Ceres (in the asteroid belt) and the Jovian planet Uranus were unknown. Indeed, the idea that undiscovered planets could exist between the orbits of Mars and Jupiter and beyond Saturn was strongly suggested by Bode in 1772. The curious gap separating Mars and Jupiter had, however, already been noted by Kepler.

The astronomers looked for new planets taking into account the predictions of the Titius–Bode rule. In 1781

Herschel (Dreyer, 1912) discovered Uranus, and in 1801 Piazzi (1801) discovered the dwarf planet Ceres. Both Ceres and Uranus fit the predictions of the Titius–Bode rule relatively well.

In the early 19th century, following Herschel and Piazzi's discoveries, the Titius–Bode rule became widely accepted as a "law" of nature. However, the discovery of Neptune in 1846 created a severe problem because its semi-major axis length $a_{\rm Ne} = 30.047$ AU does not satisfy the Titius–Bode prediction for $n = 7$, $a_7 = 38.80$ AU. The discovery of Pluto in 1930 confounded the issue still further. In fact, Pluto's semi-major axis length, $a_{\rm pl} = 39.482$ AU, would be inconsistent with the Titius–Bode rule unless Pluto is given the position $n = 7$ that the rule had predicted for Neptune (see Table 1).

The Titius–Bode rule is clearly imperfect or incomplete and no rigorous theoretical explanation of it still exists. However, it is unlikely that the relationship among the planets of the solar system that it approximately models is purely coincidental. Very likely any stable planetary system may satisfy a Titius–Bode-type relationship due to a combination of orbital resonance and shortage of degrees of freedom. Dubrulle and Graner (1994a, b) have shown that Titius–Bode-type rules could be a consequence of collapsing-cloud models of planetary systems possessing two symmetries: rotational invariance and scale invariance.

4 The asteroid belt "mirror" symmetry rule

Following the discovery of Ceres in 1801, numerous asteroids were discovered at approximately the same orbital distance. The region in which these asteroids were found lies between Mars and Jupiter and it is known as the asteroid belt. No planet could form in this region because of the gravitational perturbations of Jupiter that has prevented the accretion of the asteroids into a small planet. Ceres, with its spherical shape of ~ 500 km radius, is the largest asteroid and the only dwarf planet in the inner solar system.

A curious mathematical relationship linking the four terrestrial inner planets (Mercury, Venus, Earth and Mars) and the four giant gaseous outer planets (Jupiter, Saturn, Uranus and Neptune) exists (Geddes and King-Hele, 1983). The semi-major axes of these eight planets appear to *reflect* about the asteroid belt. This mirror symmetry associates Mercury with Neptune, Venus with Uranus, Earth with Saturn and Mars with Jupiter. Geddes and King-Hele (1983) found that the mutual relations among the planets could all be approximately given as relations between the mean frequency notes in an octave: $b = 2\exp(1/8)$.

For example, using the semi-major axis lengths reported in Table 1 for the eight planets and labeling these distances with the first two letters of the planet's name, it is easy to obtain

$$\begin{aligned} \mathrm{Me}\times\mathrm{Ne} &= 1.214\cdot\mathrm{Ea}\times\mathrm{Sa} \\ \mathrm{Ve}\times\mathrm{Ur} &= 1.194\cdot\mathrm{Me}\times\mathrm{Ne} \\ \mathrm{Ea}\times\mathrm{Sa} &= 1.208\cdot\mathrm{Ma}\times\mathrm{Ju}, \end{aligned} \tag{2}$$

where we have $b^2 \approx 1.19$, and

$$\begin{aligned} \mathrm{Ve}\times\mathrm{Ma} &= 2.847\cdot\mathrm{Me}\times\mathrm{Ea} \\ \mathrm{Sa}\times\mathrm{Ne} &= 2.881\cdot\mathrm{Ju}\times\mathrm{Ur}, \end{aligned} \tag{3}$$

where we have $b^{12} \approx 2.83$. Combining the equations yields

$$\frac{\mathrm{Me}\times\mathrm{Ne}}{\mathrm{Ea}\times\mathrm{Sa}} \approx \frac{\mathrm{Ve}\times\mathrm{Ur}}{\mathrm{Me}\times\mathrm{Ne}} \approx \frac{\mathrm{Ea}\times\mathrm{Sa}}{\mathrm{Ma}\times\mathrm{Ju}} \tag{4}$$

and

$$\frac{\mathrm{Me}\times\mathrm{Ea}}{\mathrm{Ve}\times\mathrm{Ma}} \approx \frac{\mathrm{Ju}\times\mathrm{Ur}}{\mathrm{Sa}\times\mathrm{Ne}}. \tag{5}$$

These relations relate the four inner and the four outer planets of the solar system. Even if the Geddes and King-Hele rule is not perfect, it does suggest the existence of a specific ordered structure in the planetary system where the asteroid belt region acts as a kind of mirroring boundary condition between the inner and outer regions of the solar system.

Geddes and King-Hele (1983) concluded that "the significance of the many near-equalities is very difficult to assess. The hard-boiled may dismiss them as mere playing with numbers; but those with eyes to see and ears to hear may find traces of something far more deeply interfused in the fact that the average interval between the musical notes emerges as the only numerical constant required – a result that would surely have pleased Kepler."

5 The matrix of planetary resonances

Molchanov (1968, 1969a) showed that the periods of the planets could be approximately predicted with a set of simple linear equations based on integer coefficients describing the mutual planetary resonances. Molchanov's system is reported below:

$$\begin{pmatrix} 1 & -1 & -2 & -1 & 0 & 0 & 0 & 0 & 0 \\ 0 & 1 & 0 & -3 & 0 & -1 & 0 & 0 & 0 \\ 0 & 0 & 1 & -2 & 1 & -1 & 1 & 0 & 0 \\ 0 & 0 & 0 & 1 & -6 & 0 & -2 & 0 & 0 \\ 0 & 0 & 0 & 0 & 2 & -5 & 0 & 0 & 0 \\ 0 & 0 & 0 & 0 & 1 & 0 & -7 & 0 & 0 \\ 0 & 0 & 0 & 0 & 0 & 0 & 1 & -2 & 0 \\ 0 & 0 & 0 & 0 & 0 & 0 & 1 & 0 & -3 \end{pmatrix} \begin{pmatrix} \omega_{\rm Me} \\ \omega_{\rm Ve} \\ \omega_{\rm Ea} \\ \omega_{\rm Ma} \\ \omega_{\rm Ju} \\ \omega_{\rm Sa} \\ \omega_{\rm Ur} \\ \omega_{\rm Ne} \\ \omega_{\rm Pl} \end{pmatrix} = \begin{pmatrix} 0 \\ 0 \\ 0 \\ 0 \\ 0 \\ 0 \\ 0 \\ 0 \\ 0 \end{pmatrix}, \tag{6}$$

where $\omega = T^{-1}$ is the orbital frequency corresponding to the planetary period T. By imposing $\omega_{\rm Ea}^{-1} = T_{\rm Ea} = 1$ yr the system

(Eq. 6) predicts the following orbital periods:

$$
\begin{array}{lcllll}
\text{period} & & & & \text{calculated} & \text{observed} & \text{error} \\
T_{\mathrm{Me}} & = & 2484/10\,332 & = & 0.240 & 0.241 & (0.4\%) \\
T_{\mathrm{Ve}} & = & 2484/4044 & = & 0.614 & 0.615 & (0.2\%) \\
T_{\mathrm{Ea}} & = & 1 & = & 1.000 & 1.000 & (0.0\%) \\
T_{\mathrm{Ma}} & = & 2484/1320 & = & 1.880 & 1.880 & (0.0\%) \\
T_{\mathrm{Ju}} & = & 2484/210 & = & 11.83 & 11.86 & (0.3\%) \\
T_{\mathrm{Sa}} & = & 2484/84 & = & 29.57 & 29.46 & (0.4\%) \\
T_{\mathrm{Ur}} & = & 2484/30 & = & 82.80 & 84.01 & (1.4\%) \\
T_{\mathrm{Ne}} & = & 2484/15 & = & 165.6 & 164.8 & (0.5\%) \\
T_{\mathrm{Pl}} & = & 2484/10 & = & 248.4 & 248.1 & (0.1\%),
\end{array}
\tag{7}
$$

where the last column gives the observed orbital periods of the planets in years. The absolute percent divergence between the predicted and observed orbital periods is given in parentheses.

Using simple linear algebra, the system (Eq. 6) can also be used to find alternative resonance relations. For example, summing the first two rows gives the following relation between Mercury, Earth, Mars and Jupiter: $\omega_{\mathrm{Me}} - 2\omega_{\mathrm{Ea}} - 4\omega_{\mathrm{Ma}} - \omega_{\mathrm{Sa}} = 0$.

Molchanov (1968) showed that analogous tables of integers work also for describing planetary satellite systems such as the moon systems of Jupiter and Saturn. The provided physical explanation was that the resonant structure in a gravitationally interacting oscillating system could be inevitable under the action of dissipative perturbations of mutually comparable size. However, Molchanov (1969a) noted that alternative resonance relations yielding slightly different results could also be formulated. Nevertheless, even if it is the case that the system (Eq. 6) is neither unique nor perfectly descriptive of the orbital characteristics of the planets of the solar system, it does suggest that the planets are mutually synchronized. Molchanov (1969b) quantitatively evaluated that the probability of formation of a given resonant structure by chance is not very likely: the probability that the resonant structure of the solar system could emerge as a random chance was calculated to be less than $p = 10^{-10}$.

6 The gravitational harmonics of the solar system

The simplest way to determine whether the solar system is characterized by a harmonic order is to study its natural frequencies and find out whether they obey some general rule. The main set of frequencies that characterize the solar planetary system can be found by studying the power spectra of physical measures that are comprehensive of the motion of all planets such as the functions describing the dynamics of the Sun relative to the center of mass of the solar system. In fact, the Sun is wobbling around the center of mass of the solar system following a very complex trajectory due to the gravitational attraction of all planets. Figure 3 shows the wobbling of the Sun during specific periods.

Several functions of the coordinates of the Sun relative to the center of mass of the solar system can be chosen such as the distance, the speed, the angular momentum, etc. (e.g., Jose, 1965; Bucha et al., 1985). However, simple mathematical theorems establish that generic functions of the orbits of the planets must by necessity share a common set of planetary frequencies. Only the amplitudes associated with each harmonic are expected to depend on the specific chosen observable. Thus, unless one is interested in a given observable for a specific purpose, any general function of the orbits of the planets should suffice to determine the main harmonic set describing the planetary motion of the solar system as a whole.

Herein I extend the frequency analysis of the Sun's motion made in Bucha et al. (1985) and Scafetta (2010). The JPL's HORIZONS Ephemeris system is used to calculate the speed of the Sun relative to the center of mass of the solar system from 12 December 8002 BC to 24 April 9001 AD (100-day steps). Power spectra are evaluated using the periodogram and the maximum entropy method (Press et al., 1997).

Figure 4a depicts the result and highlights the main planetary frequencies of the solar system. Slightly different values may be found using different observables and subintervals of the analyzed period because of statistical variability and because of the relative amplitude of the frequencies' change with the specific function of the planets' orbits that are chosen for the analysis. An estimate of the statistical theoretical error associated with each measured frequency could be obtained using the Nyquist theorem of the Fourier analysis and it is given by $\nabla f = \pm 1/2L$, where $L = 17\,003$ yr is the length of the analyzed time sequence. Thus, if P_0 is the central estimate of a period, its range is given by $P \approx P_0 \pm P_0^2/2L$ (cf. Tan and Cheng, 2012).

Several spectral peaks can be recognized, such as the ~ 1.092 yr period of the Earth–Jupiter conjunctions; the ~ 9.93 and ~ 19.86 yr periods of the Jupiter–Saturn spring (half synodic) and synodic cycles, respectively; the ~ 11.86, ~ 29.5, ~ 84 and ~ 165 yr orbital period of Jupiter, Saturn, Uranus and Neptune, respectively; the ~ 61 yr cycle of the tidal beat between Jupiter and Saturn; and the periods corresponding to the synodic cycle between Jupiter and Neptune (~ 12.8 yr), Jupiter and Uranus (~ 13.8 yr), Saturn and Neptune (~ 35.8 yr), Saturn and Uranus (~ 45.3), and Uranus and Neptune (~ 171.4 yr), as well as many other cycles including the spring (half-synodic) periods. Additional spectra peaks at ~ 200–220, ~ 571, ~ 928 and ~ 4200 yr are also observed. Clustered frequencies are typically observed. For example, the ranges 42–48 yr, 54–70 yr, 82–100 yr (Gleissberg cycle) and 150–230 yr (Suess–de Vries cycle) are clearly observed in Fig. 4 and are also found among typical main solar activity and aurora cycle frequencies (Ogurtsov et al., 2002; Scafetta and Willson, 2013a). The subannual planetary harmonics together with their spectral coherence with satellite total solar irradiance records and other solar records are discussed in Scafetta and Willson (2013b, c), and are not reported here.

The curious fact is that the numerous spectral peaks observed in the solar motion do not seem to be randomly distributed. They could be approximately reproduced using a

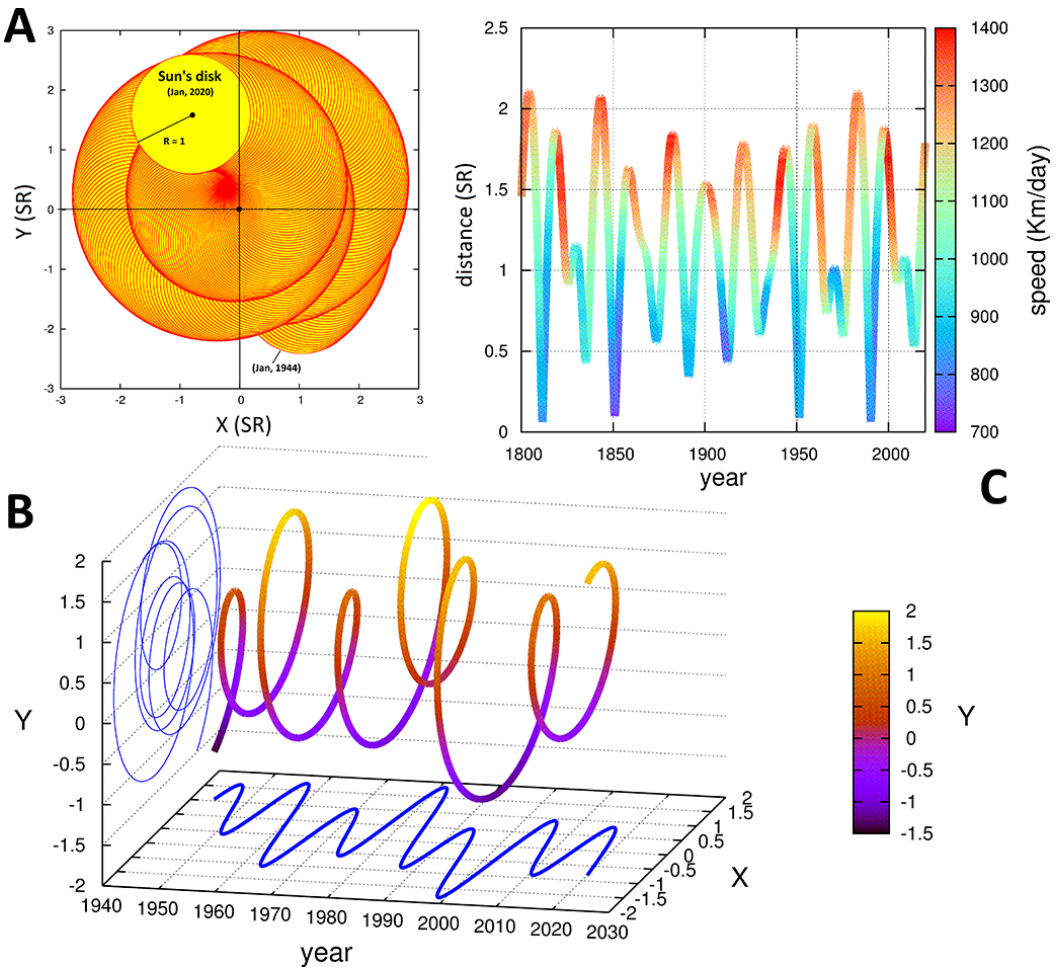

Figure 3. The wobbling of the Sun relative to the center of mass of the solar system. **(A)** Monthly scale movement of the Sun from 1944 to 2020 as seen from the z axis perpendicular to the ecliptic. The Sun is represented by a moving yellow disk with a red circumference (cf. Ebner, 2011). **(B)** The trajectory of the center of the Sun from 1944 to 2020. **(C)** The distance and the speed of the Sun from 1800 to 2020: note the evident ~ 20 yr oscillation and the less evident ~ 60 and ~ 170 yr oscillation. The Sun's coordinates are estimated using the Jet Propulsion Lab's (JPL) HORIZONS Ephemeris system. The coordinates are expressed in solar radius (SR) units.

simple empirical harmonic formula of the type (Jakubcová and Pick, 1986)

$$p_i = 178.38/i \text{ yr}, \qquad i = 1,2,3,\ldots, \tag{8}$$

where the basic period of ~ 178.38 yr is approximately the period that Jose (1965) found in the Sun's motion and in the sunspot record (cf. Charvátová and Hejda, 2014). A comparison between the observed frequencies and the prediction of the resonance model, Eq. (8), is shown in Fig. 4b.

Although Eq. (8) is not perfect, and not all the modeled frequencies are clearly observed in Fig. 4a, the good agreement observed between most of the observed periods and the harmonic model predictions suggests that the solar system is characterized by a complex synchronized harmonic structure. Jakubcová and Pick (1986) also noted that several spectral peaks in the solar motion approximately correspond to the periods of various solar and terrestrial phenomena suggesting that the Sun itself, and the Earth's climate, could be modulated by the same planetary harmonics (see also Charvátová and Hejda, 2014). This issue is further discussed below.

7 The planetary synchronization and modulation of the ~ 11 yr solar cycle

In the 19th century, solar scientists discovered that sunspot activity is modulated by a quasi-11 yr oscillation called the Schwabe cycle. In a letter to Mr. Carrington, Wolf (1859) proposed that the observed solar oscillation could be caused by the combined influence of Venus, Earth, Jupiter and Saturn upon the Sun.

The planetary theory of solar variation is today not favored among solar scientists because, according to Newtonian

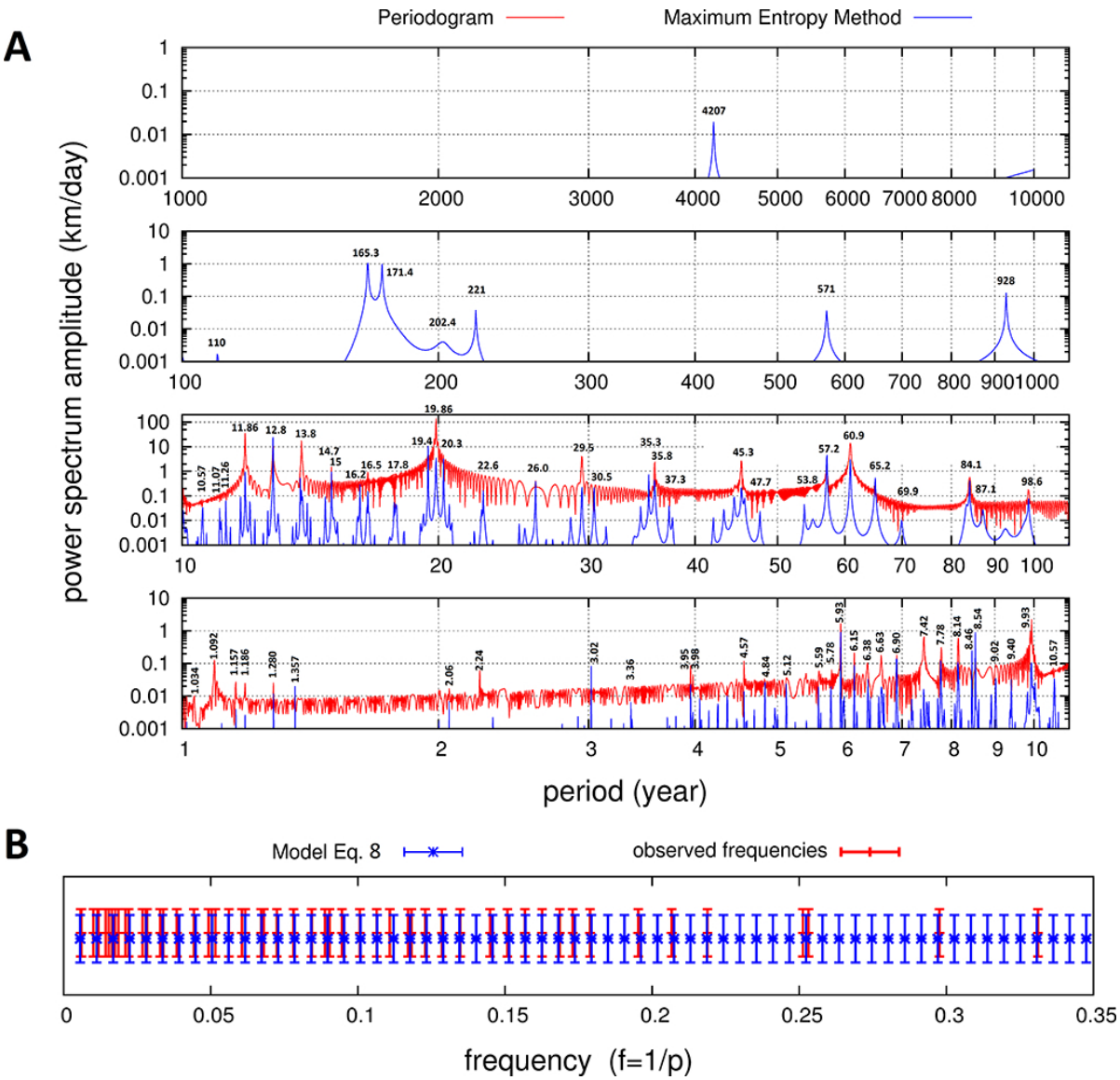

Figure 4. **(A)** Periodogram (red) and the maximum entropy method (blue) of the speed of the Sun relative to the center of mass of the solar system from Dec 12 8002 BC to 24 Apr 9001 AD. For periods larger than 200 yr the periodogram becomes unstable and is thus not shown. **(B)** Comparison between the frequencies observed and listed in **(A)** in the range 3 to 200 yr (red) and the frequency predictions of the resonance model Eq. (8) (blue). Note the good spectral coherence of the harmonic model with the observed frequencies.

physics, the planets appear too far from the Sun to modulate its activity, for example by gravitationally forcing the Sun's tachocline (Callebaut et al., 2012). The planets could modulate solar activity only if a mechanism exists that strongly amplifies their gravitational and/or electromagnetic influence on the Sun. Scafetta (2012c) showed that a strong amplification mechanism could be derived from the mass–luminosity relation: the gravitational energy dissipated by planetary tides on the Sun was proposed to modulate the nuclear fusion rate yielding a variable solar luminosity production. It was calculated that the proposed mechanism could yield a 4×10^6 energetic amplification of the tidal signal. The derived oscillating luminosity signal could be sufficiently strong to modulate the Sun's tachocline and convective zone (cf. Abreu et al., 2012; Mörner, 2013; Solheim, 2013a). Electromagnetic interactions between the planets and the Sun via Parker's spiral magnetic field of the heliosphere, which could be modulated by functions related to the wobbling dynamics of the Sun such as its speed, jerk, etc., could also be possible in principle. Evidence for planet-induced stellar activity has been also observed in other stars (e.g., Scharf, 2010; Shkolnik et al., 2003, 2005).

It is important to stress that the contemporary view of solar science is that solar magnetic and radiant variability is

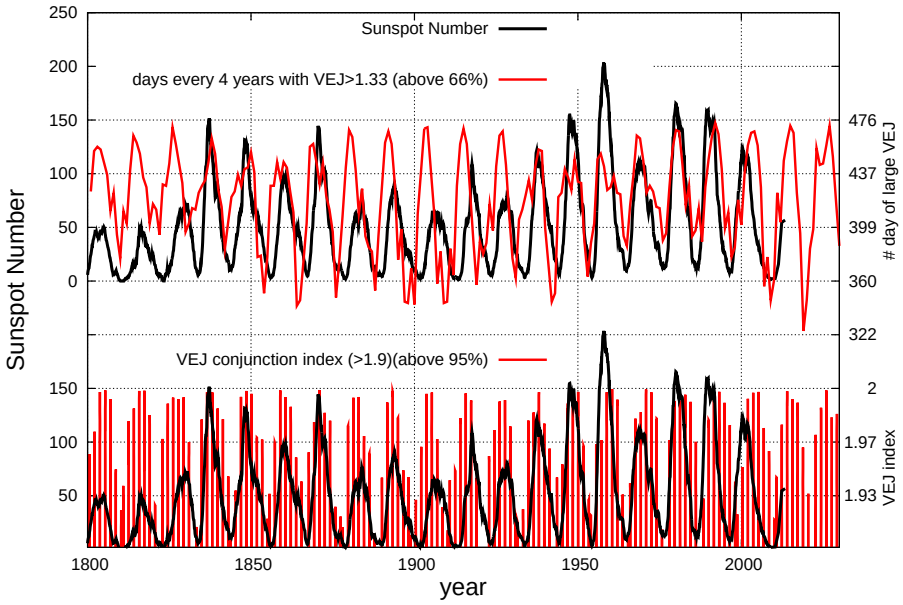

Figure 5. (Top) The sunspot number record (black) is compared against the number of days (every 4 yr) (red) when the alignment index $I_{VEJ} > 66\,\%$. (Bottom) The sunspot number record (black) is compared against the most aligned days with $I_{VEJ} > 95\,\%$ (red). For details see Hung (2007) and Scafetta (2012c).

intrinsically chaotic, driven by internal solar dynamics alone and characterized by hydromagnetic solar dynamo models (Tobias, 2002). However, as also admitted by solar physicists (e.g., de Jager and Versteegh, 2005; Callebaut et al., 2012), present hydromagnetic solar dynamo models, although able to generically describe the periodicities and the polarity reversal of solar activity, are not yet able to quantitatively explain the observed solar oscillations. For example, they do not explain why the Sun should present an ~ 11 yr sunspot cycle and a ~ 22 yr Hale solar magnetic cycle. Solar dynamo models are able to reproduce a ~ 11 yr oscillation only by choosing specific values for their free parameters (Jiang et al., 2007). These dynamo models are not able to explain also the other solar oscillations observed at multiple scales such as the 50–140 yr Gleissberg cycle, the 160–260 yr Suess–de Vries cycle, the millennial solar cycles, etc. (cf. Ogurtsov et al., 2002), nor are they able to explain the phases of these cycles. Thus, the present solar dynamo theories appear to be incomplete. They cannot predict solar activity and they have not been able to explain the complex variability of the solar dynamo including the emergence of the ~ 11 yr oscillation. Some mechanism, which is still missed in the solar dynamo models, is needed to *inform* the Sun that it needs to oscillate at the observed specific frequencies and at the observed specific phases.

However, since Wolf (1859), several studies have highlighted that the complex variability of the solar dynamo appears to be approximately synchronized to planetary harmonics at multiple timescales spanning from a few days to millennia (e.g., Abreu et al., 2012; Bigg, 1967; Brown, 1900; Charvátová, 2009; Charvátová and Hejda, 2014; Fairbridge and Shirley, 1987; Hung, 2007; Jakubcová and Pick, 1986; Jose, 1965; Scafetta, 2010, 2012a, b, c, d, 2013b; Salvador, 2013; Scafetta and Willson, 2013b, a, c; Sharp, 2013; Solheim, 2013a; Tan and Cheng, 2012; Wilson, 2013a; Wolff and Patrone, 2010; and others).

Hung (2007) also reported that 25 of the 38 largest known solar flares were observed to start when one or more tide-producing planets (Mercury, Venus, Earth, and Jupiter) were either nearly above the event positions (less than 10 deg. longitude) or at the opposing side of the Sun. Hung (2007) estimated that the probability for this to happen at random was 0.039 % and concluded that "the force or momentum balance (between the solar atmospheric pressure, the gravity field, and magnetic field) on plasma in the looping magnetic field lines in solar corona could be disturbed by tides, resulting in magnetic field reconnection, solar flares, and solar storms."

As Wolf (1859) proposed, the ~ 11 yr solar cycle could be produced by a combined influence of Venus, Earth, Jupiter and Saturn. There are two main motivations for this proposal:

1. The first model relating the 11 yr solar cycle to the configuration of Venus, Earth and Jupiter was proposed by Bendandi (1931); later Bollinger (1952), Hung (2007) and others developed equivalent models. It was observed that Venus, Earth and Jupiter are the three major tidal planets (e.g., Scafetta, 2012c). By taking into account the combined alignment of Venus, Earth and Jupiter, it is easy to demonstrate that the gravitational configuration of the three planets repeats every

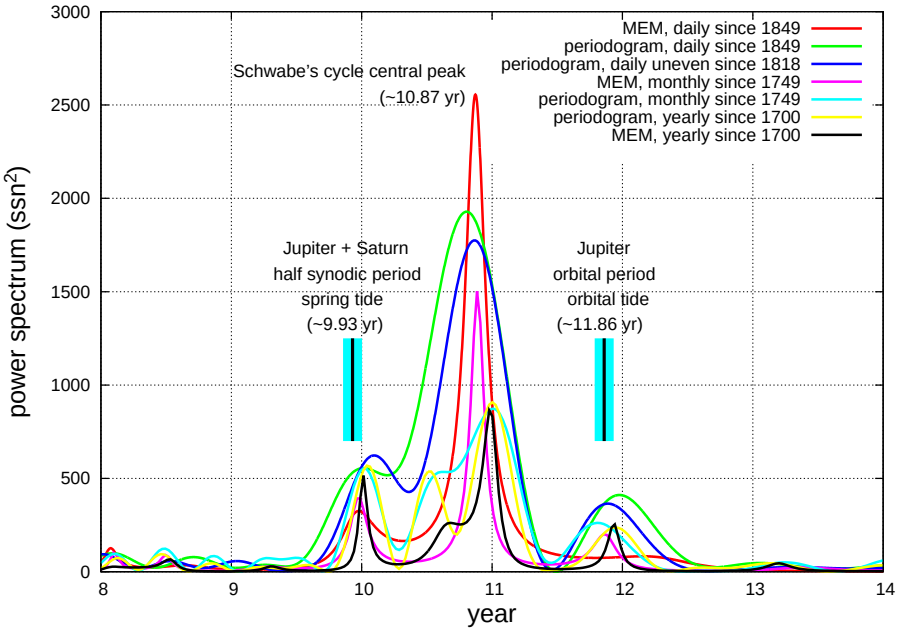

Figure 6. The three-spectral-peak structure of Schwabe's ~ 11 yr sunspot cycle as resolved by power spectra estimated using the maximum entropy method (MEM) and the periodogram (Press et al., 1997). The two side peaks at ~ 9.93 yr and ~ 11.86 yr correspond to the periods of Jupiter's and Saturn's spring tide and of Jupiter's orbital tide on the Sun, respectively (cf. Scafetta, 2012b, c; Solheim, 2013a). Daily, monthly and yearly resolved sunspot number records are used covering periods from 1700 to 2013: http://sidc.oma.be/sunspot-data/.

$$P_{\mathrm{VEJ}} = \left(\frac{3}{P_{\mathrm{Ve}}} - \frac{5}{P_{\mathrm{Ea}}} + \frac{2}{P_{\mathrm{Ju}}} \right)^{-1} = 22.14\,\mathrm{yr}, \qquad (9)$$

where $P_{\mathrm{Ve}} = 224.701$ days, $P_{\mathrm{Ea}} = 365.256$ days and $P_{\mathrm{Ju}} = 4332.589$ days are the sidereal orbital periods of Venus, Earth and Jupiter, respectively (Scafetta, 2012c). The 22.14 yr period is very close to the ~ 22 yr Hale solar magnetic cycle. Moreover, because the configurations Ea–Ve–Sun–Ju and Sun–Ve–Ea–Ju are equivalent about the tidal potential, the tidal cycle presents a recurrence of half of the above value (i.e., a period of 11.07 yr). This is the average solar cycle length observed since 1750 (e.g., Scafetta, 2012b). Figure 5 shows that a measure based on the most aligned days among Venus, Earth and Jupiter is well correlated, in phase and frequency, with the ~ 11 yr sunspot cycle: for details about the Venus–Earth–Jupiter 11.07 yr cycle see Battistini (2011, Bendandi's model), Bollinger (1952), Hung (2007), Scafetta (2012c), Salvador (2013), Wilson (2013a) and Tattersall (2013).

2. The main tides generated by Jupiter and Saturn on the Sun are characterized by two beating oscillations: the tidal oscillation associated with the orbital period of Jupiter (~ 11.86 yr period) and the spring tidal oscillation of Jupiter and Saturn (~ 9.93 yr period) (Brown, 1900; Scafetta, 2012c). Scafetta (2012b, c) used detailed spectral analysis of the sunspot monthly record since 1749 and showed that the ~ 11 yr solar cycle is constrained by the presence of two spectral peaks close to the two theoretical tidal periods deduced from the orbits of Jupiter and Saturn (see Fig. 6). These two frequencies modulate the main central cycle at ~ 10.87 yr period. The beat generated by the superposition of the three harmonics is characterized by four frequencies at about 61, 115, 130, and 983 yr periods that are typically observed in solar records (e.g., Ogurtsov et al., 2002; Scafetta, 2012b). Scafetta (2012b) proposed a harmonic model for solar variability based on three frequencies at periods of ~ 9.93, ~ 10.87 and ~ 11.86 yr. The phases of the three harmonics were determined from the conjunction date of Jupiter and Saturn (2000.475), the sunspot record from 1749 to 2010 (2002.364) and the perihelion date of Jupiter (1999.381), respectively. This simple three-frequency solar model not only oscillates with a ~ 11 yr cycle, as it should by mathematical construction, but it also manifests a complex multidecadal to millennial beat modulation that has been shown to hindcast all major patterns observed in both solar and climate records throughout the Holocene (Scafetta, 2012b). For example, the model was shown to efficiently hindcast: (1) the quasi-millennial oscillation (~ 983 yr) found in both climate and solar records (Bond et al., 2001); (2) the grand solar minima during the last millennium such as the Oort, Wolf, Spörer, Maunder and Dalton minima; (3) seventeen ~ 115 yr long oscillations found

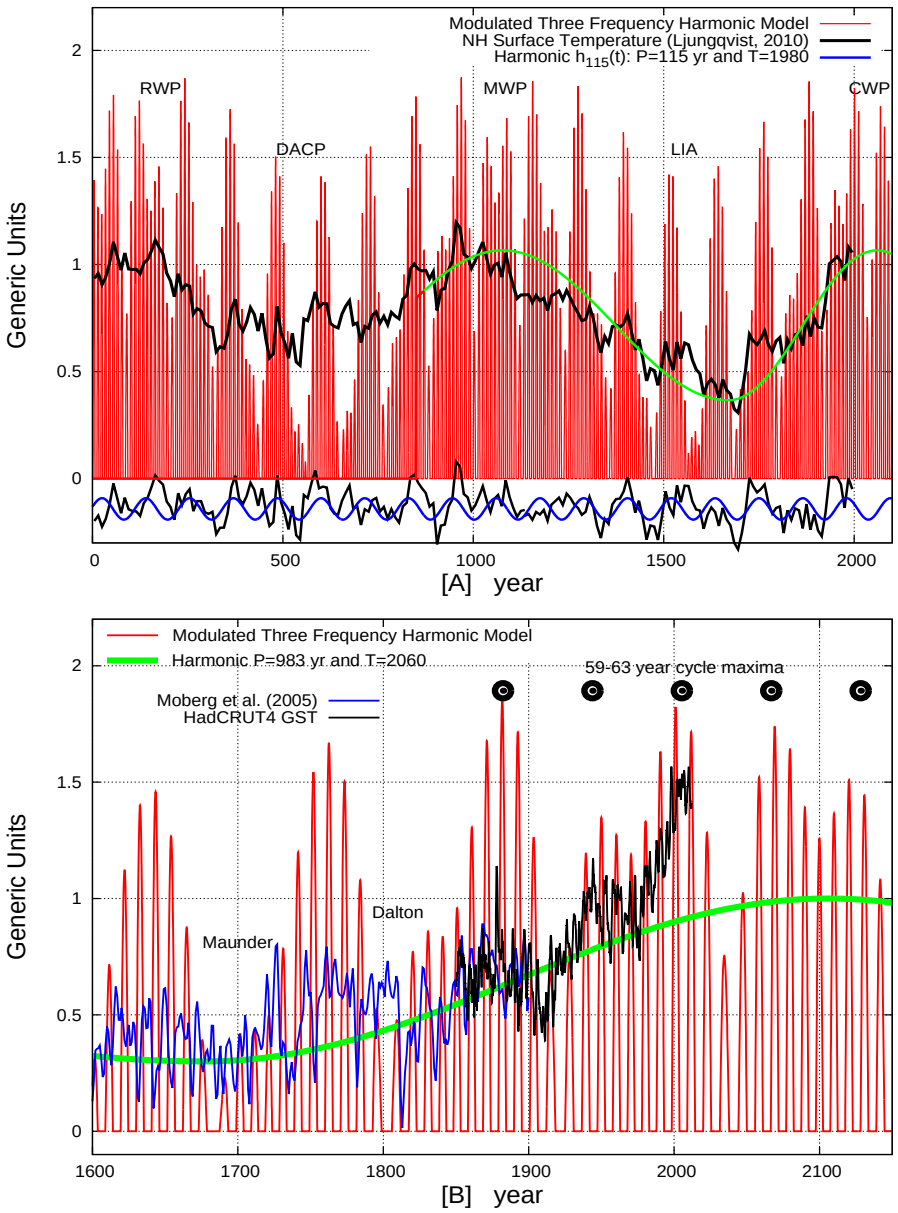

Figure 7. Scafetta (2012b) three-frequency solar model (red). **(A)** Against the Northern Hemisphere temperature reconstruction by Ljungqvist (2010) (black). The bottom section depicts a filtering of the temperature reconstruction (black) that highlights the 115 yr oscillation (blue). **(B)** The same solar model (red) is plotted against the HadCRUT4 global surface temperature (black) merged in 1850–1900 with the proxy temperature model by Moberg et al. (2005) (blue). The green curves highlight the quasi-millennial oscillation with its skewness that approximately reproduces the millennial temperature oscillation from 1700 to 2013. Note the hindcast of the Maunder and Dalton solar minima and relative cool periods as well as the projected quasi 61 yr oscillation from 1850 to 2150. Adapted from Scafetta (2013a, b).

in a detailed temperature reconstruction of the Northern Hemisphere covering the last 2000 yr; and (4) the ~ 59–63 yr oscillation observed in the temperature record since 1850 and other features. Scafetta's (2012b) three-frequency solar model forecasts that the Sun will experience another moderate grand minimum during the following decades and will return to a grand maximum in the 2060s similar to the grand maximum experienced in the 2000s (see Fig. 7b).

Solheim (2013a) observed that if the longer sunspot yearly resolved record is used (1700–2012), then the central spectral peak observed in Fig. 6 at ~ 10.87 yr could be split into two peaks as ~ 11.01 yr and ~ 10.66 yr period. My own reanalysis of the periodogram of the sunspot annual record

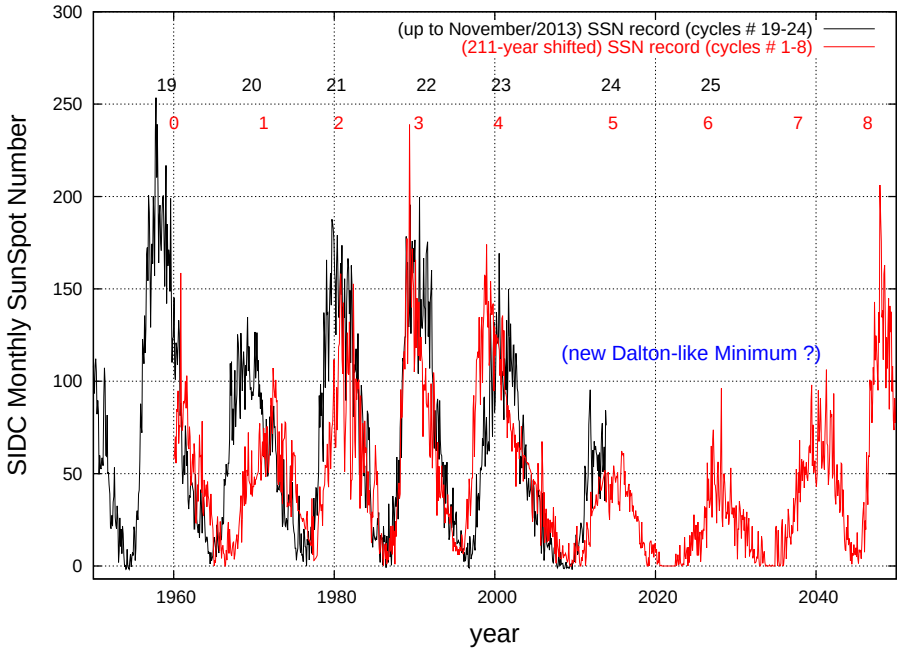

Figure 8. Comparison between latest sunspot cycles #19–24 (black) and the sunspot cycles #1–5 (red) immediately preceding the Dalton Minimum (1790–1830). A new Dalton-like solar minimum is likely approaching and may last until 2045. The 211 yr temporal lag approximately corresponds to a Suess–de Vries solar cycle, which approximately corresponds to the ~ 210 yr beat period between the ~ 60 yr Jupiter–Saturn beat (Figs. 2c and 4a) and the 84 yr Uranus orbital cycle. From Scafetta (2012b).

since 1700 shows that the split produces a secondary peak at 10.52 ± 0.2 yr and a main peak at 11.00 ± 0.2 yr. This result suggests that the central peak at ~ 10.87 yr, which was interpreted in Scafetta (2012b, c) as being produced by an internal dynamo cycle, could indeed emerge from the Venus–Earth–Jupiter recurrent cycles at ~ 11.07 yr period plus a possible minor cycle at ~ 10.57 yr period. Figure 4 shows that these two spectral peaks, plus another one at ~ 11.26 yr period, are among the planetary harmonics. This issue needs further analysis. As for the ocean tidal system on Earth, it is possible that multiple planetary oscillations regulate the ~ 11 yr solar cycle.

The physical meaning of the three-frequency solar model is that solar variability at the multidecadal to millennial scales is mostly determined by the interference among the harmonic constituents that make up the main ~ 11 yr solar oscillation. When these harmonics interfere destructively the Sun enters into a prolonged grand minimum; when they interfere constructively the Sun experiences a grand maximum. Additional oscillations at ~ 45, ~ 85, ~ 170 and ~ 210 yr period, also driven by the other two giant planets, Uranus and Neptune (see Fig. 4), have been observed in long solar and auroral records (Ogurtsov et al., 2002; Scafetta, 2012b; Scafetta and Willson, 2013a) but not yet included to optimize the three-frequency solar model.

Note that the three-frequency solar model proposed by Scafetta (2012b) is a semi-empirical model because it is based on the two main physical tidal harmonics generated by Jupiter and Saturn plus a statistically estimated central ~ 11 yr solar harmonic. Therefore, this model is based on both astronomical and empirical considerations, and its hindcasting capability have been tested for both centuries and millennia. Alternative empirical models of solar variability directly based on long-range harmonics determined using power spectra and linear regressions of solar records have been also proposed (e.g., Scafetta and Willson, 2013a; Solheim, 2013a; Salvador, 2013; Steinhilber and Beer, 2013). However, models based on as many astronomical and physical considerations as possible should be preferred to purely statistical or regressive models because the former are characterized by a lower number of degrees of freedom than the latter for the same number of modeled harmonics.

The proposed semi-empirical and empirical harmonic solar models agree about the fact that the Sun is entering into a period of grand minimum. Indeed, the latest sunspot cycles #19–24 are closely correlated to the sunspot cycles #1–5 immediately preceding the Dalton Minimum (1790–1830) (see Fig. 8). Battistini (2011) noted that the 11 yr solar cycle model proposed by Bendandi (1931) based on the Venus–Earth–Jupiter configuration is slightly out of phase with both the sunspot cycles #2–4 preceding the Dalton Minimum and with the sunspot cycles #22–24. This result may also be further evidence suggesting that the situation preceding the

Dalton Minimum is repeating today and could be anticipated by a planetary configuration.

8 Astronomically based semi-empirical harmonic climate models

As already understood since antiquity (cf. Ptolemy, 2nd century), Kepler (1601) recognized that the moon plays a crucial role in determining the ocean tidal oscillations, and in doing so, he anticipated Newton (1687) in conceiving invisible forces (gravity and electromagnetism) that could act at great distances. Kepler also argued that the climate system could be partially synchronized to multiple planetary harmonics (Kepler, 1601, 1606). The main long-scale harmonics that Kepler identified were a ~ 20 yr oscillation, a ~ 60 yr oscillation and a quasi-millennial oscillation. These oscillations were suggested by the conjunctions of Jupiter and Saturn and by historical chronological considerations (Kepler, 1606; Ma'Sar, 9th century). The quasi-millennial oscillation was associated with the slow rotation of the *trigon* of the conjunctions of Jupiter and Saturn, and Kepler (1606) claimed that this cycle was ~ 800 yr long (see Fig. 2c). Kepler's calculations were based on the tropical orbital periods of Jupiter and Saturn, which is how the orbits of Jupiter and Saturn are seen from the Earth. However, using the sidereal orbital periods this oscillation should be 850–1000 yr long (Scafetta, 2012a), as suggested in the power spectrum analysis shown in Fig. 4. Since antiquity equivalent climatic oscillations have been noted (Iyengar, 2009; Ma'Sar, 9th century; Temple, 1998) and inserted in traditional calendars. For example, the Indian and Chinese traditional calendars are based on a 60 yr cycle known in the Indian tradition as the *Brihaspati* (which means Jupiter) cycle.

The existence of climatic oscillations at about 10, 20, 60 and 1000 yr (and others) have been confirmed by numerous modern studies analyzing various instrumental and proxy climatic records such as the global surface temperature, the Atlantic Multidecadal Oscillation (AMO), the Pacific Decadal Oscillation (PDO), the North Atlantic Oscillation (NAO), ice core records, tree ring records, sea level records, fishery records, etc. (e.g., Bond et al., 2001; Chylek et al., 2011; Klyashtorin et al., 2009; Knudsen, 2011; Jevrejeva et al., 2008; Mörner, 1989; Scafetta, 2012a, 2013c; Wyatt and Curry, 2013). Indeed, numerous authors have also noted a correlation at multiple scales between climate oscillations and planetary functions – for example, those related to the dynamics of the Sun relative to the barycenter of the solar system (e.g., Charvátová, 1997; Charvátová and Hejda, 2014; Fairbridge and Shirley, 1987; Jakubcová and Pick, 1986; Landscheidt, 1989; Scafetta, 2010, 2012b; Solheim, 2013a).

In particular, global surface temperature records, which are available from 1850, present at least four major spectral peaks at periods of about 9.1, 10–11, 20 and 60 yr, plus three minor peaks at about 12, 15 and 30 yr (see Fig. 1 in Scafetta, 2013b, which is partially reproduced in Solheim, 2013b). Subdecadal astronomical oscillations are also observed in climatic records (Scafetta, 2010). In addition, multisecular and millennial oscillations (e.g., there are major ~ 115 and ~ 983 yr oscillations and others) can be deduced from paleoclimatic proxy temperature models. As also shown in Fig. 4, these oscillations can be associated with planetary harmonics (Scafetta, 2010, 2012b). Astronomically based semi-empirical harmonic models to reconstruct and forecast climatic changes are being proposed by several authors (e.g., Abdusamatov, 2013; Akasofu, 2013; Lüdecke et al., 2013; Salvador, 2013; Scafetta, 2010, 2012a, b, d, 2013a; Solheim, 2013a).

For example, Scafetta (2013b) proposed a semi-empirical harmonic climate model based on astronomical oscillations plus an anthropogenic and volcano contribution. In its latest form this model is made of the following six astronomically deduced harmonics with periods of 9.1, 10.4, 20, 60, 115, 983 yr:

$$\begin{aligned} h_{9.1}(t) &= 0.044\cos(2\pi(t-1997.82)/9.1) \\ h_{10.4}(t) &= 0.030\cos(2\pi(t-2002.93)/10.4) \\ h_{20}(t) &= 0.043\cos(2\pi(t-2001.43)/20) \\ h_{60}(t) &= 0.111\cos(2\pi(t-2001.29)/60) \\ h_{115}(t) &= 0.050\cos(2\pi(t-1980)/115) \\ h_{983}(t) &= 0.350\cos(2\pi(t-2060)/760). \end{aligned} \quad (10)$$

In the last equation a 760 yr period from 1680 to 2060 is used instead of a 983 yr period because the millennial temperature oscillation is skewed. While its maximum is predicted to occur in 2060, the minimum occurs around 1680 during the Maunder Minimum (1645–1715) (see Fig. 7a above and Fig. 8 in Humlum et al., 2011).

The 9.1 yr cycle was associated with a soli-lunar tidal oscillation (e.g., Scafetta, 2010, 2012d). The rationale was that the lunar nodes complete a revolution in 18.6 yr and the Saros soli-lunar eclipse cycle completes a revolution in 18 yr and 11 days. These two cycles induce 9.3 yr and 9.015 yr tidal oscillations corresponding respectively to the Sun–Earth–Moon and Sun–Moon–Earth symmetric tidal configurations. Moreover, the lunar apsidal precession completes one rotation in 8.85 yr, causing a corresponding lunar tidal cycle. The three cycles cluster between 8.85 and 9.3 yr periods producing an average period around 9.06 yr. This soli-lunar tidal cycle peaked in 1997–1998, when the solar and lunar eclipses occurred close to the equinoxes and the tidal torque was stronger because centred on the Equator. Indeed, the ~ 9.1 yr temperature cycle was found to peak in 1997.82, as expected from the soli-lunar cycle model (Scafetta, 2012d).

The other five oscillations of Eq. (10) were deduced from solar and planetary oscillations. The 10.4 yr cycle appears to be a combination of the ~ 10 yr Jupiter–Saturn spring cycle and the ~ 11 yr solar cycle and peaks in 2002.93 (i.e., ~ 1 yr after the maximum of solar cycle 23) that occurred in ~ 2002. The ~ 20 and ~ 60 yr temperature cycles are synchronized

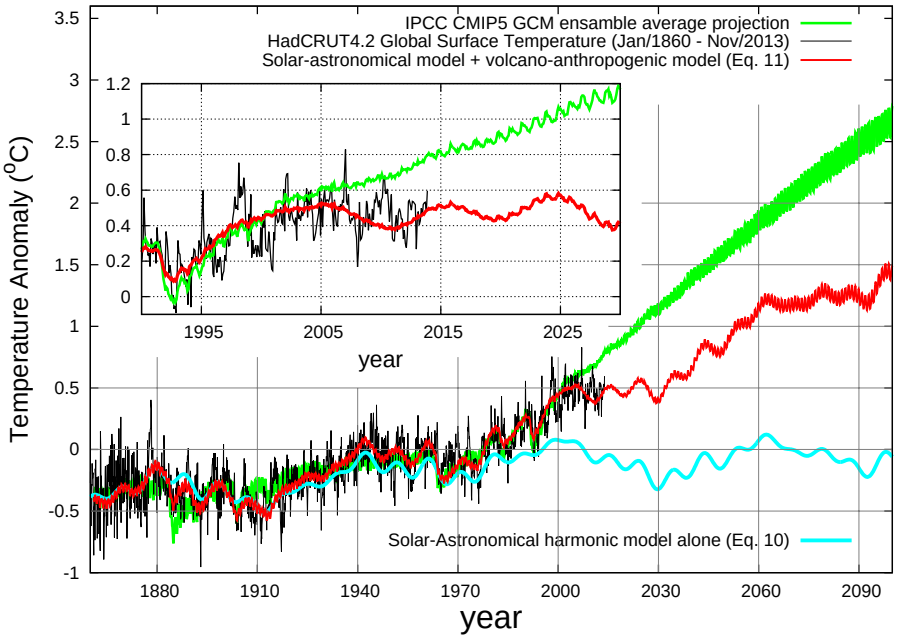

Figure 9. The semi-empirical model (Eq. 11) using $\beta = 0.5$ (red) attenuation of the CMIP5 GCM ensemble mean simulation vs. HadCRUT4 GST record from Jan 1860 to Nov 2013 (black). The cyan curve represents the natural harmonic component alone (Eq. 10). The green curve represents the CMIP5 GCM average simulation used by the IPCC in 2013. The model reconstructs the 20th century warming and all decadal and multidecadal temperature patterns observed since 1860 significantly better than the GCM simulations such as the standstill since ~ 1997, which is highlighted in the insert (cf. Scafetta, 2010, 2012d, 2013b).

with the ~ 20 and ~ 60 yr oscillations of the speed of the Sun relative to the center of mass of the solar system (Scafetta, 2010) and the ~ 61 yr beat cycle of the Jupiter–Saturn tidal function, which peaked around the 1880s, 1940s and 2000s (Scafetta, 2012b, c) (see also Fig. 7b). I note, however, that Wilson (2013b) proposed a complementary explanation of the ~ 60 yr climatic oscillation, which would be caused by planetary induced solar activity oscillations resonating with tidal oscillations associated to specific lunar orbital variations synchronized with the motion of the Jovian planets.

The ~ 115 and ~ 983 yr oscillations are synchronized with both the secular and millennial oscillations found in climatic and solar proxy records during the Holocene (Scafetta, 2012b). The amplitude of the millennial cycle is determined using modern paleoclimatic temperature reconstructions (Ljungqvist, 2010; Moberg et al., 2005). The six oscillations of Eq. (10) are quite synchronous to the correspondent astronomical oscillations (see Fig. 7 and Scafetta, 2010, 2013b). Only the amplitudes of the oscillations are fully free parameters that are determined by regression against the temperature record. See Scafetta (2010, 2012b, 2013b) for details.

To complete the semi-empirical model, a contribution from anthropogenic and volcano forcings was added. It could be estimated using the outputs of typical general circulation models (GCMs) of the Coupled Model Intercomparison Project 5 (CMIP5) simulations, $m(t)$, attenuated by half, $\beta =$ 0.5 (Scafetta, 2013b). The attenuation was required to compensate for the fact that the CMIP3 and CMIP5 GCMs do not reproduce the observed natural climatic oscillations (e.g., Scafetta, 2010, 2012d, 2013b). This operation was also justified on the ground that the CMIP5 GCMs predict an almost negligible solar effect on climate change and their simulations essentially model anthropogenic plus volcano radiative effects alone. Finally, the adoption of $\beta = 0.5$ was also justified by the fact that numerous recent studies (e.g., Chylek et al., 2011; Chylek and Lohmann, 2008; Lewis, 2013; Lindzen and Choi, 2011; Ring et al., 2012; Scafetta, 2013b; Singer, 2011; Spencer and Braswel, 2011; Zhou and Tung, 2012) have suggested that the true climate sensitivity to radiative forcing could be about half (~ 0.7–2.3 °C for CO_2 doubling) of the current GCM estimated range (~ 1.5 to 4.5 °C; IPCC, 2013).

Scafetta's (2013b) semi-empirical climate model was calculated using the following formula:

$$H(t) = h_{9.1}(t) + h_{10.4}(t) + h_{20}(t) + h_{60}(t) + h_{115}(t) + h_{983}(t) + \beta \times m(t) + \text{const.} \quad (11)$$

Figure 9 shows that the model (Eq. 11, red curve) successfully reproduces all of the decadal and multidecadal oscillating patterns observed in the temperature record since 1850, including the upward trend and the temperature standstill since 2000. However, the decadal and multidecadal temperature oscillations and the temperature standstill since ~ 2000

are macroscopically missed by the CMIP5 GCM simulations adopted by the Intergovernmental Panel on Climate Change (IPCC, 2013) (cf. Scafetta, 2013b). As Fig. 9 shows, Eq. (11) projects a significantly lower warming during the 21st century than the CMIP5 average projection.

Alternative empirical models for the global surface temperature have been proposed by Scafetta (2010, 2012a, d, 2013a), Solheim (2013b), Akasofu (2013), Abdusamatov (2013), Lüdecke et al. (2013), Vahrenholt and Lüning (2013) and others. These models are based on the common assumption that the climate is characterized by specific quasi-harmonic oscillations linked to astronomical–solar cycles. However, they differ from each other in important mathematical details and physical assumptions. These differences yield different performances and projections for the 21st century. For example, Scafetta's (2010, 2012a, d, 2013a, b) models predict a temperature standstill until the 2030s and a moderate anthropogenic warming from 2000 to 2100 modulated by natural oscillations such as the ~ 60 yr cycle (see the red curve in Fig. 9). Scafetta's model takes into account that the natural climatic variability, driven by a forecasted solar minimum similar to a moderate Dalton solar minimum or to the solar minimum observed during ~ 1910 (see Figs. 7b and 8) would yield a global cooling of ~ 0.4 °C from ~ 2000 to ~ 2030 (see cyan curve in Fig. 9), but this natural cooling would be mostly compensated by anthropogenic warming as projected throughout the 21st century by Scafetta's β-attenuated model (see Eq. 11). Although with some differences, the climatic predictions of Solheim (2013b), Akasofu (2013) and Vahrenholt and Lüning (2013) look quite similar: they predict a steady to moderate global cooling from 2000 to 2030 and a moderate warming for 2100 modulated by a ~ 60 yr cycle. However, Abdusamatov (2013, Fig. 8) predicted an imminent cooling of the global temperature beginning from the year 2014 that will continue throughout the first half of the 21st century and would yield a Little Ice Age period from ~ 2050 to ~ 2110, when the temperature would be ~ 1.2 °C cooler than the 2000–2010 global temperature. Abdusamatov's predicted strong cooling would be induced by an approaching Maunder-like solar minimum period that would occur during the second half of the 21st century. Steinhilber and Beer (2013) also predicted a grand solar minimum occurring during the second half of the 21st century, but it would be quite moderate and more similar to the solar minimum observed during ~ 1910; thus, this solar minimum will not be as deep as the Maunder solar minimum of the 17th century.

An analysis and comparison of the scientific merits of each proposed harmonic constituent solar and climate model based on astronomical oscillations elude the purpose of this paper and it is left to the study of the reader. In general, harmonic models based only on statistical, Fourier and regression analysis may be misleading if the harmonics are not physically or astronomically justified. Nonetheless, harmonic constituent models can work exceptionally well in reconstructing and forecasting the natural variability of a system if the dynamics of the system are sufficiently harmonic and the constituent physical/astronomical harmonics are identified with great precision. For example, the astronomically based harmonic constituent models currently used to predict the ocean tides are the most accurate predictive geophysical models currently available (Doodson, 1921; http://en.wikipedia.org/wiki/Theory_of_tides).

Scafetta (2012b, d, 2013b) carefully tested his solar and climate models based on astronomical oscillations using several hindcasting procedures. For example, the harmonic solar model was tested in its ability to hindcast the major solar patterns during the Holocene and the harmonic climate model was calibrated during the period 1850–1950 and its performance to obtain the correct 1950–2010 patterns was properly tested, and vice versa. Future observations will help to better identify and further develop the most reliable harmonic constituent climate model based on astronomical oscillations.

9 Conclusions

Pythagoras of Samos (Pliny the Elder, 77 AD) proposed that the Sun, the Moon and the planets all emit their own unique *hum* (orbital resonance; cf. Tattersall, 2013) based on their orbital revolution, and that the quality of life on Earth reflects somehow the tenor of the celestial *sounds* (from http://en.wikipedia.org/wiki/Musica_universalis). This ancient philosophical concept is known as *musica universalis* (universal music or music of the spheres). However, it is with Copernicus' heliocentric revolution that the harmonic structure of the solar system became clearer. Kepler (1596, 1619) strongly advocated the *harmonices mundi* (the harmony of the world) concept from a scientific point of view.

Since the 17th century, scientists have tried to disclose the fundamental mathematical relationships that describe the solar system. Interesting resonances linking the planets together have been found. I have briefly discussed the Titius–Bode rule and other resonant relationships that have been proposed during the last centuries. In addition, planetary harmonics have been recently found in solar and climate records, and semi-empirical models to interpret and reconstruct the climatic oscillations, which are not modeled by current GCMs, have been proposed (e.g., Scafetta, 2013b).

How planetary harmonics could modulate the Sun and the climate on the Earth is still unknown. Some papers have noted that a tidal-torquing function acting upon hypothesized distortions in the Sun's tachocline present planetary frequencies similar to those found in solar proxy and climate records (e.g., Abreu et al., 2012; Wilson, 2013a). However, whether planetary gravitational forces are energetically sufficiently strong to modulate the Sun's activity in a measurable way remains a serious physical problem and reason for skepticism. Also, basic Newtonian physics, such as simple evaluations of tidal accelerations on just the Sun's tachocline, does not

seem to support the theory due to the fact that planetary tidal accelerations on the Sun seem are too small (just noise) compared to the strengths of the typical convective accelerations (Callebaut et al., 2012).

However, the small gravitational perturbation that the Sun is experiencing are harmonic, and the Sun is a powerful generator of energy very sensitive to gravitational and electromagnetic variations. Thus, the Sun's internal dynamics could synchronize to the frequency of the external forcings and it could work as a huge amplifier and resonator of the tenuous gravitational *music* generated by the periodic synchronized motion of the planets. Scafetta (2012c) proposed a physical amplification mechanism based on the mass–luminosity relation. In Scafetta's model the Sun's tachocline would be forced mostly by an oscillating luminosity signal emerging from the solar interior (cf. Wolff and Patrone, 2010). The amplitude of the luminosity anomaly signal driven by the planetary tides, generated in the Sun's core and quickly propagating as acoustic-like waves in the radiative zone into the Sun's tachocline, has to oscillate with the tidal and torquing planetary gravitational frequencies because function of the gravitational tidal potential energy dissipated in the solar interior. The energetic strength of this signal was estimated and found to be sufficiently strong to synchronize the dynamics of the Sun's tachocline and, consequently, of the Sun's convective zone. The quasi-harmonic and resonant structure observed in the solar system should further favor the emergence of collective synchronization patterns throughout the solar system and activate amplification mechanisms in the Sun and, consequently, in the Earth's climate.

Although a comprehensive physical explanation has not been fully found yet, uninterrupted aurora records, solar records and long solar proxy records appear to be characterized by astronomical harmonics from monthly to the millennial timescales, and the same harmonics are also present in climate records, as has been found by numerous authors since the 19th century (e.g., Wolf, 1859; Brown, 1900; Abreu et al., 2012; Charvátová, 2009; Charvátová and Hejda, 2014; Fairbridge and Shirley, 1987; Hung, 2007; Jakubcová and Pick, 1986; Jose, 1965; Salvador, 2013; Scafetta, 2010, 2012a, b, c, d, 2013b; Scafetta and Willson, 2013b, a, c; Sharp, 2013; Solheim, 2013a; Tan and Cheng, 2012; Wilson, 2011, 2013a; Wolff and Patrone, 2010). Thus, gravitational and electromagnetic planetary forces should modulate both solar activity and, directly or indirectly, the electromagnetic properties of the heliosphere. The climate could respond both to solar luminosity oscillations and to the electromagnetic oscillations of the heliosphere and synchronize to them. The electromagnetic oscillations of the heliosphere and the interplanetary electric field could directly influence the Earth's cloud system through a modulation of cosmic ray and solar wind, causing oscillations in the terrestrial albedo, which could be sufficiently large (about 1–3 %) to cause the observed climatic oscillations (e.g., Mörner, 2013; Scafetta, 2012a, 2013b; Svensmark, 2007; Tinsley, 2008; Voiculescu et al., 2013).

Although the proposed rules and equations are not perfect yet, the results of this paper do support the idea that the solar system is highly organized in some form of complex resonant and synchronized structure. However, this state is dynamical and is continuously perturbed by chaotic variability, as it should be physically expected. Future research should investigate planets–Sun and space–climate coupling mechanisms in order to develop more advanced and efficient analytical and semi-empirical solar and climate models. A harmonic set made of the planetary harmonics listed in Fig. 4 plus the beat harmonics generated by the solar synchronization (e.g., Scafetta, 2012b) plus the harmonics deducible from the solilunar tides (e.g., Wang et al., 2012) perhaps constitutes the harmonic constituent group that is required for developing advanced astronomically based semi-empirical harmonic climate models.

As Pythagoras, Ptolemy, Kepler and many civilizations have conjectured since antiquity, solar and climate forecasts and projections based on astronomical oscillations appear physically possible. Advancing this scientific research could greatly benefit humanity.

Acknowledgements. The author thanks R. C. Willson (ACRIM science team) for support, the referees for useful suggestions and the editors for having organized the special issue *Pattern in solar variability, their planetary origin and terrestrial impacts* (Pattern Recognition in Physics, 2013; Editors: N.-A. Mörner, R. Tattersall, and J.-E. Solheim), where 10 authors try to further develop the ideas about the planetary–solar–terrestrial interaction.

Edited by: N.-A. Mörner
Reviewed by: two anonymous referees

References

Abdusamatov, Kh. I.: Grand minimum of the total solar irradiance leads to the little ice age, Geology & Geosciences, 28, 62–68, 2013.

Abreu, J. A., Beer, J., Ferriz-Mas, A., McCracken, K. G., and Steinhilber, F.: Is there a planetary influence on solar activity?, Astron. Astrophys., 548, A88, doi:10.1051/0004-6361/201219997, 2012.

Akasofu, S.-I.: On the Present Halting of Global Warming, Climate, 1, 4–11, 2013.

Battistini, A.: Il ciclo undecennale del sole secondo Bendandi (The 11-year solar cycle according to Bendandi). New Ice Age, http://daltonsminima.altervista.org/?p=8669, 2011.

Bendandi, R.: Un principio fondamentale dell'Universo (A fundamental principle of the Universe). (Faenza, Osservatorio Bendandi), 1931.

Bigg, E. K.: Influence of the planet Mercury on sunspots, Astron. J., 72, 463–466, 1967.

Brown, E. W.: A Possible Explanation of the Sun-spot Period, Mon. Not. R. Astron. Soc., 60, 599–606, 1900.

Bode, J. E.: Anleitung zur Kenntnis des gestirten Himmels, 2nd Edn., Hamburg, p. 462, 1772.

Bollinger, C. J.: A 44.77 year Jupiter-Earth-Venus configuration Sun-tide period in solar-climate cycles, Academy of Science for 1952 – Proceedings of the Oklahoma, 307–311, http://digital.library.okstate.edu/oas/oas_pdf/v33/v307_311.pdf, 1952.

Bond, G., Kromer, B., Beer, J., Muscheler, R., Evans, M. N., Showers, W., Hoffmann, S., Lotti-Bond, R., Hajdas, I., and Bonani, G.: Persistent solar influence on North Atlantic climate during the Holocene, Science, 294, 2130–2136, 2001.

Bucha, V., Jakubcová, I., and Pick, M.: Resonance frequencies in the Sun's motion, Stud. Geophys. Geod., 29, 107–111, 1985.

Callebaut, D. K., de Jager, C., and Duhau, S.: The influence of planetary attractions on the solar tachocline, J. Atmos. Sol.-Terr. Phy., 80, 73–78, 2012.

Charvátová, I.: Solar-terrestrial and climatic phenomena in relation to solar inertial motion, Surv. Geophys., 18, 131–146, 1997.

Charvátová, I.: Long-term predictive assessments of solar and geomagnetic activities made on the basis of the close similarity between the solar inertial motions in the intervals 1840–1905 and 1980–2045, New Astron., 14, 25–30, 2009.

Charvátová, I. and Hejda, P.: Responses of the basic cycle of 178.7 years and 2402 years in solar-terrestrial phenomena during Holocene, Pattern Recogn. Phys., in preparation, 2014.

Chylek, P. and Lohmann, U.: Aerosol radiative forcing and climate sensitivity deduced from the Last Glacial Maximum to Holocene transition, Geophys. Res. Lett., 35, L04804, doi:10.1029/2007GL032759, 2008.

Chylek, P., Folland, C. K., Dijkstra, H. A., Lesins, G., and Dubey, M. K.: Ice-core data evidence for a prominent near 20 year timescale of the Atlantic Multidecadal Oscillation, Geophys. Res. Lett., 38, L13704, doi:10.1029/2011GL047501, 2011.

Copernicus, N.: De revolutionibus orbium coelestium. (Johannes Petreius), 1543.

de Jager, C. and Versteegh, J. M.: Do planetary motions drive solar variability?, Sol. Phys., 229, 175–179, 2005.

Doodson, A. T.: The harmonic development of the tide-generating potential, Proc. R. Soc. Lon. Ser. A, 100, 305–329, 1921.

Dreyer, J. L. E.: The Scientific Papers of Sir William Herschel, edited by: Dreyer, J. L. E. (2 Vols., London), Vol. 1, p. xxviii, 1912.

Dubrulle, B. and Graner, F.: Titius-Bode laws in the solar system. Part I: Scale invariance explains everything, Astron. Astrophys., 282, 262–268, 1994a.

Dubrulle, B. and Graner, F.: Titius–Bode laws in the solar system. Part II: Build your own law from disk models, Astron. Astrophys., 282, 269–276, 1994b.

Ebner, J. E.: Gravity, Rosettes and Inertia, The General Science Journal, 16 October, 1–11, http://gsjournal.net/Science-Journals/Essays/View/3700, 2011.

Fairbridge, R. W. and Shirley, J. H.: Prolonged minima and the 179-year cycle of the solar inertial motion, Sol. Phys., 10, 191–210, 1987.

Geddes, A. B. and King-Hele, D. G.: Equations for Mirror Symmetries Among the Distances of the Planets, Q. J. Roy. Astron. Soc., 24, 10–13, 1983.

Goldreich, P. and Peale, S. J.: Resonant Rotation for Venus?, Nature, 209, 1117–1118, 1966a.

Goldreich P. and Peale, S. J.: Resonant Spin States in the Solar System, Nature, 209, 1178–1179, 1966b.

Humlum, O., Solheim, J.-E., and Stordahl, K.: Identifying natural contributions to late Holocene climate change, Global Planet. Change, 79, 145–156, 2011.

Hung, C.-C.: Apparent Relations Between Solar Activity and Solar Tides Caused by the Planets, NASA report/TM-2007-214817, available at: http://ntrs.nasa.gov/search.jsp?R=20070025111, 2007.

Intergovernmental Panel on Climate Change (IPCC) Fifth Assessment Report (AR5), Climate Change 2013: The Physical Science Basis, 2013.

Iyengar, R. N.: Monsoon rainfall cycles as depicted in ancient Sanskrit texts, Curr. Sci., 97, 444–447, 2009.

Jakubcová, I. and Pick, M.: The planetary system and solar-terrestrial phenomena, Stud. Geophys. Geod., 30, 224–235, 1986.

Jelbring, H.: Celestial commensurabilities: some special cases, Pattern Recogn. Phys., 1, 143–146, doi:10.5194/prp-1-143-2013, 2013.

Jevrejeva, S., Moore, J. C., Grinsted, A., and Woodworth, P.: Recent global sea level acceleration started over 200 years ago?, Geophys. Res. Lett., 35, L08715, doi:10.1029/2008GL033611, 2008.

Jiang, J., Chatterjee, P., and Choudhuri, A. R.: Solar activity forecast with a dynamo model, Mon. Not. R. Astron. Soc., 381, 1527–1542, 2007.

Jose, P. D.: Sun's motion and sunspots, Astron. J., 70, 193–200, 1965.

Kepler, J.: Mysterium Cosmographicum (The Cosmographic Mystery), 1596.

Kepler, J.: On the more certain fundamentals of astrology. 1601, in: Proceedings of the American Philosophical Society, edited by: Brackenridge, J. B. and Rossi, M. A., 123, 85–116, 1979.

Kepler, J.: De Stella Nova in Pede Serpentarii (On the new star in Ophiuchus's foot), 1606.

Kepler, J.: Astronomia nova (New Astronomy), 1609. Translated by Donahue, W. H., Cambridge, Cambridge Univ. Pr., 1992.

Kepler, J.: Harmonices mundi (The Harmony of the World), 1619. Translated by Field, J., The American Philosophical Society, 1997.

Klyashtorin, L. B., Borisov, V., and Lyubushin, A.: Cyclic changes of climate and major commercial stocks of the Barents Sea, Mar. Biol. Res., 5, 4–17, 2009.

Knudsen, M. F., Seidenkrantz, M.-S., Jacobsen, B. H., and Kuijpers, A.: Tracking the Atlantic Multidecadal Oscillation through the last 8,000 years, Nat. Commun., 2, 178, doi:10.1038/ncomms1186, 2011.

Landscheidt, T.: Sun-Earth-Man, a mesh of cosmic oscillations, Urania Trust, 1989.

Lewis, N.: An objective Bayesian, improved approach for applying optimal fingerprint techniques to estimate climate sensitivity, J. Climate, doi:10.1175/JCLI-D-12-00473.1, 2013.

Lindzen, R. S. and Choi, Y.-S.: On the observational determination of climate sensitivity and its implications, Asia Pac. J. Atmos. Sci., 47, 377–390, 2011.

Ljungqvist, F. C.: A new reconstruction of temperature variability in the extratropical Northern Hemisphere during the last two millennia, Geogr. Ann. A, 92, 339–351, 2010.

Lüdecke, H.-J., Hempelmann, A., and Weiss, C. O.: Multi-periodic climate dynamics: spectral analysis of long-term instrumental and proxy temperature records, Clim. Past, 9, 447–452, doi:10.5194/cp-9-447-2013, 2013.

Ma'Sar, A.: On Historical Astrology – The Book of Religions and Dynasties (On the Great Conjunctions), 9th century, Translated by Yamamoto, K. and Burnett, C., Brill Academic Publishers, 2000.

Moberg, A., Sonechkin, D. M., Holmgren, K., Datsenko, N. M., and Karlén, W.: Highly variable Northern Hemisphere temperatures reconstructed from low- and highresolution proxy data, Nature, 433, 613–617, 2005.

Molchanov, A. M.: The Resonant Structure of the Solar System: The Law of Planetary Distances, Icarus, 8, 203–215, 1968.

Molchanov, A. M.: The Reality of Resonances in the Solar System, Icarus, ll, 104–110, 1969a.

Molchanov, A. M.: Resonances in Complex Systems: A Reply to Critiques, Icarus, 11, 95–103, 1969b.

Mörner, N.-A.: Changes in the Earth's rate of rotation on an El Nino to century basis, in: Geomagnetism and Paleomagnetism, edited by: Lowes, F. J., Collinson, D. W., Parry, J. H., Runcorn, S. K., Tozer, D. C., and Soward, A., Kluwer Acad. Publ., 45–53, 1989.

Mörner, N.-A.: Planetary beat and solar–terrestrial responses, Pattern Recogn. Phys., 1, 107–116, doi:10.5194/prp-1-107-2013, 2013.

Mörner, N.-A., Tattersall, R., and Solheim, J.-E.: Preface: Pattern in solar variability, their planetary origin and terrestrial impacts, Pattern Recogn. Phys., 1, 203–204, doi:10.5194/prp-1-203-2013, 2013.

Newton, I.: Philosophiæ Naturalis Principia Mathematica (Mathematical Principles of Natural Philosophy), 1687.

Ogurtsov, M. G., Nagovitsyn, Y. A., Kocharov, G. E., and Jungner, H.: Long-period cycles of the sun's activity recorded in direct solar data and proxies, Sol. Phys., 211, 371–394, 2002.

Piazzi, G.: Risultati delle Osservazioni della Nuova Stella (Palermo), 3–6, 1801.

Pikovsky, A., Rosenblum, M., and Kurths, J.: Synchronization, a universal concept in nonlinear science, Cambridge University Press, Cambridge, UK, 2001.

Pliny the Elder: Natural History, books I–II, 77AD, Translated by Rackham, H., Harvard University Press, 1938.

Press, W. H., Teukolsky, S. A., Vetterling, W. T., and Flannery, B. P.: Numerical Recipes in C, 2nd Edn., Cambridge University Press, 1997.

Ptolemy, C.: Tetrabiblos: on the influence of the stars, 2nd century, Translated by Ashmand, J. M., Astrology Classics, Bel Air, MD, 1980.

Ring, M. J., Lindner, D., Cross, E. F., and Schlesinger, M. E.: Causes of the global warming observed since the 19th century, Atmos. Clim. Sci., 2, 401–415, 2012.

Salvador, R. J.: A mathematical model of the sunspot cycle for the past 1000 yr, Pattern Recogn. Phys., 1, 117–122, doi:10.5194/prp-1-117-2013, 2013.

Scafetta, N.: Empirical evidence for a celestial origin of the climate oscillations and its implications, J. Atmos. Sol.-Terr. Phy., 72, 951–970, doi:10.1016/j.jastp.2010.04.015, 2010.

Scafetta, N.: A shared frequency set between the historical mid-latitude aurora records and the global surface temperature, J. Atmos. Sol.-Terr. Phy., 74, 145–163, doi:10.1016/j.jastp.2011.10.013, 2012a.

Scafetta, N.: Multi-scale harmonic model for solar and climate cyclical variation throughout the Holocene based on Jupiter-Saturn tidal frequencies plus the 11 yr solar dynamo cycle, J. Atmos. Sol.-Terr. Phy., 80, 296–311, doi:10.1016/j.jastp.2012.02.016, 2012b.

Scafetta, N.: Does the Sun work as a nuclear fusion amplifier of planetary tidal forcing? A proposal for a physical mechanism based on the mass-luminosity relation, J. Atmos. Sol.-Terr. Phy., 81–82, 27–40, doi:10.1016/j.jastp.2012.04.002, 2012c.

Scafetta, N.: Testing an astronomically based decadal-scale empirical harmonic climate model versus the IPCC (2007) general circulation climate models, J. Atmos. Sol.-Terr. Phy., 80, 124–137, doi:10.1016/j.jastp.2011.12.005, 2012d.

Scafetta, N.: Solar and planetary oscillation control on climate change: hind-cast, forecast and a comparison with the CMIP5 GCMs, Energy & Environment, 24, 455–496, doi:10.1260/0958-305X.24.3-4.455, 2013a.

Scafetta, N.: Discussion on climate oscillations: CMIP5 general circulation models versus a semi-empirical harmonic model based on astronomical cycles, Earth-Sci. Rev., 126, 321–357, doi:10.1016/j.earscirev.2013.08.008, 2013b.

Scafetta, N.: Multi-scale dynamical analysis (MSDA) of sea level records versus PDO, AMO, and NAO indexes, Clim. Dynam., doi:10.1007/s00382-013-1771-3, in press, 2013c.

Scafetta, N. and Willson, R. C.: Planetary harmonics in the historical Hungarian aurora record (1523–1960), Planet. Space Sci., 78, 38–44, doi:10.1016/j.pss.2013.01.005, 2013a.

Scafetta, N. and Willson, R. C.: Empirical evidences for a planetary modulation of total solar irradiance and the TSI signature of the 1.09 yr Earth-Jupiter conjunction cycle, Astrophys. Space Sci., 348, 25–39, doi:10.1007/s10509-013-1558-3, 2013b.

Scafetta, N. and Willson, R. C.: Multiscale comparative spectral analysis of satellite total solar irradiance measurements from 2003 to 2013 reveals a planetary modulation of solar activity and its nonlinear dependence on the 11 yr solar cycle, Pattern Recogn. Phys., 1, 123–133, doi:10.5194/prp-1-123-2013, 2013c.

Scharf, C. A.: Possible Constraints on Exoplanet Magnetic Field Strengths from Planet–star Interaction, Astrophys. J., 722, 1547–1555, 2010.

Sharp, G. J.: Are Uranus & Neptune Responsible for Solar Grand Minima and Solar Cycle Modulation?, Int. J. Astron. Astrophys., 3, 260–273, 2013.

Shirley, J. H., Sperber, K. R., and Fairbridge, R. W.: Sun's internal motion and luminosity, Sol. Phys., 127, 379–392, 1990.

Shkolnik, E., Walker, G. A. H., and Bohlender, D. A.: Evidence for Planet-induced Chromospheric Activity on HD 179949, ApJ, 597, 1092–1096, 2003.

Shkolnik, E., Walker, G. A. H., Bohlender, D. A., Gu, P.-G., and Kurster, M.: Hot Jupiters and Hot Spots: The Short- and Long-Term Chromospheric Activity on Stars with Giant Planets, ApJ, 622, 1075–1090, 2005.

Singer, S. F.: Lack of consistency between modeled and observed temperature trends, Energy Environ., 22, 375–406, 2011.

Solheim, J.-E.: The sunspot cycle length – modulated by planets?, Pattern Recogn. Phys., 1, 159–164, doi:10.5194/prp-1-159-2013, 2013a.

Solheim, J.-E.: Signals from the planets, via the Sun to the Earth, Pattern Recogn. Phys., 1, 177–184, doi:10.5194/prp-1-177-2013, 2013b.

Spencer, R. W. and Braswell, W. D.: On the misdiagnosis of surface temperature feedbacks from variations in earth's radiant energy balance, Remote Sens., 3, 1603–1613, 2011.

Steinhilber, F. and Beer, J.: Prediction of solar activity for the next 500 years, J. Geophys. Res., 118, 1861–1867, 2013.

Svensmark, H.: Cosmoclimatology: a new theory emerges, Astron. Geophys., 48, 18–24, 2007.

Tan, B. and Cheng, Z.: The mid-term and long-term solar quasi-periodic cycles and the possible relationship with planetary motions, Astrophys. Space Sci., 343, 511–521, 2013.

Tattersall, R.: The Hum: log-normal distribution and planetary–solar resonance, Pattern Recogn. Phys., 1, 185–198, doi:10.5194/prp-1-185-2013, 2013.

Temple, R.: The Sirius mystery. Appendix IV "Why Sixty Years?", Destiny Books, Rochester, Vermont, http://www.bibliotecapleyades.net/universo/siriusmystery/siriusmystery_appendix03.htm, 1998.

Tinsley, B. A.: The global atmospheric electric circuit and its effects on cloud microphysics, Rep. Prog. Phys., 71, 066801, doi:10.1088/0034-4885/71/6/066801, 2008.

Titius, J. D.: Betrachtung über die Natur, vom Herrn Karl Bonnet (Leipzig, 1766), pp. 7–8; transl. by Jaki, S., in: The early history of the Titius-Bode Law, Am. J. Phys., 40, 1014–1023, 1972.

Tobias, S. M.: The Solar Dynamo, Phil. Trans. A, 360, 2741–2756, 2002.

Vahrenholt, F. and Lüning, S.: The neglected Sun, why the Sun precludes climate catastrophe, Stacey International, London, 2013.

Voiculescu, M., Usoskin, I., and Condurache-Bota, S.: Clouds blown by the solar wind, Environ. Res. Lett., 8, 045032, doi:10.1088/1748-9326/8/4/045032, 2013.

Wang, Z., Wu, D., Song, X., Chen, X., and Nicholls, S.: Sun–moon gravitation-induced wave characteristics and climate variation, J. Geophys. Res., 117, D07102, doi:10.1029/2011JD016967, 2012.

Wilson, I. R. G.: Are Changes in the Earth's Rotation Rate Externally Driven and Do They Affect Climate? The General Science Journal, 3811, 1–31, 2011.

Wilson, I. R. G.: The Venus–Earth–Jupiter spin–orbit coupling model, Pattern Recogn. Phys., 1, 147–158, doi:10.5194/prp-1-147-2013, 2013a.

Wilson, I. R. G.: Long-Term Lunar Atmospheric Tides in the Southern Hemisphere, The Open Atmospheric Science Journal, 7, 51–76, 2013b.

Wolf, R.: Extract of a letter to Mr. Carrington, Mon. Not. R. Astron. Soc., 19, 85–86, 1859.

Wolff, C. L. and Patrone, P. N.: A new way that planets can affect the Sun, Sol. Phys., 266, 227–246, 2010.

Wyatt, M. G. and Curry, J. A.: Role for Eurasian Arctic shelf sea ice in a secularly varying hemispheric climate signal during the 20th century, Clim. Dynam., doi:10.1007/s00382-013-1950-2, in press, 2013.

Zhou, J. and Tung, K.-K.: Deducing multi-decadal anthropogenic global warming trends using multiple regression analysis, J. Atmos. Sci., 70, 3–8, doi:10.1175/JAS-D-12-0208.1, 2012.

Part III

The Hum: log-normal distribution and planetary–solar resonance.

Tattersall, R.: Pattern Recogn. Phys., 1, 185-198, doi:10.5194/prp-1-185-2013, 2013.

Pattern Recogn. Phys., 1, 185–198, 2013
www.pattern-recogn-phys.net/1/185/2013/
doi:10.5194/prp-1-185-2013

Pattern Recognition in Physics
Open Access

The Hum: log-normal distribution and planetary–solar resonance

R. Tattersall

University of Leeds, Leeds, UK

Correspondence to: R. Tattersall (rog@tallbloke.net)

Received: 30 September 2013 – Revised: 11 November 2013 – Accepted: 12 November 2013 – Published: 16 December 2013

Abstract. Observations of solar and planetary orbits, rotations, and diameters show that these attributes are related by simple ratios. The forces of gravity and magnetism and the principles of energy conservation, entropy, power laws, and the log-normal distribution which are evident are discussed in relation to planetary distribution with respect to time in the solar system. This discussion is informed by consideration of the periodicities of interactions, as well as the regularity and periodicity of fluctuations in proxy records which indicate solar variation. It is demonstrated that a simple model based on planetary interaction frequencies can well replicate the timing and general shape of solar variation over the period of the sunspot record. Finally, an explanation is offered for the high degree of stable organisation and correlation with cyclic solar variability observed in the solar system. The interaction of the forces of gravity and magnetism along with the thermodynamic principles acting on planets may be analogous to those generating the internal dynamics of the Sun. This possibility could help account for the existence of strong correlations between orbital dynamics and solar variation for which a sufficiently powerful physical mechanism has yet to be fully demonstrated.

1 Introduction

An epoch at which a strong 2 : 1 orbital resonance existed between Jupiter and Saturn is thought to have later ejected most of the planetesimals from the system (Levison et al., 2008) and brought about the re-organisation of the planets with the planetesimal Kuiper Belt beyond Neptune. These are now found in log-normally distributed stable orbits which are close to but not at destructively resonant frequencies. The stability of the solar system at the present epoch is, however, not due to the avoidance of resonance through randomness.

As can be seen in Lykawka and Mukai (2007, Fig. 3) the semi-major axes of planetesimals in the Kuiper Belt cluster at equivalent orbital periods resonant with Neptune in the ratios 2 : 1, 3 : 2, 4 : 3, 5 : 2, 5 : 3, 5 : 8, 7 : 4, and 9 : 4. The 3 : 2 resonance is the strongest of these. It is apparent in many other solar system ratio pairs including the differential rotation of the Sun, spin–orbit ratios of Mercury and Venus, and the rates of precession of synodic conjunction cycles.

As the following observations demonstrate, these evident patterns strongly suggest that the stability of the solar system is maintained by the interaction of the gravity and the heliomagnetic field acting on planets to bring about a variety of resonant couplings. The power laws of gravity and magnetism also evidently act to bring about a log-normal distribution conforming to the numerical series which converge to phi, such as the Fibonacci and Lucas series. The timing patterns generated by the motion of the planets relative to one another are well correlated to solar variation and changes in Earth's length of day. This is further evidence suggesting that a cybernetic feedback is operating in the solar system. The effects evidently assist in maintaining stability, rather than leading to positive feedback and destructive resonance. According to Koyré (1973), Johannes Kepler, in his treatise "Nova Astonomia" wrote: "… because the Earth moves the Moon by its species, and is a magnetic body; and because the sun moves the planets in a similar manner by the species which it emits, therefore the Sun, too, is a magnetic body."

This insight may prove to be prescient, if it is eventually found that the effects of the forces of gravity and magnetism interact to bring about the simple harmonic ratios observed

Table 1. Relationships between the semi-major axes (SMA) of the solar system planets.

Planet Pair	Ratio of SMAs	Error (%)	Add/subtract unity to/from ratio units	Simplified SMA ratios
Mercury–Venus	28 : 15	0.07	28 : (15 – 1) = 28 : 14	2 : 1
Venus–Earth	18 : 13	0.15	18 : (13 – 1) = 18 : 12	3 : 2
Earth–Mars	32 : 21	0.01	(32 + 1) : (21 + 1) = 33 : 22	3 : 2
Mars–Jupiter	34 : 10	0.44	(34 + 1) : 10 = 35 : 10	5 : 2
Jupiter–Saturn	11 : 6	0.002	(11 + 1) : 6 = 12 : 6	2 : 1
Saturn–Uranus	344 : 171	0.004	344 : (171 + 1) = 344 : 172	2 : 1
Uranus–Neptune	47 : 30	0.01	(47 + 1) : 30 = 48 : 30	8 : 5

Table 2. Proximity of solar system orbital period ratios to resonant ratios.

Planet pair	Ratio of orbital periods	Error	Add/subtract unity to/from ratio units	Simplified orbital ratios
Mercury–Venus	23 : 9		(23 + 1) : 9 = 24 : 9	8 : 3
Venus–Earth	13 : 8		(13 – 1) : 8 = 12 : 8	3 : 2
Earth–Jupiter	83 : 7		(83 + 1) : 7 = 84 : 7	12 : 1
Mars–Jupiter	19 : 3		(19 – 1) : 3 = 18 : 3	6 : 1
Jupiter–Saturn	149 : 60		(149 + 1) : 60 = 150 : 60	5 : 2
Uranus–Neptune	102 : 52		102 : (52 – 1) = 102 : 51	2 : 1

between planetary and solar orbital and rotational timings. The resonances which arise from these harmonic ratios were recognised by Kepler as "The music of the spheres", and in the modern idiom, we can refer to these inter-related solar system resonances as "The Hum".

This paper examines the relationships of ratios observed in the solar system. In Sect. 2, close-to-resonant ratios are shown between planets and their synodic periods. Section 3 extends these observations to show that as well as being close to resonant ratios as planet pairs, the entire solar system lies in close relation to the log-normally distributed Fibonacci series. Section 4 shows that as well as orbital and synodic periods, the rotation rate ratios of the planet pairs are also related to the Fibonacci series. In Sect. 5 an overview of the long-term convergences and ratios of the orbital and synodic periods is given and the observations summarised.

In Sect. 6 periodicities identified in terrestrial proxy data (^{14}C and ^{10}Be) are compared with synodic periods and the number series they form, which also relate to the Fibonacci series and powers of the irrational number phi, which this series' adjacent ratios converge to. Since these proxies relate to solar activity levels, a method of correlating the planetary interaction timings of Jupiter, Earth, and Venus with solar variation is demonstrated.

Results are discussed in Sect. 7. The possible mechanisms underlying the apparently coupled phenomena are considered in relation to analogous phenomena for which theory is already developed. This discussion leads to the paper's conclusions given in Sect. 8.

2 Periodic resonance

Traditionally, the distribution of planets in the solar system has been characterised by the spacing of their semi-major axes (Bode–Titius). A short survey of the ratios between the semi-major axes of adjacent planets reveals an unusual feature whereby their almost exact ratios can be converted to a simple ratio by the addition/subtraction of unity to/from one side of the ratio, as seen in Table 1.

It should be noted that this type of relationship is not limited to the solar system. Star HD 200964 is orbited by two gas giants with orbital periods of 830 days and 630 days (Johnson et al., 2011). These periods put their semi-major axes in the ratio 6 : 5. Subtracting unity from 5 makes the ratio 3 : 2. The ratio between their orbital periods is 63 : 83. Adding unity to 83 makes the ratio 3 : 4, a resonant ratio. Similar situations occur with the ratios of orbital periods in the solar system, summarised in Table 2.

Many of the ratios in Table 2 are not strongly resonant. However, resonances which are capable of transferring angular momentum between planets and moons are evident in the ratios between the periods of synodic cycles and the orbital periods of more massive planets such as Jupiter. To understand the numerical phenomenon observed in the ratios of planets' semi-major axes seen in Table 1, we need to investigate not only the relationships between the planets' orbital periods seen in Table 2 but also their synodic cycles, which also help determine those semi-major axes via stronger resonances appearing periodically as gravitational perturbations. These are summarised in Table 3.

Table 3. Inner solar system relations with Jupiter.

Planet–planet pair	Period (years)	Ratio of relations	Error (%)	Add/subtract unity to/from ratio units	Simplified ratios	Deviation (%)
Me–Ve synodic cycle Ea–Ve synodic cycle	1.97 7.99	215 : 53	0.01	(215 + 1) : (53 + 1) = 216 : 54	4 : 1	1.3
Me–Ve synodic cycle Jupiter orbital period	1.97 11.86	6 : 1	0.33	6 : 1	6 : 1	0.33
Ratio of ratios above					3 : 2	1.05
Ea–Ve synodic cycle Jupiter orbital period	7.99 11.86	46 : 31	0.03	(46 – 1) : (31 – 1) = 45 : 30	3 : 2	1.05
Ea–Ma synodic Jupiter orbital period	4.27 11.86	50 : 9	0.005	50 : (9 + 1) = 50 : 10	5 : 1	10

3 Log-normal distribution of periodic phenomena

It is found that the orbital and synodic periods of all the planets and the two main dwarf planets Pluto and Eris lie close to simple relations with the log-normally distributed Fibonacci series, a simply generated sequence of ratios which rapidly converges towards the irrational number phi. A time period of sufficient length to cover the periodicities within the scope of this paper is considered in relation to the Fibonacci series.

In Table 4, the highest number in the Fibonacci series used (6765) is allowed to stand for the number of orbits of the Sun made by Mercury, the innermost planet. The number of orbits made by the other planets and dwarf planets during the time period of ∼1630 yr is calculated. Additionally, the number of synodic conjunctions between adjacent planet pairs made in the same period is calculated using the method derived by Nicolaus Copernicus: Period = 1/((1/faster orbit) – (1/slower orbit))

The results are then compared to the descending values of the Fibonacci series and the deviations from the series calculated. Juno is selected as representative of the Asteroid Belt as it lies near the middle of the main core at a distance of 2.67 AU (Fig. 1). By Kepler's third law this object has an orbital period of $P = \sqrt{2.67^3} = 4.36$ yr.

The synodic conjunction cycles of principal planet pairs form distinctive geometric shapes with respect to the sidereal frame of reference. Mercury–Venus and Venus–Earth conjunctions return close to their original longitudes after 5 synodic conjunctions forming five-pointed star shapes, Jupiter and Saturn after 3 synodic conjunctions forming a triangle shape, and Uranus and Neptune after 21 synodic conjunctions which alternately occur nearly oppositely. The numbers 3, 5, and 21 are all Fibonacci numbers. The time periods over which these synodic conjunction cycles precess either completely or by subdivisions of the number of synodic conjunctions in their cycles relate to each other by simple numerical operations also involving Fibonacci numbers. Their ratios are included in Table 2 in red for further discussion in Sect. 4.1.

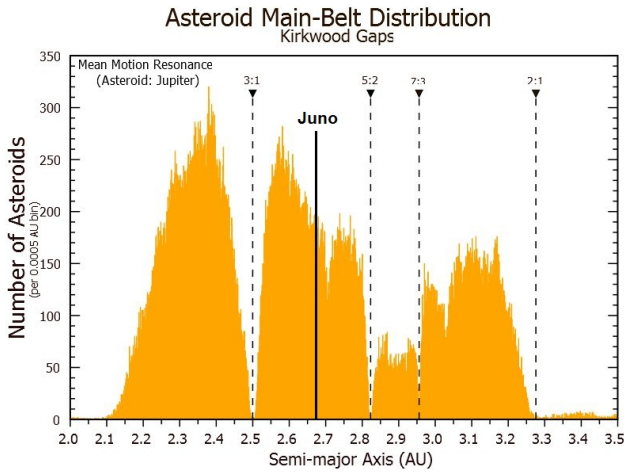

Figure 1. Dwarf planet Juno in relation to the main Asteroid Belt.

PSD analysis of the sunspot record reveals cyclic concentrations of higher sunspot numbers near the Schwabe, 1/2 Jupiter–Saturn synodic, and Jupiter orbital periods (Scafetta, 2012a). The relationship of these periods to planetary interaction periods is included, along with terrestrial climate cycle periods relating to luni–solar variation evident in proxy records such as the De Vries and Halstatt cycles.

4 Sidereal planetary rotation

4.1 The adjacent planetary pairs

It is observed in Table 5 that the numbers of completed sidereal axial rotations made by adjacent planets in proximate elapsed times form close-to-whole number ratios whose numerators and denominators sum to numbers in the Fibonacci sequence. Additional non-adjacent pair ratios are included in Table A1 of the Appendix. A test against a set of random

Table 4. Comparing the Fibonacci series to orbits and synodic conjunctions. The solar harmonics shown are the positive beat frequencies of the periods found in a power spectral density (PSD) analysis of sunspot numbers (SSN) which match the Jupiter–Saturn synodic period and the Jupiter orbital period (Scafetta, 2012b). The synodic precession cycles have simple relationships: Uranus–Neptune ~ 3600 yr is in 2 : 3 ratio with Jupiter–Saturn ~ 2400 yr, which is in 1 : 2 ratio with Earth–Venus ~ 1200 yr. One-fifth of the latter is in 1 : 5 ratio with Venus–Mercury ~ 48 yr. This suggests coupled relationships.

Fibonacci number	Period (years)	Period (years)	Relationship	Number of cycles	Deviation
6765	0.24	0.24	Orbit	6765: Mercury	+0 (baseline)
4181	0.389	0.395	Synodic	4162.2: Mercury–Venus	+0.46 %
2584	0.63	0.615	Orbit	2628.1: Venus	−1.72 %
1597	1.02	1	Orbit	1629.7: Earth	−2.04 %
987	1.65	1.6	Synodic	1019.41: Venus–Earth	−3.28 %
610	2.67	2.67	Destructive resonance orbit		
377	4.32	4.36 4.27	Orbit Synodic	372.9: Juno 381.4: 2 × Earth–Mars	+1.1 % −1.18 %
233	6.99	6.99 6.99 6.89	Harmonic Harmonic Synodic	232.955: J-S+Solar10.8yr 232.85: 2×J+0.5J-S:PSD-SSN 235.3: Juno–Jupiter	−0.01 % +0.07 % −1.1 %
144	11.32	11.28 11.86 11.07	Orbit Orbit Harmonic	144.4: 6 × Mars 137.4: Jupiter 147.7 Schwabe cycle	−0.27 % +4.6 % −2.2 %
89	18.31	19.86	Synodic	82.1: Jupiter–Saturn	+4.1 %
55	29.63	29.46 30 29.77	Orbit Harmonic Synodic	55.3: Saturn 54.32: 1/2 × AMO 54.74: 9 × Mars–Juno	−0.43 % +1.3 % +0.48 %
34	47.93	47.5 45.36	Synodic precession cycle Synodic	34.28 Mercury–Venus 35.93: Saturn–Uranus	−0.9 % −5.4 %
21	77.6	84.01	Orbit	19.4: Uranus	+7.6 %
13	125.4	122.04	Harmonic	13.36: 2 × J+J-S PSD-SSN	−2.77 %
8	203.7	247.67 208	Orbit Harmonic	7.6: Pluto 7.83: De Vries cycle	+5.26 % +2.1 %
5	325.9	329.58 342.78	Orbit Synodic	4.9: 2 × Neptune 4.75: 2 × Uranus–Neptune	+2.0 % +5.0 %
3	543.2	557 492.44	Orbit Synodic	2.9: Eris 3.31: Neptune–Pluto	+2.5 % −10.7 %
2	814.9	796	Synodic precession cycle	2.04: 1/3 Jupiter–Saturn	−2.4 %
1	1629.7	1601 1598.6 1617.7	Harmonic Synodic precession cycle Synodic precession cycle	0.98 2/3 Halstatt cycle 0.98: 4/3 Venus–Earth 0.99: 4/9 Uranus–Neptune	−1.7 % −1.9 % −0.8 %
				Average deviation of relationships from the Fibonacci series Sum of all deviations	2.51 % −2.23 %

rotation periods finds that the set of real rotation periods has 50 % lower numbers in their ratios (Appendix Table A2).

Solar rotation and the terrestrial planets: Sun and Mercury

Notwithstanding the Sun's axial tilt with respect to the invariant plane, the planets approximately orbit the Sun's equator. Due to its proximity to the Sun, Mercury has a higher orbital inclination from the plane of invariance than other planets, being more affected by the quadrupole moment from the Sun's slight equatorial bulge. The sidereal solar equatorial rotation rate is such that a fixed point on the solar equator lies directly between Mercury and the solar core every 33.899 days. From the frame of reference of solar rotation, Mercury makes exactly one axial rotation every two sidereal orbits, while Mercury completes exactly three axial rotations in the sidereal frame of reference during those two orbits. The Fibonacci numbers involved in this relationship are 1, 2, and 3.

4.2 Mercury and Venus

This planet pair forms a synodic conjunction every 144.565 Earth days, advancing 142° in the sidereal frame of reference. Every fifth conjunction is formed within 8° of the first, during a period of 1.97 yr. The precession of this sequence translates the longitude of one conjunction to the adjacent synodic conjunction point 142° away over a period of 18.72 yr. Within 9 days of this period Venus completes 28 sidereal axial rotations, while Mercury completes 116 (see Table 2) Adding unity to 28 creates a 4 : 1 ratio. The precession of the five-conjunction cycle takes on average 47.53 yr. After five of these 47.53 yr periods, plus one more five-synod cycle of 1.97 yr, the five-synod-conjunction cycle of Venus and Earth precesses 1/5 in 239.8 yr. The Fibonacci numbers involved in this relationship are 5 and 144.

Every 28 synodic conjunctions, Venus completes 18 orbits and Mercury completes 46 orbits. In this same period Mercury completes exactly 69 axial rotations. Therefore Mercury presents the same face to Venus every 28 synodic conjunctions. This is also the length of the Jupiter–Earth–Venus cycle. It is also the same period of time as the average solar cycle length (11.08 yr).

4.3 Venus and Earth

The planet Venus has a slow, retrograde axial rotation period of 243.013 days. Due to the relative rates at which Venus and Earth orbit the Sun, this means Venus will present the same face to Earth each time they meet in synodic conjunction, every 1.598 yr. This also means Venus' sidereal axial rotation is in a 3 : 2 relationship with Earth's orbital period. As seen from Earth, Venus completes two rotations in the same period.

Every 13 orbits of Venus, Earth orbits 8 times and they form 5 synodic conjunctions, the final one occurring near the sidereal longitude of the first. This conjunction cycle precesses by 1/5 in 239.8 yr after exactly 150 conjunctions. The full precession cycle is 1199 yr, and this period is close to a 3 : 2 ratio with the synodic conjunction longitude translation period of the Jupiter–Saturn synodic cycle precession of 796 yr. A closer ratio is 360 : 239. The former number of the ratio, 360, is 3 times the number of Jupiter–Saturn synodic periods in the full precession of the "triple conjunction cycle". The latter number, 239, is also the number of completed Earth orbits in 1/5 of the Earth–Venus synodic precession period of 1199 yr.

A further observation linking the rates of axial rotation and orbital motion of these three terrestrial planets and the Sun is the fact that Mercury rotates 4.14 times in the same time that Venus rotates once, and Mercury completes 4.15 orbits of the Sun while Earth orbits once.

To further underline the non-random nature of the orbital arrangement of these planets and their axial rotation periods, it is observed that the ratio of Venus and Earth's rotation rates divided by their orbital periods is 1.08 : 0.0027. This is equivalent to the ratio 400 : 1. During their respective synodic periods with Jupiter, Venus completes 1.03 rotations and Earth completes 398.88. Venus would not be able to fulfil a near 1 : 1 rotation per synod relationship with both Earth and Jupiter if it were rotating prograde. The force of gravity exerted on Venus by Jupiter and the Earth is of a similar magnitude. This suggests that a transfer of angular momentum is taking place and an orbit–spin coupling is operating to synchronise Venus' orbital and spin relations with these two planets.

The Fibonacci numbers involved in these relationships are 2, 3, 5, 8, and 13

4.4 The gas giant planets

Rotation

As we saw in Table 2, the rotation rate ratios of both the outer and inner pairs of the Jovian group is 46 : 43. The other adjacent pair in the group is Uranus–Saturn, in a 2 : 3 ratio. The ratio between the outer and inner pair's summed rotation periods is 1.618 or phi.

That calculation uses a figure of 642 min for Saturn's rotation. However, the radio signals on which the rotation rate is based are variable. Starting with the combined figures, and assigning a notional average of 642 to Saturn, Ur + Ne = 2001 min. Ju + Sa = 1237.5 min. Dividing to obtain the ratio, 2001/1237.5 = 1.617. Since phi is just over 1.618 it is an extremely close match.

Ur / Ju = 1.623. Ne / Sa = 1.611 (using 642 min for Saturn rotation) = 1.624 (using 637 min) = 1.599 (using 647 min)

Table 5. Comparing the Fibonacci series to rotation ratios. Saturn's rotation rate is variable according to the radio signal metric used as the metric. Figures in bold indicate members of the Fibonacci series.

Primary pairs	Rotation period	Rotations	Elapsed time	Ratio/sum	% match	Notes
1 Mercury 2 Venus	58.65 days 243.02 days	116 28	6803.4 d 6804.56 d	116 : 28 = **144**	99.983	
1 Earth 2 Mars	24 hours 24.6229 hours	118 115	2832 h 2831.6335 h	118 : 115 = **233**	99.987	
1 Jupiter 2 Saturn	595.5 min 640 min (N1)	46 43	27 393 min 27 520 min	46 : 43 = **89**	Up to 100 (variable)	(N1) Re. Saturn: 637.0465 = 100 % match (N1) Sat. rotation varies: est. 636–648 min
1 Uranus 2 Neptune	16.11 hours 17.24 hours	46 43	741.06 h 741.32 h	46 : 43 = **89**	99.965	
1 Pluto 2 Eris	153.29 hours 25.9 hours (N2)	8 47	1226.32 h 1217.3 h	8 : 47 = **55**	99.26	(N2) Eris rotation may not be 100 % correct

Table 6. Comparing the Fibonacci series and synodic periods to solar proxy data from McCracken et al. (2013a). Values in bold indicate periods within the error range of the peaks found in the C^{14} and ^{10}Be spectral analysis.

Period (years)	Saturn–Uranus synodic periods	Fibonacci number	Series in proxy data	Series in proxy data	Series in proxy data
45	45.36 = 1 × 45.36 = 1× S–U	1			
90	90.72 = 2 × 45.36 = 2× S–U	2	**88** × 3/2 = **132**		
130	136.1 = 3 × 45.36 = 3× S–U	3	**130** × 8/5 = **208**		
232	226.8 = 5 × 45.36 = 5× S–U	5	**208** × 5/3 = **347**		
351	362.9 = 8 × 45.36 = 8× S–U	8	**351** × 8/5 = **562**	**282** × 8/5 = **451**	
593∗	589.7 = 13 × 45.36 = 13× S–U	13		**450** × 8/5 = **720**	
974	952.6 = 21 × 45.36 = 21× S–U	21		**705** × 8/5 = **1128**	**610** × 8/5 = **976**
1550∗	1542 = 34 × 45.36 = 34× S–U	34		**1128** × 8/5 = **1805**	**976** × 8/5 = **1562**
2403	2494 = 55 × 45.36 = 55× S–U	55			**1562** × 3/2 = **2342**

These figures range from 8/5 (1.6) to 13/8 (1.625) but on the known data all are compatible with a phi–Fibonacci relationship.

5 Orbital and synodic periods

Jupiter and Saturn's successive 19.86 yr conjunctions form a slowly precessing triangle which rotates fully in the course of 2383 yr. One additional synodic conjunction brings the elapsed time to 2403 yr. This is the longer Halstatt cycle period found in proxy records of ^{14}C and ^{10}Be. It is almost coincident with double the 1199 yr Earth–Venus synodic cycle precession period mentioned in Sect. 4.4. Fourteen Uranus–Neptune synodic conjunctions total 2399 yr. This is 2/3 of the full Uranus–Neptune precession cycle.

The close integration of the orbital, synodic, and rotation periods of the inner planets suggests that their orbital and axial rotation periods are dynamically coupled.

The pattern we observe at the larger timescale (45–2400 yr) is that the precession of the five-synodic-conjunction cycles of the terrestrial pairs is also coupled. Mercury–Venus relates by multiples of 5 to Venus–Earth, which relates to 1/3 of the precession of the triangular synodic conjunction cycle of Jupiter–Saturn in a 3 : 2 ratio. In turn, the full Jupiter–Saturn synodic precession cycle is in a 3 : 2 ratio with the Uranus–Neptune synodic precession cycle of just over 21 conjunctions totalling 3599 yr. This period is also in a 3 : 2 relationship with the longer Halstatt cycle of around 2400 yr, which is a broad, prominent peak in the ^{10}Be and ^{14}C solar proxy records. Adding the longer and shorter Halstatt periods to a total of 4627 yr, there is a convergence of 27 Uranus–Neptune and 233 Jupiter Saturn conjunctions. There are 34 × 3 Saturn–Uranus synodic conjunctions in the same period, and 4237 Jupiter–Earth synodic conjunctions, 1 % away from the Fibonacci number 4181.

The Fibonacci numbers involved in these relationships are 1, 2, 3, 5, 21, 34, 233, and 4181

Table 7. Inner solar system cyclic convergence.

Period (years)	Synodic periods	Number series	Notes
44.704	20 × Mars–Jupiter	20	= 41 – 21
44.841	21 × Mars–Earth	21	= 41 – 20
44.763	28 × Venus–Earth	28	= 69 – 21
44.774	41 × Earth–Jupiter	41	= 69 – 28 = 21 + 20
44.770	69 × Venus–Jupiter	69	= 28 + 20 + 21 = 28 + 41
44.7254	113 × Venus–Mercury	113	= 4 × 28 + 1

6 Solar-terrestrial variation and replication with planetary periods

6.1 Longer term variation

McCracken et al. (2013) identified 15 periodicities in the ^{10}Be and ^{14}C records which relate predominantly to cosmic ray modulation by solar variation. These periodicities include ~ 90, 208, 351, 517, 705, 978, and 1125 yr. McCracken et al. (2013b) will discuss possible planetary relations with these periods. Without pre-empting their work, there are some observations highly relevant to the present study which are independent from their methodology.

A number of periods evident in the data presented in McCracken et al. (2013a) are not listed but are relevant to the present study as shown in Table 6. These include periodicities at 153, 282, 450, 562, 593, 612, and 856 yr. It is observed that the multiples are within the range of the peaks and at the centre of troughs (marked "*") in the data, and follow the Fibonacci series. At 856 yr there is a triple synodic conjunction of Jupiter, Uranus, and Neptune. Table 6 shows periodicities found in McCracken et al. (2013a) against multiples of the synodic period of Saturn and Uranus. Additionally, other series of Fibonacci-ratio-linked periods found in the proxy data are shown. These require further investigation.

6.2 Medium-term solar–terrestrial variation

Prominent cycles are evident in terrestrial and solar data at the periods of the Schwabe cycle (11.07 yr), the Hale cycle (~ 22.3 yr), the Gleissberg cycle (~ 90 yr), and in terrestrial beach ridge data (~ 45, ~ 90, ~ 179 yr) (Fairbridge and Hillaire-Marcel, 1977). We have seen the Saturn–Uranus synodic period is close to the 45 yr period and its multiples. Many inner solar system synodic periods converge in the 44–45 yr range, as shown in Table 7.

This period is in 2 : 3 Hale cycle ratio with the period of the Atlantic Multi-decadal Oscillation. It is bounded on either side by the period of five Jupiter–Neptune synods (63.9 yr), and five Jupiter–Uranus synods (69.05 yr). The 44.7 yr period is also in a 1 : 2 ratio with the ~ 90 yr Gleissberg cycle and a 1 : 4 ratio with the ~ 179 yr Jose cycle (José, 1965).

Table 8. Planetary periodicities near the period of the major ocean oscillations.

Period (years)	Orbital and synodic periods	Fibonacci number
61.75	1 × 61.75 = U–N : U–S harmonic beat period	1
58.9	2 × 29.45 = 2× Saturn	2
59.58	3 × 19.86 = 3× Jupiter–Saturn	3
63.9	5 × 12.78 = 5× Jupiter–Neptune	5
66.42	5 × 11.07 = 5× Jupiter–Earth–Venus cycle	5
63.92	8 × 7.99 = 8× Venus–Earth synodic period cycle	8

Table 8 lists periods close to the ~ 60 yr period identified as an important terrestrial climate oscillation (Mörner, 2013; Scafetta, 2012b; Akasofu, 2013; Solheim, 2013). This oscillation is observed in phenomena such as the ~ 66 yr Alantic Multi-decadal Oscillation (AMO) and the ~ 60 yr Pacific Decadal Oscillation (PDO). It is in approximate 2 : 3 ratio with the 44.7 yr period and 3 : 2 ratio with the Gleissberg cycle ~ 90 yr. These interwoven relationships are suggestive of resonant effects amplifying the terrestrial responses to solar system stimuli.

At around the period of the Gleissberg cycle, the relationships in Table 9 are observed.

The resulting number series in Table 6 matches a series used in the generation of the powers of phi.

$$
\begin{aligned}
\mathrm{Phi}^1 &= 0 + 1\,\mathrm{Phi} = (\sqrt{5} + 1)/2\\
\mathrm{Phi}^2 &= 1 + 1\,\mathrm{Phi} = (\sqrt{5} + 3)/2\\
\mathrm{Phi}^3 &= 1 + 2\,\mathrm{Phi} = (2\sqrt{5} + 4)/2\\
\mathrm{Phi}^4 &= 2 + 3\,\mathrm{Phi} = (3\sqrt{5} + 7)/2\\
\mathrm{Phi}^5 &= 3 + 5\,\mathrm{Phi} = (5\sqrt{5} + 11)/2\\
\mathrm{Phi}^6 &= 5 + 8\,\mathrm{Phi} = (8\sqrt{5} + 18)/2\\
\mathrm{Phi}^7 &= 8 + 13\,\mathrm{Phi} = (13\sqrt{5} + 29)/2\\
\mathrm{Phi}^8 &= 13 + 21\,\mathrm{Phi} = (21\sqrt{5} + 47)/2
\end{aligned}
$$

6.3 The Schwabe and Hale cycles

The Schwabe solar cycle averaging around 11.07 yr and the solar magnetic Hale cycle of around 22.3 yr have been extensively studied and the planetary relations investigated by several researchers, including Wilson et al. (2008) and Scafetta (2012b). The Jupiter–Earth–Venus conjunction cycle contains several periodicities including the Schwabe and Hale cycles, and the 44.7 yr inner solar system cycle. Using a modification of a model based on the planetary index devised by Hung (2007) (R. Martin, personal communication, 2010), the present author found that alignment along the Parker spiral adjusted for solar wind velocity in accordance with the reconstruction by Svalgaard and Cliver (2007) was able to replicate the general shape and varying period of the Schwabe solar cycle well, although their varying amplitudes were not well reproduced. The result is shown in Fig. 2.

Table 9. Gleissberg cycle length planetary periods.

Period (years)	Orbital and synodic periods	Number series
84.01	$1 \times 84.01 = 1\times$ Uranus orbital period	1
90.72	$2 \times 45.36 = 2\times$ Saturn–Uranus synodic period	2
88.38	$3 \times 29.46 = 3\times$ Saturn orbital period	3
88.56	$4 \times 22.14 = 4\times$ Jupiter–Earth–Venus cycle	4
89.47	$7 \times 12.78 = 7\times$ Jupiter–Neptune synodic period	7
87.89	$11 \times 7.99 = 11\times$ Venus–Earth synodic cycle	11
94.84	$29 \times 3.27 = 29\times$ Earth–Mars synodic period	29
92.59	$47 \times 1.97 = 47\times$ Venus–Mercury synodic period cycle	47

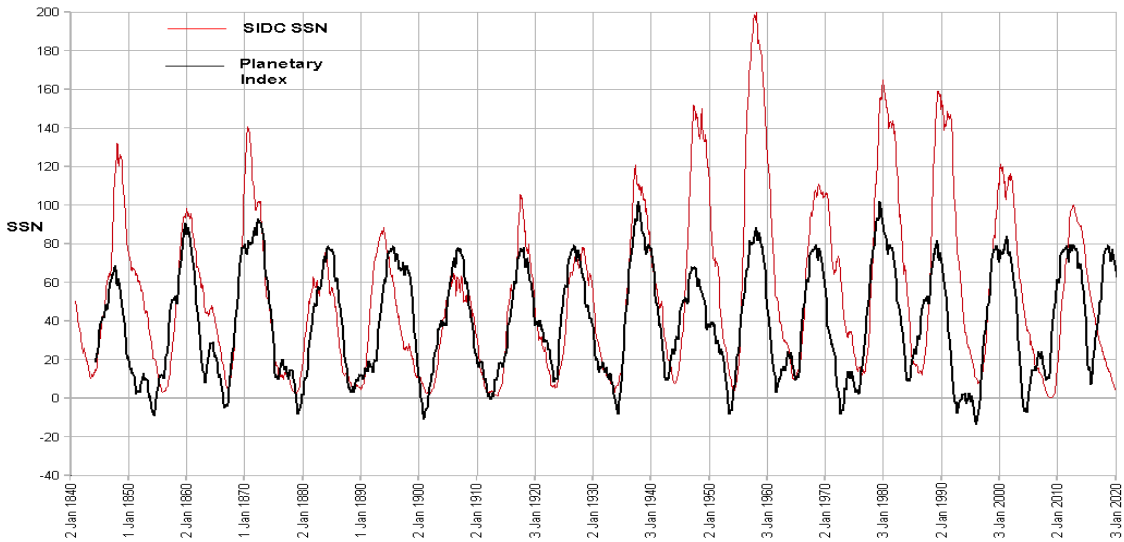

Figure 2. Reconstruction of sunspot number variation using the planetary alignment index devised by Hung (2007), modified to test alignment along the curve of the Parker spiral. Coupling this model with the solar–planetary model created by Salvador (2013) could improve the representation of amplitude and potentially lead to useful forecasting of solar variation.

7 Discussion

This paper provides observations which show that log-normally distributed numerical series which converge to phi, such as the Fibonacci and Lucas series, match the temporal–spatial distribution of matter in the solar system. Further, observations suggest that the patterns which evolve as a result of this non-random distribution of matter in the time evolution of the planetary orbits reflect changes in solar activity and the climate cycles observed on Earth. Currently, widely accepted theory concerning the evolution of the solar system considers the forces of magnetism and gravity capable of highly organising the planets' orbits and rotation rates, but the theory that the planets are capable of causing solar variation is contested (Callebaut et al., 2012, 2013; Scafetta et al., 2013).

Three theoretical mechanisms have been put forward to support the idea that the tidal and angular momentum effects of the planets could be amplified in the solar interior (Scafetta, 2012a; Wolf and Patrone, 2010; Abreu et al., 2012). The present paper adopts a different approach to tidal and angular momentum based theories by asking the following question: why phi?

As well as the convergence of the Fibonacci series to phi, the series can be generated from phi by a process of quantisation. This quantised series is log-normally distributed. The planets' orbital elements, inter-relations, and physical attributes also exhibit log-normally distributed, quantised relationships, some involving powers of phi. The following are two examples of these:

1. The inner and outer gas giant pairs' summed rotation rates are in a phi relationship, and their summed diameters are in a phi^2 relationship, to within margin of error for observation.

2. The orbital distance ratios of the Galilean moons from Jupiter can be approximated with powers of phi and more accurately calculated with Fibonacci ratios.

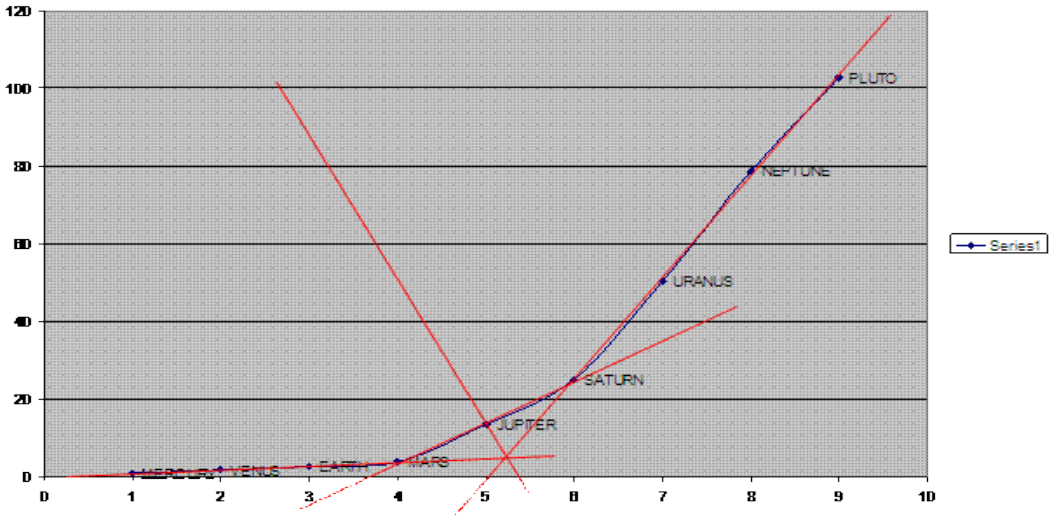

Figure 3. Planet positions against semi-major axis scaled from Earth (1) using phi^2.

The Fibonacci series has the property of containing powers of phi within itself. Adjacent numbers in the series are in approximate phi relation with their ratios converging towards phi as the series moves to higher numbers. Fibonacci numbers two positions apart in the series are in a phi^2 relationship, and those Fibonacci numbers three positions apart in a phi^3 relationship, etc.

A possible reason for the Fibonacci series evident in solar system mass and motion ratios is given by Barrow (1982):

> If we perturb a system that has a rational frequency ratio, then it can easily be shifted into a chaotic situation with irrational frequencies. The golden ratio is the most stable because it is farthest away from one of these irrational ratios. In fact, the stability of our solar system over long periods of time is contingent upon certain frequency ratios lying very close to noble numbers.

The relationship between log-normally distributed numerical series and power series has been investigated by Mitzenmacher (2004), who found that "double Pareto distributions" exhibit log-normal and power-law tails in the two halves of the distributions of randomly generated word lengths. Moreover, these power-law and log-normal distributions can interchangeably arise from randomly generated indices:

> The double Pareto distribution falls nicely between the log-normal distribution and the Pareto distribution. Like the Pareto distribution, it is a power law distribution. But while the log-log plot of the density of the Pareto distribution is a single straight line, for the double Pareto distribution the log-log plot of the density consists of two straight line segments that meet at a transition point.

Analogously, the inner and outer solar system exhibit log-normal and power-law-like tails. The difference between the Jovian outer planets and the inner solar system is illustrated in Fig. 3.

It should be noted that Jupiter's, Saturn's, and Mars' synodic periods are in 9 : 80 : 89 ratio, i.e. 9(= 3 × 3) Jupiter–Saturn = 80(= 2 × 5 × 8) Jupiter–Mars = 89(Fibonacci) Saturn–Mars.

It is clear that Jupiter is the transition point in the solar system: from rocky, terrestrial planets to gas giants, and from semi-major axes which scale with phi to scaling with approximate doubling. Nonetheless, all the planet pairs relate numerically with their synodic precession cycle periods in simple ratios involving Fibonacci numbers. The break point at Jupiter indicates that the outcome of force interactions and mass scales brings about a different regime in the inner and outer parts of the solar system. At the distance of the Jovian planets the Sun's gravity is weak compared to the situation in the inner solar system, and the more massive planets have a relatively much bigger effect on each other gravitationally.

What we see in the heliosphere is that which is left after 4.5 Byr evolution of the solar system. A recent model of the way in which log-normally distributed condensing gases form a star by condensation proposes that the rate of condensation is accelerated by the power law of gravity as condensation proceeds (Cho and Kim, 2011). The process causes the axial rotation to increase in rate, spinning off matter in a proto-planetary disc. Rebull (2013) proposes that the solar system's proto-planetary disc was magnetically coupled to the spinning Sun and may have acted as a brake on its rotational angular momentum. This would cause a coupling of the periodicities of solar rotation and the concentric rings of the proto-planetary disc at various distances.

Cho and Kim (2011) find that

> core (star) formation rates or core (stellar) mass functions predicted from theories based on the log-normal density PDF need some modifications. Our result of the increased volume fraction of density PDFs after turning self-gravity on is consistent with power law like tails commonly observed at higher ends of visual extinction PDFs of active star-forming clouds.

8 Conclusions

The observations made in the present study demonstrate the outcome of interactions between the power-law-based forces of gravity and magnetism and the interactions both between the Sun and planets, as well as between the planets themselves. These interactions tend to quantise their orbital and internal dynamics in ways which cause the system to evolve a log-normally distributed spatio-temporal distribution of inter-orbital relations, axial rotation rates, and orbits. The most stable interactions are in the ratios 1 : 1, 2 : 3, 3 : 5, 5 : 8, etc. This is why the Fibonacci series is the most clearly observed log-normally distributed series in the solar system. Apart from the ubiquitous 1 : 1 relationship of spin : orbit displayed by nearly every moon in the solar system tidally locked to its planet, the next most frequently observed ratio is 2 : 3. Out of the numerous examples, those most relevant to periods at which we see cycles in solar proxy records and solar observations are Mercury's 3 : 2 spin : orbit of the Sun, Venus' 3 : 2 spin against Earth's orbital period, and the 2 : 3 of Earth–Venus' synodic cycle precession period against the Jupiter–Saturn synodic cycle precession period converging at the longer Halstatt cycle length of ~ 2400 yr.

We also see 2 : 3 behaviour on the Sun itself. The rate of rotation at the equator (24.47 days) is close to a 2 : 3 ratio with the rate of rotation near the poles (~ 36 days). The rise time from Schwabe cycle minimum to maximum is, on average, in approximate 2 : 3 ratio to the period from maximum to minimum.

It is evident that the same mass distributions and forces which originally formed the Sun, a log-normally distributed gas cloud condensing under self-gravity, continue to influence its cyclic variation. The same is the case for the continual "cogging" and re-alignment of the planets as the interplay of forces with their neighbours and the Sun causes continual adjustment of their orbital periods and rates of rotation, maintaining an orderly log-normal spatio-temporal distribution.

Systems which maintain stability through cybernetic feedback oscillate about a mean. Such oscillation is observed throughout the solar system: variation in Earth's length of day, the 0.1 % variation of total solar irradiance measured during the Schwabe cycle, the long-term oscillations observed in solar proxies, and exchanges of angular momentum between Uranus and Neptune. The inexact periodic relationships undergo phase drift, and leave "standing waves" of modulated magnitude near the convergent frequencies identified in this study. To understand how the motion of the planets could be linked to terrestrial climatic variation, both via solar variation and directly, we must additionally consider the thermodynamic, gravitational, and magnetic forces to which both the planets and the Sun are currently subjected and were originally formed by.

The Sun's decadal variation in total solar irradiance is around 0.1 % of its output. If the strong correlations observed between planetary motion and solar variation are indicative of cybernetic feedback, then such a minor variation at around the orbital period of the largest planet in the system may indicate a well-attuned system very close to boundary conditions. Small resonantly amplified forces regularly applied to such systems could account for the observed variation. Until further research can establish the magnitude of forces required to sustain cybernetic feedback, a causal explanation for the correlations observed can be no more than tentative. The author wishes to stimulate the interest of those with better access to data and better analytic capability so progress can be made on this subject. The goal is accurate shorter and longer term prediction of changing solar activity. This ability will become more policy relevant as natural cyclic variations are increasingly recognised as important climate variables.

Table A1. Rotation ratios of secondary and non-adjacent planet pairs. Figures in bold indicate members of the Fibonacci series.

Other pairs	Rotation period	Rotations	Elapsed time	Ratio/sum	% match	For general interest only
1 Venus	243.02 days	1	243.02 d	243 + 1 =	99.99	(N3) 244 × (5/2) = 610
2 Earth	1 day (N3)	243	1 d	244 (N4)		(N4) Ve compared to 365.25 = 3 : 2 (99.8 %)
1 Mars	24.6229 hours	67	1649.7343 h	67 + 166 =	99.87	
2 Jupiter	9.925 hours	166	1647.55 h	**233**		
1 Saturn	640 min (N5)	3	1920 min	3 + 2 =	Up to 100	(N5) Re. Saturn: 644.4 min = 100 % match
2 Uranus	966.6 min	2	1933.2 min	**5**	(N1)	
1 Neptune	17.24 hours	80	1379.2 h	80 + 9 =	99.97	
2 Pluto	153.29 hours	9	1379.61 h	**89**		
Non-neighbours	Rotation period	Rotations	Elapsed time	Ratio/sum	% match	For general interest only
1 Jupiter	9.925 hours	13	129.025 h	13 + 8 =	99.888	
2 Uranus	16.11 hours	8	128.88 h	**21** (N6)		(N6) 13/8 = 1.625
1 Saturn	10.666 hours (N7)	21	223.986 h	21 + 13 =	Up to 100	(N7) 10.666 h = 640 min
2 Neptune	17.24 hours	13	224.12 h	**34** (N8)	(N1)	(N8) 21/13 = 1.6153846
1 Jupiter	9.925 hours	148	1468.9 h	148 + 85 =	99.76	
2 Neptune	17.24 hours	85	1465.4 h	**233**		
1 Uranus	16.11 hours	19	306.09 h	19 + 2 =	99.84	
2 Pluto	153.29 hours	2	306.58 h	**21**		
1 Neptune	17.24 hours	3	51.72 h	3 + 2 =	99.85	
2 Eris	25.9 hours (N2)	2	51.8 h	**5**		
1 Uranus	16.11 hours	8	128.88 h	8 + 5 =	99.52	
2 Eris	25.9 hours (N2)	5	129.5 h	**13**		
1 Jupiter	9.925 hours	63	625.275 h	63 + 26 =	99.8	63 = 21 × 3
2 Earth	24 hours	26	624 h	**89**		26 = 2 × 13
1 Mars	24.6229 hours	14	344.7206 h	14 + 20 =	99.977	
2 Neptune	17.24 hours	20	344.8 h	**34**		
1 Mars	24.6229 hours	57	1403.5053 h	57 + 87 =	99.86	
2 Uranus	16.11 hours	87	1401.57 h	**144**		
1 Mars	24.6229 hours	27	664.8183 h	27 +62 =	Up to 100	
2 Saturn	10.666 hours (N7)	62	661.33 h	**89**	(N1)	
1 Earth	24 hours	4	96 h	4 + 9 =	Up to 100	
2 Saturn	10.666 hours (N7)	9	96 h	**13**	(N1)	
1 Earth	24 hours	58	1392 h	58 + 86 =	99.53	
2 Uranus	16.11 hours	86	1385.46 h	**144**		

Table A2. In comparing real against randomly generated rotation ratios it is found that the real ratios obtain Fibonacci numbers around 50 % lower in value. This indicates that the real values are related in a non-random way. This makes the current theory that planetary rotation rates reflect the circumstances of the last collision the planetary bodies were involved in unlikely.

Real ratios		
Me Ve	99.797 %	116 + 28 = 144
Me Ve	99.851 %	795 + 192 = 987
Me Ve	99.986 %	1286 + 311 = 1597
Me Ve	99.992 %	8814 + 2132 = 10946
Me Ea	99.338 %	1570 + 27 = 1597
Me Ea	99.670 %	4111 + 70 = 4181
Me Ma	99.860 %	972 + 15 = 987
Me Ju	99.014 %	978 + 9 = 987
Me Ju	99.342 %	4143 + 38 = 4181
Me Ju	99.861 %	6704 + 61 = 6765
Me Sa	99.422 %	143 + 1 = 144
Me Sa	99.756 %	1586 + 11 = 1597
Me Ur	99.474 %	2554 + 30 = 2584
Me Ur	99.573 %	4132 + 49 = 4181
Me Ur	99.935 %	6686 + 79 = 6765
Me Ne	99.146 %	602 + 8 = 610
Me Ne	99.304 %	4127 + 54 = 4181
Me Ne	99.970 %	6677 + 88 = 6765
Ve Ea	99.214 %	2574 + 10 = 2584
Ve Ea	99.663 %	4165 + 16 = 4181
Ve Ea	99.905 %	6739 + 26 = 6765
Ve Ma	99.996 %	983 + 4 = 987
Ve Ju	99.996 %	6753 + 12 = 6765
Ve Ur	99.480 %	608 + 2 = 610
Ve Ne	99.558 %	6743 + 22 = 6765
Ea Ma	99.933 %	46 + 43 = 89
Ea Ma	99.988 %	510 + 477 = 987
Ea Ma	99.999 %	9151 + 8560 = 17 711
Ea Ju	99.421 %	70 + 19 = 89
Ea Ju	99.815 %	297 + 80 = 377
Ea Ju	99.848 %	777 + 210 = 987
Ea Ju	99.858 %	1258 + 339 = 1597
Ea Ju	99.971 %	2035 + 549 = 2584
Ea Ju	99.992 %	8620 + 2326 = 10 946
Ea Sa	99.902 %	64 + 25 = 89
Ea Sa	99.974 %	710 + 277 = 987
Ea Sa	99.995 %	4866 + 1899 = 6765
Ea Ur	99.219 %	88 + 56 = 144
Ea Ur	99.924 %	142 + 91 = 233
Ea Ur	99.997 %	973 + 624 = 1597
Ea Ur	99.999 %	6669 + 4277 = 10 946
Ea Ne	99.539 %	32 + 23 = 55
Ea Ne	99.838 %	84 + 60 = 144
Ea Ne	99.989 %	931 + 666 = 1597
Ea Ne	99.995 %	6381 + 4565 = 10 946
Ma Ju	99.809 %	101 + 43 = 144
Ma Ju	99.941 %	692 + 295 = 987
Ma Ju	99.982 %	2931 + 1250 = 4181
Ma Ju	99.986 %	4742 + 2023 = 6765
Ma Ju	99.998 %	7673 + 3273 = 10 946
Ma Sa	99.612 %	95 + 49 = 144

Table A2. Continued.

Real ratios		
Ma Sa	99.844 %	154 + 79 = 233
Ma Sa	99.948 %	249 + 128 = 377
Ma Sa	99.972 %	403 + 207 = 610
Ma Sa	99.997 %	652 + 335 = 987
Ma Ur	99.396 %	19 + 15 = 34
Ma Ur	99.743 %	211 + 166 = 377
Ma Ur	99.862 %	342 + 268 = 610
Ma Ur	99.987 %	553 + 434 = 987
Ma Ur	99.992 %	6133 + 4813 = 10 946
Ma Ur	99.994 %	9924 + 7787 = 17 711
Ma Ne	99.137 %	22 + 12 = 34
Ma Ne	99.676 %	93 + 51 = 144
Ma Ne	99.768 %	243 + 134 = 377
Ma Ne	99.871 %	637 + 350 = 987
Ma Ne	99.941 %	1030 + 567 = 1597
Ma Ne	99.987 %	1667 + 917 = 2584
Ma Ne	99.996 %	4364 + 2401 = 6765
Ju Sa	99.925 %	101 + 132 = 233
Ju Sa	99.992 %	692 + 905 = 1597
Ju Sa	99.994 %	4743 + 6203 = 10 946
Ju Sa	99.999 %	7674 + 10037 = 1771
Ju Ur	99.840 %	39 + 16 = 55
Ju Ur	99.967 %	1132 + 465 = 1597
Ju Ur	99.983 %	4795 + 1970 = 6765
Ju Ur	99.996 %	7758 + 3188 = 10 946
Ju Ne	99.969 %	75 + 69 = 144
Ju Ne	99.994 %	514 + 473 = 987
Ju Ne	99.995 %	3523 + 3242 = 6765
Ju Ne	99.998 %	9223 + 8488 = 17 711
Sa Ur	99.120 %	103 + 41 = 144
Sa Ur	99.835 %	167 + 66 = 233
Sa Ur	99.876 %	708 + 279 = 987
Sa Ur	99.949 %	1145 + 452 = 1597
Sa Ur	99.984 %	1853 + 731 = 2584
Sa Ur	99.990 %	2998 + 1183 = 4181
Sa Ur	100.000 %	4851 + 1914 = 6765
Sa Ne	99.040 %	2 + 1 = 3
Sa Ne	99.277 %	59 + 30 = 89
Sa Ne	99.688 %	155 + 78 = 233
Sa Ne	99.955 %	656 + 331 = 987
Sa Ne	99.970 %	1717 + 867 = 2584
Sa Ne	99.997 %	7274 + 3672 = 10 946
Ur Ne	99.095 %	27 + 28 = 55
Ur Ne	99.519 %	44 + 45 = 89
Ur Ne	99.949 %	71 + 73 = 144
Ur Ne	99.999 %	2062 + 2119 = 4181
Randomly generated rotation ratios		
Me Ve	99.962 %	116 + 28 = 144
Me Ve	99.984 %	795 + 192 = 987
Me Ve	99.998 %	8817 + 2129 = 10 946
Me Ea	99.409 %	1567 + 30 = 1597
Me Ea	99.630 %	2535 + 49 = 2584
Me Ea	99.995 %	4102 + 79 = 4181
Me Ma	99.718 %	1569 + 28 = 1597
Me Ma	99.858 %	4108 + 73 = 4181
Me Ju	99.133 %	1588 + 9 = 1597

Table A2. Continued.

Randomly generated rotation ratios		
Me Sa	99.844 %	2559 + 25 = 2584
Me Ur	99.728 %	1577 + 20 = 1597
Me Ur	99.939 %	6680 + 85 = 6765
Me Ne	99.828 %	230 + 3 = 233
Me Ne	99.858 %	4127 + 54 = 4181
Ve Ea	99.800 %	1590 + 7 = 1597
Ve Ma	99.361 %	6732 + 33 = 6765
Ve Ju	99.296 %	6753 + 12 = 6765
Ve Sa	99.457 %	2579 + 5 = 2584
Ve Ur	99.074 %	6745 + 20 = 6765
Ve Ne	99.184 %	1592 + 5 = 1597
Ea Ma	99.593 %	46 + 43 = 89
Ea Ma	99.748 %	195 + 182 = 377
Ea Ma	99.936 %	316 + 294 = 610
Ea Ma	99.943 %	511 + 476 = 987
Ea Ma	99.989 %	827 + 770 = 1597
Ea Ma	99.999 %	9172 + 8539 = 17 711
Ea Ju	99.601 %	101 + 43 = 144
Ea Ju	99.862 %	264 + 113 = 377
Ea Ju	99.936 %	1119 + 478 = 1597
Ea Ju	99.957 %	1810 + 774 = 2584
Ea Ju	99.998 %	2929 + 1252 = 4181
Ea Sa	99.989 %	65 + 24 = 89
Ea Sa	99.999 %	7994 + 2952 = 10 946
Ea Ur	99.732 %	32 + 23 = 55
Ea Ur	99.957 %	575 + 412 = 987
Ea Ur	99.984 %	1505 + 1079 = 2584
Ea Ur	99.989 %	6376 + 4570 = 10 946
Ea Ne	99.657 %	132 + 101 = 233
Ea Ne	99.889 %	214 + 163 = 377
Ea Ne	99.937 %	346 + 264 = 610
Ea Ne	99.996 %	560 + 427 = 987
Ma Ju	99.352 %	114 + 30 = 144
Ma Ju	99.459 %	184 + 49 = 233
Ma Ju	99.910 %	298 + 79 = 377
Ma Ju	99.979 %	2043 + 541 = 2584
Ma Ju	99.994 %	8654 + 2292 = 10 946
Ma Sa	99.623 %	64 + 25 = 89
Ma Sa	99.756 %	271 + 106 = 377
Ma Sa	99.848 %	438 + 172 = 610
Ma Sa	99.999 %	709 + 278 = 987
Ma Ur	99.114 %	93 + 51 = 144
Ma Ur	99.985 %	150 + 83 = 233
Ma Ur	99.993 %	7047 + 3899 = 10 946
Ma Ne	99.800 %	129 + 104 = 233
Ma Ne	99.985 %	546 + 441 = 987
Ma Ne	99.995 %	3742 + 3023 = 6765
Ma Ne	99.998 %	9797 + 7914 = 17 711
Ju Sa	99.860 %	58 + 31 = 89
Ju Sa	99.931 %	1041 + 556 = 1597
Ju Sa	99.962 %	1685 + 899 = 2584
Ju Sa	99.997 %	2726 + 1455 = 4181
Ju Ur	99.251 %	62 + 27 = 89
Ju Ur	99.354 %	163 + 70 = 233
Ju Ur	99.714 %	263 + 114 = 377
Ju Ur	99.932 %	426 + 184 = 610

Table A2. Continued.

Randomly generated rotation ratios		
Ju Ur	99.933 %	689 + 298 = 987
Ju Ur	99.985 %	1115 + 482 = 1597
Ju Ur	99.986 %	7643 + 3303 = 10 946
Ju Ne	99.240 %	31 + 24 = 55
Ju Ne	99.587 %	132 + 101 = 233
Ju Ne	99.787 %	213 + 164 = 377
Ju Ne	99.974 %	345 + 265 = 610
Ju Ne	99.997 %	6190 + 4756 = 10 946
Sa Ur	99.613 %	5 + 3 = 8
Sa Ur	99.680 %	235 + 142 = 377
Sa Ur	99.788 %	381 + 229 = 610
Sa Ur	99.992 %	616 + 371 = 987
Sa Ur	100.000 %	4222 + 2543 = 6765
Sa Ne	99.931 %	3 + 2 = 5
Sa Ne	99.985 %	592 + 395 = 987
Sa Ne	99.995 %	1550 + 1034 = 2584
Ur Ne	99.802 %	104 + 129 = 233
Ur Ne	99.986 %	441 + 546 = 987
Ur Ne	99.993 %	3023 + 3742 = 6765
Ur Ne	99.995 %	4891 + 6055 = 10 946
Ur Ne	100.000 %	7914 + 9797 = 17 711

Acknowledgements. The author wishes to thank the following people for their generous assistance in the production of this unfunded work: Stuart Graham, Ian Wilson, Roy Martin, Wayne Jackson, Graham Stevens, Roger Andrews, and many other people offering insight and comment at “Tallbloke’s Talkshop”.

Edited by: N.-A. Mörner
Reviewed by: H. Jelbring and one anonymous referee

References

Abreu, J. A., Beer, J., Ferriz-Mas, A., McCracken, K. G., and Steinhilber, F.: Is there a planetary influence on solar activity?, Astron. Astrophys., A88, 1–9, 2012.

Akasofu, Syun-Ichi: On the Present Halting of Global Warming, Climate, 1, 4–11, 2013.

Barrow, J. D.: Chaotic Behaviour in General Relativity, Phys. Rep., 85, 1, 1982.

Callebaut, D. K., de Jager, C., and Duhau, S.: The influence of planetary attractions on the solar tachocline, J. Atmos. Sol.-Terr. Phy., 80, 73–78, 2012.

Callebaut, D. K., de Jager, C., and Duhau, S.: Reply to “The influence of planetary attractions on the solar tachocline” by N. Scafetta, O. Humlum, J. E. Solheim, K. Stordahl, J. Atmos. Sol.-Terr. Phy., 102, p. 372, 2013.

Cho, W. and Kim, J.: Enhanced core formation rate in a turbulent cloud by self-gravity, Mon. Not. R. Astron. Soc. Letters, 410, L8–L12, doi:10.1111/j.1745-3933.2010.00968.x, 2011.

Fairbridge, R. W. and Hillaire-Marcel, C.: An 8,000-yr palaeoclimatic record of the “Double-Hale” 45-yr solar cycle, Nature, 268, 413–416, 1977.

Hung, Ching-Cheh: Apparent Relations Between Solar Activity and Solar Tides Caused by the Planets, NASA/TM-2007-14817, 2007.

Johnson, J. A., Payne, M., Howard, A. W., Clubb, K. I., Ford, E. B., Bowler, B. P., Henry, G. W., Fischer, D. A., Marcy, G. W., Brewer, J. M., Schwab, C., Reffert, S., and Lowe, T. B.: Retired A Stars and Their Companions. VI. A Pair of Interacting Exoplanet Pairs Around the Subgiants 24 Sextanis and HD 200964 Astron. J., 141, 10 pp., 2011.

José, P. D.: Sun's motion and sunspots, Astron. J., 70, p. 193, 1965.

Koyré, A.: The Astronomical Revolution, Hermann Paris, Cornell University, 1973.

Levison, H. F., Morbidelli, A., Van Laerhoven, C., Gomes, R., and Tsiganis, K.: Origin of the Structure of the Kuiper Belt during a Dynamical Instability in the Orbits of Uranus and Neptune, Icarus, 196, 258–271, 2008.

Lykawka, P. S. and Mukai, T.: Dynamical classification of trans-neptunian objects: Probing their origin, evolution, and interrelation, Icarus, 189, 213–232, 2007.

McCracken, K. G., Beer, J., Steinhilber, F., and Abreu, J.: A phenomenological study of the cosmic ray variations over the past 9400 years, and their implications regarding solar activity and the solar dynamo, Sol. Phys., 286, 609–627, 2013.

Mitzenmacher, M.: A Brief History of Generative Models for Power Law and Log-normal Distributions, Internet Mathematics, 1, 226–251, 2004.

Mörner, N. A.: Solar Wind, Earth's Rotation and Changes in Terrestrial Climate, Physical Review & Research International, 3, 117–136, 2013.

Rebull, L. M., Johnson, C. H., Gibbs, J. C., Linahan, M., Sartore, D., Laher, R., Legassie, M., Armstrong, J. D., Allen, L. E., McGehee, P., Padgett, D. L., Aryal, S., Badura, K. S., Canakapalli, T. S., Carlson, S., Clark, M., Ezyk, N., Fagan, J., Killingstad, S., Koop, S., McCanna, T., Nishida, M. M., Nuthmann, T. R., O'Bryan, A., Pullinger, A., Rameswaram, A., Ravelomanantsoa, T., Sprow, H., and Tilley, C. M.: New Young Star Candidates in BRC 27 and BRC 34, Astron. J., 145, 15, doi:10.1088/0004-6256/145/1/15, 2013.

Scafetta, N.: Does the Sun work as a nuclear fusion amplifier of planetary tidal forcing? A proposal for a physical mechanism based on the mass-luminosity relation, J. Atmos. Sol. Terr. Phy., 81–82, 27–40, 2012a.

Scafetta, N.: Multi-scale harmonic model for solar and climate cyclical variation throughout the Holocene based on Jupiter-Saturn tidal frequencies plus the 11-year solar dynamo cycle, J. Atmos. Sol.-Terr. Phy., 80, 296–311, doi:10.1016/j.jastp.2012.02.016, 2012b.

Scafetta, N., Humlum, O., Solheim, J.-E., and Stordahl, K.: Comment on "The influence of planetary attractions on the solar tachocline" by Callebaut, de Jager and Duhau, J. Atmos. Sol.-Terr. Phy., 102, 368–371, 2013.

Solheim, J.-E.: The sunspot cycle length – modulated by planets?, Pattern Recogn. Phys., 1, 159–164, doi:10.5194/prp-1-159-2013, 2013.

Svalgaard, L. and Cliver, E. W.: A Floor in the Solar Wind Magnetic Field Astrophys. J., 661, L203–L206, 2007.

Wilson, I. R. G., Carter, B. D., and Waite, I. A.: Does a Spin-Orbit Coupling Between the Sun and the Jovian Planets Govern the Solar Cycle?, Publ. Astron. Soc. Aust., 25, 85–93, 2008.

Wolff, C. L. and Patrone, P.: A New Way that Planets Can Affect the Sun, Sol. Phys., 266, 227–246, 2010.

Part IV

Energy transfer in the solar system.

Jelbring, H.: Pattern Recogn. Phys., 1, 165-176, doi:10.5194/prp-1-165-2013, 2013.

Pattern Recogn. Phys., 1, 165–176, 2013
www.pattern-recogn-phys.net/1/165/2013/
doi:10.5194/prp-1-165-2013

Pattern Recognition in Physics
Open Access

Energy transfer in the solar system

H. Jelbring

Tellus, Stockholm, Sweden

Correspondence to: H. Jelbring (hans.jelbring@telia.com)

Received: 5 October 2013 – Revised: 3 November 2013 – Accepted: 16 November 2013 – Published: 5 December 2013

Abstract. Different types of energy transfer are presented from the literature and are approached and commented on. It follows from these articles that energy transfer in addition to solar irradiation is less well understood by contemporary scientist. The transformation of energy between kinetic and potential energy in planetary orbits might be of crucial importance for understanding energy transfer between celestial bodies and the development of commensurabilities. There is evidence pointing to interactions (friction) between space and satellites producing volcanism. The reversible transfer of energy between the orbit of Moon and Earth's rotational energy is crucial to the creation of the 13.6-day and 27.3-day periods in both solar variables and Earth bound climate variables. It is hypothesized that the Earth–Moon system is modulating the sunspot numbers and creating both these periods, and that the great planets are responsible for the 11 yr solar cycle.

1 Introduction

The title might seem ambitious but it is chosen for emphasizing the importance of grasping the whole picture related to energy transfer. Doing so makes it easier to identify the most important subsystems, narrowing the perspective and focus on what is most needed to investigate in the very complex system where we all live, our solar system.

We know that the source of solar energy has a nuclear origin. We also know that nuclear energy is produced inside Earth and that this type of energy, to a very small extent, is reaching the surface of Earth. This situation is different on Jupiter and the other giant planets. On these planets, a prominent part of the energy flux leaving the planets seems to come from their interiors. However, most scientists are persuaded that the satellites of our planets do not produce nuclear power that melts their interior. Still, the most volcanic celestial body in the solar system is Io, the innermost Galilean satellite orbiting Jupiter (Hamilton, 2013). There was great surprise among scientists when it turned out that the biggest of Neptune's moons, Triton, was also actively volcanic, despite an outer surface temperature of around 38 K, not very far from absolute zero temperature. Neptune itself is the windiest planet among the atmosphere bearing planets.

There is little doubt that solar irradiation energy is the main reason for deciding the approximate steady state temperature situation on the surfaces of celestial bodies in our solar system. However, when an atmosphere exists on a planet or satellite the situation becomes more complex. The outer part of Venus' thick atmosphere is in thermal balance with solar energy flux and is about −89 °C, which is in stark contrast to its surface temperature around +460 °C. The corresponding values on Earth are −18 and +15 °C (NASA, 2013). We know from our own experience that the tilt of Earth's axis and the distance from our Sun affects the surface temperature of Earth producing summers and winters as well as polar and tropical climate. We also understand that an enormous energy flux is carried by winds to keep the polar winter temperatures, although low, to stay away from the neighborhood of absolute zero temperature.

We should ask ourselves if there are other prominent sources of energy other than solar nuclear energy which is mostly lost to space and of which only a minor fraction is caught by Earth's surface, its atmosphere and other celestial bodies in our solar system. Let us just for a moment look into the vast universe; there are both spiral and elliptical galaxies containing billions of stars.

There has to be reasons (physical causes) why some galaxies are three-dimensional rather than two-dimensional. In a similar way there have to be physical processes causing our solar system to become approximately flat and to keep the inner satellites of the giant planets close to the equatorial

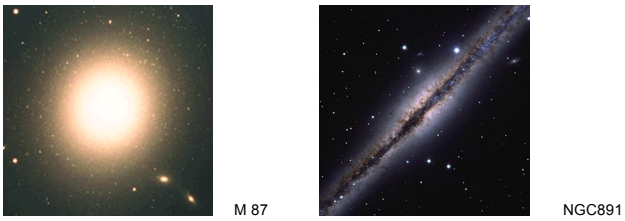

Figure 1. Geometry of galaxies; Left: M 87, Right: NGC 891.

planes of these planets. A similar situation seems to exist among atoms where the closest electrons are moving in an "equatorial" plane. Apparently, there are forces which act on all scales and which indicate a strong relationship between orbital motions and rotational directions and which might transfer energy between kinetic orbital motion and rotational energy.

The celestial bodies in the solar system are bound together by gravitational energy. Newton's law of gravity can be used to calculate how much energy is needed to separate the planets from the Sun, and the satellites from the planets. Nothing says that the total of this amount of energy has to be constant in the long run. In fact, data from planetary bodies imply that the solar system is contracting and that potential energy is lost to space. As an example, tidal friction does exist in our atmosphere and oceans. Heat escapes to space sooner or later. It is reasonable to suggest that the rotation rate of the Sun has slowed down and that Venus once rotated as Earth still does. It is known that Earth's rotation is slowing down on a long-term bases (Marsden and Cameron, 1966). The above arguments support the notion that one energy source in our solar system is "friction" energy in a contracting solar system in which rotating bodies also loose rotational energy. However, there is no doubt that there exist physical processes that cause both slowdowns and speed-ups on Earth's rotational rate. Earth is hardly an exception in this respect.

Processes involving energy transfer can be regarded as reversible and/or irreversible. A pendulum, for example, is switching its total energy between potential energy and kinetic energy. Still, friction exists and the pendulum is bound to stop its motion sooner or later. Its total energy content is dissipating and lost to the environment and ultimately to space. Any planet that does not move exactly in a circular orbit is constantly switching potential energy with kinetic energy when moving from perihelion to aphelion and vice versa. The idea that these energy pulsations would create friction energy is not farfetched.

In conclusion, the solar nuclear energy provides all celestial bodies in our solar system with average temperatures that can be considered as fairly stable over orbital periods. An approximate *steady state* situation has evolved for each planet. The system is gradually loosing energy in an irreversible process because of "friction" and is contracting seen in a very long-term perspective. However, (quasi) reversible energy processes in our solar system do exist and energy is constantly shifting between potential and kinetic energy; a statement valid for any celestial body in the solar system. Reversible energy processes involve both orbital and rotational energy (as further discussed below). A prime topic of this paper deals with the reversible processes causing rotational spin-ups and slowdowns of celestial bodies.

2 Aim of the article

One aim of this article is to show that there is a severe lack of understanding related to energy transfer in our solar system when looking beyond electromagnetic energy transfer. Presented observational evidence and theoretical reasoning are intended to demonstrate that most generally accepted theories relating to the evolution of the solar system and energy transfer between celestial bodies have severe shortcomings. There is a vast pool of observations from a number of sources where the results often seem to be contradictive. Hopefully this article will stimulate to deeper thoughts about such evidence, making it possible to identify dominating subsystems in the solar system and to increase our understanding how celestial bodies interact with each other. Therefore, the present paper is focused on the basic energy transfer processes between celestial bodies. Some statements are made by the author more to stimulate other scientists than to claim them as truths. A controversial hypothesis is formulated (Sect. 8) with the hope that it will be disproved or confirmed by other scientists in the near future.

3 Method

The results are obtained by a combination of

a. gathering information relating to all types of motion in the solar system from adequate scientific papers and data sources;

b. a special investigation of a few key articles dealing with the solar terrestrial interaction and especially the 13.6-days period found in both solar bound and Earth bound data;

c. research on the commensurabilities (Jelbring, 2013);

d. further theoretical considerations.

The combined information under (a) to (d) might persuade the reader that the subject of solar terrestrial interaction is in a severe need of scientific rework. This article is just scanning an ocean of mostly old research results that deserve to be remembered and treated seriously. The results here presented should not be treated on a strict "proof" basis. It is the author's opinion, however, that there exists a number of detailed information that has been published and can be published in the future to defend most of what is stated in this paper.

4 Key sources of information and key variables relating to energy transfer

"It appears that the world scientific community is indeed capable of undertaking a concerted effort to unravel the mysteries of solar activity effects on meteorological phenomena. The success of such an effort ultimately depends on the wisdom of those assigned to assimilate the divers results into predictions schemes for weather and climate. The ultimate beneficiary is mankind" (Herman and Goldberg, 1978). Their book contains 370 references where 170 directly treat solar–Earth correlations and connections. This is just an example indicating that scientific valuable information does exist but that it sometimes have been forgotten or disqualified (for different reasons). In this article, other similar examples will be presented.

After the above statements, irradiation will not be included in the paper. It is well known that it heats celestial bodies in the solar system and we will concentrate on less known processes. The energy processes causing the almost constant "quiet" solar wind will also be dismissed. Let me separate the treated types of energy transfer into two categories. One will relate to solar–Earth connections and the other will not depend on earth bound factors. One way to track down energy transfer is to investigate "all" types of motion that occur among celestial bodies in the solar system and describe how they vary.

4.1 Rotation rates

According to NASA the rotation period of the Sun is 25.38 days at 16 degrees latitude. The Sun has a differential rotation with the equatorial period being 25.05 days and the polar being 34.35 days (NASA, 2013). The rotation period (at a specific latitude) can and does change between years. The Carrington synodic period (as seen from Earth) is defined as a constant period of 27.275 days. Rotation rates faster than the Carrington rate usually occur at less than 20 degrees latitude (Gigolashvili et al., 2010). In the same reference it is stated: "The phenomenon of the solar differential rotation has been known for centuries but it is still not properly understood." Notice that an exact rotation rate of the Sun cannot be determined based on observations. It is remarkable that the sidereal rotation period of our Moon is so close to the Carrington period. The latter has been decided as an approximate period for sunspots to move around the Sun as seen from Earth, but very few sunspots live that long. The observed 27-day activity cycle of the Sun can, therefore, not be a result of sunspot groups surviving Sun's rotational period. It is more a question of intermittent revival of sunspots around every fourth week than survival of the same.

All the giant planets have a super rotation at the equatorial region as the Sun has. Estimating a fixed rotation period for the planet is quite hard since the atmosphere moves very differently at various latitudinal bands. On the other hand the true rotation rate for an assumed solid body can be determined by the rotation rate of its magnetic field, which is assumed to be fixed to the solid body below the atmosphere (Glatzmeier, 2009; Drobyshevskij, 1977). Surprisingly enough, the strongest winds in the solar system were found on the very cold planets Uranus and Neptune (Kaspi et al., 2013). On Neptune the equatorial winds move about 250 $\mathrm{m\,s^{-1}}$ faster than the solid body and at higher latitudes the winds move about 250 $\mathrm{m\,s^{-1}}$ slower (Kaspi et al., 2013). The coldest planet (except Pluto) has the fastest mowing winds among planets. It is not probable that these winds are primarily caused by solar irradiation energy variations. Earth absorbs a maximum around 940 $\mathrm{W\,m^2}$ and Neptune a maximum of 1.1 $\mathrm{W\,m^2}$ in their equatorial planes. Earth's equatorial winds show little or no super rotation (study the QBO) and Neptune has the most extreme rotation in the solar system.

Comets can be spectacular to watch when, for unknown reasons, their orbits choose to become very elliptical and they closely approach the Sun. What we see is the gas and particle emission from the comet. The mass loss can be substantial and the mass will diminish as time passes on. The comet C/Levy was losing about 4500 $\mathrm{kg\,s^{-1}}$, mostly water molecules, in the neighborhood of the Sun. The rotation rate of comets is hard to observe but most measured periods are included in the interval of 5–20 h (Jewitt, 1998, Table 1). Jewitt (1998) stated: "The current challenge to cometary astronomers is to quantify the interaction between the spin, the outgassing, and the resultant torque on the nucleus, and to understand the role of rotation in determining the basic physical properties of the nucleus." Experts expect the rotation to be caused by the emitted gas jets, a conclusion which might only be partially true since all "free" celestial bodies do rotate whether they emit gas or not.

The causes of asteroid rotation are hard to understand but there are several physical processes involved. "Asteroids larger than tens of kilometers spin with a mean rotation period around 10 h, with some minor variations with size" and "the distribution is close to normal" (Harris and Pravec, 2005; Pravec et al., 2002). There is an upper limit on spin rate called the "Rubble pile spin barrier" of around 2 h indicating that asteroids would lose mass because of the centrifugal force and disappear if rotating faster. Nowadays a large number of smaller asteroids have been possible to detect and observe, and spin periods down to around 1 min have been measured (Pravec and Harris, 2000; Ryan and Ryan, 2008). Collisions are believed to be the cause of the fast rotation but it is also recognized that there has to exist one or several "spin-up" processes. One suggestion is that infrared radiation is causing the spin-up but there are also other suggestions.

The inner satellites (up to about 20 planetary radiuses) of the giant planets have their rotation rates bound to its orbital period (NASA, 2013). The rotation period of the planets vary between 9 h (Jupiter) and 243 days (Venus). The rotation

period of Venus and Mercury seem to be affected by the orbital period of Earth (Jelbring, 2013).

4.2 Orbital periods

Orbital changes among comets and asteroids are probably caused by other processes than the Newtonian gravitational force. The existence of the Kirkwood gaps in orbital periods of asteroids is a clear indication that energy transfer between celestial bodies does occur. Asteroids, close to resonances with Jupiter's orbital period, have been observed to change their orbital parameters quicker than other asteroids (Sinclair, 1968; Yoshikawa, 1989). Emelyanenko (1985) found that a small number of comets also moved in resonance with Jupiter. Carusi et al. (1988) showed that the most famous comet of all, Halley's comet, has changed its eccentricity from about 0.953 to 0.968 during the last 9 millennia. Most celestial bodies exhibit a decrease in eccentricity with time, which is supported by the fact that all inner satellites move in almost circular orbits close to the equatorial plane of their parent planets. The same tendency is found among planets in the solar system. The possible variability of planetary orbital periods is clearly shown by a rather strange example from another solar system. Two more than Jupiter sized planets orbit the star Kepler-9 in 19.2 and 38.9 days, which is close to a 1 : 2 commensurability. The strange fact is that the inner planet is increasing its orbital period by 4 min/revolution and the other one is decreasing its period by 39 min each revolution (Holman, 2010).

Lately, Nugent et al. (2012) have performed an extensive investigation of semi major axis drift on near-Earth asteroids. They found 54 asteroids "that exhibit some of the most reliable and strongest drift rates" among a larger number of such asteroids. Nugent et al. (2012) attribute this drift to the Yarkowsky effect, which means that solar irradiation pressure should be responsible for the drift. However, this hypothesis cannot explain all the observed drifts quantitatively, which the authors were well aware of.

An amazing work on asteroids named "asteroids harmonics" has been presented on the web by Ross (2013). This work has not been peer reviewed. The results ought to be checked out thoroughly. In short, Ross calculates the "center of mass" for thousands of asteroids by measuring average mass/time unit in each orbit. This center of mass for each individual asteroid is close to the second focal point in the elliptical orbit where the Sun is in the other focal point. He divides the asteroids into 5 groups decided by the Kirkwood gaps. Finally, he shows that each group has their "centers of mass" in different *circular* "energy states" almost symmetrically spaced around the Sun and the "center of mass" of Jupiter's orbit. Ross (2013) is uncertain about the interpretation. Given that these calculations are correct, they do show that most asteroids are moved into specific energy states that are decided by the Sun and Jupiter. These are not possible to calculate using Newtonian gravity models. If the Ross (2013) calculations are correct, these circular symmetric "energy states" are observational evidence that cannot be refuted.

4.3 Commensurabilities

The tendency of celestial bodies to have orbital periods described by integers, has been known for a long time. As an example of this, it is mentioned in Herman and Goldberg (1978, p. 23) that

- 46 siderial revolutions of Mercury = 11.079 (yr)
- 18 siderial revolutions of Venus = 11.074
- 137 synodic revolutions of Moon = 11.077

Commensurabilities are probably major evidence indicating that celestial bodies exchange energy with each other in a way that cannot be explained by applying the Newtonian gravity model. Boeyenes (2009) gives a limited overview of commensurabilities. Commensurabilities are treated in a separate paper (Jelbring, 2013) where examples of three to four body commensurabilities are presented. Some of these have not been mentioned in the literature before. Jelbring (2013) also claims that a number of strong commensurabilities, like the one mentioned above, hardly can be produced by chance. If so, every celestial body in the solar system has found its recent energy state (orbit) by interacting with other celestial bodies during long time periods.

4.4 Volcanisms on celestial bodies

Active volcanism has only been observed on three celestial bodies in the solar system; viz. on Earth, Jupiter's moon Io and Neptune's moon Triton. Io is close to the size of our own Moon and is the most volcanic celestial body in the solar system. The reason for volcanisms is declared by Hamilton (2013): "As it (Io) gets closer to Jupiter, the Giant planet's powerful gravity deforms the moon towards it, and then, as Io moves further away the gravitational pull decreases and the moon relaxes. The flexing from gravity causes tidal heating." This simple mechanical model is not unchallenged. Recently, Cook (2013) wrote an article with the title "Scientists to Io: Volcanoes are in the wrong spot". He quoted the research-leader Christoffer Hamilton: "… but we found that volcanic activity is located 30–60 degrees east from where we expected it to be." More information from NASA about active volcanism is found in "Triton's volcanic plains" on the web (NASA/JPL, 2008).

The title "Cryovolcanism on the icy satellites" (Kargel, 1995) is motived by the fact that the surfaces of several satellites far away from the Sun are more or less lacking scars from meteoritic impacts as seen on the surfaces on our Moon and Mercury, which is indicating a relatively young surface. Kargel (1995) mentions that there is evidence of past volcanic activity on the surfaces of Ganymede, Europa (Jupiter), Enceladus, Tethys, Dione (Saturn), Miranda and

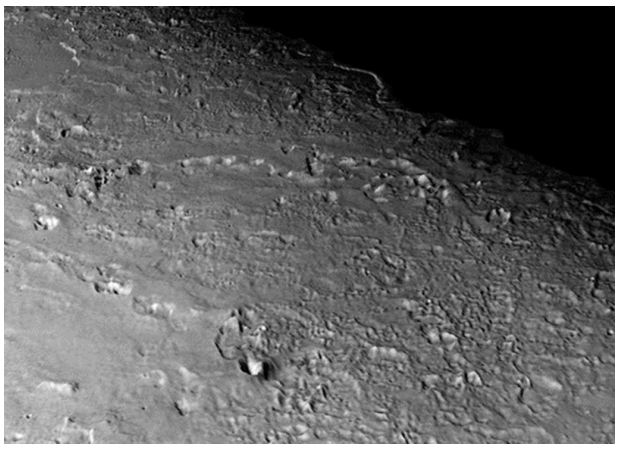

Figure 2. This view of the volcanic plains of Neptune's moon Triton was made from topographic mapping of images obtained by NASA's Voyager spacecraft during its August 1989 flyby. Credit: NASA/JPL/Universities Space Research Association/Lunar & Planetary Institute.

Table 1. Some characteristics of satellites in our solar system.

Satellite	Orbital/ equatorial	Lunar mass	Albedo	Eccentricity	Retrograde rotation
Moon	60.27	1.00	0.12	0.026–0.077	No (3.6 %)
Io	5.91	0.82	0.62	0.004	Yes
Europa	9.40	0.65	0.68	0.0101	Yes
Ganymede	14.97	2.02	0.44	0.015	No (83 %)
Enceladus	3.95	0.0015	1.0	0.0045	Yes
Tethys	4.89	0.0084	0.8	0.0000	Yes
Dione	6.26	0.015	0.7	0.0022	Yes
Miranda	5.08	0.00090	0.27	0.0027	Yes
Ariel	7.48	0.018	0.35	0.0034	No (81 %)
Triton	5.88	0.29	0.76	0.000016	No (81 %)

Data according to NASA satellite fact sheets and CRC Handbook of Chemistry and Physics.

Ariel (Uranus). Adding Io and Triton to the list, it should be noted that all of the satellites indicating volcanic activity are orbiting close to the parent planets. In Table 1, the first column shows the ratio between the radius of orbit to the radius of planet, the second the satellite mass relative lunar mass, the third the visual geometric albedo, the fourth the eccentricity of orbit and the last column tells if the satellite at any times moves in a retrograde direction relative to the Sun. The percentage tells how far the satellite is from achieving such a retrograde motion indicated by 100 %.

Table 1 is quite interesting in that the values in column 1 only vary within a factor of 4, excluding our Moon. The mass of these satellites varies with a factor of 1350. The albedos are extremely high which seems to indicate that "new" satellite surfaces have high albedos. Compare the albedo of the old lunar surface. Our Moon is also special in having an exceptionally variable eccentricity. All the satellites, but our Moon and Ganymede, move very close to circular orbits. All of the volcanic ones can move or do move close to a retrograde direction around the Sun during short periods of their orbits. These factors will be discussed below.

Figure 3. The Hudson Bay "staircase" of 185 successively uplifted shorelines, documented in Richmond Gulf on the eastern side of Hudson Bay, Canada (Hillaire-Marcel and Fairbridge, 1978). The sand gravel beaches recur with great regularity about every 45 yr, representing the cycle of storminess. There are also longer cycles of 111 yr and 317 yr evident in the sequence of beach ridges, which are linked with planetary cycles according to Fairbridge and Hillaire-Marcel (1977) (Credit: Fairbridge).

5 Irrefutable evidence from Earth

From Earth itself, we may obtain some "irrefutable evidence" relating to inner planetary energy exchange as discussed below.

5.1 Evidence of storminess and sunspot cycles in sediments

There is no trace left of variable energy states in the atmosphere. Fortunately such variations will affect wind systems on Earth and ultimately they will show up as secondary effects in sediments, in wind blasted rocks, in glacial drill cores and as below in beach ridges during 9000 yr. The combined processes of land uplift and cyclic storminess has produced an impressive testimony of energetic variations in Earth's atmosphere since the end of the last glacial period. No one knows for sure why the cycle, forming the ridges in the image below, is close to 45 yr. Fairbridge and Hillaire-Marcel (1977) suggested that it had to do with the beat period between Saturn and Uranus, which is 45.392 yr.

Fairbridge was a pioneer in trying to gather all types of information relating to solar–Earth connections and was the scientist who pushed attention towards the importance of commensurabilities (Mackey, 2007; Jelbring, 2013). Fairbridge was not the first scientist claiming that celestial bodies

are causing sunspots. There is a one hundred year old story waiting to being told about this topic.

Physical sunspots–Earth connection impacts have occurred for a long time according to an exceptional research performed by an Australian geologist investigating drill cores in the Elatina formation that was formed about 680 million years ago (Williams et al., 1985). The variations in varve thickness were analyzed and treated by signal processing methods (Williams and Sonett, 1985). The results conclusively indicate that solar–Earth processes have created the observed variations (still, alternative implausible interpretations have been published).

5.2 Evidence of long-term solar wind influence

The production of the isotopes ^{10}Be and ^{14}C occurs in the atmosphere due to cosmic radiation. These variations do confirm the existence of solar wind variability during the investigated period. The paths of these isotopes into sediments and biological matter vary in complicated ways. Still, it has been possible to extract probable periodicities during a time interval of 9400 yr. Some of these might be coupled to planetary orbital periods even if such a statement is not made by the authors of an interesting article based on advance signal processing methods (McCracken et al., 2013). Another interesting article (Georgieva et al., 2005) shows that there are at least two physical processes affecting solar wind speed (and thus ^{10}Be and ^{14}C isotope production). One of them is correlated with sunspot numbers and the other with coronal holes which do not correlate with sunspot numbers. It is advocated that geomagnetic activity correlates with the sum of these processes. Geomagnetic activity is also claimed to be better correlated with global temperature variations than with sunspot numbers alone (Georgieva et al., 2005).

5.3 Evidence of planetary influence on climate and Earth's axis

A few earthbound physical processes are critical when examining the energy transfer between celestial bodies. One is the quasi-biennial oscillation (QBO), which is an equatorial stratospheric wind that changes direction about every 27 month. There is no plausible physical earthbound process that can generate this type of wind shift so the cause should be looked for from outside Earth itself.

The QBO variations are correlated both with variations in AAM and LOD according to Abarca del Rio et al. (2003) and several other researchers. AAM is the atmospheric angular momentum and LOD is the length of the day on Earth. Much research has shown very strong correlations between LOD and AAM in the decal and interannual ranges (Abarca del Rio et al., 2003; Morgan et al., 1985). The former also claims correlation between solar activity and QBO: "At interannual times scales we present results regarding associations between the decadal cycle in solar activity and the amplitude and phase of the stratospheric QBO."

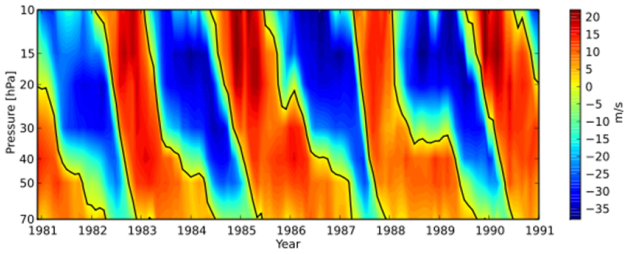

Figure 4. The quasi-biennial oscillation, QBO (Credit: Free University of Berlin).

The Earth's axis is wobbling. The polar axis moves about 9 m back and forth. The orbital year of Earth is affecting the wobble and so is another period, which is around 433 days. The interference between these two components produces the approximately 6.5 yr envelope seen in Fig. 5. The physical mechanism providing the excitations energy causing the Chandler wobble is unknown. The existence of the wobble proves that there is an external torque affecting Earth's axis.

6 Evidence of solar terrestrial connections

ENSO, LOD, QBO, SOI, AAM, Chandler wobble, 11 yr Sunspot cycle, 27- and 13.6-day sunspot cycles all describe energy states on Earth or parts of Earth. Much research effort has been made to find correlations between these variables (e.g., Herman and Goldberg, 1978) and these efforts have continued. The coupling between sunspots cycles and the stratospheric Aleutian High is described by Soukarev and Labitzke (2001) as an example also including the 27-day sunspot cycle. A similar message is given by Fioletov (2009) and Shapiro et al. (2012). The former recognizes, besides the 27-day cycle, a 13.5-day cycle, which is found in the tropical upper stratospheric ozon concentration. Generally, authors are persuaded that the 27-day sunspot cycle is caused by the solar rotation period. Fioletov (2009) states that "the analyses shows that during the periods of high solar activity, about half of the variance for periods of 13.5 and 27 days near 40 km can be attributed to the fluctuation of the Mg II index", which is a solar index originating from the solar chromosphere.

In an analysis focusing on outgoing long-wave radiation (OLR), where it is considered as a proxy for cloudiness, Takahashi et al. (2010) showed that there is a distinct 27-day periodicity over the warm pool of water in the Western Pacific during the period 1980 to 2003. An intriguing fact is that the 27-day periodicity was only found during sunspot maxima periods (1979–1982, 1990–1992, 2000–2002). The 27-day period was also compared with the $F10.7$ index from the solar surface. The authors state: "Identification of the physical mechanism for physical 27-day periodicity is not an easy

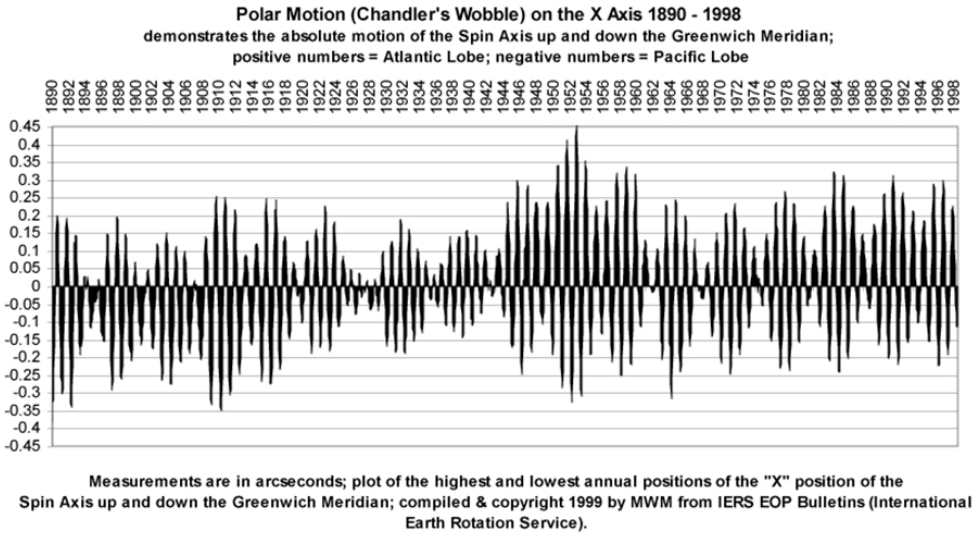

Figure 5. Chandler's Wobble 1890–1998 (Credit: MWM from IERS EOP Bullentins, 1999).

task since most solar parameters, including total solar irradiance, solar UV, and galactic cosmic ray (GCR) intensity, vary with the period of solar rotation and are modulated by the 11 yr solar cycle." The result proves that Earth's atmospheric system has filtered OLR power ($W\,m^{-2}$) geographically and temporally to match sunspot data in the solar atmosphere. Similar processes must have been at work producing the sunspot bound data in the Elatina formation reported by Williams (1985).

It is of a special interest that LOD is a true *global* variable. The same can only be claimed for the Chandler Wobble among the solar terrestrial variables mentioned above. The amplitude of LOD is around 1 ms in most of the treated time ranges. Several articles informs us that (1) LOD is slowly decreasing due to tidal friction, (2) LOD is correlated with ENSO events in the decadal range of periods (Fong Chao, 1988), (3) LOD is strongly correlated with AAM on the interannual range (Abarca del Rio et al., 2003) and (4) LOD is strongly correlated with lunar declination and atmospheric geopotential height (Gouqing, 2004). Gouqing (2004) states: "It is found that there are a 27.3 and a 13.6-day east-west oscillation in the atmosphere circulation following the lunar phase change. The lunar revolution around the Earth strongly influences the atmospheric circulation. During each lunar cycle… (change in)… atmospheric zonal wind, atmospheric angular momentum and LOD. The dominant factor producing such an oscillation in atmospheric circulation is the period change of lunar declination during the lunar revolution around the Earth. The 27.3- and 13.6-day atmospheric oscillatory phenomenon is akin to a strong atmospheric tide, which is different from the weak atmospheric tides, diurnal and semidiurnal, previously documented in the literature. Also it is different from the tides in the ocean in accordance with their frequency and date of occurrences."

These are indeed strong statements written in 2004, but is seems to have had little impact on climate scientists. Gouqing's (2004) work proves that the 27.3-day and 13.6-day oscillations in wind circulation emanate from the Earth–Moon system and that the critical parameter is the declination of the Moon (27.321 days period) and not the synodic month (29.53-days period).

Mursula and Zieger (1996) are analyzing the 13.5-day and 27-day periodicity of a number of mostly solar variable using advanced signal processing during 3 solar cycles. All variables were normalized to make quantitative comparisons between them possible. The variables are the near-Earth solar wind speed, solar wind temperature, ion density, geomagnetic activity (Kp index), sunspot number, IMF radial component, IMF direction, IMF *z* component, IMF radial magnitude, CA-plage index, X-ray intensity.

Correlation between the solar wind speed and four other variables (solar wind temperature, ion density, IMF radial component and Kp index) were carried out using raw data and data filtered around 13.5 days to find out the time lag between these variables. The authors show that existing data gaps in solar wind data and IMF field variables can be handled in a satisfactory way. The analysis is a high quality investigation. It is hard to imagine an analysis that involves more relevant variables and which is more suitable as a foundation for deductions.

Background information is given by Mursula and Zieger (1996) in the introduction: "First evidence or the fact that geomagnetic activity and auroral occurrence reflect the solar rotation period of approximately 27 days were obtained already more than a century ago" and "in most early and even some later studies, these peaks at the second harmonic of the fundamental solar rotational period were not considered to correspond to a real physical periodicity related to certain

specific heliospheric conditions but rather to be due to mathematical artifacts related, for example, to numerical effects when calculating power spectra." With these words in mind, it is quite a scientific feat to find out that the 13.5-day period is for real in all the variables mentioned above.

The 13.5-day period is only lacking for the IMF z component and is rather weak for sunspot numbers and X-rays. On the other hand the amplitude of the 13.5-day cycle beats the amplitude of its "fundamental" 27-day cycle for solar wind velocity, solar wind temperature, ion density and IMF radial magnitude (Fig. 1 of Mursula and Zieger, 1996). Regarding the chromosphere variables Ca plage index and Mg ratio, the 27-day cycle is dominating, but the 13.5-day period is clearly recognized. It is reasonable to suggest that both these periods should emanate from the same physical process.

The autocorrelation function tells how "persistent" a specific period is. This persistence can be counted in days based on Fig. 2 of Mursula and Zieger (1996), which covers a year. A persistence during 1 yr means that the 13.5-period amplitude has been well detected about 27 times during that year. The most persistent variables (>1 yr or close to 1 yr) are the IMF radial component in the average IMF direction, Ca plage index, solar wind speed, Mg ratio, solar wind temperature and ion density. The variables are ordered relating to amplitude by the present author based on Fig. 2 of Mursula and Ziegler (1996). The persistence of other variables is shorter such as sunspot numbers (250 days) and Kp index (100 days). A very interesting fact is that all the chromosphere variables show a secondary period around 290 days. After that time the X-ray amplitude is 180 degrees phase shifted compared to the Ca plage index and the Mg ratio which is an interesting result.

The cross-correlation calculations on filtered data show phase shifts between variables (Fig. 3, Mursula and Zieger, 1996). It should be noticed that both the Kp index and solar wind temperature peaks 1 day before the maximum value of solar wind speed. The correlations between both these variables and solar wind speed are above 0.8, which is highly significant.

Mursula and Zieger (1996) have demonstrated very strong connections between the Earth bound geomagnetic Kp index and a number of solar variables relating both to the 13.5-day period and to the 27.5 period in a scientifically qualified manner. Gouqing (2004) has, in an equally qualified manner, showed that periods of 13.6 days and 27.3 days are found in major atmospheric air oscillations and that these are caused by the dynamics of our Moon when rotating around Earth.

7 Theoretical considerations

The aim of all disciplines in natural sciences is to increase our knowledge about what happens and what could happen in our environment, atmosphere, solar system, galaxy and in the Universe. When we believe that we know enough of a subsystem, we can make models aimed for predictions or better understanding. However, there is a golden rule in natural sciences: If there exists undeniable observational evidence these will always beat the result of any model whatever its output is. Models always have to be adjusted to nature since nature can never adjust to a model output. Models are and will always be incomplete copies of a partial piece of nature.

Regarding knowledge related to the creation and functioning of the solar system, human knowledge is far from complete. The unknown and "unsolvable" problems are often left aside or forgotten since there is little reward for pointing out limitations in scientific research and contemporary understanding. This article deals with this problem by trying to locate types of energy transfer in our solar system which shows up in observational evidence but which may seem unexpected (and therefore often are neglected).

The models predicting positions of celestial objects in the solar system are very effective and precise. Solar and lunar eclipses can be predicted within minutes many years in advance. Still, that model might have been constructed without a real understanding of what causes energy transfer between celestial bodies. It may rely on Newton's gravity force model in an average sense and Kepler's observations that the momentum of planets orbiting the Sun is approximately constant. But a number of "perturbation terms" have been added to each planet to increase the accuracy of the model to fit observational evidence gathered for hundreds of years, demonstrating how the orbits of planets actually deviate from the theoretical exact elliptical paths.

To be more specific some additional examples will be treated below. Earth moves in an approximate elliptical path. Its closest distance from the Sun is called perihelion and its longest is called aphelion. Newton's gravity law only describes where the *average* distance between the Earth and the Sun should be located. It can be used to calculate the energy required to move Earth away from Sun. It can, however, not be directly used to calculate the energy needed to move the Earth away from the Sun when Earth is in the perihelion and aphelion positions. The orbital velocities in these positions are 30.29, 29.78 (average value) and 29.29 $\mathrm{km\,s^{-1}}$ according to NASA fact sheet where the velocity at average position is added. The corresponding distances are 1.4707, 1.4957 and 1.5207E11 m (according to West, 1960). At aphelion Earth has gained potential energy and lost kinetic energy but it has lost more kinetic energy than it has gained in potential energy according to Newton's law. To understand this statement, the gravitational binding energy of Earth and Sun is expressed by Eq. (1) where the subscript "a" means average value over an orbital period:

$$1/2 M_j \times M_s \times G/R_\mathrm{a} = 1/2 M_j \times V_\mathrm{a}^2\,, \qquad (1)$$

where M denotes masses, G is the gravitational constant and V is velocity.

Now assume that the distances mentioned above are all average distances and put them into Eq. (1). The resulting

velocities (V_a) are then: 30.03, 29.78 and 29.05 km s^{-1}. Thus, applying the approximate formula that kinetic energy is $E_{kin} = 0.5 \times M \times V^2$ the following statement and questions seem proper. When Earth is at perihelion it has gained more kinetic energy than the potential energy it has lost. The question arises, where is the part of excess or missing kinetic energy physically located when Earth is in its aphelion or perihelion positions? We assume that the law of conservation of energy is valid, implying that energy cannot be created from nothing and not disappear without a trace of it.

Hence, the missing energy has to be found at some physical place especially since it disappear and reappear once every orbital period and has done so for billions of years. The answer ought to be either inside the Earth (and the Sun) or in space between these bodies. Space seems to be a good guess. In that case, there should be some type of field in space where amplitude depends on how much Earth deviates from its average energy state, which can be calculated by Newton's gravity formula. Such a field should act as a gravity field, which can change signs and should be responsible for an attraction when Earth is further from the Sun than its average distance and repulsion when Earth is closer than its average distance. The resultant orbit is the one Kepler observed and which he assumed to be an ellipse. Such a field should be called a dynamic gravity field.

If variable energy fields in our solar system constantly interfere with each other there is no wonder that celestial bodies will be trapped in commensurabilities with each other (Jelbring, 2013) meaning that one specific body has found a "lowest" energy level in relation to several other celestial bodies. If so, commensurabilities should be found between all the celestial bodies, if enough time has passed for their binding energies to adjust to each other. This would also mean that individual celestial bodies can both loose or gain binding energy to their parent body although there would always exist a "friction" loss due to tidal action between bodies in any "energy cycle".

The Chandler wobble has two prominent components, which have been estimated as 1.000 yr and 433 days. Few persons seem to have asked why the 1-yr component exists. They take for granted that Earth should be the reason but do not investigate the case further. Is Earth most affected when it is at perihelion or aphelion or at some other longitudinal position? In that case what physical situation would excite the 1 yr wobble component? The interaction when Earth is exactly at perihelion based on the Newtonian gravity formula might be one reason. Another option is to investigate when Earth's and Sun's axis point "most" towards each other. It should be noticed that 3 times the beat period of Mercury and Venus is very close to the observed Chandler period. It is 433.57 days according to the orbital periods preferred by Jelbring (2013) and 433.70 days according to NASA fact sheets (2013). It is the opinion of the author that there is an energetic coupling between Mercury, Venus and Earth causing the 433-day Chandler component and causing Earth's axis to wobble. This is a novel finding proposed here.

8 Location of sunspot generator

The major issue relating to the sunspots generating process is whether it is located inside or outside the surface of the Sun. The view held by the established experts favors the former view. The sunspot period is generally known as the 11 yr cycle. A long-term analysis of its length based on Schove's (1955) data indicates a cycle length of 11.11–11.12 yr. The 27-day period is much less recognized, but has been known for a long time. Carrington determined the solar rotation period from low latitude sunspots in the 1850s and found it to be 25.38 days. Looking from Earth, a spot rotating at that period would cross our line of sight every 27.275 days. This is why this period has been termed Carrington Rotation. Since then the Sun has been hypothesized to harbor the physical mechanism generating sunspots.

There are several objections to why the cause of sunspots should be situated inside the surface of the Sun. Consider the hypothetical situation that the Sun would have no planets or other objects circling it. Would 11-yr, 27.3-day and 13.5-day sunspot periods still be present if seen from a non-existing imaginary Earth? How would the Sun be aware of the length of its rotation period? How would the Sun know about its own 25.5-day rotation period when its closest reference point in space is 4 light years away (the closest star)? There is no way it could sense its own rotation rate in such a hypothetical situation and that argument alone places the physical mechanism generating sunspots outside the Sun itself.

Consider the following alternatives if the conclusion above is not persuading. If the answer is yes, it would imply that the inner part of the Sun would have a clock administrating (1) the start of the activity, (2) the stop of activity, (3) distribute this activity over an immense surface area and (4) control the intensity of these periodicities of which the longest one is of a very quasi-periodic nature and the two others are relatively stable. If the answer is no, planets have to be involved in the sunspot generating process and they have to be responsible for the forces producing the described actions.

This paper has listed a number of observational evidence and analytical results that do diminish the probability that there is a sunspot generating process hidden in the interior of the Sun. There is another advantage with a sunspot generating process coupled to planetary dynamics and it is that any hypothesis can be checked since measurements can be made outside the surface of the Sun. The latter is essential if we want to apply scientific methods. An hypothesis that cannot be tested has little or no scientific value. The following hypothesis can be checked in the future and hopefully it will turn into a verified theory.

9 A hypothesis suggesting that Earth–Moon is modulating sunspot activity

The 13.6-day and 27.3-day periodicity in a number of variables that have been observed in the atmosphere of the Sun and in the atmosphere of the Earth are all caused by our Moon due to its motion back and forth to high declinations above and below the equatorial plane of the Earth.

If so, it follows that the Earth–Moon system modulates other sunspot generating processes caused by the action of the great planets, preferentially Jupiter and Saturn. When the action from these big planets are strong, the 27.3-day variations gets stronger and when the action of the bigger planets reduces, the 13.6-day period gets stronger. When the big planets are in energetic balance with the Sun (sunspot minimum), the 13.6 and 27.3-day periods are hardly detectable except in LOD. When the energetic balance prevails for longer times Earth gets cold and we will experience both Little Ice Ages and larger glaciations.

The period of the Moon crossing the equatorial plane of the Earth varies between 12–15 days because of the Moon's variable orbital motion. The forcing period thus varies in the interval 13.6 ± 1.5 days. The dates for minimum LOD (at highest absolute declination) follow the actual lunar variations but the variations increases to 13.6 ± 2.5 days (during 2012). The advocated forcing mechanism is thus phase stable and there are no phase shifts even if the variation occasionally gets bigger than what is mentioned above during solar maxima. The solar activity variables can show phase shifts depending on the influence from the bigger planets. The most spectacular phenomenon might be that the 13.6-day periodicity gets almost eliminated in sunspot numbers and to a large extent in the Ca plage index and in the Mg II ratio (Mursula and Zieger, 1996), the reason being that the amplitude of the 11 yr sunspot period is bigger than the amplitude of the 13.6-day period. The 13.6-day signal during moderate solar activity turns into a 27.3-day modulating signal during maximum solar activity.

The 27.3-day signal can almost always be found in the Mg II ratio except at sunspot minima. It is harder to find it in the sunspot number signal as Mursula and Ziger (1996) have demonstrated. H. Jelbring (unpublished data) found the strongest long-lasting sunspot 27.3-day signal component during the 1937 solar maximum (during 9 consecutive months). A similar phenomenon can be found in the Earth's atmosphere according to Takahashi et al. (2010), who state: "Based on FFT analysis for OLR (Outgoing Longwave Radiation) compared with the $F10.7$ index, we clearly demonstrate a 27-day variation in the cloud amount in the region of the Western Pacific warm pool, which is only seen in the maximum years of 11-year solar activity."

These finding are also consistent with the following statement relating to the 13.5 day-period: "For each of the three solar cycles studied, the largest two-stream structures were found in the *late* declining phase of the cycle" (Mursula and Zieger, 1996). It is hard to avoid the conclusion that the 13.6-day period and 27.3-day period in both solar variables and in Earth bound climate variables have the same identical cause and that that cause is the motion of our Moon in relation to the Earth's equatorial plane. LOD is for sure a function of lunar declination and the same seems to be true regarding a part of Earth's climate variations.

10 Discussion and conclusions

This article has focused on surveying non-thermal energy transfer in our solar system. It has raised questions as to what such energy transfer means for the geometry of galaxies, solar system and planetary systems. It makes it probable that such energy transfer affects solid celestial bodies and the atmospheres of planets and that it also is the reason for all observed commensurabilities.

There exists an undeniable reversible exchange of energy between Earth's rotation energy and our Moon with 13.6-day and 27.3-day periodicities. Non-thermal energy exchange could be called tidal energy exchange, but it covers more than the normal concept of tidal action. The lunar impact on LOD is quite independent of the distance between the Earth and the Moon and it does correlate well with the atmospheric angular momentum. This type of energy exchange has the potential to explain why meteorological predictions are limited to an absolute maximum of about one week and why glacials and interglacials exist. It also explains why climate models are hopelessly wrong since the influence of our Moon on atmospheric and oceanic mass motion is ignored in these models.

The transfer of energy to and from Earth's rotation energy is a fact. It happens on a number of timescales. One timescale is definitely locked to the orbital sidereal period of the Moon and the cause has to be coupled to physical processes related to the maximum absolute declination the Moon reaches above or below the equatorial plane twice each rotation. Earth rotation slows down when the Moon passes the equator plane and speeds up when it is at high or low absolute declinations. This has occurred at every rotation since consistent LOD measurement started in 1973 (H. Jelbring, unpublished data). The Moon is very special as a big satellite because it is not orbiting in the equatorial plane of its mother planet. In fact the Moon is more like a planet than a satellite just for this reason, which is also why we do observe a strong 13.6-day period in LOD variations. These variations would not be there if the Moon was orbiting Earth close to Earth's equatorial plane. Still, there would be long-term, interannual and decadal variations of LOD even if our Moon was equator bound. The 13.6-day variation in LOD constitutes a key factor when investigating energy transfer in the solar system, and is to a great help for an improved understanding of many of its subsystems.

All the satellites showing active or former volcanic activity are moving very fast close to their mother planet in

Table A1. List of acronyms.

AAM	Atmospheric angular momentum (Global wind index)
Ca pla. index	Calcium plage index (solar activity index)
ENSO	El Niño–Southern Oscillation
GCR	Galactic cosmic rays (Semantic ambiguous concept)
IERS–EOP	International Earth Rotation Service – Earth Orientation Parameters
IMF	Interplanetary magnetic field
JPL	Jet Propulsion Laboratory
Kp-index	3 h global geomagnetic activity index
LOD	Length of day
Mg II	Magnesium II wing index (solar activity index)
NASA	National Aeronautics and Space Administration
OLR	Outgoing long wave radiation
QBO	Quasi-biennial oscillation (stratospheric wind variations)
SOI	Southern Oscillation index (atmospheric mass variations)
X-ray	Electromagnetic radiation within a specified frequency range

orbits with eccentricities close to zero. What might be even more important is that they move faster than or almost as fast as the orbital motion of their mother parent planets. All these satellites move very close to the equatorial plane of its parent planet except Triton, which shares this property with Earth's moon. Our Moon is active in influencing the Earth's jet wind system. Neptune has the fastest super rotation in its equatorial wind system among all great planets despite the fact that it is the coldest one; which is remarkable. Is this feature connected with Triton passing at high absolute declinations just as Moon does? Information in Table 1 opens the question if there is friction between "space" and celestial objects. Another way to look at it is to ask if a dynamical gravity field is created when celestial bodies are energetically unbalanced. In that case there would always be an interaction between celestial bodies and such a field would create forces, torques and friction. Unexplained observational evidence such as QBO and the Chandler Wobble would be seen in a new light together with a number of other observational evidence if such a dynamical gravity field really exists. Solar system dynamics is a scientific field of great importance which involves a number of scientific disciplines.

Let us never forget the impressive uplifted shorelines in Hudson Bay (Fig. 3) or the sedimentary layers in the Elatina formation mimicking solar sunspots variations 680 million years ago. These and other evidence have written down the history of Earth for billions of years. It would be a waste of scientific talent and opportunity to ignore this history "book". It seems that we are just scratching at the surface of a sea of potential knowledge related to our solar system, our planets and all other celestial bodies it consists of.

Acknowledgements. Many thanks to my parent who always supported me whatever innovative ideas I had in mind and Inventex Aqua AB for financial support. Thanks to Nils-Axel Mörner who has had the patience to transform a manuscript to a readable scientific article and to the advice of one anonymous reviewer for positive recommendations.

Edited by: N.-A. Mörner
Reviewed by: two anonymous referees

References

Abarca del Rio, R., Gambis, D., Salstein, D., Nelson, P., and Dai, A.: Relationship between solar activity, Earth rotation and atmospheric angular momentum, Poster based on Solar activity and Earth rotation variability, J. Geodynam., 36, 423–443, 2003.

Boeyenes, J. C. A.: Commensurability in the solar system, Unit for Advanced Study, University of Pretoria, 2009.

Carusi, A., Kresak, L., Perozzi, E., and Valsecchi, G. B.: On the past orbital history of comet P/Halley, Celestial Mech., 43, 319–322, 1988.

Cook, J. R.: Volcanoes are in the wrong spot (on IO), Jet propulsion laboratory, http://www.jpl.nasa.gov/news/news.php?release=2013-125, 2013.

Drobyshevskij, E. M.: Differential rotation of the atmosphres of Jupiter and Saturn, Astr. Zh., 56, 595–605, 1977.

Emelyanenko, V. V.: Comet resonances with Jupiter, Sov. AQstron. Let., 11, 388–390, 1985.

Fairbridge, R. W. and Hillaire-Marcel, C.: An 8,000-yr palaeoclimatic record of the "Double-Hale" 45-yr solar cycle, Nature, 268, 413–416, 1977.

Fioletov, V. E.: Estimating the 27-day and 11-year solar cycle variations in tropical upper Stratospheric ozon, J. Geophys. Res., 114, 2302, doi:10.1029/2008JD010499, 2009.

Fong Chao, B.: Correlation of Interannual Length-of-day Variation with El Nino/southern oscillation, 1972–1986, J. Geophys. Res., 93, 7709–7715, 1988.

Georgiova, K., Bianchi, C. and Kirov, B.: Once again about global warming and solar activity, Mem. S. A. It., 7, 969–972, 2005.

Gigolashvili, M. Sh., Japaridze, D. R., and Kukhianidze, V. J.: Investigation of the Differential Rotation by Hα Filaments and Long-Lived Magnetic Features for Solar Activity Cycles 20 and 21, E.K. Kharadze Abastumani Astrophysical University at Ilia state University, Tbilisi, Georgia, 2010.

Glatzmaier, G. A.: Differential rotation in giant planets maintained by density-stratified turbulent convection, Geophys. Astro. Fluid, 103, 31–51, 2009.

Gouqing, Li: 27,3-day and 13.6-day Atmospheric Tide and Lunar forcing on Atmospheric Circulation, institute of Atmospheric Physics, Chinese Academy of Sciences, 2004.

Hamilton, C.: Volcanism on Jupiter's moon Io and its relation to interior processes, EGU General Assembly, held 7–12 April, 2013.

Harris, A. W. and Pravec, P.: Rotational properties of asteroids. Comets and TNOs, International astronomoical Union, doi:10.1017/S1743921305006903, 2005.

Herman, J. R. and Goldberg, R. A.: Sun, weather and Climate, NASA, Washington DC, 1978.

Hillaire-Marcel, C. and Fairbridge, R. W.: Isostasy and eustasy of Hudson Bay, Geology, 6, 117–122, doi:10.1130/0091-7613(1978)6<117:IAEOHB>2.0.CO;2, 1978.

Holman, J. M.: Kepler-9: A system of multiple planets transiting a sun-like star, confirmed by timing variations, Science, 330, 51–54, doi:10.1126/science.1195778, 2010.

Jelbring, H. R.: Celestial commensurabilities: some special cases, Pattern Recogn. Phys., in preparation, 2013.

Jewitt, D.: Cometary rotation: an overview, Institute for Astronomy, University of Hawaii, 1998.

Kargel, J. S.: Cryovolcanism on the icy satellites, Earth Moon Planets, 67, 101–113, 1995.

Kaspi, Y., Showman, A. P., Hubbard, W. B., Aharanson, O., and Helled, R.: Atmospheric confinement of jet streams on Uranus and Neptune, Nature, 497, 334–347, 2013.

Marsden, B. G. and Cameron, A. G. (Eds.): The Earth–Moon system, Plenum Press, NY, 1966.

McCracken, K. G., Beer, J., Steinhilber, F., and Abreu, J.: A phenomenological Study of the Cosmic ray Variations over the Past 9400 years, and Their Implications regarding Solar Activity and the Solar Dynamo, Solar Phys., 286, 609–627, 2013.

Mackey, R.: Rhodes Fairbridge and the idea that the solar system regulates the Earth's climate, J. Coastal Res., 50, 955–968, 2007.

Morgan, P. J., Margot, J. L., Chesley, S. R., and Vokrouhlicky, D.: Length of day and atmospheric angular momentum: a comparison for 1981–1983, J. Geophys. Res., 90, 1978–2012, 1985.

Mursula, K. and Zieger, B.: The 13.5-day periodicity in the Sun, solar wind and geomagnetic activity: The last three solar cycles, J. Geophys. Res., 101, 27077–27090, 1996.

NASA: http://nssdc.gsfc.nasa.gov/planetary/factsheet/, last access: November 2013.

NASA/JPL: Triton's volcanic plains, www.nasa.gov/mission_pages7voyager/pia12184.html (last access: November 2013), 2008.

Nugent, C. R., Margot, J. L., Chesley, S. R., and Vokrouhlický, D.: Detection of semi major Axis Drifts in 54 Near-Earth Asteroids: New Measurements of the Yarkovsky Effect, Astron. J., 144, 13 pp., doi:10.1088/0004-6256/144/2/60, 2012.

Pravec, P. and Harris, A. W.: Fast and slow rotations of Asteroids, Icarus, 148, 12–20, 2000.

Pravec, P., Harris, A. W., and Michalowski, T.: Asteroid Rotations, Astronomical Institute of the Czech Republic Academy of Sciences, Science, 000, 114–122, 2002.

Ross, J.: Asteroid Harmonics, Research Update, http://science.larouchepac.com/weekly/20130320/20130320AsteroidUpdate.pdf, 2013.

Ryan, W. H. and Ryan, E. V.: Rotational rates of recently discovered Small near-earth asteroids, Magdalena Ridge Observatory, New Mexico Institute of Mining and Technology, 2008.

Schove, D.: The sunspot cycle, 649 BC to AD 1986, J. Geophys. Res., 60, 127–146, 1955.

Shapiro, A. V., Rozanov, E., Shapiro, A. I., Wang, S., Egorova, T., Schmutz, W., and Peter, Th.: Signature of the 27-day solar rotation cycle in mesospheric OH and H_2O observed by the Aura Microwave Limb Sounder, Atmos. Chem. Phys., 12, 3181–3188, doi:10.5194/acp-12-3181-2012, 2012.

Sinclair, A. T.: The motion of Minor Planets close to Commensurabilities with Jupiter, Mon. Not. R. Astr. Soc., 142, 289–294, 1968.

Soukharev, B. and Labitzke, K.: The 11-year solar cycle, the 27-day Sun's rotation and the area of the stratospheric Aleutain High, Metorol. Z., 10, 29–36, 2001.

Takahashi, Y., Okazaki, Y., Sato, M., Miyahara, H., Sakanoi, K., Hong, P. K., and Hoshino, N.: 27-day variation in cloud amount in the Western Pacific warm pool region and relationship to the solar cycle, Atmos. Chem. Phys., 10, 1577–1584, doi:10.5194/acp-10-1577-2010, 2010.

West, R. C.: CRC Handbook of chemistry and Physics, CRC Press, Florida, 1960.

Williams, G. E.: Solar affinity of Sedimentary Cycles in the late Precambrian Elatina Formation, Austr. J. Physics, 38, 1027–1043,1985.

Williams, G. E. and Sonett, C. P.: Solar signature in sedimentary cycles from the late Precambrian Elatina Formation, Australia, Nature, 318, 523–527, 1985.

Yoshikawa, M.: Eccentricity variations of Orbits of asteroids at the mean motion resonancies with Jupiter, Astron. Astrophys., National Astronomical Observatory, Mitaka, Japan, 213, 436–458, 1989.

Part V

Planetary beat and solar–terrestrial responses. Mörner, N.-A.: Pattern Recogn. Phys., 1, 107-116, doi:10.5194/prp-1-107-2013, 2013.

Pattern Recogn. Phys., 1, 107–116, 2013
www.pattern-recogn-phys.net/1/107/2013/
doi:10.5194/prp-1-107-2013

Pattern Recognition in Physics
Open Access

Planetary beat and solar–terrestrial responses

N.-A. Mörner

Paleogeophysics & Geodynamics, Saltsjöbaden, Sweden

Correspondence to: N.-A. Mörner (morner@pog.nu)

Received: 10 September 2013 – Revised: 23 October 2013 – Accepted: 24 October 2013 – Published: 1 November 2013

Abstract. Solar activity changes with time in a cyclic pattern. The origin of those changes may be caused by planetary motion around the Sun, affecting the position of the Sun's motion with respect to the centre of mass and subjecting the Sun to changes in angular momentum and gravitational tidal forces. With modern achievements, this multi-body problem can now be addressed in a constructive way. Indeed, there are multiple criteria suggesting that the solar variability is driven by a planetary beat also affecting a number of terrestrial variables: ^{14}C and ^{10}Be production, Earth's rotation, ocean circulation, paleoclimate, geomagnetism, etc. The centennial changes between grand solar maxima and minima imply that we will soon be in a new solar minimum and, in analogy with past events, probably also in Little Ice Age climatic conditions.

1 Introduction

The geocentric model of the Universe can be regarded as the world's first and oldest model. It was presented in the middle of the 3rd century BC by Eudoxus of Cnidus and Aristotle. In the fully developed Aristotelian system, the spherical Earth is at the centre of the universe, and all other heavenly bodies (the Moon, Sun, planets and stars) are attached to 47–56 transparent concentric spheres, which rotate around the Earth (at different uniform speeds to create the rotation of bodies around the Earth). This model came to dominate science and Christian religion (where it was even elevated to a dogma) for 1800 yr until Copernicus in 1543 revealed that it was all totally wrong and the Sun must be in the centre – the heliocentric concept was re-established. In the three Keplerian laws, Kepler (1619) defined the planetary motions along very strict elliptical paths. Still in 1633, Galilei faced inquisition for his belief in the heliocentric concept. In the 1970s, it was realized (although suggested before; e.g. José, 1965) that the true centre of our planetary system is the centre of mass (CM), which even the Sun has to move around in response to the planetary beat (Landscheidt, 1976, 1979). The evolution in ruling concept over the last 2500 yr is illustrated in Fig. 1.

Although Rudolf Wolf himself proposed that the sunspot cycle was driven by the impact from Venus, the Earth, Jupiter and Saturn (Wolf, 1859) and this was further discussed by de la Rue et al. (1872), it took a century until the planetary beat theory became seriously considered (e.g. Bureau and Craine, 1970; Wood, 1975; Kuklin, 1976; Mörth and Schlamminger, 1979).

Others (e.g. Okal and Anderson, 1975) have reported the absence of any tidal effects from the planets on the Sun, the solar orbital motions being another thing, however.

2 A multi-body problem

Our solar–planetary system is a perfect example of the multi-body problem, which in principle means that the interaction of all the bodies involved – the Sun, the planets, their moons – is unsolvable with respect to gravitational interaction and individual motions.

Still, it was understood that this interaction might affect the solar activity (e.g. Mörth and Schlamminger, 1979) as well as the Sun's motion with respect to the centre of mass (e.g. José, 1965; Landscheidt, 1976).

2.1 Qualitative approaches

Personally, I tried to express these effects in different qualitative ways (Mörner, 1984a, Figs. 1 and 13; 1984b, 2013a) as illustrated in Fig. 2.

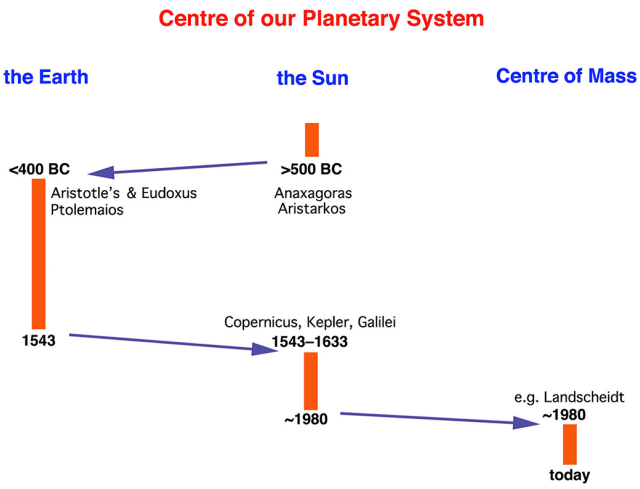

Figure 1. Changes in leading concepts of the centre of our planetary system (from Mörner, 2006).

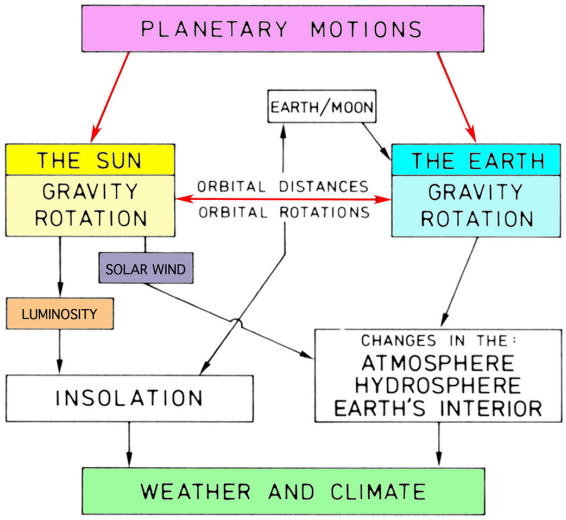

Figure 2. Planetary beat on the Sun and the Earth (rightly the Earth–Moon system) and various lines by which weather and climate may be affected (from Mörner, 1984a).

2.2 Extraterrestrial climate stress

Fairbridge (1984) formulated the situation as follows:

Extraterrestrial climate stress is applied to the planet Earth by four deterministic processes:

1. Planetary orbital motions, dominated by Jupiter and Saturn, transmit momentum by gravitational torques, causing changes in velocity and spin rate to successive planets and the Sun itself. On Earth, spin rate changes appear to trigger seismicity and volcanicity (and therefore dust veils).

2. The Sun accordingly develops its own mini-orbit around the systemic barycentre, with abrupt changes in its acceleration and turning angle that are expressed in the 11 and 22 yr solar cycle of sunspots, electromagnetic radiation of particles and particulate emission that reach the Earth and beyond as the "solar wind".

3. The Earth's geomagnetic field is modulated by the solar wind, which triggers geochemical reactions within the gases of the upper atmosphere.

4. Lunar tidal cycles, identified in many terrestrial climate series, develop standing waves in the atmosphere and help to trigger major seismic and volcanic events with contribution to the dust veil. The 18.6 yr nodal periodicity also corresponds to a nutation of the precession parameter and is commensurable in turn with the basic cycles of category 1.

2.3 Modern achievements

Obviously, we were on to something in the 1980s, but we could not yet quantify the effects. With modern achievements in statistics and computer modelling, the situation has changed considerably in theory (e.g. Wang, 1991; Diacu, 1996) as well as in practice (e.g. Scafetta, 2010, 2013a; Abreu et al., 2012).

"Is there a chronometer hidden in the Sun", Dicke asked (1978), and in opposition Wilson (2011) asked: "Do periodic peaks in the planetary tidal forces acting upon the Sun influence the sunspot cycle?". I think we are now ready to say no to Dicke and yes to Wilson, and add the following: it is an effect of the planetary beat acting upon the Sun.

3 The planetary beat

The multi-body interaction of the planetary motions on the Sun's motion is so large that the Sun's motion around the centre of mass is perturbed by up to about 1 solar radius. The planetary beat also includes the transfer of angular momentum and tidal forces (Fig. 2; further dealt with in this volume; e.g. Jelbring, 2013; Solheim, 2013; Tattersall, 2013).

The motions of the Sun around the centre of mass – in response to the planetary beat – follow cyclic pattern of 79 yr (Landscheidt, 1979) in close agreement with the main sunspot cycle over the last 2200 yr (below; Jelbring, 1995), 179 yr (José, 1965; Fairbridge and Shirley, 1987; Charvatova, 1995) not really recorded in sunspot records (Jelbring, 1995; Abreu et al., 2012) and 2160 yr (Charvatova, 1995), which may relate to the somewhat unclear Hallstatt cycle of about 2400 yr (e.g. Vasiliev and Dergachev, 2002).

The 11 yr solar cycle is well synchronized with the alignment of Venus, Earth and Jupiter (Hung, 2007; cf. Wolf, 1859; Mörth and Schlamminger, 1979; Wilson, 1987; Wilson et al., 2008; Scafetta, 2010). According to Scafetta (2010) Jupiter, Saturn, Uranus and Neptune all modulate

solar dynamics (cf. Mörth and Schlamminger, 1979). According to Fairbridge (1984) and Fairbridge and Sanders (1995a), the principle cycle generated by the planets is the Saturn–Jupiter lap of 19.857 yr. Scafetta (2010) showed that the orbital periods of Jupiter and Saturn generate significant gravitational oscillation cycles of ~ 20 and ~ 60 yr. A 9.1 yr cycle refers to the Moon's orbital cycle (Scafetta, 2010). This, however, is also the cycle of solar flares according to Landscheidt (1984).

As for the longer term effects from Jupiter and Saturn, Scafetta (2012) finds "major beat periods" of about 61, 115, 130 and 983 yr. Steinhilber et al. (2007) found major power peaks in the radionuclides record of the last 9400 yr of 86, 207, 499 and 978 yr (cf. McCracken et al., 2013). Abreu et al. (2012) "estimated the planetary torque exerted on the tachocline" and found peaks at 88, 104, 150, 208 and 506 yr, which all correlated well with similar peaks in the radionuclides record of the last 9400 yr.

4 The solar variability

The variation in the solar activity is a well-established fact, and the solar–terrestrial linkage has been addressed in numerous papers (Fairbridge and Sanders, 1995b). The Schwabe–Wolf (11 yr), Hale (22 yr), Gleissberg (88 yr) and de Vries (208 yr) cycles have all become widely recognized; their driving forces are still far from solved, however.

Observations of the changes in solar activity are limited to the last 400 yr. By considering a number of different indirect observations, Schove (1955) was able to extend the record back to 649 BC. Jelbring (1995) analysed Schove's data from 300 BC up to 1990. He found the date to be "of high quality concerning sunspot cycle length and phase information … at least 2200 yr back in time". He identified seven cycles of 200, 133, 79, 50, 42, 33 and 29 yr length.

Because the intensity of the heliomagnetic field controls the galactic cosmic ray in-fall to the upper atmosphere and hence the production of the ^{10}Be and ^{14}C radionuclides, the solar activity can be reconstructed over 9400 yr or more by recording the variability of those isotopes in different terrestrial time series (e.g. Bard et al., 2000; Solanki et al., 2004; Usoskin et al., 2007; Steinhilber et al., 2007; Abreu et al., 2012; McCracken et al., 2013).

4.1 The planetary hypothesis

The idea that the planetary beat affects and controls the solar activity is old. Generally, it was held that the impact was too small to drive solar variability. The planets may perturb the solar dynamo, however, and the effects are then likely to become amplified by some internal mechanism (Abreu et al., 2012; cf. Scafetta, 2012b).

Abreu et al. (2012; cf. Steinhilber et al., 2007) were able to show that there is an "excellent spectral agreement between the planetary tidal effects acting on the tachocline and the solar magnetic activity". This is illustrated in Fig. 3. It implies a benchmark in the planetary–solar research. The planetary hypothesis took an important step towards a planetary theory.

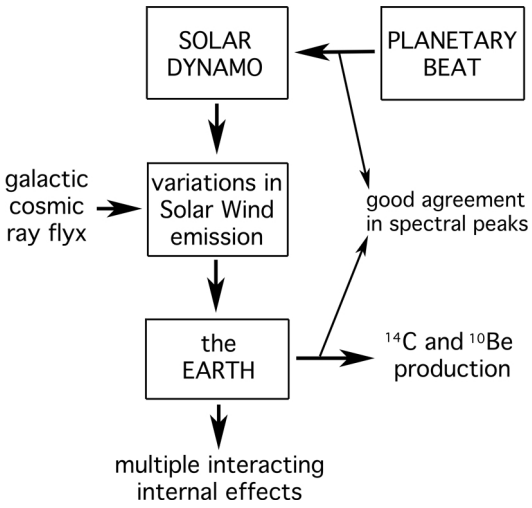

Figure 3. The planetary beat on the solar dynamo generates changes in the solar magnetic emission which controls the galactic cosmic ray flux and hence the production of ^{14}C and ^{10}Be in the Earth's upper atmosphere. The relations are evidenced by the good agreement in spectral peaks between planetary beat and production of ^{14}C and ^{10}Be (as shown by Abreu et al., 2012; these relations are further discussed and developed in Sect. 5.3).

4.2 The tachocline

The tachocline (Spiegler and Zahn, 1992; Hughes et al., 2012) seems to be the sensitive zone picking up and amplifying the planetary signals (as proposed by Abreu et al., 2012). The stratification of the outer 50 % of the Sun is illustrated in Fig. 4.

According to Scafetta (2012b), however, the Sun may operate like a nuclear fusion reactor with the capacity of amplifying the planetary tidal force signals.

5 The terrestrial responses

Planet Earth and the coupled Earth–Moon system are affected by four different solar–planetary variables, viz.

1. Transfer of heat (luminosity, irradiance) from the Sun to the Earth;
2. Solar wind interaction with the Earth's magnetosphere (Mörner, 1996a, 2012, 2013a);
3. Solar–planetary gravity interaction with the coupled Earth–Moon system;
4. Transfer of angular momentum to the coupled Earth–Moon system.

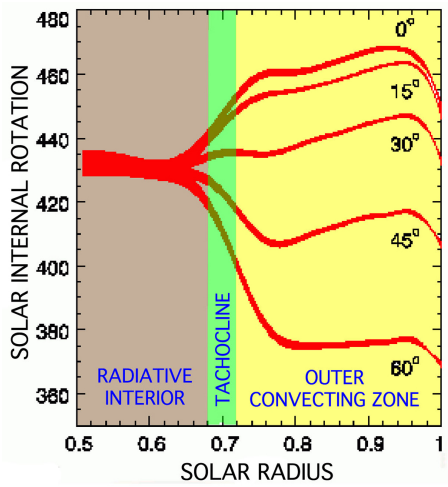

Figure 4. The tachocline at about one-third depth (~ 0.7) in the Sun separates the rigidly rotating inner part from the differentially rotating and convecting outer part generating variations in sunspots and solar flares, and the emission of solar wind.

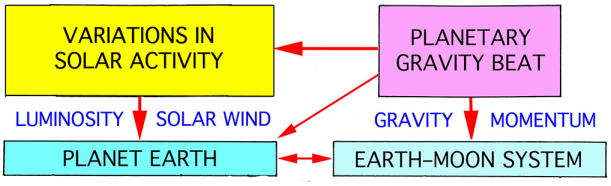

Figure 5. Planetary beat affects the Earth and the Earth–Moon system via luminosity, solar wind, gravity and momentum. Changes within the Earth–Moon system may also affect the Sun (as further discussed in Sects. 5.4 and 5.6).

This is illustrated in Fig. 5 (cf. Fig. 2). The planetary beat may hence affect the Earth both directly via its gravity pulse and indirectly via its effects on the solar dynamo. The 208 yr de Vries cycle has been identified both in the terrestrial cosmogenic radionuclides (cf. above; Abreu et al., 2012) and in the motions within the Earth–Moon system (Wilson, 2013). Consequently, this gives evidence of a twofold effect of the planetary beat; a direct gravity beat on the Earth–Moon system, and a simultaneous beat on the solar dynamo, which, via the solar wind controls of incoming cosmic rays, also controls the production of cosmogenic radionuclides (Fig. 3).

5.1 Internal effects

The cyclic planetary beat affecting the Earth (Figs. 2 and 5) gives rise to a spectrum of different processes within the Earth system. This is illustrated in Fig. 6, and has been separately addressed before (Mörner, 1984a, 1989b, 2010, 2011, 2012, 2013a).

The fact that there is a good correlation between changes in solar activity and changes in Earth's rate of rotation (LOD

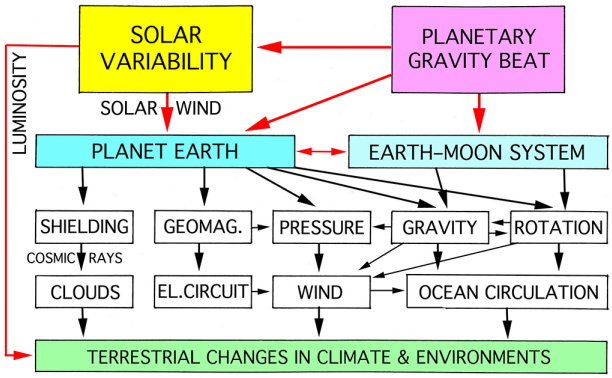

Figure 6. Planetary beat processes and the spectrum of terrestrial variables affected (from Mörner, 2012).

– length of day) can hardly be understood in other ways than that Earth's spin rate is strongly controlled by the interaction between the solar wind and the magnetosphere (Mörner, 1996a, 2010, 2012, 2013a). This is illustrated in Fig. 6 indicating that variations in solar wind (initiated by the planetary beat) affect the shielding (in-fall of cosmic rays), the geomagnetic field strength, the pressure, the gravity and the rotation.

The causation chain – solar wind variations, interaction with the magnetosphere, changes in the Earth's rate of rotation and effects on the ocean circulation – plays a central role according to the present author (Mörner, 1996a, 2010, 2011, 2012, 2013a).

5.2 Geomagnetic field changes

The strength of the magnetospheric field surrounding planet Earth is the combined effect of the interaction of the heliomagnetic field (the solar wind) and the Earth's own internal geomagnetic field. Consequently, it has both an internal and an external component, which together control the deflection of cosmic rays and hence the production of ^{14}C and ^{10}Be in the atmosphere (as illustrated in Fig. 6 of Mörner, 1984b).

Therefore some of the peaks in ^{14}C production and in-fall of ^{10}Be may have an internal origin and hence may not represent a solar activity signal. This should be considered in the spectral analyses of cosmogenic radionuclides (Fig. 3).

The strong ^{14}C peak at 2700 BP, for example, seems to be the direct effect of an internal geomagnetic anomaly (Mörner, 2003). This may well be the case with some of the other peaks, too: for example at 1000–1100 AD when there was a trans-polar geomagnetic shift (Mörner, 1991) and a major change in rotation and ocean circulation (Mörner, 1995).

Therefore, it is interesting to note that Nilsson et al. (2011) determined a 1350 yr cyclicity in the Earth's geomagnetic dipole tilt over the last 9000 yr. This cycle peaked at 2650 BP – i.e. virtually just at the above-mentioned ^{14}C peak and geomagnetic anomaly (Mörner, 2003). Furthermore, there is a

close correlation of the dipole tilt and the changes in rotation during the last 3000 yr (Nilsson et al., 2011), indicating that we are dealing with a differential rotation (Fig. 9; cf. Mörner, 1984a, 1996a) between the core and the mantle. The finding that there are two preferential dipole regions in northwestern Russia and northern Canada is consistent with the observation of flux tubes in the core and trans-polar VGP (virtual geomagnetic pole) shift indicating the displacement of the symmetry axis of two rotating bodies (Mörner, 1991).

Neither the ^{10}Be, the ^{14}C, nor the planetary beat have any peaks at around this 1350 yr cycle (McCracken et al., 2013; Tattersall, 2013) indicating that this cycle refers to an internal terrestrial cycle (as suggested by Nilsson et al., 2011). Therefore, these cyclic changes should be removed from the terrestrial cosmogenic nuclide records when trying to reconstruct solar variability from those records (e.g. Bard et al., 2000; Usoskin et al., 2007; Abreu et al., 2012; McCracken et al., 2013).

5.3 Production of cosmogenic radionuclides

The production of ^{14}C and ^{10}Be is a function of the amount of cosmic rays reaching the upper atmosphere. Variations in ^{14}C content in the atmosphere are measured in the deviation between absolute dendrochronological ages and relative radiocarbon ages, known with high accuracy for the last 9500 yr and with reasonable accuracy for the last 12 000 yr. The ^{10}Be content is distributed with precipitation, and its variations are recorded in ice cores, sediment cores, speleothems, etc.

It has often been assumed that the concentration of cosmogenic nuclides is a virtually direct function of solar variability (e.g. Bard et al., 2000; Solanki et al., 2004; Usoskin et al., 2007; Steinhilber et al., 2007; Abreu et al., 2012; McCracken et al., 2013). This is not the case, however.

The production of ^{14}C in the upper atmosphere is a function of the amount of cosmic rays being able to penetrate the magnetosphere, where the variations in shielding capacity are driven both by the solar wind (Sect. 4.1) and the Earth's own geodynamo (Sect. 5.2). This implies a double origin. Furthermore, the concentration of ^{14}C is also affected by the ocean/air ventilation and interchange of isotopes. This implies a third mode of origin. This is illustrated in Fig. 7.

The production of ^{10}Be is a function solar wind and Earth's geodynamo. Its concentration in terrestrial records is strongly controlled by precipitation. Therefore, not even ^{10}Be is a direct measure of changes in solar activity; it is only a proxy.

Therefore, the terrestrial records of ^{14}C and ^{10}Be variations must be split up into their different causation components before they can be used as true records of solar variability and analysed with respect to cyclic behaviour; if not, they only provide relative proxies.

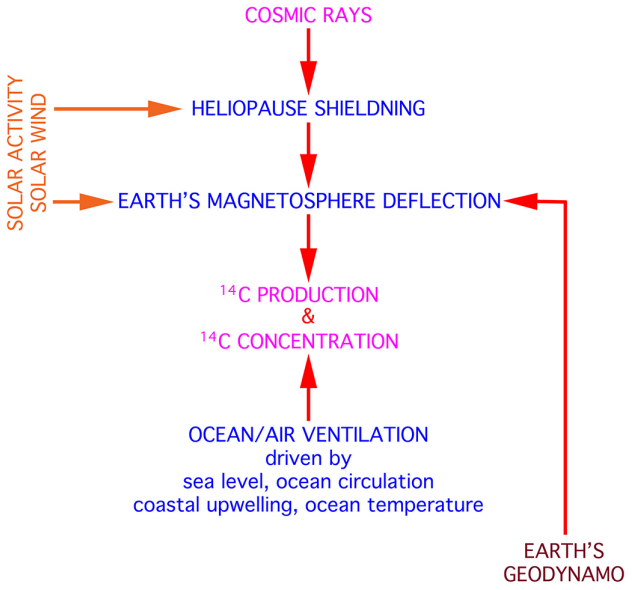

Figure 7. Illustration of the three factors controlling the ^{14}C production and concentration. Not until each factor is quantified, do we have a clear record of the solar variability.

5.4 The Earth–Moon distance

The Earth and the Moon constitute a double planet system in its motions with respect to each other and with respect to the Sun and the other planets of our solar system (i.e. a multi-body system as discussed above). The barycentre in the Earth–Moon system is located in the Earth's mantle at a depth of about 1700 km below the surface.

The Earth's rate of rotation is constantly changing. These changes must be compensated in the Earth–Moon distance (Dicke, 1966) or by interchange of angular momentum within the terrestrial system (Mörner, 1984a, 1987, 1989b, 1996a).

Dicke (1966) showed that the postglacial sea level rise after the last glaciation had to lead to a general deceleration, which had to be compensated for within the Earth–Moon system by an increased distance between the two bodies. Therefore, Mörner (1995) transferred the sea level curve of the last 30 000 yr into a curve of the changes in Earth's rate of rotation: a speed-up at the build-up of the 20 ka glaciation maximum and sea level fall to a maximum speed of an about 1800 ms higher speed at the glaciation maximum when sea level was about 120 m lower than today, and a deceleration during the sea level rise in response to the glacial melting from about 18 000 to 6000 C14 yr BP (about 22 000 to 6800 cal. yr BP). These changes had, of course, to be compensated in the Earth–Moon distance to keep the total momentum constant. When this general deceleration had finished, the Earth came into another mode dominated by regular interchanges of angular momentum between the

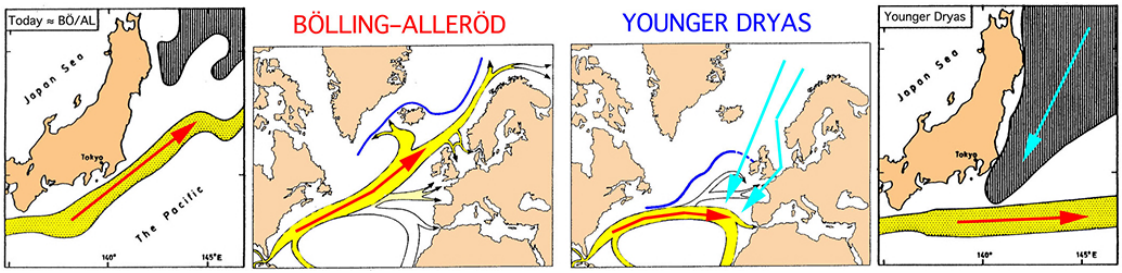

Figure 8. The strong ocean current changes in the Atlantic (middle) and in the Pacific (sides) in association with the BÖ/AL and YD high-amplitude changes in climate (based on Mörner, 1996b). These changes must be coupled with corresponding interchanges of angular momentum between the solid Earth and the hydrosphere (Mörner, 1993).

solid Earth and the hydrosphere (Mörner, 1984a, 1987, 1988, 1995, 1996a, 2013a).

The general glacial eustatic rise in sea level can be approximated by two superposed exponential curves (Mörner and Rickard, 1974). During the transitional period 13–10 C14 ka BP or 16–11.5 cal. ka BP, a sequence of extreme events occurred (Mörner, 1993): the geomagnetic pole made a sudden trans-polar shift, the onset of central uplift of Fennoscandia indicating a deformation of the gravitational potential surface; climate first underwent a sudden high-amplitude amelioration with a sudden swing of the Gulf Stream high up into the northeast Atlantic reaching into the Barents Sea, and then a high-amplitude cooling (the well-known Younger Dryas (YD) event) with extensive glacial expansion, a polar-front displacement to mid-Portugal and with large distances deflections of the Gulf Stream as well as the Kuro Siwo Current towards the Equator (Fig. 8). These changes are far too large and rapid to be understood in terms of solar variability itself. Therefore, Mörner (1993) proposed that it perhaps might be understood in terms of the strong deceleration and a delay in its compensation in the Earth–Moon system, so that it instead had to be compensated by anomalous displacements of the water masses: first to high latitudes (generating the Bölling–Alleröd warm phase – BÖ/AL) and then to low latitudes (generating the Younger Dryas cold phase). Therefore, the high-amplitude changes at around 13–10 C14 ka BP appear like the beat on a cord (Mörner, 1993).

The high-amplitude changes of the BÖ/AL warm period and the YD cold period are also recorded in the production of ^{14}C (e.g. Hughen et al., 2000; Muscheler et al., 2008). The BÖ/AL period has a low ^{14}C production due to strong shielding and high solar activity, whilst the YD period has a high ^{14}C production due to weak shielding and low solar activity (as illustrated in Fig. 7). This implies that changes in solar activity are involved in the climatic changes of the BÖ/AL and YD periods. Therefore, it seems we are facing a double origin – an internal and an external – of the high-amplitude changes within the period 16–11.5 cal. ka BP.

The question now arises of weather we can combine the internal and external factors. Indeed, Jelbring (2013) has proposed that changes in the Earth–Moon system may affect the solar activity. This opens the possibility of a cause–response relationship as follows: changes in the Earth's rotation affect the Earth–Moon system (and related parameters), which affects the solar activity.

5.5 Earth's differential rotation

The Earth consists of many different layers and sub-layers, which may move with respect to each other (Mörner, 1984a, 1987, 1988, 1996a), which, in principles, act as a multi-body system (cf. Sect. 2).

First of all it is an interchange of momentum between different layers (Fig. 9) where one speed-up has to be compensated by another slow-down in order to keep the total angular momentum constant. I have made much effort on the interchange of angular momentum between the hydrosphere (the ocean circulation) and the solid Earth, which strongly affects regional sea level (the redistribution of water masses) and climate (the redistribution of ocean-stored heat). This is well recorded in the El Niño–Southern Oscillation changes (Mörner, 1988, 1989b, 1996a, 2012), in the climatic–eustatic 60 yr cycle (cf. below; Sect. 5.7), in the atmosphere/ocean 60 yr changes (Wyatt and Curry, 2013), and the general centennial changes in ocean circulation (Mörner, 1984a, 1995, 1996a, 2010). Differential rotation between the core and the mantle has been discussed by several authors (e.g. Hide, 1970; Cortillot et al., 1978; Mörner, 1980; Braginskiy, 1982; Roberts et al., 2007; Livermore et al., 2013).

An excellent and direct example of the interchange of angular momentum between the solid Earth (LOD) and the hydrosphere comes from the 2004 Sumatra earthquake and tsunami in the Indian Ocean. In response to the tsunami wave, the solid Earth speeded up by 2.68 ms. Similarly, at the 2011 Japan earthquake the Earth speeded up by 1.8 ms.

Secondly, this internal multi-layer system, of course, sensitively picks up gravitational and rotational signals from the Sun, the planets and the Moon as illustrated in Figs. 5 and 6.

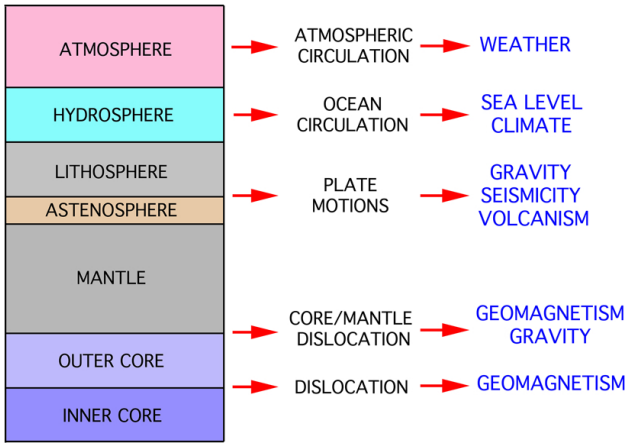

Figure 9. The Earth consists of several layers and sub-layers, which experience differential rotation with interchange of angular momentum (Mörner, 1984a, 1987, 1989b). Ocean circulation changes generate sea level changes and changes in climate (Mörner, 1989b, 1995, 2010, 2013a). Differential rotation is partly generated from internal sources (feedback interchange of angular momentum) and partly from external sources (gravitational and rotational impact from the Sun, the planets and from the Moon).

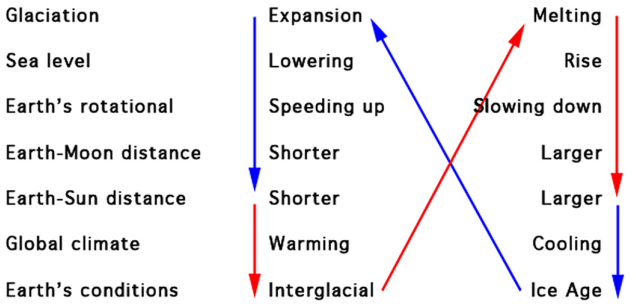

Figure 10. Hypothetical chain effects of changes in glaciation, sea level and rotation, and their effects on Earth's rotation and by that the Sun–Earth distance (Mörner, 1984b).

5.6 The Sun–Earth distance

The postglacial sea level rise and linked general rotational deceleration must be compensated as discussed above (Sect. 5.4). It should also be compensated in Earth's orbital velocity and/or the Sun–Earth distance (Mörner, 1984b, Fig. 4). According to Mörner "one may therefore hypothesize that the Earth's climate could be strongly influenced by this in some sort of feed-back mechanism" as illustrated in Fig. 10.

Even if the glacial/interglacial alterations are primarily driven by the Milankovitch variables (e.g. Roe, 2007), the Fig. 10 mechanism may imply an additional effect to account for in the Sun–Earth and planetary–Earth interactions, and hence merit at least mentioning in this volume.

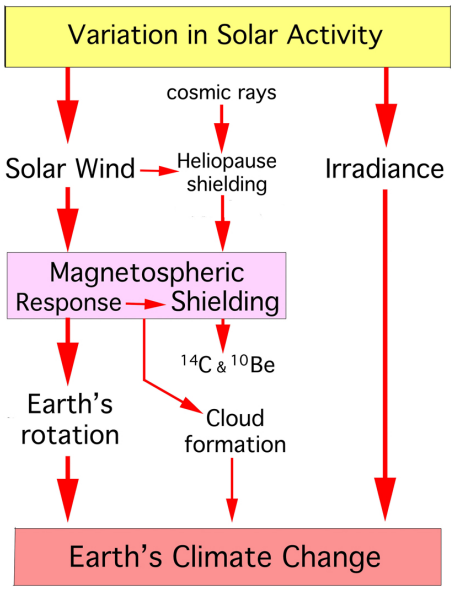

Figure 11. Three ways of affecting Earth's climate all ultimately driven by planetary beat cycles (slightly modified from Mörner, 2010, 2011).

5.7 Climatic changes

Without the constant heat energy supply from the Sun (the luminosity or irradiance), there would have been no life on planet Earth. The variations in solar activity seem to follow strict cyclic patterns. The driving forces for those cycles seem to be found in the planetary beat.

An alternative way of affecting Earth's climate is the multiple effects of the solar wind interaction with the magnetosphere, and, not least, its effects on Earth's rate of rotation and by that the ocean circulation (Mörner, 1996a, 2010, 2011, 2012, 2013a).

A third way of affecting climate is via the cloud formation as a function of cosmic ray flux (Svensmark, 1998, 2007; Svensmark et al., 2013).

These three ways of affecting Earth's climate are illustrated in Fig. 11.

According to Scafetta (2010, 2013a), the beat of Jupiter and Saturn generates a 60 yr cycle, which is also present in global temperature records (close to the 65–70 yr global temperature cycle of Schlesinger and Ramankutty, 1994). The 60 yr cycle is recorded in the atmospheric circulation (Mazzarella, 2007; Wyatt and Curry, 2013), different oceanic parameters (in ocean circulation by Mörner, 2010, 2013a; in the Gulf Stream beat by Mörner, 2010, 2013a; in Barents Sea fish catch by Klyashtorin et al., 2009; in sea level changes by Chambers et al., 2012; Mörner, 2013b; Parker, 2013 and Scafetta, 2013b), in climate (e.g. Akasofu, 2013), in rotation (e.g. Mazzarella, 2007) and in geomagnetics (Braginskiy, 1982; Roberts et al., 2007). This cycle is not present in the cosmogenic radionuclide records, however (Abreu et

al., 2012, Fig. 5). Therefore, its origin may be a direct gravitational effect on the Earth–Moon system and the differential rotation of the Earth (Figs. 5–6; Mörner, 1884a, 2013a), rather than an effect of solar wind interaction with the Earth's magnetosphere. In the power spectrum of the cosmogenic changes according to Bard et al. (2000), there is a peak at 63–66 yr (Scafetta, 2012a), implying that a solar wind origin cannot be ruled out, however.

5.8 Grand minima

At the Spörer, Maunder and Dalton solar minima, the Earth experienced a rotational speed-up (decreased LOD), a deflection of the Gulf Stream to its southern course and a southward penetration of Arctic water all the way down to mid-Portugal (Mörner, 1995, 2010, 2011). This generated Little Ice Age conditions in the Arctic, northern Atlantic and northwest Europe. At around 2030–2050, we will be in a new grand minimum situation (as evidenced by a large number of authors: e.g. Mörner, 2010, 2011; Cionco and Compagnucci, 2012; Casey and Humlum, 2013; Salvador, 2013). The driving forces seem to be the planetary beat and its effects on the solar activity, and the effects of the solar wind upon the Earth (Fig. 6). During previous solar minima, the Earth experienced Little Ice Age climatic conditions. Therefore, we may once again experience such climatic conditions when the new grand minimum occurs (Mörner, 2010, 2011).

6 Conclusions

The planetary motion generates a beat on the Sun in the form of gravity (tidal force), angular momentum and motions with respect to the centre of mass. This beat generates cyclic changes in the Sun's activity. The sensitive zone in the Sun is likely to be the tachocline.

The changes in solar activity control the solar luminosity (irradiance) and solar wind emission, both factors of which affect the Earth as illustrated in Figs. 6 and 11.

The planetary beat also affects the Earth–Moon system directly via tidal forces and angular momentum.

The correlation between changes in solar activity and Earth's rate of rotation (LOD) seems primarily to be a function of the solar wind interaction with the magnetosphere.

At the next solar minimum, to occur around 2030–2050, there might be a return to Little Ice Age climatic conditions (as was the case during the Dalton, Maunder and Spörer minima).

The planetary beat hypothesis has become a theory. There is, of course, much more to learn, decode and improve, but the theory is here to stay.

Edited by: S.-A. Ouadfeul
Reviewed by: J.-E. Solheim and one anonymous referee

References

Abreu, J. A., Beer, J., Ferriz-Mas, A., McCracken, K. G., and Steinhilber, F.: Is there a planetary influence on solar activity?, Astron. Astrophys., A88, 1–9, 2012.

Akasofu, S.-I.: On the present halt of global warming, Climate, 1, 4–11, 2013.

Bard, E., Raisbeck, G., Yiou, F., and Jouzel, J.: Solar irradiance during the last 1200 years based on cosmogenic nuclides, Tellus, 52B, 985–992, 2000.

Braginskiy, S. I.: Analytical description of the secular variations of the geomagnetic field and the rate of rotation of the Earth, Geomagn. Aeronomy, 22, 88–94, 1982.

Bureau, R. A. and Craine, L. B.: Sunspots and planetary orbits, Nature, 228, 984, doi:10.1038/228984a0, 1970.

Casey, J. and Humlum, O.: Global Climate Status Report for 2013, Space and Science Research Corporation (SSRC), September 2013, 1–15, www.spaceandscience.net, 2013.

Chambers, D. P., Merrifield, M. A., and Nerem, R. S.: Is there a 60-year oscillation in global mean sea level, Geophys. Res. Lett., 39, L18607, doi:10.1029/2012GL052885, 2012.

Charvatova, I.: Solar-terrestrial and climatis variability during the last several millennia in relation to solar intertial motion, in: Climate: History, Periodicity and Predictability, edited by: Rampino, M. R., Sanders, J. E., Newman, W. S., and Königsson, L. K., van Nostrand Reinhold, 1343–1354, 1995.

Cionco, R. G. and Compagnucci, R. H.: Dynamicas characterization of the last prolonged solar minima, Adv. Space Res., 50, 1434–1444, 2012.

Copernicus, N.: De revolutionibus orbium coelestium, 1543.

Cortillot, V., Ducroix, J., and Le Mouel, J.-L.: Sur une acélérationrécente de la variation séculaire du champmagnétique terrestre, C.R. Acad. Sci. Paris, 287, 1095–1098, 1978.

de la Rue, W., Stewart, B., And Loewy, B.: Further investigations on planetary influence upon solar activity, http://tallbloke.wordpress.com/2012/11/06, 1872.

Diacu, F.: The solution of the n-body problem, Math. Intell., 18, 66–70, 1996.

Dicke, R. H.: The secular acceleration of the Earth's rotation and cosmology, in: The Earth–Moon system, edited by: Marsden, B. G. and Cameron, A. G., 98–164, Plenum Press, NY, 1966.

Dicke, R. H.: Is there a chronometer hidden in the Sun?, Nature, 276, 676–680, 1978.

Fairbridge, R. W.: Planetary periodicities and terrestrial climate stress, in: Climatic Changes on a Yearly to Millennial Basis, edited by: Mörner, N.-A. and Karlén, W., 509–520, Reidel Publ. Co. (Dordrecht/Boston/Lancaster), 1984.

Fairbridge, R. W. and Sanders, J. E.: The Sun's orbit, A.D. 750–2050: Basis for new perspectives on planetary dynamics and Earth-Moon linkage, in: Climate: History, Periodicity and Predictability, edited by: Rampino, M. R., Sanders, J. E., Newman, W. S., and Königsson, L. K., 446–471, van Nostrand Reinhold, 1995a.

Fairbridge, R. W. and Sanders, J. E.: Selected bibliography on Sun–Earth relationships and cycles having periods less than 10,000 years, in: Climate: History, Periodicity and Predictability, edited by: Rampino, M. R., Sanders, J. E., Newman, W. S., and Königsson, L. K., 475–541, van Nostrand Reinhold, 1995b.

Fairbridge, R. W. and Shirley, J. H.: Prolonged minima and the 179-yr cycle or the solar inertial motion, Sol. Phys., 110, 191–220, 1987.
Galilei, G.: Mumbling "E pur si muove" (sic movit) at facing the inquisition in 1633.
Hide, R.: Interaction between the Earth's liquid core and solid mantle, Nature, 222, 1055–1056, 1970.
Hughen, K. A., Southon, J. R., Lehman, S. J., and Overpeck, J. T.: Synchronous radiocarbon and climate shifta during the last deglacialtion, Science, 290, 1951–1954, 2000.
Hughes, D. W., Rosner, R., and Weiss, N. O.: The Solar Tachocline, Cambridge Univ. Press, 2012.
Hung, C.-C.: Apparent relations between solar activity and solar tides caused by the planets, Report NASA/TM-2007-214817, http://gltrs.grc.nasa.gov/Citations.aspx?id=330S, 2007.
Jelbring, H.: Analasis of sunspot cycle phase variations – based on D. Justin Schove's proxy data, J. Coastal. Res., S.I. 17, 363–369, 1995.
Jelbring, H.: Energy transfer in the Solar System, Pattern Recogn. Phys., in preparation, 2013.
José, P. D.: Sun's motion and sunspots, Astron. J., 70, 193–200, 1965.
Kepler, J.: Harmonice mundi, 1619.
Klyashtorin, L. B., Borisov, V., and Lyubushin, A.: Cyclic changes of climate and major commercial stocks of the Barents Sea, Mar. Biol. Res., 5, 4–17, 2009.
Kuklin, G. V.: Cyclical and secular variations in solar activity, in: Basic Mechanisms of Solar Activity, edited by: Bumba, V. and Kleczek, J., IAU Symp. 71, 147–190, Reidel Publ. Co., 1976.
Landscheidt, T.: Beziehungen zwischen der Sonnenaktivität und dem Massen-zentrum des Sonnensystem, Nachr. Olders-Ges. Bremen, 100, 2–19, 1976.
Landscheidt, T.: Swinging Sun, 79-year cycle, and climate change, J. Interdiscipl. Cycle, 12, 3–19, 1979.
Landscheidt, T.: Cycles of solar flares and weather, in: Climatic Changes on a Yearly to Millennial Basis, edited by: Mörner, N.-A. and Karlén, W., 473–481, Reidel Publ. Co. (Dordrecht/Boston/Lancaster), 1984.
Livermore, P. W., Hollerbach, R., and Jackson, A.: Elecromagnetically driven westward drift and inner-core superrotation in Earth's core, P. Natl. Acad. Sci., 110, 15914–15918, 2013.
Mazzarella, A.: The 60-year solar modulation of global air temperature: the Earth's rotation and atmospheric circulation connection, Theor. Appl. Climatol., 88, 193–199, 2007.
McCracken, K. G., Beer, J., Steinhilber, F., and Abreu, J.: A phenomenological study of the cosmic ray variations over the past 9400 years, and their implication regarding solar activity and solar dynamo, So. Phys., 286, 609–627, 2013.
Mörner, N.-A.: Eustasy and geoid changes as a function of core/mantle changes, in: Earth Rheology, Isostasy and Eustasy, edited by: Mörner, N.-A., 535–553, Wiley (Chichester/New York/Brisbane/Toronto), 1980.
Mörner, N.-A.: Planetary, solar, atmospheric, hydrospheric and endogene processes as origin of climatic changes on the Earth, in: Climatic Changes on a Yearly to Millennial Basis, edited by: Mörner, N.-A. and Karlén, W., 483–507, Reidel Publ. Co. (Dordrecht/Boston/Lancaster), 1984a.
Mörner, N.-A.: Terrestrial, solar and galactic origin of the Earth's geophysical variables, Geogr. Ann., 66A, 1–9, 1984b.
Mörner, N.-A.: Short-term paleoclimatic changes; observational data an a novel causation model, in: Climate; History, Periodicity and Predictability, edited by: Rampino, M. R., Sanders, J. E., Newman, W. S., and Königsson, L.-K., 256–269, van Nostrand Reinhold Co, 1987.
Mörner, N.-A.: Terrestrial variations within given energy, mass and momentum budgets; Paleoclimate, sea level, paleomagnetism, differential rotation and geodynamics, in: Secular Solar and Geomagnetic Variations in the Last 10,000 Years, edited by: Stephenson, F. R. and Wolfendale, A. W., 455–478, Kluwer Acad. Press, 1988.
Mörner, N.-A.: Global Change: The lithosphere: Internal processes and Earth's dynamicity in view of Quaternary observational data, Quaternary Int., 2, 55–61, 1989a.
Mörner, N.-A.: Changes in the Earth's rate of rotation on the El Niño to century basis, in: Geomagnetism and Paleomagnetism, edited by: Lowes, F. J. et al., 45–53, Kluwer Acad. Press, 1989b.
Mörner, N.-A.: Trans-polar VGP shifts and Earth's rotation, Geophysics Astrophysics Fluid Dynamics, 60, 149–155, 1991.
Mörner, N.-A.: Global change: the high-amplitude changes 13–10 ka ago – novel aspects, Global Planet. Change, 7, 243–250, 1993.
Mörner, N.-A.: Earth rotation, ocean circulation and paleoclimate, GeoJournal, 37, 419–430, 1995.
Mörner, N.-A.: Global Change and interaction of Earth rotation, ocean circulation and paleoclimate, An. Brazilian Acad. Sc., 68 (Supl. 1), 77–94, 1996a.
Mörner, N.-A.: Earth rotation, ocean circulation and paleoclimate: the North Atlantic–European example, Geol. Soc. Spec. Publ., 111, 359–370, 1996b.
Mörner, N.-A.: The 2700 BP solar-terrestrial signal, EGS-AGU-EUG meeting, Nice, 6–11 April, Abstracts ST1, 2003.
Mörner, N.-A.: 2500 years of observations, deductions, models and geoethics, Boll. Soc. Geol. It., 125, 259–264, 2006.
Mörner, N.-A.: Solar Minima, Earth's Rotation and Little Ice Ages in the Past and in the Future. The North Atlantic – European case, Global Planet. Change, 72, 282–293, 2010.
Mörner, N.-A.: Arctic environment by the middle of this century, Energy & Environment, 22, 207–218, 2011.
Mörner, N.-A.: Planetary beat, Solar Wind and terrestrial climate, in: Solar Wind: Emission, Technology and Impacts, edited by: Escaropa, C. D. and Berós Cruz, A. F., 47–66, Nova, 2012.
Mörner, N.-A.: Solar Wind, Earth's rotation and changes in terrestrial climate, Physical Review & Research International, 3, 117–136, 2013a.
Mörner, N.-A.: Sea level changes: past records and future expectations, Energy & Environment, 24, 509–536, 2013b.
Mörner, N.-A. and Rickard, D.: Quantitative analyses of eustatic changes and climate cycles, Colloque Int. CNRS, 219, 142–153, 1974.
Mörth, H. T. and Schlamminger, L.: Planetary motions, sunspots and climate, in: Solar-Terrestrial influences on Weather and Climate, edited by: McCormac, B. M. and Seliga, T. A., 193–207, Reidel Publ. Co, 1979.
Muscheler, R., Kromer, B., Björck, S., Svensson, A., Friedrich, M., Kaiser, K. F., and Southon, J.: Tree rings and ice cores reveal ^{14}C calibration uncertainties during the Younger Dryas, Nat. Geosci., 1, 263–267, 2008.

Nilsson, A., Muscheler, R., and Snowball, I.: Millennial scale cyclicity in the geodynamo inferred from dipole reconstructions, Earth Planet. Sc. Lett., 311, 299–305, 2011.
Okal, E. and Anderson, D. L.: On the planetary theory of sunspots, Nature, 253, 511–513, 1975.
Parker, A.: Natural oscillations and trends in long-term tide gauge records from the Pacific, Pattern Recogn. Phys., 1, 11–23, doi:10.5194/prp-1-11-2013, 2013.
Roberts, P. H., Yu, Z. J., and Russell, C. T.: On the 60-year signal from the core, Geophys. Astro. Fluid, 101, 11–35, 2007.
Roe, G.: In defense of Milankovitch, Geophys. Res. Lett., 33, L24703, doi:10.1029/2006GL027817, 2007.
Salvador, R. J.: A mathematical model of the sunspot cycle for the past 1000 years, Pattern Recogn. Phys., in preparation, 2013.
Scafetta, N.: Empirical evidence for a celestial origin of the climate oscillations and its implications, J. Atmos. Sol.-Terr. Phy., 72, 951–970, 2010.
Scafetta, N.: Multi-scale harmonic model for solar and climate cyclical variation throughout the Holocene based on Jupiter-Saturn tidal frequencies plus the 11-year solar dynamo cycle, J. Atmos. Sol.-Terr. Phy., 80, 296–311, 2012a.
Scafetta, N.: Does the Sun work as a nuclear fusion amplifier of planetary tidal forcing? A proposal for a physical mechanism based on the massluminosity relation, J. Atmos. Sol.-Terr. Phy., 81–82, 27–40, 2012b.
Scafetta, N.: Solar and planetary oscillation control on climate change: hind-cast, forecast and comparison with the CMIP5 GCMS, Energy & Environment, 24, 455–496, 2013a.
Scafetta, N.: Discussion on common errors in analyzing sea level accelerations, solar trends and global warming, Pattern Recogn. Phys., 1, 37–57, doi:10.5194/prp-1-37-2013, 2013b.
Schlesinger, M. E. and Ramankutty, N.: An oscillation in the global climate system of period 65–70 years, Nature, 367, 723–726, 1994.
Schove, D.: The sunspot cycle, 649 BC to AD 1986, J. Geophys. Res., 60, 127–146, 1955.
Solanki, S. K., Usoskin, I. G., Kromer, B., Schüssler, M., and Beer, J.: An unusually active Sun during recent decades compared to the previous 11,000 years, Nature, 431, 1084–1087, 2004.
Solheim, J. E.: Signals from the planets, via the Sun to the Earth, Pattern Recogn. Phys., in preparation, 2013.
Spieger, E. and Zahn, J.-P.: The solar tachocline, Astron. Astrophys., 265, 106–114, 1992.
Steinhilber, F., Abreu, J. A., Beer, J. et al.: 9,400 years of cosmic radiation and solar activity from ice cores and tree rings, P. Natl. Acad. Sci., 109, 5967–5971, 2007.
Svensmark, H.: Influence of cosmic rays on Earth's climate, Phys. Rev. Lett., 81, 5027–5030, 1998.
Svensmark, H.: Cosmoclimatology: A new theory emerges, Astron. Geophys., 48, 1.18–1.24, 2007.
Svensmark, H., Enghoff, M. B., and Pedersen, J. O. P.: Response of cloud condensation nuclei (> 50 nm) to change in ion-nucleation, Phys. Lett., A377, 2343–2347, 2013.
Tattersall, R.: Are solar variation and terrestrial climate influenced by the spatio-temporal distribution of mass in the Heliosphere?, Pattern Recogn. Phys., in preparation, 2013.
Usoskin, I. G., Solanki, S. K., and Kovaltsov, G.A .: Grand minima and maxima of solar activity: new observational constrains, Astron. Astrophys., 471, 301–307, 2007.
Vasiliev, S. S. and Dergachev, V. A.: The ~2400-year cycle in atmospheric radiocarbon concentration: bispectrum of ^{14}C data over the last 8000 years, Ann. Geophys., 20, 115–120, doi:10.5194/angeo-20-115-2002, 2002.
Wang, Q.: The global solution of the n-body problem, Celes. Mech. Dyn. Astr., 50, 73–88, 1991.
Wilson, I.: Connecting the 208 year de Vries cycle with the Earth-Moon system, http://tallbloke.wordpress.com/, 22 August, 2013.
Wilson, I. R. G.: Do periodic peaks in the planetary tidal forces acting upon the Sun influence the sunspot cycle?, General Science Journal, 1–25, 2011.
Wilson, I. R. G., Carter, B. D., and Waite, I. A.: Does a spin-orbit coupling between the Sun and the Jovian Planets govern the solar cycle?, Publ. Astronomical Society of Australia, 25, 85–93, 2008.
Wilson, R. M.: On the distribution of sunspot cycle periods, J. Geophys. Res., 92, 10101–10104, 1987.
Wolf, R.: Extract of a letter to Mr. Carrington, Mon. Not. R. Astron. Soc., 19, 85–86, 1859.
Wood, R. M.: Comparison of sunspot periods with planetary synodic period resonances, Nature, 255, 312–313, 1975.
Wyatt, M. G. and Curry, J. A.: Role of Eurasian Arctic shelf sea ice in a secularly varying hemispheric climate signal during the 2oth century, Clim. Dynam., in press, 2013.

Part VI

Signals from the planets, via the Sun to the Earth. Solheim, J.-E.: Pattern Recogn. Phys., 1, 177-184, doi:10.5194/prp-1-177-2013, 2013.

Pattern Recogn. Phys., 1, 177–184, 2013
www.pattern-recogn-phys.net/1/177/2013/
doi:10.5194/prp-1-177-2013

Pattern Recognition in Physics
Open Access

Signals from the planets, via the Sun to the Earth

J.-E. Solheim

formerly at: Department of Physics and Technology, University of Tromsø, Norway

Correspondence to: J.-E. Solheim (janesol@online.no)

Received: 7 October 2013 – Revised: 21 November 2013 – Accepted: 22 November 2013 – Published: 10 December 2013

Abstract. The best method for identification of planetary forcing of the Earth's climate is to investigate periodic variations in climate time series. Some natural frequencies in the Earth climate system seem to be synchronized to planetary cycles, and amplified to a level of detection. The response by the Earth depends on location, and in global averaged series, some planetary signals may be below detection. Comparing sea level rise with sunspot variations, we find phase variations, and even a phase reversal. A periodogram of the global temperature shows that the Earth amplifies other periods than observed in sunspots. A particular case is that the Earth amplifies the 22 yr Hale period, and not the 11 yr Schwabe period. This may be explained by alternating peak or plateau appearance of cosmic ray counts. Among longer periods, the Earth amplifies the 60 yr planetary period and keeps the phase during centennials. The recent global warming may be interpreted as a rising branch of a millennium cycle, identified in ice cores and sediments and also recorded in history. This cycle peaks in the second half of this century, and then a 500 yr cooling trend will start. An expected solar grand minimum due to a 200 yr cycle will introduce additional cooling in the first part of this century.

1 Introduction

The near similarity of the length of the 11 yr sunspot cycle and the 11.8 yr orbital period of Jupiter has led to speculations about a possible connection between the planets and solar activity periods. This is discussed in other papers in this issue (Mörner, 2013a; Scafetta and Willson, 2013b; Solheim, 2013; Tattersall, 2013; Wilson, 2013).

The general argument against the hypothesis that the planets may have some control on the Earth's climate is that the effect of gravity on the Earth or the Sun from the planets is too small to have any direct effect (de Jager and Verdsteegh, 2005). In addition, the giant planets may be too far away to interact with the magnetic fields of the Earth or the Sun. In order to have an effect, the weak signal from the planets needs to be amplified, maybe of the order of 10^4–10^5. Recently two possible mechanisms for amplification in the Sun have been proposed.

Abreu et al. (2012) propose that tidal torque from the planets may introduce deformation of a non-spherical tachocline and change its capacity for storage of magnetic flux tubes, which may develop into sunspots. The amplification can be the result of a resonance effect meditated by gravity waves. A non-spherical tachocline is consistent with helioseismological observations.

Another mechanism proposed by Scafetta (2012a) is that the nuclear burning in the solar core is modulated by tidal interaction from the planets. From mass–luminosity relations for solar type stars, he calculates that the amplification can be of the order of 4×10^6, which is enough to explain the TSI (total solar irradiance) variations observed. The cyclic variation in nuclear burning is assumed to be transferred to the surface of the Sun by gravity waves.

These amplification mechanisms are not proved, but strongly supported by similarities in periodicities calculated from planetary orbits and observed in ^{10}Be, ^{14}C and other solar activity indicators (Scafetta, 2010; Abreu et al., 2012).

In the following we will assume that an amplification of a tiny planetary signal takes place in the Sun, and that this signal is imbedded in the solar wind or in TSI variations. We will investigate the response to some of these planetary signals in our climate system. There are many processes between the Sun and the climate system, which may modify the frequency, amplitude and phase of a planetary–solar signal (Mörner, 2013a, Fig. 6). The response to a solar signal may differ at various places on the Earth, and the response may

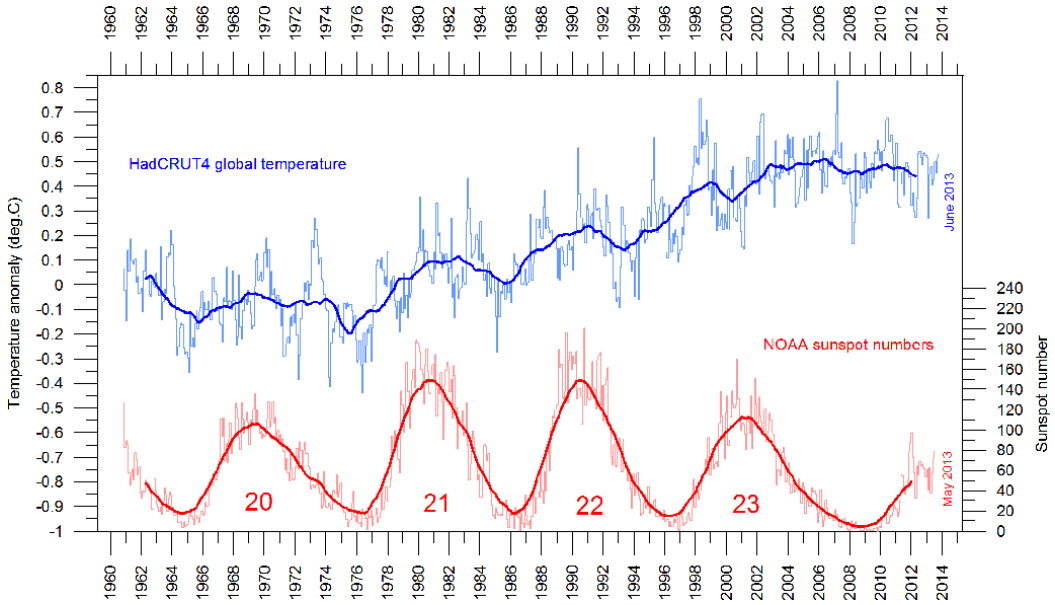

Figure 1. The thin lines show monthly sunspot numbers (red) since 1960 and HadCRUT4 monthly values of global temperature (blue). The thick lines are 3 yr running averages. Sunspot cycle numbers for SC20–23 are indicated (graph provided by Ole Humlum).

be phase-shifted due to the thermal inertia and heat transported by air and ocean or other processes. We may therefore not expect to find the same response everywhere, and in global averages some signals may be below detection. On the other hand, if we find phase-locked solar periods, it is a high probability that they are from the Sun. In addition there may be natural frequencies in the Earth's climate system that respond to external periodic forcing. Scafetta (2010) found 11 periods between 5 and 100 yr in global temperature series, corresponding approximately to periods calculated from the orbits of the planets (see Fig. 7).

In this investigation we will first compare global temperature and solar activity (Sect. 2), then sea-level change and solar activity (Sect. 3). In Sect. 4 we will investigate if periods between 5 and 80 yr observed in the Sun, with assumed planetary origin, also are present in global temperature series, and show how cosmic rays may modulate the signal. In Sect. 5 we look for solar signals in the climate on centennial and millennial timescales, including historical evidence of solar activity-related climate periods. Finally, in Sect. 6 we discuss our findings, and what this may tell us about the Earth's future climate.

2 Global temperature and solar activity

A comparison of the variations of sunspots numbers with the global temperature is shown in Fig. 1. The general picture is that the temperature roughly follows the sunspot variations up and down, indicating a heating and cooling sequence. The effect is of the order of 0.1–0.2 °C in a solar cycle (SC) and largest in SC21. In SC21–23, it looks as if the global temperature does not return to the same level as in the previous minima. One explanation may be that the cycle is too short for a complete cooling, and the temperature increase in 1980–2000 is a result of the higher solar activity in SC21–22 compared to SC20 and 23. Another possibility is that a warming trend started in about 1976 and leveled off after 2000. We shall later (Fig. 3) see that this warming trend may be interpreted as part of a 60 yr warming/cooling cycle.

A detailed analysis of the relation between the cycle-averaged sunspot number and global temperature in the same interval, delayed 3 yr, shows a correlation of $r = 0.77$ for SC10–21, and $r = 0.975$ if SC16–19 are excluded (Stauning, 2011). In this period (1923–1964) solar activity increased significantly, and the temperature variations were for a while leading the sunspot number variations. The maximum temperature increase during one cycle was 0.05 °C, which corresponds to about 0.1 % irradiance increase over a cycle. He concludes that changes in terrestrial temperatures are related to sources different from solar activity after 1985 (SC22).

A much stronger response is observed by comparing the sea surface temperature (SST) global ocean heat content (OHC) and Atlantic OHC variations folded over solar cycles since 1950. The correlations between the reconstructed solar flux and SST, OHC global and OHC Atlantic are $r = 0.83$, 0.79 and 0.86, respectively (Shaviv, 2008), and the peak-to-peak sea surface temperature varies from 0.08 to 0.10 °C over a solar cycle. This is a factor of five larger than that calculated from the TSI variations, and requires an amplification mechanism, which is not identified, but could be low cloud cover modulated by the galactic cosmic ray (GCR) variations (Shaviv, 2008, Fig. 3).

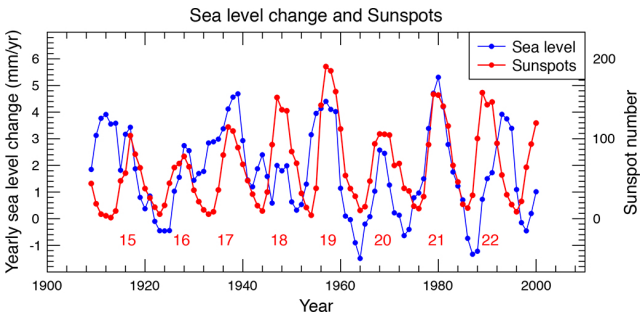

Figure 2. A comparison of yearly sea level change (Holgate, 2007) and yearly averaged sunspot numbers.

3 Sea level change and solar activity

A stronger effect related to solar cycles is seen in Fig. 2, where the yearly averaged sunspot numbers are plotted together with the yearly change in coastal sea level (Holgate, 2007). The sea level rates are calculated from nine distributed tidal gauges with long records, which were compared with a larger set of data from 177 stations available in the last part of the century. In most of the century the sea level varied in phase with the solar activity, with the Sun leading the ocean, but in the beginning of the century they were in opposite phases, and during SC17 and 19 the sea level increased before the solar activity.

The coastal sea level variation cannot be explained as due to expansion/contraction of the oceans due to heating/cooling during a solar cycle as proposed by Shaviv (2008) simply because, near the shore, the thermal expansion becomes zero since the expansion is proportional to the depth (Mörner, 2013b). The good correlation and nearly in-phase response between solar activity and sea level indicates that this is a direct mechanical response – and not a thermal response that needs time to heat up and cool, and therefore shows delayed response. This may be seen comparing Figs. 1 and 2.

An explanation for the sea level variations is found in the extremely good correlation between sunspots and rotation of the Earth expressed as semi-annual length of day (LOD) variations (Le Moël et al., 2010, their Fig. 1). The sunspot numbers are leading approximately 1 yr, and the correlation coefficient is $r = 0.76$ after detrending. They attribute the 10.5 yr modulation of LOD through a modulation of the excitation function of the zonal wind, and also show that GCR (see Fig. 5) correlates extremely well with the semi-annual LOD variations. This indicates that the GCR may act as a link between solar activity variations and the Earth rotation through various proposed mechanisms such as seasonal cloud variations, variations in the Earth's electric circuits or atmospheric aerosols, which again are modulated by the solar wind (Svensmark and Friis-Christensen, 1997; Svensmark et al., 2013; Tinsley et al., 2007). If the solar wind carries signals from the planets, either from their control of the solar activity by tidal effects or by direct electro-magnetic interaction, this signal may be transferred to the Earth's climate system.

4 The strong 60, 22 and 9 yr periods, but weak 11 yr period in the global temperature

A periodogram of sunspot number variations since 1850 shows that the strongest periods are in the 10–12 yr Schwabe band (Fig. 3a), while the Hale period at 22 yr is quite weak. Figure 3b shows a periodogram for the same period for the HadCRUT4 global temperature. Here the dominant periods are 155, 66, 21.6 and 9.14 yr. The difference means that the Earth as a whole does not respond to the dominant solar periods. This will be discussed later.

The global temperature variations since 1850 can be modeled with a linear trend of $+0.0047\,^{\circ}\mathrm{C\,yr^{-1}}$ and the four dominant periods: 155, 66, 21.6 and 9.14 yr as shown in the periodogram in Fig. 3b. The resulting temperature curve with this model is shown in Fig. 4.

We had expected a strong signal at $P = 10$–12 yr, where the sunspot variation is strongest, as shown in Fig. 3a, but instead we observe a strong 22 yr period, and an even stronger 66 yr component. The differences between Fig. 3a and b may tell us something about filtering and amplification of solar signals in our climate system.

The dominance of a 22 yr period compared with a 10–12 yr period can be explained by GCR variations. The 22 yr Hale period is the Sun's magnetic period, and represents a polarity change in the two hemispheres of the Sun. This is observed in the GCR variations as shown in Fig. 5. During solar cycles with negative polarity of the Sun's northern polar field, the GCR variation has a peaked form. In the other phase it has a plateau. This is an effect of the differences in cosmic ray drift in the positive and negative phases of the magnetic cycle. Integrated GCR counts are higher in plateau cycles compared with peak cycles (Ogurtsov et al., 2003), and this may be the reason for the amplification of the 22 yr component in the global temperature curve.

The difference between 11 and 22 yr climate response is also seen in the latitudinal difference in the rhythm of growth in pine trees, as shown in Fig. 6, where the 20 yr period dominates north of 65 degrees latitude, while the 10 yr period dominates at lower latitudes. This may be a result of differences in atmospheric circulation or effects of cosmic rays of lower energies reaching deeper at higher latitudes. For Svalbard at 78° N, an analysis by Humlum et al. (2011) shows that periods 17 and 26 yr are much stronger than those at 10–12 yr.

The filtering, phase changes, and response of natural frequencies make it difficult to find exact correspondence between the solar and planetary periods in the Earth's climate system. One possibility is to search for quasi-periodic oscillations in the same frequency bands as forced by the

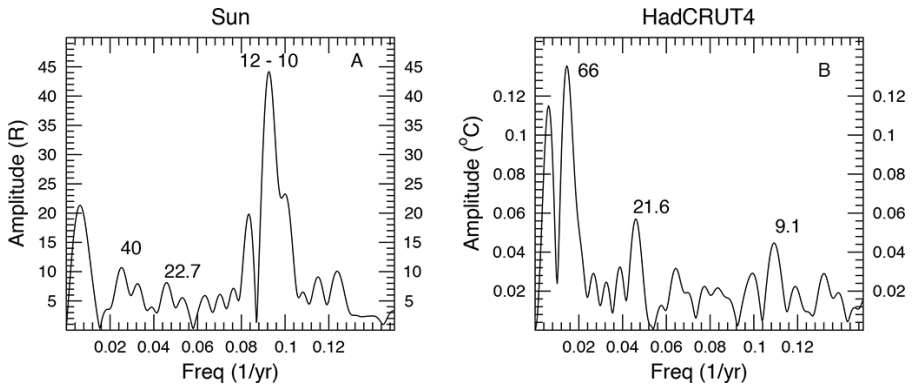

Figure 3. Periodogram of the sunspot record from 1850 **(A)** and the global temperature for the same period **(B)**. The periods (in yr) of the strongest peaks are indicated. *R* is the average yearly sunspot number. The strongest periods (in yr) are shown.

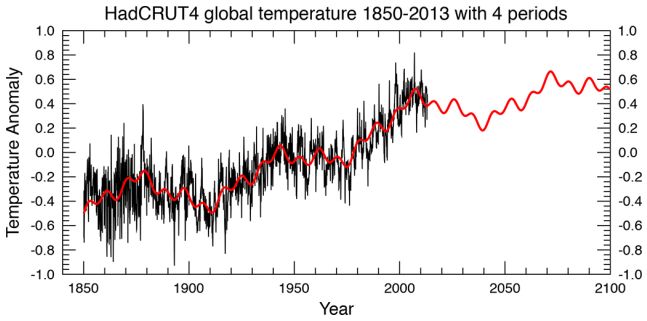

Figure 4. HadCRUT4 monthly averages of global temperature anomalies compared with a simple model consisting of a linear trend (0.0047 °C yr^{-1}) and four harmonic components with periods 155, 66, 21.6 and 9.14 yr.

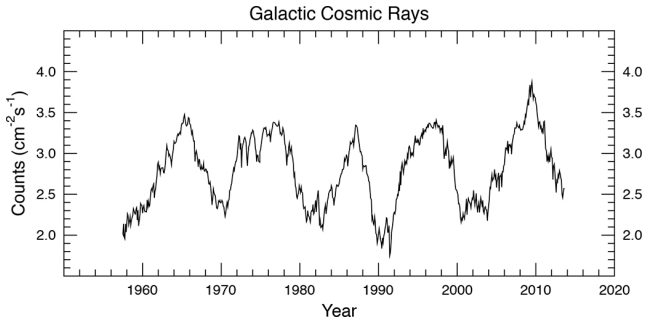

Figure 5. Monthly values of cosmic ray intensity measured in the Murmansk region, 1965–2013 at an altitude of ≈ 25 km, with a cut-off of 0.6 GV (Stozhkov et al., 2007, 2009).

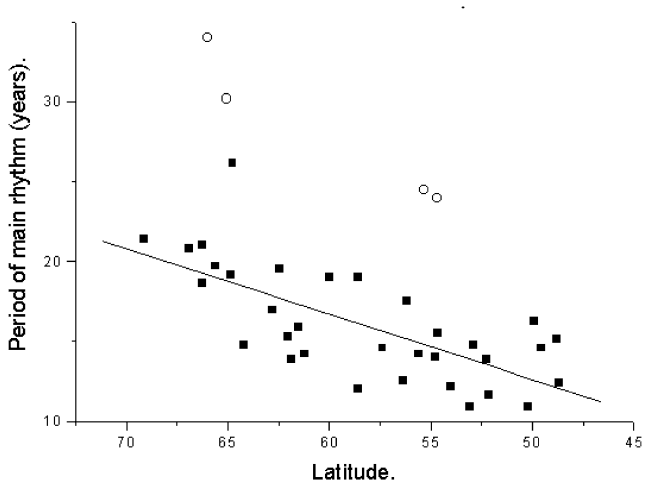

Figure 6. Latitudinal dependence of the rhythmic periods of pine growth along the Murmansk–Carpathians profile (Konstantinov et al., 1986). Squares – normal conditions, open circles – bog conditions.

planetary system. This is done by Scafetta (2010, 2012a, b, c, 2013a, b). One example is his power spectra analysis of the HadCRUT4 temperature series (Fig. 7), which show six peaks present in the Northern and Southern hemispheres, land and ocean separately (Scafetta, 2010). The same peaks can be found in power spectra of the velocity of the Sun relative to the solar system center of mass (SSCM). In the temperature series there is also a strong component of a 9.1 yr lunar cycle. The 20 and 60 yr modulations may be explained as a signal due to the orbits of Jupiter and Saturn (Scafetta, 2010, 2013b).

The 60 yr cycle is clearly present in the Pacific decadal oscillation (PDO) and the Atlantic multi-decadal oscillation (AMO), with phases coherent with a planetary signal since at least 1650. This is also the case for the Indian summer monsoon variations and many other climate series (Scafetta, 2012b, c).

Yndestad et al. (2008) have shown that a 74.4 yr sub-harmonic of the lunar 18.6 yr nodal tide cycle controls the decadal temperature and salinity of the North Atlantic Water current, which has a major influence on the climate in northern Europe. The lunar 74 yr period may also contribute to the global average temperature's 60 yr cycle.

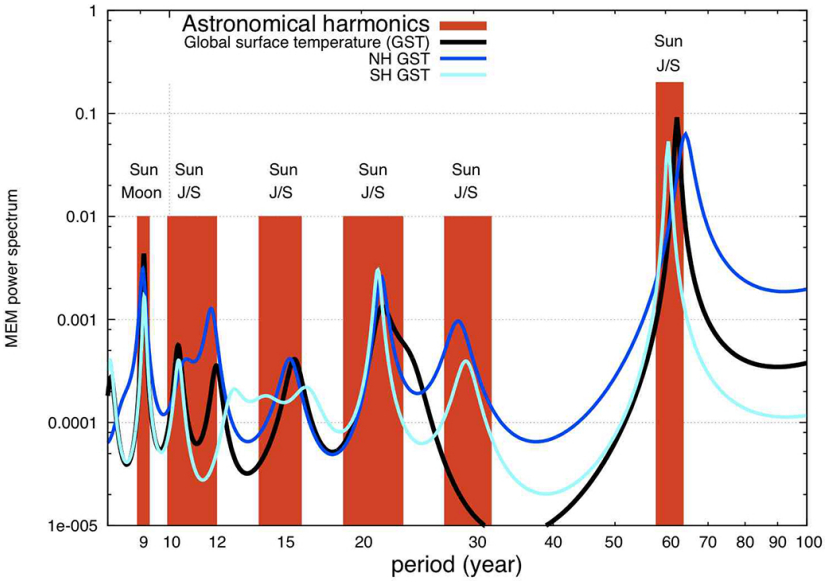

Figure 7. Power spectra of the HadCRUT4 global surface temperature (GST) (1850–2012) (black) and of the Northern Hemisphere and Southern Hemisphere GSTs using the maximum entropy method (MEM); red boxes represent major astronomical oscillations associated with a decadal solilunar tidal cycle (about 9.1 yr), and the major heliospheric harmonics associated with Jupiter and Saturn (from Scafetta and Willson, 2013a).

5 Sun and planets control the climate on centennial and millennial timescales

Galactic cosmic rays are modulated by the magnetic field transported from the Sun to the Earth by the solar wind. The variation of GCR can be determined from dating of ^{14}C abundances in tree rings, and ^{10}Be in ice cores. Two 9400 yr long ^{10}Be data records from the Arctic and the Antarctica, and a ^{14}C record of equal length, have been analyzed by McCracken et al. (2013). They determined 15 significant periodicities between 40 and 2320 yr. The oscillations may either originate in the Sun, or be imprinted in the solar wind by other members of the solar system.

If we look at the relative amplitude of the 15 periods (McCracken et al., 2013, Fig. 4), the periods 2310, 976, 708, and 208 yr are strongest, while the periods 1768, 1301, 1125, 508 and 351 yr are weaker. Also periods 65, 87.3, 104.5, 129.8, 148 and 232 yr are detected.

Many of these periods may be related to the planets (Abreu et al., 2012). Scafetta (2012b) has constructed a simple harmonic model based on three periods in the Schwabe sunspot cycle 11 yr band: 9.93, 10.87 and 11.86 yr, and the beat cycles between them. The 9.93 yr period is the Jupiter/Saturn spring period (half the synodic beat period), 11.86 yr the Jupiter orbital period, and 10.87 yr a quasi-11 yr solar dynamo period theoretically deduced. From these three periods, four beat periods of 63, 118, 135 and finally 970 yr are created. Solheim (2013) shows that the 10.87 yr dynamo period splits into two periods (11.01 and 10.66 yr) when sunspot series back to 1700 are analyzed. He also finds modulation periods of 440, 190 and 86 yr in the length of solar cycles.

The amplitudes of the climate periods in Scafetta's harmonic model were determined from the relative amplitudes in the sunspot power spectrum, and the phases were determined from the perihelion date for Jupiter and the date for the strongest spring tide of the Jupiter–Saturn conjunction. The phase of maximum amplitude for the combined beat period (T_{123} = 970 yr) was determined from the beat of the other two beat periods, and its amplitude from two reconstructions of total solar irradiance since 800 AD (Bond et al., 2001; Steinhilber et al., 2009). The result is quasi-periodic regular periods of about 120–140 yr plus a quasi-millennium cycle, which has a maximum around 2060. The quasi-millennium cycle could also be forced on the Sun by the rotation of the Trigon, the great conjunctions of Jupiter and Saturn with a period of 960 yr (Scafetta, 2012b).

Another interesting period is a combination of the synodic period of the Uranus–Neptune conjunction of 171.44 yr and the 9× Jupiter–Saturn conjunction period of 178.787 yr, which has a beat period of 4200 yr, which means that the four giant planets create quarter cycles about 55× Jupiter–Saturn synodic periods, which is 1100 yr, for the motion of the Sun around the solar system center of mass or SSCM (Charvátová, 2000).

The connection between solar activity and climate on secular and millennial timescales is documented in many studies comparing solar activity and climate. The most famous is perhaps Bond et al. (2001), who compared ice debris outside

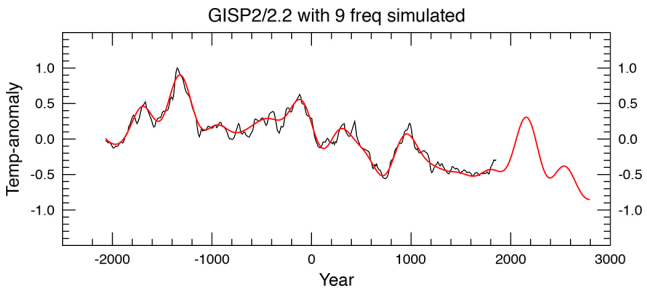

Figure 8. A simple harmonic model for the GISP2 temperature variations, with extension to 2800 AD.

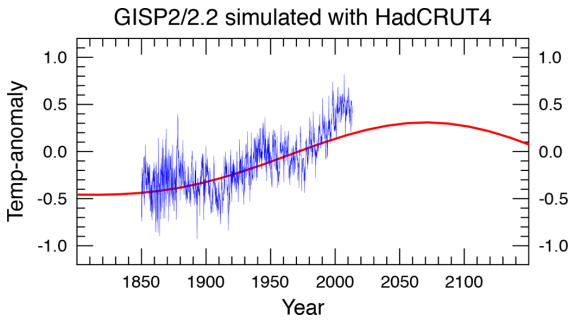

Figure 9. The red curve is the harmonic model based on the GISP2 series (Fig. 8) shifted 85 yr (earlier) and compared with the HadCRUT4 monthly global temperatures including June 2013 (blue).

Greenland with ^{14}C abundances, and found a very good correlation during 12 000 yr.

Analysis of a temperature reconstruction from the Greenland ice core GISP2 the last 4000 yr by Humlum et al. (2011) showed dominant periods of 1130, 790–770, 560 and 390–360 yr. The last period was strong in the beginning of the record, but has since weakened. In order to compare this temperature series with modern global temperatures, we compute the average and divide by 2.2, which is the relation between Arctic and global temperature variations. Figure 8 shows the resulting temperature record and a model based on nine periods where 2804, 1186 and 556 yr are the dominating in addition to a linear cooling trend since the Holocene maximum 7000 yr BP.

This simple harmonic model gives a fair reconstruction of historic warm periods – the Medieval Warm Period around 1000, the Roman Warm Period about 200 BC and the Minoan Warm Period about 1400 BC – and shows that the modern warm period is a result of periodic variations, which will have a peak in the near future.

We find that all the 10 periods observed in solar variations with $P > 200$ yr (McCracken et al., 2013) are present in the GISP2 temperature reconstruction, but that the Earth (or the Greenland ice) for some reason has amplified the period around 1000 yr and its harmonics at about 500 yr. In addition the periodogram of GISP2 temperature data shows periods of 189, 179 and 168 yr, which also are related to planets: the 178 yr period is the trefoil period where the pattern of the solar orbit around the SMMC repeats, and is also close to the 9× Jupiter–Saturn conjunction period (Jose, 1965). A 190 yr period is also found controlling the length of the sunspot cycle (Solheim, 2013).

The GISP2 may have a timing error of decades and/or show temperatures out of phase with the global temperature variation. In Fig. 9 we compare the simulation determined from the GISP2 data with the HadCRUT4 global temperature series, and find a good fit if we introduce a shift of 85 yr, which means the response in the ice core as shown in Fig. 8 is delayed 85 yr compared with the instrumental temperature record. This suggests that a modern temperature maximum will take place about 2070. This corresponds to the maximum determined by Scafetta (2012b) in his Jupiter–Saturn–Sun harmonic model discussed above. The reason for the shift we have introduced is at present unexplained, but should be investigated more closely.

If we are as close to the millennial temperature peak as indicated in Fig. 9, the global temperature will increase at most 0.2 °C due to this period in this century. The global temperature development will therefore be dominated by the shorter periods, in particular the 60 yr period as observed in Figs. 3 and 4b. Based on an analysis of the length of the solar cycle since 1610, it is concluded (Richards et al., 2009; Solheim, 2013) that a grand solar minimum is expected to occur in the first part of this century. The global temperature may then be lower than indicated by the millennium peak in Fig. 9, but still higher than during the the Little Ice Age of the Maunder Minimum (1640–1720), which happened during a minimum phase in the millennium period.

6 Conclusions

The orbits of planets represent stable periodic oscillations, which makes the Sun move in a complicated orbit around the SSMC. The variations in these orbits create periodic tides, which can be amplified by processes in the solar tachocline, which seems to have a controlling effect on the solar dynamo (Abreu et al., 2012). The tides may also modulate the nuclear burning rate in the solar center and create gravity waves, which may transmit a signal to the outer layers of the Sun (Scafetta, 2012a), which modulates the solar activity.

Luminosity variations and solar activity variations may be detected at the Earth either as TSI variations, where signals from the inner planets are detected (Scafetta and Willson, 2013a, b), or in the climate related to the Schwabe sunspot cycle or the Hale magnetic cycle. The temperature response to the Schwabe cycle is small, and may be restricted to certain geographic regions, while the Hale cycle response can be detected in the global average temperature. Since this is a magnetic cycle, and the magnetic field controls the influx of galactic cosmic ray particles, the amplification of the

Hale cycle is an indication of GCR influence on climate. The coastal sea level is strongly modulated by the Schwabe cycle, and this is explained by LOD variations modulated by zonal winds, which again are modulated by GCR controlled by the solar wind.

However, the 60 yr cycle is the dominating one in temperature measurements since 1850, and it is followed back to 1650 in the PDO cycle and the AMO cycle (Scafetta, 2012c). This period may be forced by a beat between the Jupiter orbital period and the Jupiter/Saturn spring period. The beat between these periods and the solar dynamo period creates other beat periods of 120–140 yr, which is also observed in solar activity indicators such as ^{14}C and ^{10}Be abundance variations. Of particular interest is the 178 yr SSMC variation created by a the four giant planets, which have an even stronger modulation with a period of 1100 yr, which is the period between temperature maxima the last 4000 yr.

Calibrations of the phase of the millennium cycle by two different methods give the same answer: we may expect the millennium temperature cycle to reach a maximum around 2060–2080, and then it will decline the next 5–600 yr. This means that an expected grand solar minimum this century, which is predicted to start in the period 2030–2050 due to the Sun's 200 yr cycle (Abdusamatov, 2007; Scafetta, 2010), will not result in as low temperatures as observed during the Maunder Minimum, which took place in the minimum phase of the millennial cycle. This is in line with the forecast by Mörner (2011, Fig. 6).

Acknowledgements. Special thanks to Ole Humlum, Nicola Scafetta and Maxim Ogurtsov for help with figures and data, and to the referees and the editor with very helpful comments.

Edited by: N.-A. Mörner
Reviewed by: H. Jelbring and one anonymous referee

References

Abdusamatov, Kh. I.: Optimal Prediction of the Peak of the Next 11-Year Activity Cycle and of the Peaks of Several Succeding Cycles on the Basis of Long-Term Variations in the Solar Radius or Solar Constant, Kinemat. Phys. Celest., 23, 97–100, 2007 (in Russian).

Abreu, J. A., Beer, J., Ferriz-Mas, A., McCracken, K. G., and Steinhilber, F.: Is there a planetary influence on solar activity? Astron. Astrophys., 548, A88, doi:10.1051/0004-6361/201219997, 2012.

Bond, G., Kromer, B., Beer, J., Muscheler, R., Evans, M. N., Showers, W., Hoffmann, S., Lotti-Bond, R., Hajdas, I., and Bonani, G.: Persistent solar influence on North Atlantic climate during the Holocene, Science, 294, 2130–2136, 2001.

Charvátová, I.: Can origin of the 2400-year cycle of solar activity be caused by solar inertial motion?, Ann. Geophys., 18, 399–405, doi:10.1007/s00585-000-0399-x, 2000.

de Jager, C. and Versteegh, J. M.: Do planetary Motions Drive Solar Variability?, Sol. Phys., 229, 175–179, 2005.

Holgate, S. J.: On the decadal rates of sea level change during the twentieth century, Geophys. Res. Lett., 34, L01602, doi:10.1029/2006GL028492, 2007.

Humlum, O., Solheim, J.-E., and Stordahl, K.: Identifying natural contributions to late Holocene climate change, Global Planet Change, 79, 145–156, doi:10.1016/j.gloplacha.2011.09.005, 2011.

Jose, P. D.: Sun's Motion and Sunspots, Astron. J., 70, 193–200, 1965.

Konstantinov, A. N., Ostryakov, V. M., and Stupneva, A. V.: Solar activity and tree ring widths, Solar Data (Solnechnye Dannye), 2, 84–89, 1986 (in Russian).

Le Moël, J.-L., Blanter, E., Shnirman, M., and Courtillot, V.: Solar forcing of the semi-annual variation of length-of-day, Geophys. Res. Lett, 37, L15307, doi:10.1029/2010GL043185, 2010.

McCracken, K. G., Beer, J., Steinhilber, F., and Abreu, J.: A phenomenological study of the cosmic ray variations over the past 9400 years, and their implications regarding solar activity and the solar dynamo, Sol. Phys., 286, 609–627, 2013.

Mörner, N.-A.: Arctic Environment by the middle of this century, Energ. Environ., 22, 207–218, 2011.

Mörner, N.-A.: Planetary beat and solar–terrestrial responses, Pattern Recogn. Phys., 1, 107–116, doi:10.5194/prp-1-107-2013, 2013a.

Mörner, N.-A.: Sea level changes: past records and future expectations, Energ. Environ., 24, 509–536, 2013b.

Ogurtsov, M. G., Jungner, H., Kocharov, G. E., Lindholm, M., Eronen, M., and Nagovitsyn, Yu. A.: On the link between Northern Fennoscandian climate and length of the quasi-eleven-years cycle in Galactic Cosmic Ray Flux, Sol. Phys., 218, 245–357, 2003.

Richards, M. T., Rogers, M. L., and Richard, D. St. P.: Long-Term variability in the Length of the Solar Cycle, Publ. Astron. Soc. Pac., 121, 797–809, 2009.

Scafetta, N.: Empirical evidence for a celestial origin of the climate oscillations and its implications, J. Atmos. Sol.-Terr. Phy., 72, 951–970, 2010.

Scafetta, N.: Does the Sun work as a nuclear fusion amplifier of planetary tidal forcing? A proposal for a physical mechanism based on the mass-luminosity relation, J. Atmos. Sol.-Terr. Phy., 81—82, 27–40, 2012.

Scafetta, N.: Multi-scale harmonic model for solar and climate cyclical variation throughout the Holocene based on Jupiter-Saturn tidal frequencies plus the 11-year solar dynamo cycle, J. Atmos. Sol.-Terr. Phy., 80, 296–311, 2012b.

Scafetta, N.: A shared frequency set between the historical mid-latitude aurora records and the global surface temperature, J. Atmos. Sol.-Terr. Phy., 74, 45–163, 2012c.

Scafetta, N.: Solar and Planetary Oscillation control on climate change hind-cast, forecast and an comparison with the CMIP5 GCMs, Energ. Environ., 42, 455–496, 2013a.

Scafetta, N.: Discussion on climate oscillations: CMIP5 general circulation models versus a semi-empirical harmonic model based on astronomical cycles, Earth-Sci. Rev., 126, 321–357, 2013b.

Scafetta, N. and Willson, R. C.: Empirical eveidences for a planetary modulation of total solar irradiance and the TSI signature of the 1.09-year Earth-Jupiter conjunction cycle, Astrophys. Space. Sci., doi:10.1007/s10509-013-1558-3, in press, 2013a.

Scafetta, N. and Willson, R. C.: Multiscale comparative spectral analysis of satellite total solar irradiance measurements from

2003 to 2013 reveals a planetary modulation of solar activity and its nonlinear dependence on the 11 yr solar cycle, Pattern Recogn. Phys., 1, 123–133, doi:10.5194/prp-1-123-2013, 2013.b.

Shaviv, N. J.: Using the oceans as a calorimeter to quantify the solar radiative forcing, J. Geophys. Res., 113, A11101, doi:1029/2007JA012989, 2008.

Solheim, J.-E.: The sunspot cycle length – modulated byplanets?, Pattern Recogn. Phys., in preparation, 2013.

Stauning, F.: Solar activity-climate relations: A different approach, J. Atmos. Sol.-Terr. Phy., 75, 1999–2012, 2011.

Steinhilber, F., Beer, J., and Fröhlich, C.: Total solar irradiance during the Holocene, Geophys. Res. Lett., 36, L19704, doi:10.1029/2009GL040142, 2009.

Stozhkov, Yu. I., Svirzhevsky, N. S., Bazilevskaya, G. A., Svirzhevskaya, A. K., Kvashnin, A. N., Krainev, M. B., Makhmutov, V. S., and Klochkova, T. I.: Fluxes of cosmic rays in the maximum of absorption curve in the atmosphere and at the atmosphere boundary (1957–2007), Preprint of FIAN No. 14, Moscow, FIAN, 77c, 2007.

Stozhkov, Yu. I., Svirzhevsky, N. S., Bazilevskaya, G. A., Kvashnin, A. N., Makhmutov, V. S., and Svirzhevskaya, A. K.: Long-term (50 year) measurements of cosmic ray fluxes in the atmosphere, Adv. Space. Res., 44, 1124–1137, 2009.

Svensmark, H. and Friis-Christensen, E.: Variation of cosmic ray flux and global cloud coverage – a missing link in solar-climate relationships, J. Atmos. Sol.-Terr. Phy., 59, 1225–1232, 1997.

Svensmark, H., Enghoff, M. B., and Pedersen, J. O. P.: Response of cloud condensation nuclei (> 50 nm) to changes in ion-nucleation, Phys. Lett. A, 377, 2343–2347, 2013.

Tattersall, R.: Apparent relations between Earth's length of day and the motion of the gas giant planets, Pattern Recogn. Phys., in press, 2013.

Tinsley, B. A., Burns, G. B., and Zhou, L.: The role of the global electric circuit in solar and internal forcing of clouds and climate, Adv. Space. Res., 40, 1126–1139, 2007.

Wilson, I. R. G.: The Venus–Earth–Jupiter spin–orbit coupling model, Pattern Recogn. Phys., 1, 147–158, doi:10.5194/prp-1-147-2013, 2013.

Yndestad, H., Turell, W. R., and Ozhigin, V.: Lunar nodal tide effects on variability of sea level, temperature, and salinity in the Faroe-Shetland Channel and the Barents Sea, Deep-Sea Res. Pt. I, 55, 1201–1217, 2008.

Part VII

Apparent relations between planetary spin, orbit, and solar differential rotation.

Tattersall, R.: Pattern Recogn. Phys., 1, 199-202, doi:10.5194/prp-1-199-2013, 2013.

Pattern Recogn. Phys., 1, 199–202, 2013
www.pattern-recogn-phys.net/1/199/2013/
doi:10.5194/prp-1-199-2013

Pattern Recognition in Physics
Open Access

Apparent relations between planetary spin, orbit, and solar differential rotation

R. Tattersall

University of Leeds, Leeds, UK

Correspondence to: R. Tattersall (rog@tallbloke.net)

Received: 6 October 2013 – Revised: 26 November 2013 – Accepted: 28 November 2013 – Published: 16 December 2013

Abstract. A correlation is found between changes in Earth's length of day [LOD] and the spatio–temporal disposition of the planetary masses in the solar system, characterised by the *z* axis displacement of the centre of mass of the solar system [CMSS] with respect to the solar equatorial plane smoothed over a bi-decadal period. To test whether this apparent relation is coincidental, other planetary axial rotation rates and orbital periods are compared, and spin–orbit relations are found. Earth's axial angular momentum moment of inertia, and internal dynamics are considered in relation to the temporal displacement between the potential stimulus and the terrestrial response. The differential rotation rate of the Sun is considered in relation to the rotational and orbital periods of the Earth–Moon system and Venus and Mercury, and harmonic ratios are found. These suggest a physical coupling between the bodies of an as yet undetermined nature. Additional evidence for a resonant coupling is found in the relation of total solar irradiance (TSI) and galactic cosmic ray (GCR) measurements to the resonant harmonic periods discovered.

1 Introduction

Earth's length of day [LOD] varies cyclically at various timescales. These small variations in the order of a millisecond are believed to be related to exchanges of angular momentum between the atmosphere and Earth, the displacement of oceans away from and toward the equator (Axel-Mörner, 2013), and the changing Earth–Moon distance. On longer timescales, the variation is considerably larger, on the order of several milliseconds, and these variations take place over several decades or more. It is thought by Gross (2007) that the cause of the longer-term variation is due to shifts in the circulation of convecting molten fluid in Earth's fluid outer core. If this is the case, it begs the question: what is the cause of those shifts?

2 Data and method

LOD Data from (Gross, 2007) is plotted against the *z* axis motion of the centre of mass of the solar system [CMSS] with respect to the solar equatorial plane using the NASA/JPL DE14 ephemeris. This curve is smoothed at around the period of two Jupiter orbits (24 yr) in order to mimic the damping effect of the changes of motion in a viscous fluid (like that in Earth's interior). The curve is shifted temporally to obtain the best fit to the LOD curve, and the period of the lag is found to be 30 yr (Fig. 1).

3 Result

The result is suggestive of a dynamic coupling between changes in the disposition of solar system masses, predominantly the gas giant planets. These planets possess an overwhelming percentage of the mass in the solar system outside the Sun, and also possess a high proportion of the entire system's angular momentum. Resonant coupling between Jupiter–Saturn and the inner planets in the early history of the solar system had significant impact on the planets' eventual orbits (Agnor and Lin, 2011).

If the planets are able to transfer orbital angular momentum to the axial angular momentum of neighbour planets, we might expect to see evidence of this in the axial rotation periods of smaller planets relative to the orbital periods of larger neighbours. To investigate this possibility, the rotation rates

Figure 1. *z*-axis motion of the CMSS relative to the solar equatorial plane plotted against LOD (Gross, 2010) 1840–2005.

and orbital periods of several planets are compared with the rotation rate and orbital period of Jupiter.

4 Inner planet synchrony

It is observed that the ratio of Venus and Earth's rotation rates divided by their orbital periods is 1.08 : 0.0027. This is equivalent to the ratio 400 : 1. During their respective synodic periods with Jupiter, Venus completes 1.03 rotations and Earth completes 398.88. This is close to a 400 : 1 ratio. Looking at Earth and Mars' axial rotation and orbital periods, we observe that:

- Earth 1/365.256 = 0.0027.
- Mars 1.0275/686.98 = 0.0015.
  The ratio of these numbers is
  0.0027 : 0.0015 = 1 : 0.546.
- Earth completes 1.092 orbits between synodic conjunctions with Jupiter, while
- Mars completes 1.18844. The ratio of these numbers is 1.092 : 1.18844 = 1 : 1.088.
- The ratio of the ratios is 2 : 1 (99.6 %).

The reason for the 2 : 1 ratio becomes apparent when we observe that the Mars–Jupiter synodic conjunction period is in a 2 : 1 ratio with the Earth–Jupiter synodic period (97.7 %).

Once again there appears to be a quantisation of spin and orbit into simple ratios involving the largest planet in the system, the Sun and the inner planets between them.

As a further test, it is observed that:

- The Neptune rotation rate divided by the Uranus rotation rate = 1.0701427.
- The Jupiter–Uranus synodic period divided by the Jupiter–Neptune synodic period is 1.0805873.
- 1.0805873/1.0701427 = 1.00976 (99.03 %).

These observations strongly suggest that Jupiter affects the rotation rates and orbital periods of both Earth–Venus and Earth–Mars. In combination with the other gas giant planets, the combined effect produces the curve seen in Fig. 1, notwithstanding the much smaller contributions of the inner planets. Having established that the spin and orbit of the four inner planets relates to Jupiter's orbital period, greater weight can be given to the possibility that Earth's decadal LOD anomalies may have a celestial cause in planetary motion.

4.1 Inertia and fluid damping

Earth's high axial rotation rate, along with its density, cause Earth to have a high angular momentum which resists changes in angular velocity. A theory developed from the observation of magnetic anomalies on Earth's surface suggests that columnar vortices surround Earth's core which produce flows in the viscous mantle and liquid outer core (Lister, 2008). Modelling such fluid dynamics as these is beyond the scope of this paper, but the temporal stability of these magnetic structures suggests that small, externally applied forces will take a considerable period of time to produce a terrestrial response. The effect of these stabilising structures will produce a terrestrial response which can be characterised as a fluid-damped oscillation. The signature of Jupiter's motion above and below the solar equatorial plane over the course of its orbital period of around 11.86 yr is not seen in LOD data.

If the correlation in Fig. 1 is indicative of a physically coupled relationship, it is then evident that the damping of the oscillation is sufficient to smooth out both the Jupiter orbital period and the Jupiter–Saturn conjunction period of 19.86 yr. It is found that the best fit of the celestial data to the LOD variation magnitude is at two Jupiter orbital periods. This matches well with the temporal lag between the celestial data and the LOD data of around 30 yr. The peak-to-peak oscillation period seen in the celestial data indicates a cycle of around 180 yr. This period was found by José (1965). The lag of the terrestrial response appears to be at around 1/6 of this periodic length. This is around the half period of the major oceanic oscillations observed on Earth (Axel-Mörner, 2013). These oceanic oscillations are in phase with the changes in LOD and the lagged celestial data.

4.2 Differential solar rotation rates relating to planetary motion

The periods in which the Sun's visible surface makes one sidereal rotation vary with latitude. Near the equator the period is near 24.47 days. This period is known to vary on a period relating to the orbits of Jupiter, Earth and Venus (Wilson et al., 2008). Near the poles, the period of rotation is around 35 days. These periods relate to variation in total solar irradiance (TSI) (Scafetta and Willson, 2013).

Considering the relationships between the spin and orbit of Mercury (three rotations per two orbits of the Sun) and Venus (three rotations per two Earth orbits and two rotations per synodic conjunction with Earth), a test is made to see if similarly simple harmonic relations exist between these planets and the Sun's differential rates of rotation.

Firstly, it is noted that the lengths of day of Mercury and Venus form a ratio that is close to 2 : 3 ratio, and that the equatorial and polar rotation rates of the solar surface also form a ratio close to 2 : 3.

Mercury makes one sidereal rotation per 2/3 (240 degrees) of orbit in 58.65 days. A point on the Sun rotating at a rate which brought it directly between Mercury and the solar core in the same period would have a sidereal period of 35 days (184 days making one full rotation plus 2/3 of a rotation, i.e. 240 degrees). Mercury makes two sidereal rotations per 480 degrees (1, 1/3 orbits) in 117.3 days. A point on the Sun rotating at a rate which brought it directly between Mercury and the solar core in the same period would have a sidereal period of 27.06 days, making four sidereal rotations plus 1/3 of a rotation (120 degrees). It is noted that this is close to the Carrington period.

In summary, it can be seen that Mercury has a 3 : 2 spin-orbit ratio which is in 3 : 5 spin–spin and 2 : 5 orbit–spin ratios with a solar rotation period of 35.18 days, and is in 6 : 13 spin-spin 4 : 13 orbit-spin ratios with a solar rotation period of 27.06 days.

Two Mercury rotations occur in 117.3 days. In a similar period of 116.8 days, Venus makes a full rotation with respect to the Sun, while orbiting 180 plus 6.18 degrees (0.52 orbits) and rotating (retrograde) 180 minus 6.18 degrees in the sidereal frame. A point near the solar equator rotating at a rate which brought it directly between Venus and the solar core in the same period after 4.52 rotations would have a sidereal solar rotation period of 25.84 days.

Points near the solar poles rotating at a rate which brought them directly between Venus and the solar core in the same period after 3.52 rotations would have a sidereal period of 33.2 days. It is noted that the average of these two solar rotation periods is 29.51 days, which is close to the period of rotation of the Earth–Moon system with respect to the Sun (29.53 days). A solar rotation period of 29.32 days is found to be in a 1 : 3 ratio with a period of 87.97 days; the Mercury orbital period, and 1 : 4 ratio with a period of 117.3 days; the period of two Mercury rotations and close to one Venusian day.

The relationship of Venus with the Earth–Moon system is more clearly seen by considering that the period of a Venus rotation with respect to the Sun of 116.8 days is exactly 1/5 of the Earth–Venus orbital synodic conjunction period of 1.6 yr. Five synodic conjunctions occur over a period of 8 Earth years as Venus makes 13 orbits, bringing the two planets back to within two degrees of their original longitude. At the end of this period, the various solar periods calculated in the preceding observations make whole numbers of sidereal rotations: 113×25.84 days, 108×27.06 days, 88×33.18 days, and 83 × 35.18 days.

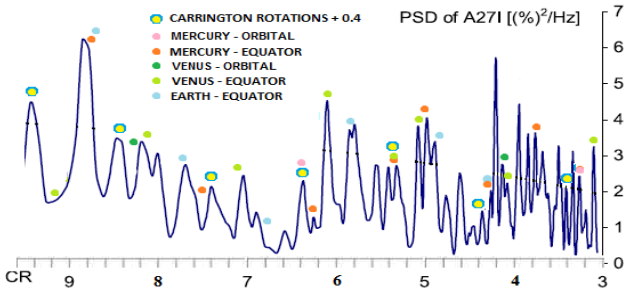

Figure 2. Comparison of GCR measurements over Carrington rotations with planetary frequencies.

5 Discussion

A physical mechanism linking solar rotation rates with planetary rotation and orbital periods may involve resonance if the ratios are 1 : 2 or ratios such as 1 : 4, 2 : 3, 2 : 5, 1 : 3, 3 : 5, 5 : 8 etc. (Agnor and Lin, 2011). As a first approximate observation, the rotation rates of the solar equator and solar poles are in a 2 : 3 ratio.

The average of the periods relating to Venus, 25.84 and 33.2 days, is 29.51 days. This is very close to the Earth–Moon system rotation period relative to the Sun (29.53 days). The ratio of 25.84 to 29.51 is 7 : 8. The ratio of 29.51 to 33.2 is 8 : 9.

The ratio of the periods relating to Mercury, 27.06 and 35.184, is 20 : 26. The average of the periods is 31.12 days. The ratio of 27.06 to 31.12 is 20 : 23. The ratio of 31.12 to 35.184 is 23 : 26. There are 12 Mercury orbits in 26 periods of 27.06 days each.

These observations indicate that in addition to resonance between the orbital and rotation periods between individual planets and the Sun, we may hypothesise that there is also resonance between the solar rotation rates at various latitudes reinforcing the effect. If there is an effect of this resonance on solar activity levels, we would expect to see evidence of it in accurate TSI measurement, such as the strong peaks seen at periods around 25–27 days and 33–35 days in spectrographic analysis of TSI (Scafetta and Willson, 2013).

6 Additional analysis

Further evidence to support the hypothesis may be found in spectrographic analysis of galactic cosmic ray incidence at Earth, which is also indicative of solar activity levels, and is found to be modulated at the Carrington-period length (Gil and Alania, 2012).

A comparison of periods at which various fractional multiples of the solar equatorial rotation rate which bring a point on the solar equator directly between the inner planets and

the solar core, and the peaks in the galactic cosmic ray measurements (A27l) is made in Fig. 2.

The coincidence of peaks in the galactic cosmic ray (GCR) curve with multiples of the Carrington Rotation (CR) period indicates a resonant effect of this frequency (27 days). Similarly, the coincidence of other peaks in the GCR curve with multiples of the periods at which a point on the solar equator passes between inner planets and the solar core is indicative of resonant effects. Also shown are Mercury and Venus orbital and half-orbital periods. Venus orbital periods lie close to multiples of the Venus–Solar rotation periods near the peaks in GCR activity at 4.15 and 8.3 CRP. The sharp, high amplitude peak at 4.2 CRP lies between the half periods of Venus' orbit and sidereal rotation, which are four days apart.

7 Conclusions

Harmonic ratios between the planets orbital periods are the principle cause of their quantised semi-major axes. These ratios also affect the rate at which planets rotate, which in turn sets their LOD. The discovery of simple ratios of LOD between planets further underlines the resonant nature of the effect which quantises their relations. These resonances also affect the Sun, which has developed a differential rotation in response to the resonant forces to which it is subjected by the planets, whose orbital elements may be modulating the resonant periods. Cyclic variations induced in the rate of rotation of various latitudinal plasma belts on the solar surface affect the Sun's activity cycles; these include the Hale, Schwabe and Gleissberg cycles, which are found to be in synchronisation with planetary alignment cycles (Wilson, 2013). Further research is required in modelling the resonant frequencies present and studying their resultant interactions in order to better understand the magnitudes of inertia and damping present in the oscillating subsystems which constitute the rotating solar surface layers.

Acknowledgements. The author wishes to thank the following people for their generous assistance in the production of this unfunded work: Stuart Graham, Ian Wilson, Roy Martin, Wayne Jackson, Graham Stevens, Roger Andrews, and many other people offering insight and comment at "Tallbloke's Talkshop".

Edited by: N. A. Mörner
Reviewed by: two anonymous referees

References

Agnor, C. B. and Lin, D. N. C.: On the migration of Jupiter and Saturn: Constraints from linear models of secular resonant coupling with the terrestrial planets, Astrophys. J., 745, p. 143, 2011.

Gil, A. and Alania, M. V.: Cycling Changes in the Amplitudes of the 27-Day Variation of the Galactic Cosmic Ray Intensity, Sol. Phys., 278, 447–455, 2012.

Gross, R. S.: Earth rotation variations – long period, in: Physical Geodesy, edited by: Herring, T. A., Treatise on Geophysics, Vol. 11, Elsevier, Amsterdam, 2007.

José, P. D.: Sun's motion and sunspots, Astron. J., 70, p. 193, 1965.

Lister, J.: Earth science, Structuring the inner core, Nature, 454, 701–702, 2008.

Mörner, N. A.: Solar Wind, Earth's Rotation and Changes in Terrestrial Climate, Physical Review & Research International, 3, 117–136, 2013.

Scafetta, N. and Willson, R. C.: Multiscale comparative spectral analysis of satellite total solar irradiance measurements from 2003 to 2013 reveals a planetary modulation of solar activity and its nonlinear dependence on the 11 yr solar cycle, Pattern Recogn. Phys., 1, 123–133, doi:10.5194/prp-1-123-2013, 2013.

Wilson, I. R. G.: The Venus–Earth–Jupiter spin–orbit coupling model, Pattern Recogn. Phys., 1, 147–158, doi:10.5194/prp-1-147-2013, 2013.

Wilson, I. R. G., Carter, B. D., and Waite, I. A.: Does a Spin-Orbit Coupling Between the Sun and the Jovian Planets Govern the Solar Cycle?, Publications of the Astronomical Society of Australia, 25, 85–93, http://www.publish.csiro.au/paper/AS06018.htm, 2008.

Part VIII

The Venus–Earth–Jupiter spin–orbit coupling model. Wilson, I. R. G.: Pattern Recogn. Phys., 1, 147-158, doi:10.5194/prp-1-147-2013, 2013.

Pattern Recogn. Phys., 1, 147–158, 2013
www.pattern-recogn-phys.net/1/147/2013/
doi:10.5194/prp-1-147-2013

Pattern Recognition in Physics
Open Access

The Venus–Earth–Jupiter spin–orbit coupling model

I. R. G. Wilson

The Liverpool Plains Daytime Astronomy Centre, Gunnedah, Australia

Correspondence to: I. R. G. Wilson (irgeo8@bigpond.com)

Received: 1 October 2013 – Revised: 30 October 2013 – Accepted: 3 November 2013 – Published: 3 December 2013

Abstract. A Venus–Earth–Jupiter spin–orbit coupling model is constructed from a combination of the Venus–Earth–Jupiter tidal-torquing model and the gear effect. The new model produces net tangential torques that act upon the outer convective layers of the Sun with periodicities that match many of the long-term cycles that are found in the ^{10}Be and ^{14}C proxy records of solar activity.

1 Introduction

The use of periodicities to investigate the underlying physical relationship between two variables can be fraught with danger, especially if reasonable due care is not applied. Any use of this technique must be based upon the following premise: if two variables exhibit common periodicities, it does not necessarily prove that there is a unique physical connection between the two. This is the dictum saying that a correlation does not necessarily imply causation.

However, there are cases where the correlation between two variables is so compelling that it makes it worthwhile to investigate the possibility that there may be an underlying physical connection between the two. One such case is the match between the long-term periodicities observed in the level of the Sun's magnetic activity and the periodicities observed in the relative motion of the planets.

Jose (1965) showed that the Sun's motion around the centre-of-mass of the solar system (CMSS) is determined by the relative orbital positions of the Jovian planets, primarily those of Jupiter and Saturn. He also showed that the time rate of change of the Sun's angular momentum about the instantaneous centre of curvature of the Sun's motion around the CMSS ($= \mathrm{d}P/\mathrm{d}T$), or torque, varies in a quasi-sinusoidal manner, with a period that is comparable to the 22 yr Hale cycle of the solar sunspot number (SSN).

Jose (1965) found that the temporal agreement between variations in $\mathrm{d}P/\mathrm{d}T$ and the SSN were so compelling that it strongly hinted that there was a physical connection between the planetary induced torques acting upon the Sun and sunspot activity. However, Jose was unable to give a physically plausible explanation as to how this connection might work.

Following Jose's original work, there were several further attempts to link the Sun's motion around the CMSS with long-term variations in solar activity (Landscheidt, 1981, 1999; Fairbridge and Shirley, 1987; Chárvátova, 1988, 1990, 2000; Zaqarashvili, 1997; Javaraiah and Gokhale, 1995; Javaraiah, 2003; Juckett, 2000). However, each of these attempts was dismissed by Shirley (2006), based upon the argument that differential forces within the Sun cannot be produced by the Sun's motion around the CMSS (hereafter referred to as the solar inertial motion or SIM), since the Sun is in a state of free-fall. Shirley (2006) claimed that the only differential forces that could be generated within the Sun by the planets were those associated with their extremely weak tidal forces.

De Jaeger and Versteegh (2005) went one step further, claiming that the observed accelerations of plasma in the base of the convective layers of the Sun, where the solar dynamo is thought to originate, were 1000 times greater than those induced by the planetary tides. This makes it very difficult to argue that planetary tidal forces can play a significant role in influencing the solar dynamo.

Despite these strong counterarguments, Wilson et al. (2008) found further observational evidence that there was a link between the SIM and long-term changes in SSN. They showed that there was a correlation between the Sun's equatorial rotation rate and its motion about the CMSS (i.e. a form of spin–orbit coupling) that was associated with long-term changes in the SSN. However, Wilson et al. (2008)

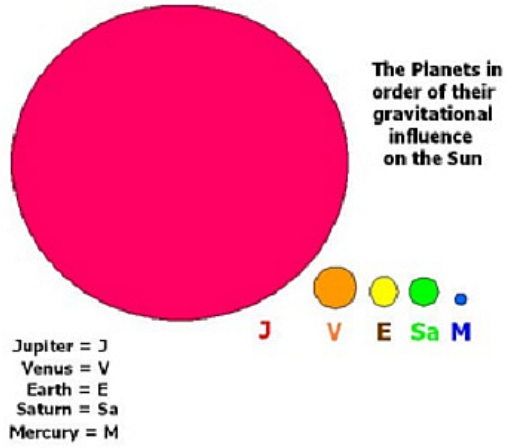

Figure 1. The relative gravitational influence of the planets upon the Sun. NB: all comparisons should be made using the circle's diameters and not their areas.

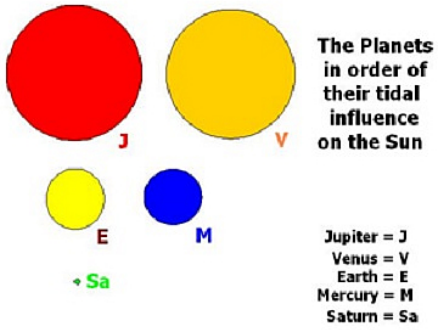

Figure 2. The relative tidal influence of the planets upon the Sun. NB: all comparisons should be made using the circle's diameters and not their areas.

could not provide a physically plausible explanation for the observed spin–orbit coupling.

At about the same time, Hung (2007) and Wilson (2011) advanced the idea that there was a connection between the tides induced in the surface layers of the Sun by periodic alignments of Jupiter, Venus and the Earth (VEJ) and long-term changes in SSN. NB: this idea was first proposed by Bollinger (1952) and Desmoulins (1989) and then further developed by others in the non-peer reviewed literature (see Acknowledgements).

Claims by Hung (2007) and Wilson (2011) were based upon the fact that there are 11.07 and 22.14 yr periodicities in the planetary tides induced in the surface layers of the Sun by Jupiter, Venus and the Earth and that these periodicities closely matched the observed Schwabe and Hale SSN cycles. However, despite the suggestive nature of the matching periods, the problem still remained that the VEJ models relied on tidal forces that were orders of magnitude too weak

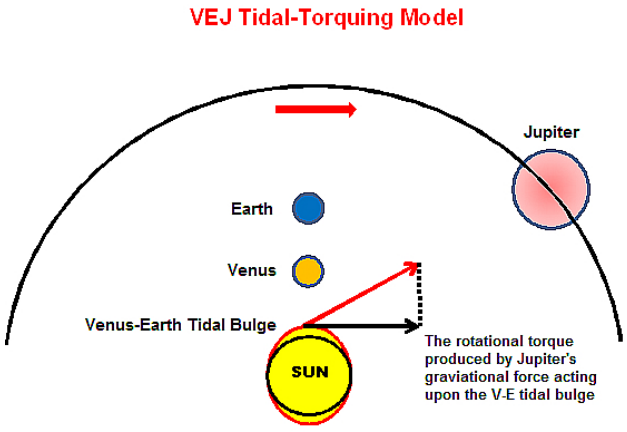

Figure 3. An over-view of the VEJ tidal-torquing model – further details in the text.

to produce any significant bulk motions at the base of the convective layer of the Sun (Callebaut et al., 2012).

One way to overcome the inadequacies of the planetary tidal models was to postulate that the layers of plasma at the base of the convective layer of the Sun (i.e. near the tachocline) were somehow aspherical, allowing the gravitational forces of the planets (primarily that of Jupiter) to apply torques that were tangential to the solar surface.

Two types of models have been proposed along these lines. The first is the model by Abreu et al. (2012) that assumes there is an intrinsically non-spherical tachocline at the base of the Sun's convective zone. The Abreu et al. (2012) model can successfully reproduce many of periodicities that are observed in the ^{10}Be and ^{14}C proxy records of solar activity over the last 9400 yr. The second type of model is the Venus–Earth–Jupiter tidal-torquing model presented and discussed here.

2 The Venus–Earth–Jupiter tidal-torquing model

The Venus–Earth–Jupiter (VEJ) tidal-torquing model is based on the idea that the planet that applies the dominant gravitational force upon the outer convective layers of the Sun is Jupiter (Fig. 1), and after Jupiter, the planets that apply the dominant tidal forces upon the outer convective layers of the Sun are Venus and the Earth (Fig. 2).

Periodic alignments of Venus and the Earth on the same or opposite sides of the Sun, once every 0.7993 sidereal Earth years, produces temporary tidal bulges on the opposite sides of the Sun's surface (Fig. 3 – red ellipse). Whenever these temporary tidal bulges occur, Jupiter's gravitational force tugs upon the tidally induced asymmetries and either slows down or speeds-up the rotation rate of plasma near the base of the convective layers of the Sun.

The VEJ tidal-torquing model proposes that it is the variations in the rotation rate of the plasma in Sun's lower

convective layer, produced by the torque applied by Jupiter upon the periodic Venus–Earth (VE) tidal bulges that modulate the Babcock–Leighton solar dynamo. Hence, the model asserts that it is the modulating effects of the planetary tidal-torquing that are primarily responsible for the observed long-term changes in the overall level of solar activity.

It is important to note that tidal bulges will be induced in the surface layers of the Sun when Venus and the Earth are aligned on the same side of the Sun (inferior conjunction), as well as when Venus and the Earth are aligned on opposite sides of the Sun (superior conjunction). This means that whenever the gravitational force of Jupiter increases/decreases the tangential rotation rate of the surface layer of the Sun at inferior conjunctions of the Earth and Venus, there will be a decrease/increase the tangential rotation rates by almost the same amount at the subsequent superior conjunction.

Intuitively, one might expect that the tangential torques of Jupiter at adjacent inferior and superior conjunctions should cancel each other out. However, this is not the case because of a peculiar property of the timing and positions of Venus–Earth alignments. Each inferior conjunction of the Earth and Venus (i.e. VE alignment) is separated from the previous one by the Venus–Earth synodic period (i.e. 1.5987 yr). This means that, on average, the Earth–Venus–Sun line moves by 144.482 degrees in the retrograde direction, once every VE alignment. Hence, the Earth–Venus–Sun line returns to almost the same orientation with respect to the stars after five VE alignments of almost exactly eight Earth (sidereal) years (actually 7.9933 yr). Thus, the position of the VE alignments trace out a five pointed star or pentagram once every 7.9933 yr that falls short of completing one full orbit of the Sun with respect to the stars by $(360 - (360 \times (7.9933 - 7.0000))) = 2.412$ degrees.

In essence, the relative fixed orbital longitudes of the VE alignments means that, if we add together the tangential torque produced by Jupiter at one inferior conjunction, with the tangential torque produced by Jupiter at the subsequent superior conjunction, the net tangential torque is in a prograde/retrograde direction if the torque at the inferior conjunction is prograde/retrograde.

What makes this simple tidal-torquing model most intriguing is the time period over which the Jupiter's gravitational force speeds up and slows down the rotation rate of the Sun's outer layers. Figure 4 shows Jupiter, Earth and Venus initially aligned on the same side of the Sun (position 0). In this configuration, Jupiter does not apply any tangential torque upon the tidal bulges (the position of the near-side bulge is shown by the black 0 just above the Sun's surface). Each of the planets, 1.5987 yr later, moves to their respective position 1s. At this time, Jupiter has moved 13.00° ahead of the far-side tidal bulge (marked by the red 1 just above the Sun's surface) and the component of its gravitational force that is tangential to the Sun's surface tugs on the tidal bulges, slightly increasing the rotation rate of the Sun's outer layers.

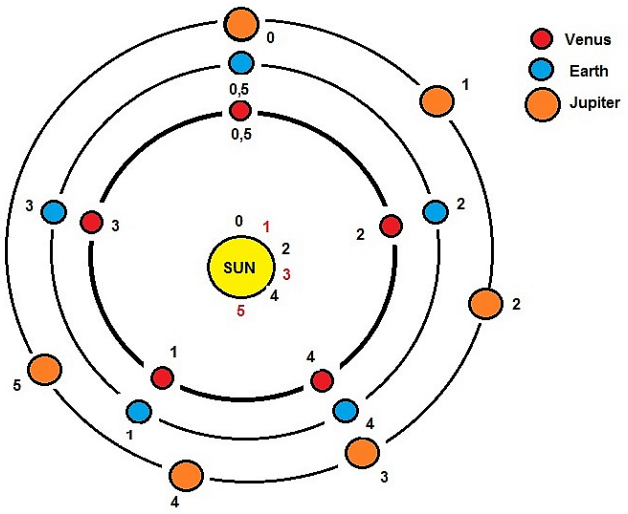

Figure 4. The VEJ tidal-torquing model produces a net increase/decrease in the rotation rate of the outer layers of the Sun that lasts for 11.07 yr, followed by a net decrease/increase in the rate of rotation of the outer layers of the Sun that lasts for another 11.07 yr. Further description in the text.

After a second 1.5987 yr, each of the planets moves to their respective position 2s. Now, Jupiter has moved 26.00° ahead of the near-side tidal bulge (marked by the black 2 just above the Sun's surface), increasing Sun's rotation rate by roughly twice the amount that occurred at the last alignment. This pattern continues with Jupiter getting 13.00° further ahead of the nearest tidal bulge, every 1.5987 yr. Eventually, Jupiter will get 90° ahead of the closest tidal bulge and it will no longer exert a net torque on these bulges that is tangential to the Sun's surface and so it will stop increasing the Sun's rotation rate.

Interestingly, Jupiter's movement of 13.00° per 1.5987 yr with respect to closest tidal bulge means that Jupiter will get 90° ahead of the closest tidal bulge in 11.07 yr. This is almost the same amount of time as to average length of the Schwabe sunspot cycle (11.1 ± 1.2 yr, Wilson, 2011). In addition, for the next 11.07 yr, Jupiter will start to lag behind the closest tidal bulge by 13.00° every 1.5987 yr, and so its gravitational force will pull on the tidal bulges in such a way as to slow down the rotation rate of the outer convective layers of the Sun. Hence, the basic unit of change in the Sun's rotation rate (i.e. an increase followed by a decrease in rotation rate) is 2×11.07 yr = 22.14 yr. This is essentially equal to the mean length of the Hale magnetic sunspot cycle of the Sun, which is 22.1 ± 2.0 yr (Wilson, 2011).

Figure 5 shows the observed variation in the SSN between 1748 and 2008 (top curve – labelled SSN). Also shown in this figure is the variation of a parameter that is directly proportional to the net tangential torque that is applied by Jupiter to the periodic VE tidal bulges, according to the VEJ tidal-torquing model (bottom curve – labelled Torque, shown in

arbitrary units and offset by −50 for comparison purposes). In order to further help with comparisons, a fifth-order binomial filter has been applied to the torque data to produce the smooth curve that is superimposed on the torque curve (Horizons On-Line Ephemeris System, 2008).

The net tangential torque calculated from the model exhibits a number of properties that closely match the observed variations that are seen in the Sun's long-term magnetic activity:

- It naturally produces a net increase/decrease in the rate of rotation of the outer layers of the Sun that lasts for 11.07 yr (i.e. equivalent to the Schwabe cycle), followed by a net decrease/increase in the rate of rotation of the outer layers of the Sun that also lasts for 11.07 yr.
- Hence, the net torque of Jupiter acting on the VE tidal bulge has a natural 22.14 yr periodicity that closely matches the observed period (and phase) of the 22.1 yr Hale (magnetic) cycle of solar activity.
- If one considers the torque of Jupiter upon the VE tidal bulge at each separate inferior and superior conjunction of Venus and Earth (*rather than their consecutive sum = net torque*), the actual magnitude of Jupiter's torque is greatest at the times that are at or near solar minimum. Even though Jupiter's torque is a maximum at these times, the consecutive torques at the inferior and superior conjunctions of Venus and the Earth almost exactly cancel each other out.
- In all but two cases between 1750 and 2013, the time for solar minimum is tightly synchronized with the times when Jupiter's *net torque* (acting on the VE tidal bulge) is zero (NB: this is the time when the net torque changes direction with respect the Sun's rotation axis, R. Martin, personal communication, 2013).
- On these two occasions where the synchronization was disrupted (i.e. the minima prior to the onset of cycle 4 (1784.7) and cycle 23 (1996.5), the timing of the sunspot minimum quickly re-synchronizes with the timing of the minimum change in Jupiter's tangential force acting upon Venus–Earth tidal bulge. Interestingly, the minimum prior to cycle 4 (1784.7) marks the onset of the Dalton Minimum and minimum prior to cycle 23 (1996.5) marks the onset of the upcoming Landscheidt Minimum.
- Remarkably, if the minimum between solar cycles 24 and 25 occurs in 2021 ± 2 yr, it will indicate a re-synchronization of the solar minima with a VEJ cycle length of 11.07 ± 0.05 yr over a 410 yr period.
- The equatorial convective layers of the Sun are sped-up during ODD numbered solar cycles and slowed-down during EVEN numbered solar cycles, thus providing a logical explanation for the Gnevyshev–Ohl (G–O) rule for the solar sunspot cycle (Gnevyshev and Ohl, 1948).

(NB: since the VEJ tidal-torquing model has a natural aliasing set by the physical alignments of Venus and the Earth, simple auto-regression analysis of the smoothed torque curve in Fig. 5 indicates that the (short-term) repetition cycle is 22.38 yr (= 7 VE alignments) rather than 22.14 yr. Essentially, what this means is that while the tangential torques affecting the convective layers of the Sun are being applied over a 22.14 yr repetition cycle, any external mechanism that uses the VE alignments to interact with the tidal-torquing mechanism, will attempt to do so over periodic cycles that are 22.38 yr long).

Figure 6 shows the smoothed torque curve from Fig. 5, replotted to highlight its long-term modulation (Horizons On-Line Ephemeris System, 2008). Superimposed on the torque are two sinusoidal envelopes with periods of 166.0 yr. In order to understand why the torque is modulated by this long-term period, we need to understand the main factors that influence long-term changes in the torque that Jupiter applies to the VE tidal bulges. These factors are the 3.3-degree tilt in the heliocentric latitude of Venus' orbit and the mean distance of Jupiter from the Sun.

Figure 7 (from Wilson, 2011) shows that the variations in the heliocentric latitude of Venus essentially mimics the variations in the mean distance of Jupiter from the Sun, provided these variables are measured at the times when Jupiter aligns with either the inferior or superior conjunctions of Venus and the Earth. What this indicates is that the long-term net tangential torque should be weakest when Venus is at its greatest positive (most northerly) heliocentric latitude, and Jupiter is at its greatest distance from the Sun (≈ 5.44 A.U.). Figure 7 shows that this condition reoccurs roughly once every 166 yr and that they correspond in time with periods of low solar activity known as Grand Solar Minimum. The one exception to this rule since 1000 AD is a period of weak planetary tidal force that peaks near 1150 AD spanning the first half of the Medieval Maximum from 1090–1180 AD. The reason for this discrepancy is unknown, although it could be explained if there is an additional countervailing factor present during this period that was working against the planetary tidal effects.

So, in summary, the Venus–Earth–Jupiter tidal-torquing model naturally produces 11.07 and 22.14 yr periodicities in the net tangential torque that Jupiter applies to the base of the convective layer of the Sun. These periodicities closely match the 11.1 yr Schwabe and the 22.1 yr Hale solar activity cycles. In addition, the model gives a natural explanation for the G–O rule for SSN and it provides a plausible physical explanation for the average spacing in time between recent Grand Solar Minima in solar activity of approximately 166 yr.

Despite all of these successes, the model is unable to easily produce the known periodicities that are associated with the

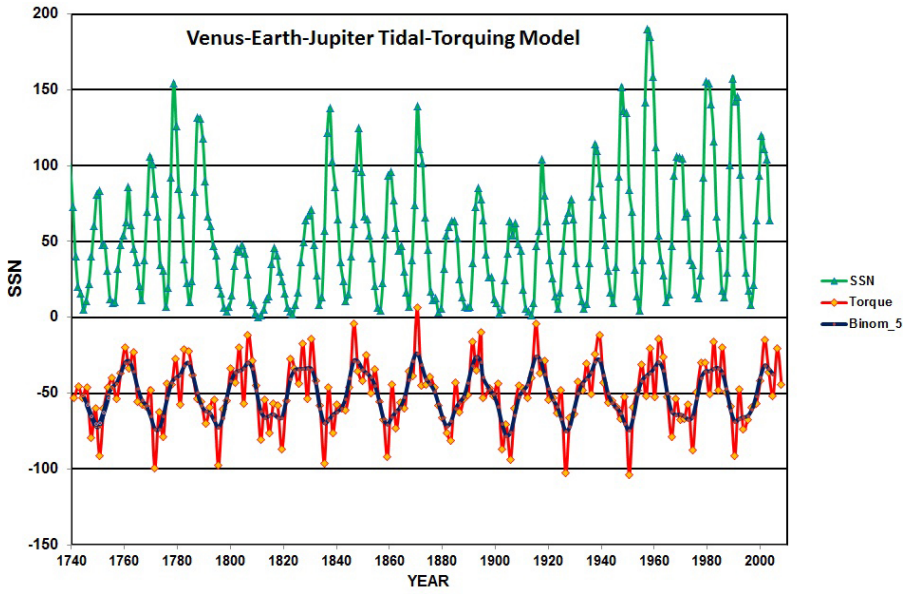

Figure 5. The observed variation in the SSN (green) between 1748 and 2008. The torque curve (red) represents a parameter that is directly proportional to the net tangential torque that is applied by Jupiter to the periodic VE tidal bulges, according to the VEJ tidal-torquing model (bottom curve shown in arbitrary units and offset by −50 for comparison purposes). A fifth-order binomial filter has been applied to the torque data to produce the smooth curve (black) that is superimposed on the torque curve.

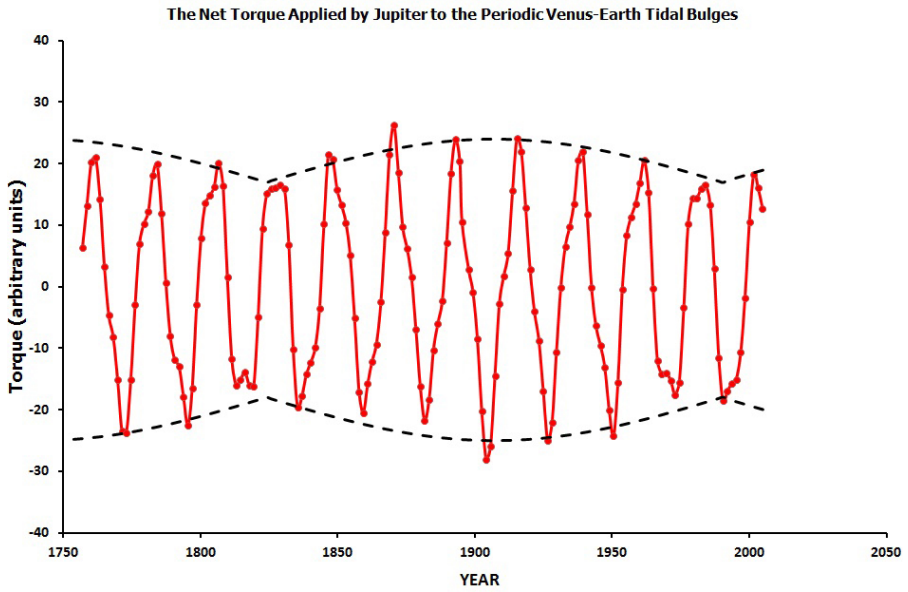

Figure 6. The smoothed torque curve from Fig. 5, replotted to highlight its long-term modulation. Superimposed on the torque are two sinusoidal envelopes (dashed) with periods of 166.0 yr.

^{10}Be and ^{14}C proxy observations of the long-term variations in the level of solar activity (column 1 of Table 1). In order to accomplish this we must combine the VEJ tidal-torquing model with the gear effect to produce a new model called the VEJ spin–orbit coupling model.

3 The Venus–Earth–Jupiter spin–orbit coupling model

3.1 The gear effect

The gear effect is the term used in golf to describe the action of a club head upon a golf ball that causes it to either slice

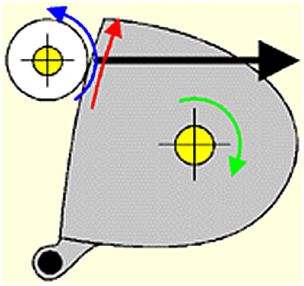

Figure 7a. An explanation as to how the gear effect can be used either to slice or to hook a golf ball off a tee. If the golf ball hits the (curved) face of the club off-centre, it applies a force (horizontal black arrow) to the club, which induces clockwise rotation of the club head (green arrow) around its centre-of-mass (bottom right yellow circle with cross-hairs). The resultant rotation of the face of the club head (red arrow) applies a side-ways force to the golf ball at the point of contact, producing an anti-clockwise rotation (blue arrow) of the golf ball.

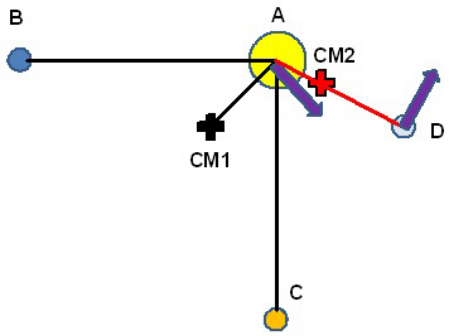

Figure 7b. A more specific example that removes many of ambiguities of the golf club analogy. In this figure, the head of the golf club is replaced by a structure that consists of three spheres A, B, and C, that are held together by rigid bars. The ABC structure is free to rotate in the plane of the page around a centre-of-mass (CM1). CM1 is located at a fixed distance from the sphere A, as well as a fixed point on the page. Similarly, the golf ball is replaced by a structure that consists of two spheres A and D. These spheres are held together by a rigid bar, as shown. The AD structure is free to rotate in the plane of the page around a centre-of-mass (CM2). CM2 is located a fixed distance from the sphere A, however it is able to move freely in the plane of the page. For more detail about how this analogy is used to describe the gear effect please refer to the text.

or hook. The gear effect occurs whenever two bodies impact at an angle or impact with misaligned centres-of-mass (i.e. the point of impact between them does not lie along the line connecting the two bodies' centres-of-mass).

Figure 7a shows how the gear effect can be used to either slice or hook a golf ball off a tee. If the golf ball hits the (curved) face of the club off-centre, it applies a force (horizontal black arrow) to the club, which induces clockwise rotation of the club head (green arrow) around its centre-of-mass (bottom right yellow circle with cross-hairs). The resultant rotation of the face of the club head (red arrow) applies a side-ways force to the golf ball at the point of contact, producing an anti-clockwise rotation (blue arrow) of the golf ball.

Table 1. Periodic variations in the level of solar activity – longer the Gleissberg cycle.

McCracken (Years)	Cycle name	Wilson (2013) (Years)
(i) Category A	Periods shorter than the Eddy cycle	
87.3 ± 0.4	Gleissberg	$88.15 = 1/2 \times 176.3$
130 ± 0.9		–
148 ± 1.3		–
350 ± 7		$352.6 = 2 \times 176.3$
510 ± 15		$528.9 = 3 \times 176.3$
708 ± 28		$705.2 = 4 \times 176.3$
(ii) Category B	Periods as long or longer than the Eddy cycle	
976 ± 53	Eddy	$974.7 = 1151.0 - 176.3$?
1126 ± 71		$1151.0 = 2 \times 575.518$
1301 ± 96		$1327.3 = 1151.0 + 176.3$?
1768 ± 174		$1726.5 = 3 \times 575.518$ (& $1763 = 10 \times 176.3$)
2310 ± 304	Hallstatt	$2302.1 = 4 \times 575.518$
(iii) Category C	Multiples of the de Vries cycle	
104.5 ± 0.6	half de Vries	–
208 ± 2.4	de Vries	208.2

The golf club analogy is good at giving a preliminary introduction to the gear effect. However, there are ambiguities in the analogy that limit its application in the current context. Figure 7b shows a more specific example that removes many of ambiguities of the golf club analogy. In this figure, the head of the golf club is replaced by a structure that consists of three spheres A, B, and C, that are held together by rigid bars (as shown in Fig. 7b). The ABC structure is free to rotate in the plane of the page about a centre-of-mass (CM1). CM1 is located at a fixed distance from the sphere A, as well as a fixed point on the page. Similarly, the golf ball is replaced by a structure that consists of two spheres A and D. These spheres are held together by a rigid bar (as shown in Fig. 7b). The AD structure is free to rotate in the plane of the page about a centre-of-mass (CM2). CM2 is located a fixed distance from the sphere A, however it is able to move freely in the plane of the page.

Now, imagine that a force is applied to sphere A that acts directly along the rigid bar AD towards the sphere D. This could be accomplished by someone pulling on sphere D. Such a force will cause the ABC structure to rotate in a clockwise direction about CM1. One direct consequence of this action is that CM2 will be moved slightly away from CM1 and that both B and D will be forced to rotate around CM2. It is this forced rotation of A and D around CM2, which the present author terms "the gear effect".

The purpose of this article is to show how the gear effect can be combined with the VEJ tidal-torquing model to

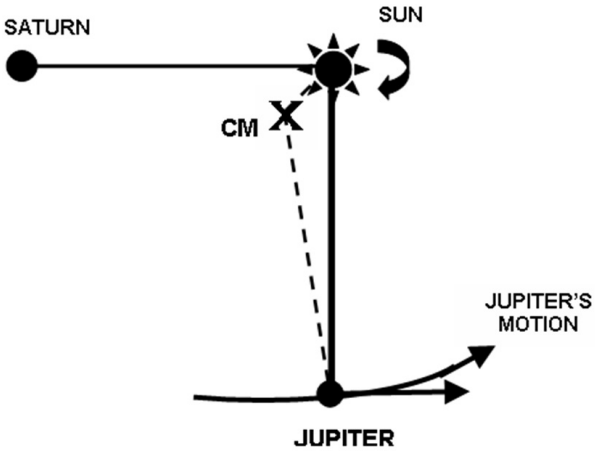

Figure 8. The orbital configuration when Jupiter and Saturn are in quadrature with Saturn following Jupiter in its orbit. Saturn drags the centre-of-mass of the Sun, Jupiter, Saturn system (CMSJSa) off the line joining the planet Jupiter to the Sun. As a result, the gravitational force of the Sun acting upon Jupiter speeds up its orbital motion around the CMSJSa. At the same time, the gravitational force of Jupiter acting on the Sun slows down the orbital speed of the Sun around the CMSJSa. The exchange of orbital angular momentum between the Sun and Jupiter is known as the quadrature effect.

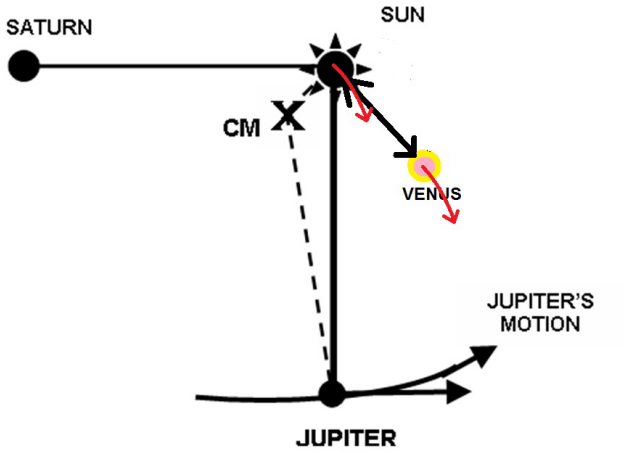

Figure 9. A re-plot of Fig. 8 with the terrestrial planet Venus preceding Jupiter in its orbit. This figure shows Saturn and Jupiter in quadrature, with Saturn following Jupiter. Under these circumstances, the quadrature effect ensures that the Sun's speed around the CMSJSa slows down. If this is the case then the same must be true for the terrestrial planets, since their orbital motions are constrained to move around the centre-of-mass of the Sun rather than the CMSJSa. The red arrows in this figure represent the decrease in speed of the Sun and Venus as they revolve in an anti-clockwise direction around the CMSJSa. This decrease in speed is shared by both the Sun and Venus so that the two bodies effectively move as one, maintaining their orientation and spacing.

produce a spin–orbit coupling model that links the rotation rate of the outer layers of the Sun to the Sun's motion around the centre-of-mass of the solar system (CMSS). In order to understand how the gear effect can be combined with the VEJ tidal-torquing model, we must, however, also discuss the quadrature effect.

3.2 The quadrature effect

Every 9.9 ± 1.0 yr, the planet Saturn is in quadrature with the planet Jupiter (i.e. the subtended angle between Saturn and Jupiter, as seen from the Sun, is 90 degrees). Figure 8 shows the orbital configuration when Jupiter and Saturn are in quadrature with Saturn following Jupiter in its orbit. Referring to this diagram, one can see that Saturn drags the centre-of-mass of the Sun, Jupiter, Saturn system (CMSJSa) off the line joining the planet Jupiter to the Sun. As a result, the gravitational force of the Sun acting upon Jupiter speeds up its orbital motion around the CMSJSa. At the same time, the gravitational force of Jupiter acting on the Sun slows down the orbital speed of the Sun about the CMSJSa. Of course, the reverse is true at the next quadrature, when Saturn precedes Jupiter in its orbit. In this planetary configuration, the mutual force of gravitation between the Sun and Jupiter slows down Jupiter's orbital motion around the CMSJSa and speeds up the Sun's orbital motion around the CMSJSa.

Hence, the Sun's orbital speed around the CMSJSa (as well as the CMSS) should periodically decrease and then increase as we move from one quadrature to the next (Jose, 1965). This change in speed of the Sun around the CMSJSa once every 19.859 yr is known as the quadrature effect (Wilson et al., 2008).

3.3 Differentiating between the quadrature effect and the gear effect

Figure 9 is a re-plot of Fig. 8 with the terrestrial planet Venus preceding Jupiter in its orbit. As with Fig. 8, Fig. 9 shows Saturn and Jupiter in quadrature, with Saturn following Jupiter. Under these circumstances, the quadrature effect ensures that the Sun's anti-clockwise motion around the CMSJSa will be slowed by the gravitational force of Jupiter. If this is the case, then the same must be true for the terrestrial planets, since their orbital motions are, for all intents and purposes, constrained to move around the centre-of-mass of the Sun rather than the CMSJSa. The red arrows in Fig. 9 represent the decrease in speed of the Sun and Venus as they revolve in an anti-clockwise direction around the CMSJSa. This decrease in speed is shared by both the Sun and Venus so that the two bodies effectively move as one, maintaining their orientation and spacing. Hence, the quadrature effect has little to no effect upon the tangential torques being applied to the outer layer of the Sun by the VEJ tidal-torquing model.

Figure 10 shows the Jupiter–Sun–Saturn system with its CM located at CMSJSa. This is the analogue of the ABC

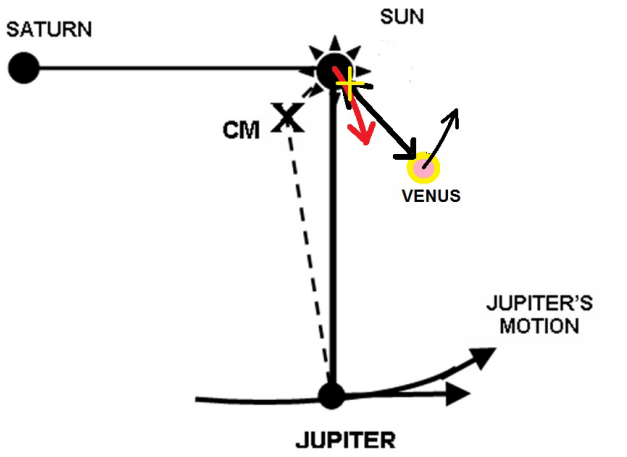

Figure 10. The Jupiter–Sun–Saturn system with its CM located at CMSJSa. This system is the analogue of the ABC structure, described in Sect. 3.1. The figure also shows the Sun–Venus system with its own independent CM. This is the analogue of the AD structure in Sect. 3.1. Now consider the situation where Venus applies a gravitational torque to the Sun that forces the Jupiter–Sun–Saturn system to reduce its orbital velocities around the CMSJSa (red arrow). One direct consequence of this is that the Jupiter–Sun–Saturn system will also apply a gravitational torque to Venus that speeds up the motion of Venus around the CMSJSa (dark curved arrow emanating from Venus). Hence, unlike the quadrature effect, the torques applied in the gear effect try to change the orientation and spacing between the Sun and Venus.

structure, described in Sect. 3.1. Figure 10 also shows the Sun–Venus system with its own independent CM. This is the analogue of the BD structure in Sect. 3.1. Now consider the situation where Venus applies a gravitational torque to the Sun that forces the Jupiter–Sun–Saturn system to reduce its orbital velocities around the CMSJSa (red arrow). One direct consequence of this is that the Jupiter–Sun–Saturn system will also apply a gravitational torque to Venus that speeds up the motion of Venus around the CMSJSa (dark curved arrow emanating from Venus).

Hence, Fig. 10 shows us that there are three critical features that distinguish the gear effect from the quadrature effect:

1. Unlike the quadrature effect, the torques involved in the gear effect try to change the orientation and spacing between the Sun and Venus, for example, in relation to the specific case shown in Fig. 10; even though these gravitational torques are very minute, they produce a net anti-clockwise rotation of the Sun and Venus around their mutual centre-of-mass (yellow cross). (NB: it is the offset between the CMSJSa and the centre-of-mass of the Sun–Venus system that is crucial for producing the net anti-clockwise rotation of the Sun and Venus around their mutual centre-of-mass.)
2. Even though the net gravitational torque tries to produce an anti-clockwise rotation of the Sun and Venus around their mutual centre-of-mass, some of the resulting angular momentum will almost certainly end up changing the rotation rates of both Venus and the outer layers of the Sun.
3. Given the minute nature of the torques applied and velocity changes involved, it is obvious that the effects of the gear effect will be greatest at the times when Venus and the Earth are aligned on the same side of the Sun (i.e. inferior conjunction). At these times, the Jupiter–Sun–Saturn system (which is at quadrature) would experience the combined gravitational force of Venus and the Earth, and the centre-of-mass of the aligned Sun–Venus–Earth system would be furthest from the centre of the Sun.

Hence, the gear effect should have an effect upon the tangential torques applied to the outer layers of the Sun by the VEJ tidal-torquing model and so it will modulate the changes in the rotation rate that are caused by the tidal-torquing mechanism.

Figure 11 shows the tangential torque applied by the alignments of Venus and Earth to the Jupiter–Sun–Saturn System (via the gear effect acting about the CMSJSa) plotted against time. It is important to note that the quantity plotted is not the actual tangential torque but a variable that is directly proportional to it. This variable is plotted in arbitrary units with positive values indicating that the torque is applied in a prograde direction and negative values indicating that it is applied in a retrograde direction. The data covers the period from October 1847 to December 2085 (Aciqra, 2008).

From Fig. 11 it is evident that both the retrograde and prograde torques varied in a quasi-sinusoidal manner throughout the 20th century and the first half of 21st century. A closer inspection reveals that the torque oscillates between being retrograde and prograde in direction over a period of 3.2 yr. These retrograde/prograde pairs persist over a 20 yr interval, with each bi-decadal period being separated from the next by two (or more) torques that act in the same direction. It is reasonable to presume that the length of the bi-decadal period is set by the 19.859 yr synodic cycle of Jupiter and Saturn.

In Fig. 12, the sums of the consecutive retrograde and pro-grade tangential torques shown in Fig. 11 are re-plotted against time. This allows us to see the long-term modulation of the net tangential torque acting upon the convective layers of the Sun between 1847 and 2085. As with Fig. 11, there is a bi-decadal pattern in the net torque produced by the gear effect that is set by the 19.859 yr synodic period of Jupiter and Saturn. However, there is also a longer term modulation of this pattern with a repetition period of approximately 193 yr.

Finally, Fig. 13 shows the angle subtended at the Sun by Venus and Earth (at inferior conjunction) and the centre-of-mass of the Sun–Jupiter–Saturn system, near each quadrature of Jupiter and Saturn, over the period from January 1003 to

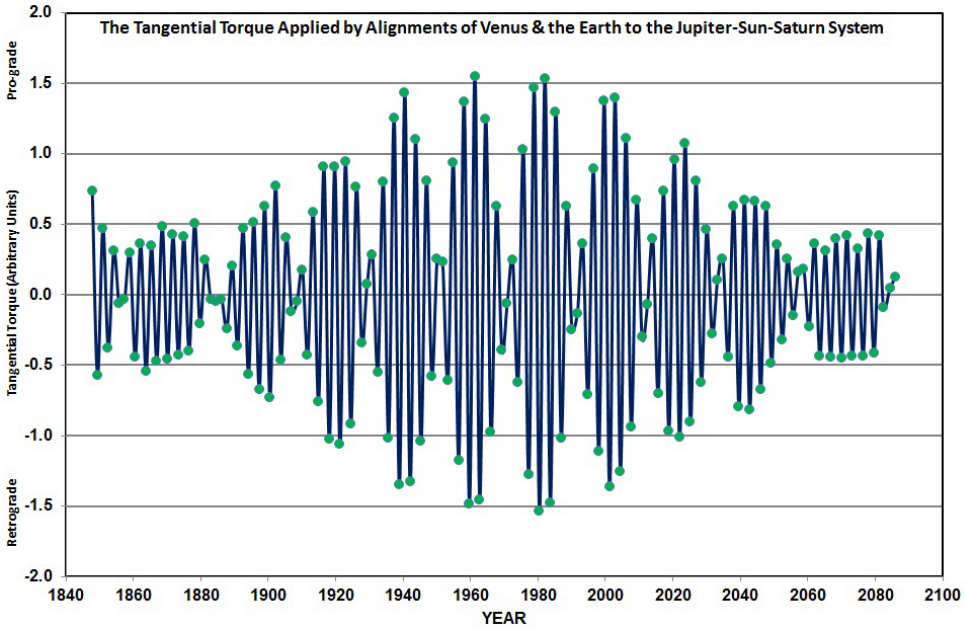

Figure 11. The tangential torque applied by the alignments of Venus and Earth to the Jupiter–Sun–Saturn System (via the gear effect acting around the CMSJSa) plotted against time. It is important to note that the quantity plotted is not the actual tangential torque but a variable that is directly proportional to it. This variable is plotted in arbitrary units with positive values indicating that the torque is applied in a pro-grade direction and negative values indicating that it is applied in a retrograde direction. The data covers the period from October 1847 to December 2085.

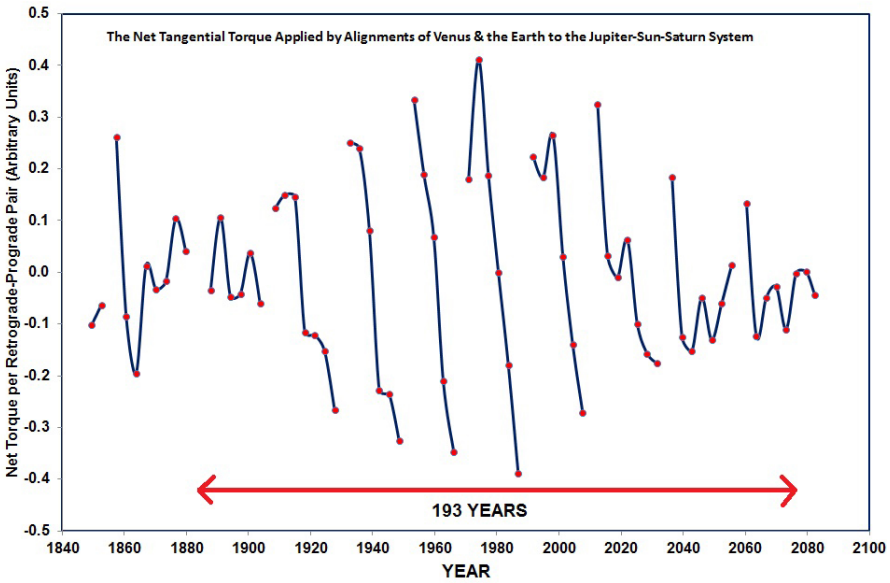

Figure 12. The sum of the consecutive retrograde and pro-grade tangential torques from Fig. 11, replotted against time. As with Fig. 11, there is a bi-decadal pattern in the net torque produced by the gear effect that is set by the 19.859 yr synodic period of Jupiter and Saturn. There is also a longer term modulation of this pattern with a repetition period of approximately 193 yr.

January 2015 (Aciqra, 2008). This plot shows that the tangential torques resulting from the gear effect are greatest when this subtended angle approaches 90° and least when the subtended angle approaches 0°.

Superimposed upon the data plotted in Fig. 13 are two sinusoidal functions with periods of 191.0 and 195.0 yr, synchronized to match in the year 1153. These two sinusoidal curves indicate that the longer term periodicity that

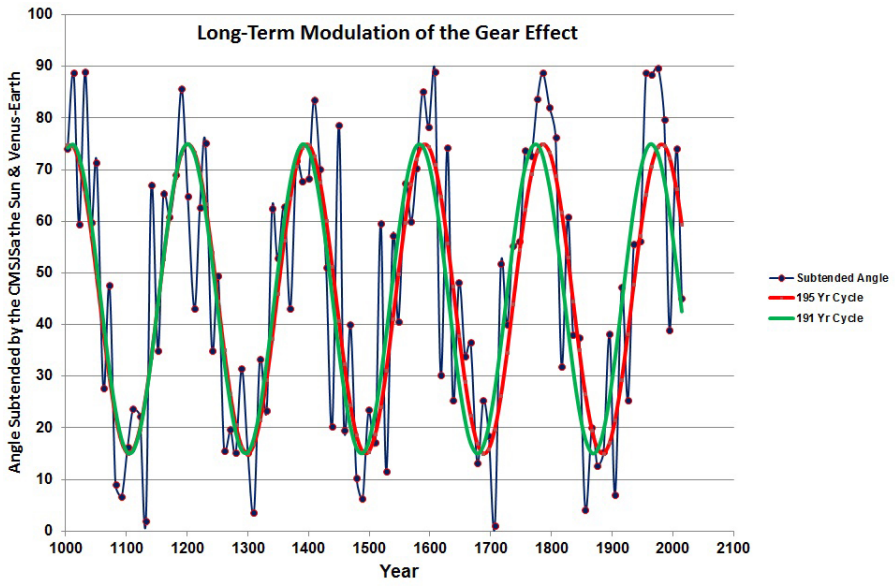

Figure 13. The angle subtended by Venus and Earth (at inferior conjunction) and the centre-of-mass of the Sun-Jupiter-Saturn system at the Sun, near each quadrature of Jupiter and Saturn over the period from January 1003 to January 2015. Superimposed upon the data are two sinusoidal functions with periods of 191.0 and 195.0 yr, synchronized to match in the year 1153. These two sinusoidal curves indicate that the longer term periodicity that is modulating the net torque produced by the gear effect has a period $\approx 193 \pm 2$ yr.

is modulating the net torque produced by the gear effect has a period $\approx 193 \pm 2$ yr. This long-term modulation cycle is almost certainly set by the time it takes for the 22.137 yr period associated with the VEJ tidal-torquing model to re-align with the 19.859 yr period associated with the gear effect:

$$(22.137 \times 19.859)/(22.137 - 19.859) = 192.98 \text{ yr}. \quad (1)$$

4 Conclusions

There are at least two ways that the Jovian and Terrestrial planets can influence bulk motions in the convective layers of the Sun. The first is via the VEJ tidal-torquing process:

- Tidal bulges are formed at the base of the convective layers of the Sun by the periodical alignments of Venus and the Earth.
- Jupiter applies a tangential gravitational torque to these tidal bulges that either speed-up or slow-down parts of the convective layer of the Sun.
- Jupiter's net tangential torque increases the rotation rate of the convective layers of the Sun for 11.07 yr (≈ 7 Venus–Earth alignments lasting 11.19 yr) and then decreases the rotation rate over the next 11.07 yr.
- The model produces periodic changes in rotation rate of the convective layers of the Sun that result a 22.14 yr (Hale-like) modulation of the solar activity cycle (≈ 14 Venus–Earth alignments lasting 22.38 yr).
- There is a long-term modulation of the net torque that has a period of ≈ 166 yr. This 166 yr modulation period results from the fact that 14 sidereal orbital periods of Jupiter (= 166.07 yr) almost equals 15 times the period required for Jupiter to move 90° in the Venus–Earth alignment reference frame $= 15 \times 11.0683$ yr (= 166.02 yr).

NB: More precisely, it is the mean time required for the 11.8622 yr periodic change in Jupiter's distance from the Sun to realign with the 11.0683 yr tidal-torquing cycle of the VEJ model.

$$(11.8622 \times 11.0683)/(11.8622 - 11.0683) = 165.38 \text{ yr} \quad (2)$$

The second way is via modulation of the VEJ tidal-torquing process via the gear effect:

- The gear effect modulates the changes in rotation rate of the outer convective layers of the Sun that are being driven by the VEJ tidal-torquing effect.
- This modulation is greatest whenever Saturn is in quadrature with Jupiter. These periodic changes in the modulation of the rotation rate vary over a 19.859 yr period.
- The gear effect is most effective at the times when Venus and the Earth are aligned on the same side of the Sun.
- There is a long-term modulation of the net torque that has a period of 192.98 yr.

While the VEJ tidal-torquing model can produces torques that have periods that closely match the length and phase of the 11.1 Schwabe cycle and the 22.1 yr Hale sunspot cycles, the model cannot easily reproduce the periods that are found by McCracken et al. (2013) for the long-term variations in the level of solar activity. In order to accomplish this, the VEJ tidal-torquing model must be combined with the gear effect to produce a new model called the VEJ spin–orbit coupling model. (NB: this new model is called a spin–orbit coupling model for the simple reason that its net outcome is to produce link between changes in the rotation rate of the convective layers of the Sun (SPIN), primarily near the Sun's equatorial regions, and changes in the Sun's motion around the CMSS (ORBIT)).

The new model produces torques with periodicities that fall into three broad categories (Table 1).

4.1 Category A – from the Gleissberg cycle, up to, but not including the Eddy cycle

These periods are produced by the synodic product of short periodicities that are associated with each of the models (i.e. 22.38 yr period for the VEJ tidal-torquing model and 19.859 yr period for the gear effect) such that

$$(22.38 \times 19.859)/(22.38 - 19.859) = 176.30 \text{ yr}. \quad (3)$$

as well as the following multiples of the 176.30 yr period:

$1/2 \times 176.30 = 88.15$ yr – Gleissberg cycle $\quad 2 \times 176.30 = 352.6$ yr

$3 \times 176.30 = 528.9$ yr $\quad 4 \times 176.30 = 705.2$ yr

It is important to note that the 22.38 yr VEJ tidal-torquing cycle is used here in the synodic product rather than the 22.14 yr cycle, since the gear effect interacts with the VEJ tidal-torquing mechanism via the VE alignments. This means that the interaction will take place at the 22.38 yr VE alignment repetition cycle. It also means that the 22.38 yr interaction cycle will slowly drift out of phase with the 22.14 yr torque application cycle, requiring some form of re-synchronization between these two cycles on longer term timescales.

4.2 Category B – the Eddy cycle and periods longer than the Eddy cycle

These periods are produced by a repetition cycle that is close to multiples of the synodic product of the longer modulating periods that are associated with each of the models (i.e. 165.35 yr period for the VEJ tidal-torquing model and 192.98 yr period for the gear effect) such that:

$$(165.38 \times 192.98)/(192.98 - 165.38) = 1156.3 \text{ yr}. \quad (4)$$

It takes Jupiter 575.518 yr to re-synchronize itself with the penta-synodic Venus–Earth alignment cycle. In addition, it takes two 575.518 yr periods (= 1151.0 yr) for Jupiter to re-synchronize itself with the penta-synodic Venus–Earth alignment cycle and also with respect to the stars (Wilson, 2013). Hence, the 1156.3 yr is most likely just a multiple of the fundamental Jupiter re-synchronization period of 575.518 yr.

These multiples of the 575.518 yr Jupiter re-synchronization cycle include:

$2 \times 575.518 = 1151.0$ yr $\quad 3 \times 575.518 = 1726.5$ yr

$4 \times 575.518 = 2302.1$ yr – Hallstatt cycle.

4.3 Category C – the de Vries cycle and sub-multiples of the de Vries cycle

Finally, the synodic product of the 176.30 yr cycle with the 1151.0 yr cycle is

$$(1151.0 \times 176.30)/(1151.0 - 176.30) = 208.2 \text{ yr}. \quad (5)$$

This is very close to the 208 yr de Vries cycle.

Hence, the new model called the VEJ spin–orbit coupling model, formed by combining the VEJ tidal-torquing model with the gear effect, is able to produce many of the long-term periods in solar activity that are found by McCracken et al. (2013) from proxy ^{10}Be and ^{14}C data spanning the last 9400 yr (compare columns 1 and 3 of Table 1).

Acknowledgements. The author would like to thank J. P. Desmoulins, Ulric Lyons, Ching-Cheh Hung, Ray Tomes, P. A. Semi, Roy Martin, Roger Tattersall, Paul Vaughan and R. J. Salvador for their contributions to the development of the VEJ tidal-torquing model and Ken McCracken for his support and encouragement of this research.

Edited by: N.-A. Mörner
Reviewed by: two anonymous referees

References

Abreu, J. A., Beer, J., Ferriz-Mas, A., McCracken, K. G., and Steinhilber, F.: Is there a planetary influence on solar activity?, Astron. Astrophys., 548, 1–9, 2012.

Aciqra Io 1.1.0 Planetarium Software Package – Caglo 2008–2009.

Bollinger, C. J.: A 44.77 year Jupiter-Earth-Venus configuration Sun-tide period in solar-climate cycles, Academy of Science for 1952 – Proceedings of the Oklahoma, 307–311, available at: http://digital.library.okstate.edu/oas/oas_pdf/v33/v307_311.pdf, 1952.

Callebaut, D. K., de Jager, C., and Duhau, S.: The influence of planetary attractions on the solar tachocline, J. Atmos. Sol.-Terr. Phy., 80, 73–78, 2012.

Charvátová, I.: The solar motion and the variability of solar activity, Adv. Space Res., 8, 147–150, 1988.

Chárvátova, I.: On the relation between solar motion and solar activity in the years 1730–1780 and 1910–60, Bull. Astr. Inst. Czech., 41, 200–204, 1990.

Charvátová, I.: Can origin of the 2400-year cycle of solar activity be caused by solar inertial motion?, Ann. Geophys., 18, 399–405, doi:10.1007/s00585-000-0399-x, 2000.

de Jager, C. and Versteegh, G. J. M.: Do Planetary Motions Drive Solar Variability?, Sol. Phys., 229, 175–179, 2005.

Desmoulins, J. P.: Sunspot cycles are they caused by Venus, Earth and Jupiter syzygies?, available at: http://jpdesm.pagesperso-orange.fr/sunspots/sun.html, last access: September 2013, 1989.

Fairbridge, R. W. and Shirley, J. H.: Prolonged Minima and the 179-yr Cycle of the Solar Inertial Motion, Sol. Phys., 110, 191–210, 1987.

Gnevyshev, M. N. and Ohl, A. I.: On the 22-year solar activity cycle, Astron. Zh., 25, 18–20, 1948.

Horizons on-Line Ephemeris System v3.32f 2008, DE-0431LE-0431 – JPL Solar System Dynamics Group, JPL Pasadena California, available at: http://ssd.jpl.nasa.gov/horizons.cgi, 2008.

Hung, C.-C.: Apparent Relations Between Solar Activity and Solar Tides Caused by the Planets, NASA report/TM-2007-214817, available at: http://ntrs.nasa.gov/search.jsp?R=20070025111, 2007.

Javaraiah, J.: Long-Term Variation in the Solar Differential Rotation, Sol. Phys., 212, 23–49, 2003.

Javaraiah, J. and Gokhale, M. H.: Periodicities in the Solar Differential Rotation, Surface Magnetic Field and Planetary Configurations, Sol. Phys., 158, 173–195, 1995.

Jose, P. D.: Sun's motion and sunspots, AJ, 70, 193–200, 1965.

Juckett, D.: Solar Activity Cycles, North/South Asymmetries, and Differential Rotation Associated with Solar Spin-Orbit Variations, Sol. Phys., 191, 201–226, 2000.

Landscheidt, T. J.: Swinging Sun, 79-Year cycle, and climatic change, Interdiscipl. Cycl. Res., 12, 3–19, 1981.

Landscheidt, T. J.: Extrema in Sunspot Cycle Linked to Sun's Motion, Sol. Phys., 189, 413–424, 1999.

McCracken, K. G., Beer, J., Steinhilber, F., and Abreu, J.: A Phenomenological Study of the Cosmic Ray Variations over the Past 9400 Years, and Their Implications Regarding Solar Activity and the Solar Dynamo, Sol. Phys., 286, 609–627, 2013.

Shirley, J. H.: Axial rotation, orbital revolution and solar spin-orbit coupling, Mon. Not. R. Astron. Soc., 368, 280–282, 2006.

Wilson, I. R. G.: Do Periodic Peaks in the Planetary Tidal Forces Acting Upon the Sun Influence the Sunspot Cycle?, The General Science Journal, 3812, 1–25, 2011.

Wilson, I. R. G.: The VEJ Tidal Torqueing Model Can Explain Many of the Long-Term Changes in the Level of Solar Activity. II. The 2300 Year Hallstatt Cycle, available at: http://astroclimateconnection.blogspot.com.au/2013/08/the-vej-tidal-torquing-model-can.html, 2013.

Wilson, I. R. G., Carter, B. D., and Waite, I. A.: Does a Spin–Orbit Coupling Between the Sun and the Jovian Planets Govern the Solar Cycle?, PASA, 25, 85–93, 2008.

Zaqarashvili, T.: On a possible generation mechanism for the solar cycle, Ap. J., 487, 930–935, 1997.

Part IX

Celestial commensurabilities: some special cases. Jelbring, H.: Pattern Recogn. Phys., 1, 143-146, doi:10.5194/prp-1-143-2013, 2013.

Pattern Recogn. Phys., 1, 143–146, 2013
www.pattern-recogn-phys.net/1/143/2013/
doi:10.5194/prp-1-143-2013

Pattern Recognition in Physics
Open Access

Celestial commensurabilities: some special cases

H. Jelbring

Tellus, Stockholm, Sweden

Correspondence to: H. Jelbring (hans.jelbring@telia.com)

Received: 5 October 2013 – Revised: 24 October 2013 – Accepted: 30 October 2013 – Published: 2 December 2013

Abstract. Commensurabilities are calculated based on published orbital periods of planets and satellites. Examples are given for commensurabilities that are strong or very strong. There are sets of commensurabilities that involve 3–4 celestial bodies. Our moon–Earth system is probably a key system forming commensurabilities with all the inner planets. The existence and structure of commensurabilities indicate that all celestial bodies in our Solar System interact energetically. The Solar System seems to include an unknown physical process capable of transferring energy between both celestial bodies (orbital energy) and between orbital energy and rotational energy. Such a process is proposed to be the major reason for the evolution of commensurabilities, which are judged as not being produced by chance. The physical reason for their creation still remains undiscovered, however.

1 Background

It is well known that orbital or rotational periods of celestial objects sometimes interlock with each other. The mathematical definition of commensurability is: "*exactly divisible by the same unit an integral number of times*". Our moon always shows the same side towards us. The moon rotates (relative to the stars) at exactly the same period as it orbits around Earth. This is an example of commensurability. As a satellite to a planet it is not alone. Almost all inner satellites to the giant planets behave like our moon does. They turn the same face towards its mother planet at all times.

The concept of commensurability became popular when the Kirkwood gaps among the asteroids were discovered. It turned out that they avoid orbiting at certain (small) rational numbers times the period of Jupiter such as $1/2$, $3/7$, $2/5$ and $1/3$. The well-known Bode–Titus law suggests fitting all the planets into approximate commensurabilities (Boeyens, 2009). This "law" does not produce commensurabilities as defined here even if it turns out to be a physical process that can explain the temporal distribution of planetary periods in some approximate way. A similar fair "law" can be found between the inner Jovian satellites, whose orbital periods approximately turn out to be related as $1 : 2 : 4$.

A more serious attempt to find commensurabilities among planets was made by Rhodes Fairbridge, who pairwise quantified a number of relationships between planetary orbital periods (see: "Commensurability", "Kirkwood", "Asteroid resonance" and "Orbital commensurability and resonance" in Shirley and Fairbridge, 1997). It remains to find out if there are commensurabilities between orbital periods and rotational periods among all bodies in the Solar System. Allan (1971) indicates (1) that the Newton gravity formula plus Kepler's law based on observations are not enough to predict long-term orbital motion, and (2) that orbital motion is affected by resonances with the rotational period of a planet (in this case Earth).

2 Purpose of article

A number of scientists claim that observed (close) commensurabilities are just produced by chance, while others consider them to be an important result of the Solar System evolution. These commensurabilities should be remarkable enough to warrant further investigation necessary for increased knowledge and understanding of the Solar System. It is the author's opinion that commensurabilities are a result of energy transfer between celestial bodies that have evolved during an extended time period, and that the physical processes responsible are as yet inadequately known. In this paper some known and some unpublished commensurabilities will be presented. The few examples mentioned here will be

Table 1. Orbital periods.

Planets/satellites	years or days	denotation
Mercury	0.2408 87.969	Tme
Venus	0.6152 224.701	Tv
Earth	1.00000	Te
Mars	1.8809	Tma
Jupiter	11.8622	Tj
Saturn	29.4577	Ts
Uranus	84.013	Tu
Neptune	164.79	Tn
Pluto	248.4	Tp
Synodic month	29.53059	Tsyn
Sidereal month	27.32166	Tsid
Anomalistic month	27.55455	Tano
Draconitic month	27.21222	Tdra
Tropical month	27.32158	Ttro
Io	1.769138	Tio
Europa	3.551181	Teu
Ganymede	7.154553	Tga
Callisto	16.689018	Tca
Saros period	6585+1/3	T(Saros)

briefly discussed in the context of Solar System evolution. The intention is to raise awareness of the fact that commensurabilities are not created by chance. The motion of celestial bodies in our Solar System is neither strictly Keplerian nor "chaotic".

3 Method

The orbital periods (Table 1) are mostly quoted from Nordling and Österman (1980). The reason for using planetary orbital periods from this source instead of modern NASA data (2013) is that the former is based on long-term visual records of celestial bodies, while the NASA records are based on short-term instrumental records. Orbital periods in the Solar System are not strictly constant. They vary considerably, but their average values are quite stable over long time scales. However, it is not known whether the long-term planetary periods are quietly diminishing or weakly pulsating. They might even be both at the same time. An examination of commensurabilities provides some answers relating to probable paths of the Solar System evolution. A number of commensurabilities will be calculated below and these will be assigned a simple quality value.

Note that the orbital periods for Mercury and Venus are given to only four significant digits and Jupiter and Saturn to six, according to Nordling and Österman (1980). NASA provides 5–6 digits for the inner planets. The quality concept that will be used in this paper is illustrated by the orbital motions of Venus and Earth. The beat frequency between Venus and Earth is here denoted by $\mathrm{Tv}\,||\,\mathrm{Te}$ (Note: The symbol "||" is used to denote the average beat period between two bodies orbiting the same centre, such that $5\times\mathrm{Tv}\,||\,\mathrm{Te}=7.9938$; $8\times\mathrm{Te}=8.00000$ yr). The ratio between these numbers is 1.000776. This level of commensurability is designated as being rather weak and will be called a 3-digit commensurability.

4 Examples of commensurabilities

4.1 The Saros cycle and lunar commensurabilities

$223\times\mathrm{Tsyn}=6585.32$; $239\times\mathrm{Tano}=6585.54$; $242\times\mathrm{Tdra}=6585.36$; $241\times\mathrm{Tsid}=6584.52$ (days)

The Saros cycle was discovered in Babylon a couple of hundred years BC. This is an excellent example of 4–5 digit commensurabilities. It should be noted that the position of the moon in relation to the stars (Tsid) only qualifies as a 3-digit commensurability. The motion of the perigee and ascending node of the moon will move in opposite directions in relation to the stars and will meet every 5.99673 yr (average value).

$6\times\mathrm{Te}=2191.538$; $1\times\mathrm{Tdra}\,||\,\mathrm{Tano}=2190.344$ (days)

This is a 4-digit commensurability. The question arises if these periods are synchronized to Earth's orbital period just by chance or not. Notice that the observed synchronicity is not exact, and that it should not be expected to be so. The Solar System is a dynamic system which has always changed and which will continue to change. However, if the change is slow, it seems that close-to-perfect commensurabilities can and will evolve.

4.2 Days on Mercury and Venus and Earth's orbital period

Many planetary satellites lock one face towards the planet. Is there evidence that the satellite had been spinning before it got locked up? There are two arguments that should be considered. Most asteroids do rotate, often with a rotation period around 10 h, and then there are the rotation periods of the planets Mercury and Venus, which provide good examples that planets might approach a steady state with a very slow rotation. In this case these periods seem coupled with Earth's orbital period, and it seems a plausible hypothesis that both Mercury and Venus once rotated much faster. According to NASA (2013), Mercury's average day is 175.2 days long and its sidereal rotation period is (on average) 58.65 days. Mercury and Earth are at closest approach every 115.88 ($\mathrm{Tme}\,||\,\mathrm{Te}$) days, which is the most favourable time for scientists to observe its surface. During such conjunctions, surface visibility is limited by strong sunlight. This is the reason why earlier it was wrongly believed that Mercury's rotation was synchronized with its orbital period. At every third inferior conjunction, Mercury presents the same side towards Earth.

$2\times175.2=350.4$; $3\times115.88=347.64$ (days)

This is a weak commensurability, but it seems to indicate an evolution in which Earth is playing a role and which might turn into a strong future commensurability. This suggestion is strengthened by the next example. Venus is slowly rotating in a retrograde direction. There are reasons to believe that Venus has gone from a fast prograde rotation to its current retrograde rotation. Every other planet rotates in a prograde direction (except Uranus, which is a special case). Venus has probably slowed down and then found a "steady state" retrograde rotation, which might be very stable. Venus' rotation period is 243.02 days. Its length of day is 116.75 days.

$6 \times 116.75 = 583.75; \quad 1 \times \mathrm{Tv} \| \mathrm{Te} = 583.95$ (days)

This is close to a 4-digit commensurability, (very probably) meaning that Earth is affecting the rotation period of Venus in a way that Venus shows the same face towards Earth every time there is an inferior conjunction between the two planets.

4.3 The Galilean satellites

The orbital periods are known to a high precision with 7 digits. A glance at the periods in Table 1 is enough to see that consecutive periods among Jupiter's inner satellites are approximately doubled. The best fit is between Europa and Io, where Teu/Tio = 2.00729, which could be called a week commensurability. However, we are looking for something more interesting. It is possible to find pairwise commensurabilities as follows.

$283 \times \mathrm{Tio} = 500.666; \quad 47 \times \mathrm{Teu} = 166.906; \quad 7 \times \mathrm{Tga} = 50.0818;$
$30 \times \mathrm{Tca} = 500.670; \quad 10 \times \mathrm{Tca} = 166.890; \quad 3 \times \mathrm{Tca} = 50.0671$ (days)

What makes these commensurabilities really intriguing is that there exists a "master" period for all of them, namely around 500.7 days or 1.371 yr. These are 4–5 digit commensurabilities, involving four celestial bodies.

$283 \times \mathrm{Tio} = 500.666; \quad 141 \times \mathrm{Teu} = 500.818; \quad 70 \times \mathrm{Tga} = 500.818$ (days)

$30 \times \mathrm{Tca} = 500.670$ (days);

All the Galilean moons seem to be energetically interlocked with each other.

4.4 The Jupiter–Earth–Mars commensurability

There is an undiscovered strong three-body commensurability between our own planet, Mars and Jupiter. The beat frequency between Earth and Mars is 2.1352(0) yr. This is coupled with the orbital period of Jupiter in the following way:

$50 \times \mathrm{Te} \| \mathrm{Tma} = 106.76(0); \quad 9 \times \mathrm{Tj} = 106.760$ (yr)

Such a 5- or 6-digit commensurability poses the question of whether there are relationships that, on average, are very close to being exact over long time periods. Besides, Earth and Mars are involved in another 4-digit commensurability in which Jupiter is left out.

$37 \times \mathrm{Te} \| \mathrm{Ma} = 79.0025; \quad 79 \times \mathrm{Te} = 79.0000$ (yr)

4.5 The Jupiter–Saturn commensurability

$149 \times \mathrm{Tj} = 1767.47; \quad 60 \times \mathrm{Ts} = 1767.46; \quad 89\,\mathrm{Tj} \| \mathrm{Ts} = 1767.47$ (yr)

This truly remarkable 6-digit commensurability is close to being exact. The orbital periods might be variable, but the commensurabilities should be of a more stable nature than the periods themselves. It is quite possible that this cycle is the Grand Cycle of our Solar System. It might be the periodicity that Jelbring (1996) discussed with respect to Shove's (1955) sunspot records. The longest periods were hard to be precise about for limitations caused by the length of the time series: "If any specific component should pointed out it is the slowly varying one with a 'period' around 1700 yr. Regarding this component Schove's data can hardly be wrong". It should be pointed out that the period in question related to the phase of sunspot numbers from about 300 BC to 1980 AD.

4.6 Commensurabilities among the inner planets

There are good reasons to consider our moon as a planet rather than a satellite. The major argument is that its orbit is more prone to staying in the ecliptic plane rather than the equatorial plane of Earth. Our moon–Earth system might play a crucial role as an "energy transfer gate" between the planets in our Solar System.

$13 \times \mathrm{Tme} \| \mathrm{Te} = 1506.06; \quad 51 \times \mathrm{Tsid} \| \mathrm{Te} = 1506.06;$
$38 \times \mathrm{Tsid} \| \mathrm{Tme} = 1506.06$ (days)

These are 3 interlocked 6-digit commensurabilities and can hardly be considered as "produced" by chance. They simply imply that there has to exist an unknown force affecting energy transfer in the Solar System. Furthermore, there is also a "master" period, which includes the remaining inner planet Venus.

$969 \times \mathrm{Tsid} \parallel \mathrm{Te} = 28615.1$ (days or 78.343 yr)
$920 \times \mathrm{Tsid} \parallel \mathrm{Tv} = 28615.2$
$722 \times \mathrm{Tsid} \parallel \mathrm{Tme} = 28615.2$
$198 \times \mathrm{Tme} \parallel \mathrm{Tv} = 28615.4$
$247 \times \mathrm{Tme} \parallel \mathrm{Te} = 28615.1$
$49 \times \mathrm{Tv} \parallel \mathrm{Te} = 28613.8$

Note that $\mathrm{Tsid} \| \mathrm{Te}$ is equal to the synodic month.

Our moon's importance for energy transfer is probably demonstrated by the fact that the $\mathrm{Tsid} \| \mathrm{Tv}$ provides a higher quality commensurability compared to $\mathrm{Tv} \| \mathrm{Te}$. It is quite amazing that 6-digit commensurabilities can arise using only 4-digit values for the periods of Mercury and Venus. A probable explanation is that the mean orbital long-term periods of Mercury and Venus are very close to 0.240800 and 0.615200 yr. The corresponding NASA (2013) values are given with 5 and 6 digits as 87.969 days (0.24084 yr) and 224.701 days (0.61519 yr). Values on planetary orbital periods by Nordling and Österman (1980) are preferred, however, for the reasons given above.

5 Discussion

A celestial commensurability is just a pair of numbers. It does not explain anything except a factual relationship between periods which happen to be described by two integers with a good accuracy. By studying commensurabilities like the ones mentioned above, it is quite hard to ignore them as stochastic phenomena. It is possible to test how much these examples deviate from a random result. Such an exercise is not hard to do. It will not be performed here for reasons of time and space. In this paper, I have focused on a few cases of quite amazing commensurabilities, indicating clear deviations from a random distribution.

This paper demonstrates the existence of 3–4 high-quality body commensurabilities among planets, which is an important discovery. This implies that celestial bodies are able to transfer energy between themselves. It also means that the energy transfer is not strictly dependent on distance between the interacting bodies, as has to be the case for interactions based on Newton's gravity formula. There is a lack of a potent theory explaining how this is possible. Some of the examples show that there are reasons to believe in a type of energy transfer between orbital and rotational energy which is unknown or at least not yet well understood, which, by itself, is an important insight. The study of commensurabilities does not provide strict evidence, but points to directions for more complex research efforts. It is easy to get the impression that all the celestial bodies in the Solar System are constantly interacting with each other.

The existence and evolution of Kirkwood gaps in the asteroid belt certainly support such a view. It seems that certain celestial bodies are more active in forming commensurabilities than others. There is little doubt that Jupiter is the major reason for the Kirkwood gaps to evolve. If the sunspot generation is proven to be caused by physical agents outside the surface of the Sun, Jupiter and Saturn would be the main suspects. The examples relating to the inner planets show, that our moon seems to be an important celestial body and that its synodic and sidereal periods are important orbital periods. There have to be identifiable physical reasons for this situation to evolve, however. This issue is discussed separately in Jelbring (2013).

The ultimate task in the context of Solar System evolution, still urgent to resolve, is the identification of the physical mechanisms creating sunspots. Firstly, it is pivotal to prove if sunspots are (mainly) caused by physical agents residing inside our Sun or outside the Sun's surface. Secondly, the present author is persuaded that advanced knowledge about when, how and why commensurabilities evolve will also give an answer to the riddle of which physical processes are responsible for creating sunspots.

Acknowledgements. Many thanks to engineers and scientists around the world producing measurements and making it possible to interpret how nature functions.

Edited by: N.-A. Mörner
Reviewed by: two anonymous referees

References

Allan, R. R.: Commensurable Eccentric Orbits near Critical Inclination, Celestial Mech., 3, 320–330, 1971.

Boeyens, J. C. A.: Commensurability in the Solar System, Unit for Advanced study, University of Pretoria, 2009.

Jelbring, H.: Analysis of sunspot cycle phase variations – based on D. Justin Schove's proxy data, J. Coastal. Res., 17, 363–369, 1996.

Jelbring, H.: Energy transfer in the Solar System, Pattern Recogn. Phys., in press, 2013.

NASA: Fact sheets, http://nssdc.gsfc.nasa.gov/planetary/planetfact.html, last access: November 2013.

Nordling, C. and Österman J.: Physics handbook, Studentlitteratur, Lund, Sweden, 1980.

Schove, D.: The sunspot cycle, 649 BC to AD 1986, J. Geophys. Res., 60, 127–146, 1955.

Shirley, J. H. and Fairbridge, R. W. (Eds.): Encyclopedia of Planetary Sciences, Chapmann & Hall, 1997.

Part X

Responses of the basic cycle of 178.7 and 2402 yr in solar–terrestrial phenomena during Holocene.

Charvátová, I., Hejda, P.: Pattern Recogn. Phys., 2, 21-26, doi:10.5194/prp-2-21-2014, 2014.

Pattern Recogn. Phys., 2, 21–26, 2014
www.pattern-recogn-phys.net/2/21/2014/
doi:10.5194/prp-2-21-2014

Pattern Recognition in Physics
Open Access

Responses of the basic cycles of 178.7 and 2402 yr in solar–terrestrial phenomena during the Holocene

I. Charvátová and P. Hejda

Institute of Geophysics, Academy of Sciences, Prague, Czech Republic

Correspondence to: P. Hejda (ph@ig.cas.cz)

Received: 11 December 2013 – Revised: 6 January 2014 – Accepted: 7 January 2014 – Published: 17 January 2014

Abstract. Reconstructions of solar–terrestrial (ST) phenomena, in sufficient quality, several thousands of years backward by means of radiocarbon (^{14}C), ^{10}Be or ^{18}O isotopes have been employed for study of possible responses of the ordered (trefoil) and disordered intervals (types) of the solar inertial motion (SIM) as well as of the 370 yr exceptional segments occurring in steps of 2402 yr in these phenomena. The trefoil intervals are about 50 yr long, and the Sun returns to the trefoil intervals always after 178.7 yr, on average. During intermediate intervals the Sun moves along chaotic (disordered) lines. It was also found that very long (nearly 370 yr) intervals of the solely trefoil orbit of the SIM occurred in steps of 2402 yr. Such exceptional intervals occurred in the years 159 BC–208 AD, 2561–2193 BC, 4964–4598 BC, etc. A stable behaviour of ST phenomena during these long segments is documented. It was also found that the deepest and longest solar (temperature) minima (of Spörer or Maunder types) occurred in the second half of the 2402 yr cycle in accordance with the respectively most disordered types of the SIM. The SIM is computable in advance: the SIM comparable with that after 1873 is before us. Corresponding behaviours of ST phenomena can be expected.

1 Introduction

In recent years many papers considering possible planetary influences on solar–terrestrial (ST) and climatic variability were published (Beer et al., 2000; Abreu et al., 2012). These authors primarily dealt with the tidal influences of the planets on the Sun and computed the spectral analyses of ST and climatic data. The results show good correlations. The papers published up to the 1970s showed that a tidal enhancement from planets is in the order of millimetres. The latest papers employ the data (reconstructions) from nearly the whole Holocene.

This paper will deal with the solar inertial motion (SIM). The SIM is not negligible, it is a very noticeable phenomenon. The Sun moves within an area of a diameter of 4.3 r_s, where r_s is the solar radius (see Fig. 1), or 3×10^6 km. Our contributions (several tools) for the SIM-ST and climatic studies have been employed as follows:

1. The periods found in the SIM (in all its motion characteristics such as the velocity, the acceleration, the radii of curvature, etc.) are higher harmonics of the basic period of 178.7 yr (Bucha et al., 1985; Jakubcová and Pick, 1987). The basic period of 178.7 yr was found by Jose (1965) and further described by Fairbridge and Shirley (1987). Charvátová and Střeštík (2004) detected such periods, between 6 and 16 yr, in European temperature series and Charvátová-Jakubcová et al. (1988) detected these periods between 10 and 60 yr in global aurora records (cf. also Scafetta, 2012b). Since the solar motion characteristics are underlaid by variable geometries of the solar orbit, the results of spectral analyses are dependent on the intervals being employed (Charvátová and Střeštík, 1995). Scafetta and Wilson (2013) detected these periods in Hungarian aurora records since 1523.

2. Separation of the SIM into two basic types, the ordered (in JS trefoils) and disordered (Charvátová, 1990, 1995).

3. The very long, regular cycle of 2402 yr represents a repetition of the exceptional, nearly 370 yr-long interval of trefoil solar motion.

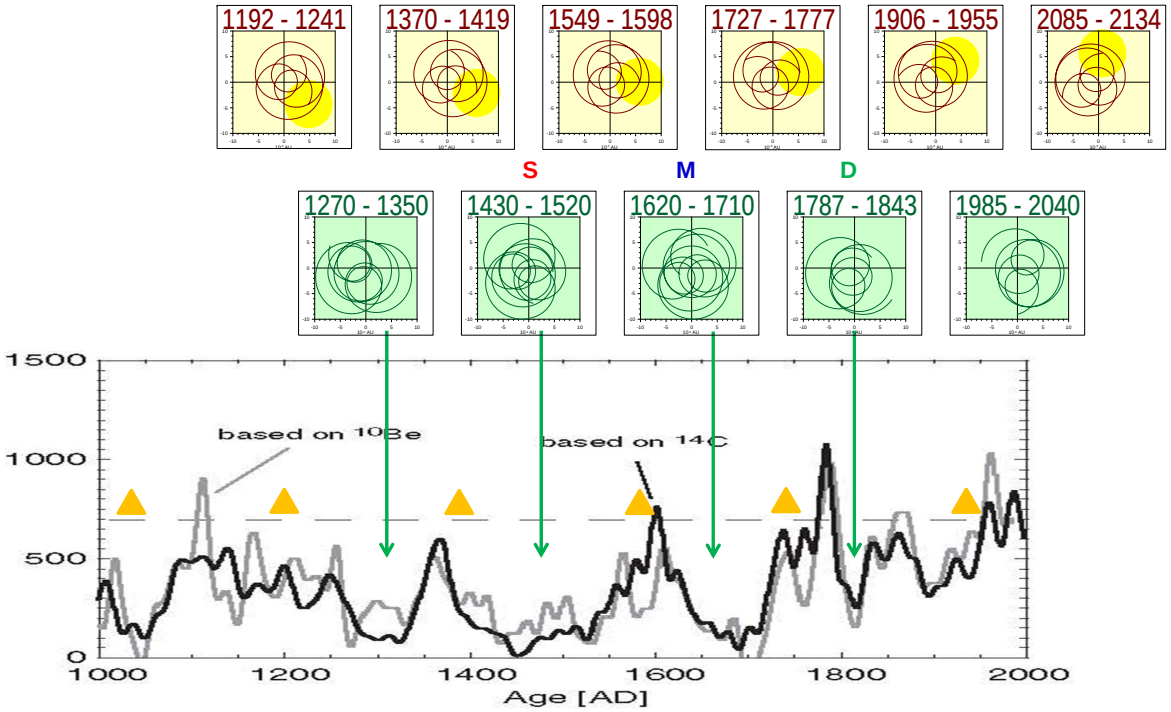

Figure 1. Above: the solar orbit divided into two basic types, the one ordered in JS (Jupiter/Saturn) trefoils (yellow) and one disordered (chaotic) (green). The Sun is returning at the trefoil orbits after 178.7 yr. The Sun moves in the area with a diameter of 4.3 r_s, where r_s is solar diameter or 3×10^6 km. The yellow circles denote the Sun. Below: a solar modulation record based on ^{14}C and on ^{10}Be since 1000 AD (taken from Muscheler et al., 2007). Long-term maxima in these records tend to coincide with the trefoil intervals (yellow triangles mark their centres). Grand prolonged minima occurred in accordance with the intervals of the chaotic motion of the Sun (see lower green orbits), S – Spörer, M – Maunder, D – Dalton minima. A moderate chaotic (green) type of the SIM (1980–2040) indicates lowered both solar activity and surface air temperature.

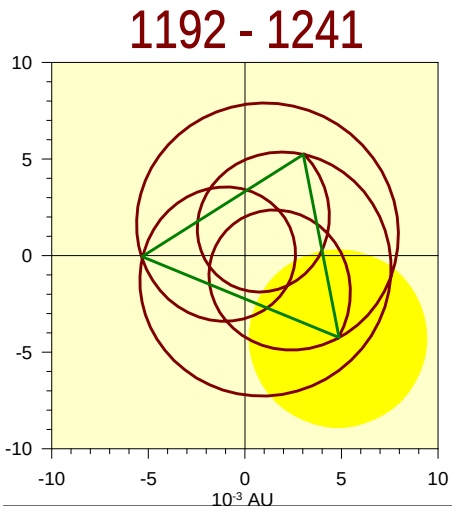

Figure 2. Triplet of loops (brown) and the characteristic triangle (green). The trefoils are characterized by nearly equilateral triangles.

4. Nearly identical parts of the SIM were found (e.g. 1840–1905 and 1980–2045 AD), which were employed for predictive assessments (Charvátová, 2009).

2 The cycle of 178.7 yr in the SIM, ST and climatic relations

Important insight into the SIM, ST and climatic relations gradually appeared since the geometry of the SIM was studied. The geometry of the SIM consists of loops and arcs. It was found that the geometry of the SIM can be divided into two basic types, the ordered (in JS trefoils) and disordered (chaotic) types (Charvátová, 1988, 1989, 1990; Charvátová and Střeštík, 1991). The average length of the loop-arc pair is 19.85 yr (Jupiter/Saturn synodic period). The Sun returns at the trefoil orbit after 9 cycles, i.e. 178.7 yr, on the average. The precise basis for the study of the relations between the SIM and solar–terrestrial and climatic variability thus arose. The SIM can be computed into the future, providing new predictive possibilities.

The trefoil is a stable shape. A movement of the Sun along one loop or arc lasts for 10 yr (JS/2). Here it seems pertinent

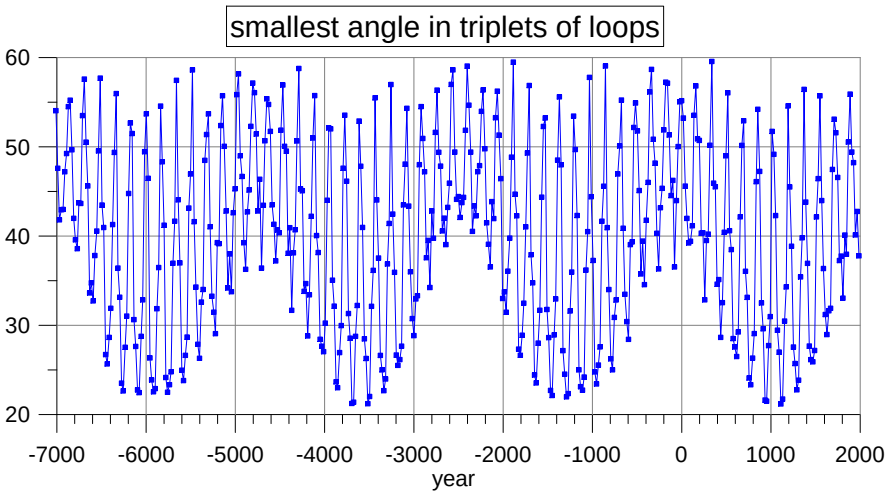

Figure 3. The smallest angle of the characteristic triangle of triplets of loops. The basic cycle of 171.4 yr (UN) as well as the long cycle of 2402 yr is well demonstrated. The cycle of 2402 yr is 14 cycles of 171.4 yr.

for a short review of our previous results dealing with behaviour of solar–terrestrial (ST) phenomena during the trefoils: the last trefoil occurred in 1906–1956. The lengths of the respective sunspot cycles (15–19) varied between 10.0 and 10.6 yr, being 10.3 yr on average, a mean value of the lengths of cycles from −1 to +3 (in the previous trefoil) is also about 10 yr. This supports a bimodality of sunspot cycle lengths with modi of 10 and 12 yr found by Rabin et al. (1986). The dominant period in geomagnetic index aa is also 10 yr (Charvátová and Střeštík, 2007). The series of sunspot cycles in the trefoil interval of the 18th century nearly coincide with that in the trefoil in the 20th century. This was also confirmed by methods of nonlinear dynamics, i.e. quantitatively (Paluš et al., 2000). Instrumental temperature series measured since 1750 in central Europe, in Jesuit monasteries, show temperature maxima in centres of the trefoils (in about 1760 and in about 1940) (Charvátová, 1995). During the trefoil intervals volcanic activity is attenuated, there is a general absence of large volcanic events (Charvátová, 1997).

Further back in time we can use reconstructed data. Figure 1 shows the reconstruction of solar activity by means of the amount of ^{14}C (radiocarbon) in tree rings and surface temperature by means of ^{10}Be since 1000 AD. It is seen that long-term maxima of both solar activity and of surface temperature tend to coincide with the mid-points of the trefoil intervals. The great prolonged minima such as the Spörer or Maunder minima, on the other hand, coincide with the chaotic motion of the Sun. The last prolonged solar minima were recently studied by Cionco and Compagnucci (2012), Mörner (2013), Salvador (2013), and Solheim (2013).

We may conclude that the SIM is the central factor which causes ST and climatic variability. It can be held as a driving force of climatic changes

3 The cycle of 2402 yr in the SIM and its response in ST phenomena

The ordered (trefoil) intervals of the SIM are characterized by a triplet of loops whose vertices form a nearly equilateral triangle (see Fig. 2). On the other hand, loops in disordered parts are often distributed along a straight-line and the corresponding triangle has at least one small angle (see e.g. Dalton period in Fig. 1). The smallest angle of the triangle is a good characteristic of this feature (if the smallest angle is close to 60°, all angles must be nearly equal). As it follows from Fig. 3, the number of loop-arc pairs between neighbouring maxima varies between 9 and 8. The average distance between maxima computed from the interval 7000 BC–2000 AD is 171.1 yr, which is very close to the Uranus/Neptune (UN) synodic period of 171.4 yr. Many solar–terrestrial phenomena thus fall between 171.4 and 178.7 yr (Scafetta and Wilson, 2013).

Figure 3 also documents a very long cycle of 2402 yr found by Charvátová (2000). It looks like a vault under the cycle of 178.7 yr. In the intervals 159 BC–208 AD, 2561–2193 BC, 4964–4598 BC, etc., the same exceptional solar orbits of trefoil type were repeated in steps of 2402 yr. These exceptional intervals are nearly 370 yr long (see Fig. 4). The period of 2400 yr was found in the time series of cosmogenic nuclide production over the last millennia (e.g. Bard et al., 1997; Vasiliiev and Dergachev, 2002; McCracken et al., 2013). Figure 5 shows reconstructions of several phenomena since 9000 BP (before present). Vertical lines define the above mentioned intervals. It is possible to see that all phenomena show very small fluctuations inside these intervals. The greatest deviations occurred in the second half of the 2402 yr cycle. They represent prolonged (grand) minima of the Spörer or Maunder types.

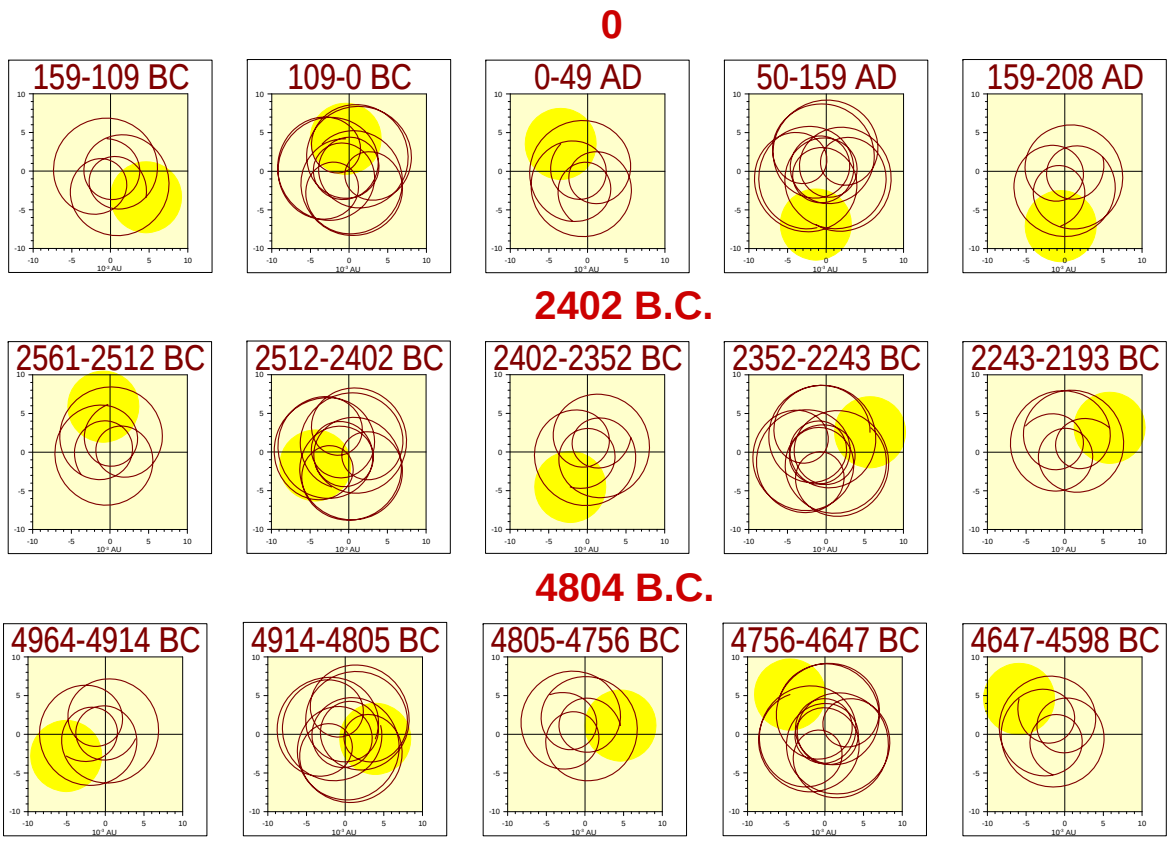

Figure 4. Alternation (in steps of 179 yr) of trefoil intervals of about 50 yr and chaotic intervals of about 130 yr of the SIM have been regularly overcome by the cycle of 2402 yr (Charvátová, 2000). The nearly 370 yr segments of the exceptional trefoil (stable) pattern of the SIM occurred in the years 159 BC–208 AD, 2561–2193 BC, 4964–4598 BC, etc. Notice the twice shortened distance of 159 yr between the three trefoils in each segment.

4 Conclusions

The results obtained indicate a primary, controlling role of the SIM in solar–terrestrial and climatic variability. The quite precise base for study of the SIM, ST and climatic relations occurred after the solar orbit had been divided into two basic types: the ordered according to trefoil, lasting for about 50 yr, and disordered, lasting for about 130 yr. The prolonged solar and temperature minima have coincided with the intervals of the chaotic SIM. Responses of two basic types of the SIM were described. A response of a stable character of very long (370 yr) trefoil intervals of the SIM was also shown (Fig. 5). The deepest and longest solar (temperature) minima (of the Spörer or Maunder types) occurred in the second half of the 2402 yr cycle in accordance with the most disordered types of the SIM.

The Sun has a layered structure and the greatest jump of physical parameters was found at the boundary between radiative and convection zones. The satellites (SOHO, etc.) found a thin shear layer between the radiative and convection zones, now called the tachocline. This layer is likely to be the place where the solar dynamo operates (Abreu et al., 2012; Mörner, 2013). The layered Sun is forced to move along the given loops and arcs, its velocity ranges between 36 and 64 km h^{-1}, its mean velocity is about 50 km h^{-1}. It would be interesting to compare a changing velocity of the Sun with a velocity of shear flows in the tachocline. Scafetta (2012a) showed that the Sun, by means of its nuclear active core, may be working as a great amplifier of the small, planetary tidal energy dissipated in it. Wolff and Patrone (2010) came to the conclusion that the Sun is subject to significant differential forces, not only from tides, but from the varying angular momenta of cells within it, which do not cancel out.

The SIM is computable in advance (celestial mechanics). This opens predictive possibilities. The intervals of the nearly identical SIMs will serve as the supporting bases in searching for mutual relations between the SIM and different types of solar–terrestrial phenomena, including climatic. Charvátová (2009) showed that the SIMs in the years 1840–1905 and 1980–2045 are nearly identical and of a moderately chaotic type. The future (forthcoming) behaviours of ST phenomena are likely to be analogous to those after 1873.

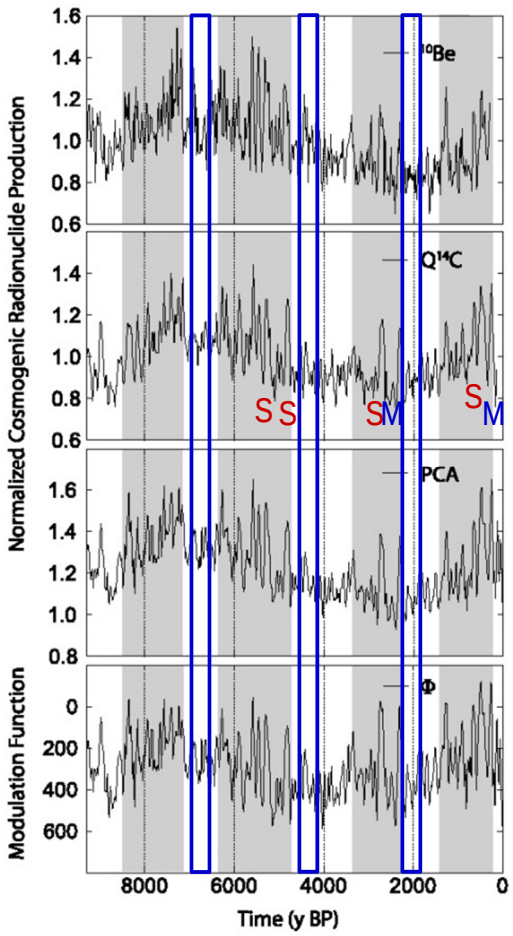

Figure 5. Normalized cosmogenic radionuclide productions since 9000 BP (taken from McCracken et al., 2013) and the cycle of 2402 yr in SIM ("present" means 1950). Blue vertical lines denote the exceptional trefoil intervals in steps of 2402 yr and the SIM is therefore of stable type within those lines. The smallest deviations occurred during these intervals, while the greatest deviations occurred in the second half of the 2402 yr cycle representing Spörer (S) or Maunder (M) type of prolonged (grand) minima in correspondence with chaotic intervals of the SIM.

Acknowledgements. This work was supported by the Ministry of Education, Youth and Sports of the Czech Republic under project OC09070. Fruitful discussions related to this topic took place during the Space Climate 5 Symposium held in Oulu in June 2013.

Edited by: N.-A. Mörner
Reviewed by: R. Tattersall and one anonymous referee

References

Abreu, J. A., Beer, J., Ferriz-Mas, A., McCracken, K. G., and Steinhilber, F.: Is there a planetary influence on solar activity?, Astronomy and Astrophysics, A88, 1–9, 2012.

Bard, E., Raisbeck, G. M., Iuou, F., and Jouzel, J.: Solar modulation of cosmogenic nuclide production over the last millennium: comparison between 14C and 10Be records, Earth Planet. Sci. Lett., 150, 453–462, 1997.

Beer, J., Mende, W., and Stellmacher, R.: The role of the Sun in climate forcing, Quaternary Sci. Rev., 19, 403–415, 2000.

Bucha, V., Jakubcová, I., and Pick, M.: Resonance frequencies in the Sun's motion, Studia Geophys. et Geod., 29, 107–111, 1985.

Charvátová, I.: The solar motion and the variability of solar activity, Adv. Space Res., 8, 147-150, 1988.

Charvátová, I.: On the relation between solar motion and the long term variability of solar activity, Studia Geophys. et Geod., 33, 230–241, 1989.

Charvátová, I.: On the relation between solar motion and solar activity in the years 1730–1780 and 1910–60, Bull. Astr. Inst. Czech., 41, 200–204, 1990.

Charvátová, I.: Solar-terrestrial and climatic variability during the last several millennia in relation to solar inertial motion, J. Coastal Res., 17, 343–354, 1995.

Charvátová, I.: Solar-terrestrial and climatic phenomena in relation to solar inertial motion, Surveys in Geophys., 18, 131–146, 1997.

Charvátová, I.: Can origin of the 2400-year cycle of solar activity be caused by solar inertial motion?, Ann. Geophys., 18, 399–405, doi:10.1007/s00585-000-0399-x, 2000.

Charvátová, I.: Long-term predictive assessments of solar and geomagnetic activities made on the basis of the close similarity between the solar inertial motions in the intervals 1840–1905 and 1980–2045, New Astronomy, 14, 25–30, doi:10.1016/j.newast.2008.04.005, 2009.

Charvátová, I. and Střeštík, J.: Solar variabilityas a manifestation of the Sun's motion, J. Atmos. Terr. Phys., 53, 1019–1025,1991.

Charvátová, I. and Střeštík, J.: Long-term changes of the surface air temperature in relation to solar inertial motion, Climatic Change, 29, 333–352, 1995.

Charvátová, I. and Střeštík, J.: Periodicities between 6 and 16 years in surface air temperature in possible relation to solar inertial motion, J. Atmos. Solar-Terr. Phys., 66, 219–227, 2004.

Charvátová, I. and Střeštík, J.: Relations between the solar inertial motion, solar activity and geomagnetic index aa since the year 1844, Adv. Space Res., 40, 1026–1031, doi:10.1016/j.asr.2007.05.086, 2007.

Charvátová-Jakubcová, I., Křvský, L. and Střeštík, J.: The periodicity of aurorae in the years 1001–1900, Studia Geophys. et Geod., 32, 70–77, 1988.

Cionco, R. G. and Compagnucci, R. H.: Dynamical characterization of the last prolonged solar minima, Adv. Space Res., 50, 1434–1444, 2012.

Fairbridge, R. W. and Shirley, J. H.: Prolonged minima and the 179-yr cycle of the solar inertial motion, Solar Phys., 110, 191–210, 1987.

Jakubcová, I. and Pick, M.: Correlation between solar motion, earthquakes and other geophysical phenomena, Ann. Geophys., 5B, 135–142, 1987.

Jose, P. D.: Sun's motion and sunspots, Astron. J., 70, 193–200, 1965.

McCracken, K. G., Beer, J., Steihilber, F., and Abreu, J.: A phenomenological study of the cosmic ray variations over the past 9400 years, and their implications regarding solar activity and the solar dynamo, Solar Phys., 286, 609–627, doi:10.1007/s11207-013-0265-0, 2013.

Mörner, N. A.: Planetary beat and solar-terrestrial responses, Pattern Recog. Phys., 1, 107–116, doi:10.5194/prp-1-107-2013, 2013.

Muscheler, R., Joos, F., Beer, J., Müller, S. A., Vonmoos, M., and Snowball, I.: Solar activity during the last 1000 yr inferred from radionucleide records, Quaternary Sci. Rev. 26, 82–97, doi:10.1016/j.quascirev.2006.07.012, 2007.

Paluš, M., Kurths, J., Schwarz, U., Novotná, D., and Charvátová, I.: Is the solar activity cycle synchronized with the solar inertial motion?, Int. J. Bifurc. Chaos, 10, 2519–2526, 2000.

Rabin, D., Wilson, R. M., and Moore, R. L.: Bimodality of the solar cycle, Geophys. Res. Lett., 13, 352–354, 1986.

Salvador, R. J.: A mathematical model of the sunspot cycle for the past 1000 yr, Pattern Recogn. Phys., 1, 117–122, doi:10.5194/prp-1-117-2013, 2013.

Scafetta, N.: Does the Sun work as a nuclear fusion amplifier of planetary tidal forcing? A proposal for a physical mechanism based on the mass-luminosity relation, J. Atmos. Solar-terr. Phys., 81–82, 27–40, 2012a.

Scafetta, N.: A shared frequency set between the historical mid-latitude aurora records and the global surface temperature, J. Atmos. Solar-terr. Phys., 74, 145–163, doi:10.1016/j.jastp.2011.10.013, 2012b.

Scafetta, N. and Wilson, R. C.: Planetary harmonics in the historical Hungarian aurora record (1523–1960), Planet. Space Sci., 78, 38–44, 2013.

Solheim, J.-E.: The sunspot cycle length - modulated by planets?, Pattern Recogn. Phys., 1, 159–164, doi:10.5194/prp-1-159-2013, 2013.

Vasiliev, S. S. and Dergachev, V. A.: The ~2400-year cycle in atmospheric radiocarbon concentration: bispectrum of ^{14}C data over the last 8000 years, Ann. Geophys., 20, 115–120, doi:10.5194/angeo-20-115-2002, 2002.

Wolff, C. L. and Patrone, P. N.: A new way that planets can affect the Sun, Solar Phys., 266, 227–247, doi:10.1007/s11207-010-9628-y, 2010.

Part XI

Multiscale comparative spectral analysis of satellite total solar irradiance measurements from 2003 to 2013 reveals a planetary modulation of solar activity and its nonlinear dependence on the 11 yr solar cycle.

Scafetta, N. and Willson, R. C.: Pattern Recogn. Phys., 1, 123-133, doi:10.5194/prp-1-123-2013, 2013.

Pattern Recogn. Phys., 1, 123–133, 2013
www.pattern-recogn-phys.net/1/123/2013/
doi:10.5194/prp-1-123-2013

Pattern Recognition in Physics
Open Access

Multiscale comparative spectral analysis of satellite total solar irradiance measurements from 2003 to 2013 reveals a planetary modulation of solar activity and its nonlinear dependence on the 11 yr solar cycle

N. Scafetta[1,2] **and R. C. Willson**[1]

[1]Active Cavity Radiometer Irradiance Monitor (ACRIM) Lab, Coronado, CA 92118, USA
[2]Duke University, Durham, NC 27708, USA

Correspondence to: N. Scafetta (nicola.scafetta@gmail.com) and R. C. Willson (rwillson@acrim.com)

Received: 28 September 2013 – Revised: 24 October 2013 – Accepted: 30 October 2013 – Published: 25 November 2013

Abstract. Herein we adopt a multiscale dynamical spectral analysis technique to compare and study the dynamical evolution of the harmonic components of the overlapping ACRIMSAT/ACRIM3 (Active Cavity Radiometer Irradiance Monitor Satellite/Active Cavity Radiometer Irradiance Monitor 3), SOHO/VIRGO (Solar and Heliopheric Observatory/Variability of solar Irradiance and Gravity Oscillations), and SORCE/TIM (Solar Radiation and Climate Experiment/Total Irradiance Monitor) total solar irradiance (TSI) records during 2003.15 to 2013.16 in solar cycles 23 and 24. The three TSI time series present highly correlated patterns. Significant power spectral peaks are common to these records and are observed at the following periods: ~ 0.070 yr, ~ 0.097 yr, ~ 0.20 yr, ~ 0.25 yr, ~ 0.30–0.34 yr, and ~ 0.39 yr. Less certain spectral peaks occur at about 0.55 yr, 0.60–0.65 yr and 0.7–0.9 yr. Four main frequency periods at ~ 24.8 days (~ 0.068 yr), ~ 27.3 days (~ 0.075 yr), at ~ 34–35 days (~ 0.093–0.096 yr), and ~ 36–38 days (~ 0.099–0.104 yr) characterize the solar rotation cycle. The amplitude of these oscillations, in particular of those with periods larger than 0.5 yr, appears to be modulated by the ~ 11 yr solar cycle. Similar harmonics have been found in other solar indices. The observed periodicities are found highly coherent with the spring, orbital and synodic periods of Mercury, Venus, Earth and Jupiter. We conclude that solar activity is likely modulated by planetary gravitational and electromagnetic forces acting on the Sun. The strength of the Sun's response to planetary forcing depends nonlinearly on the state of internal solar dynamics; planetary–Sun coupling effects are enhanced during solar activity maxima and attenuated during minima.

1 Introduction

Total solar irradiance (TSI) satellite measurements are fundamental to the investigation of solar physics and the climate change forcing of TSI variability. TSI observations follow the solar magnetic activity level (Willson and Hudson, 1991) and their variation therefore conforms to the ~ 11 yr Schwabe solar cycle. The average TSI on solar cycle time scales is sometimes referred to as the *solar constant*. TSI records are characterized by complex variability, from the quasi-monthly differential solar rotation cycles to the subannual and annual time scales (whose origins are still unknown).

An important physical issue is whether the annual and subannual TSI variability is intrinsically chaotic and unpredictable or, alternatively, is made of a complex set of harmonics and may be predicted once a sufficient number of constituent harmonics are identified. The latter possibility implies solar activity forecasts and may benefit from harmonic constituent modeling, as have the predictions of ocean tidal levels on Earth using a set of specific solar and lunar orbital harmonics (Doodson, 1921; Kelvin, 1881).

The harmonic constituent model hypothesis is important because it could provide an explanation of many solar magnetic and radiative phenomena that conventional solar

physics cannot. The conventional view of solar science is that solar magnetic and radiant variability is intrinsically chaotic, driven by internal solar dynamics alone and characterized by hydromagnetic solar dynamo models (Tobias, 2002). These models cannot predict solar activity and have not been able to explain its complex variability.

A growing body of empirical evidence suggests that solar activity on monthly to millennial time scales may be modulated by gravitational and magnetic planetary harmonic forces (e.g., Abreu et al., 2012; Brown, 1900; Charvátová, 2009; Fairbridge and Shirley, 1987; Hung, 2007; Jose, 1965; Scafetta, 2010a, b, 2012a, b, c, d; Scafetta and Willson, 2013a; Sharp, 2013; Tan and Cheng, 2012; Wilson et al., 2008; Wolf, 1859; Wolff and Patrone, 2010). For example, the 11 yr solar cycle appears to be bounded by the Jupiter–Saturn spring tide oscillation period (9.93 yr) and the Jupiter orbital tide oscillation period (11.86 yr) (Scafetta, 2012c). The 11 yr solar cycle is also in phase with major tidal resonances generated by the Venus-Earth-Jupiter system (11.07 yr period) and by the Mercury–Venus system (11.08 yr period) (Scafetta, 2012d). The multidecadal, secular and millennial solar oscillations appear to be generated by beat interferences among the multiple cycles that comprise the 11 yr solar cycles (Scafetta, 2012c).

A recent commentary in *Nature* discusses the "revival" of the planetary hypothesis of solar variation (Charbonneau, 2013). It has been pointed out that the arguments of critics of this hypothesis (e.g., Callebaut et al., 2012; Smythe and Eddy, 1977) have either not been supported by empirical evidence or have based their arguments on overly simplistic Newtonian analytical physics (e.g., Scafetta, 2012c, d; Scafetta et al., 2013b).

In a previous publication, Scafetta and Willson (2013b) analyzed the power spectra of TSI records since 1992. These were compared with theoretical power spectra deduced from the planetary orbital effects such as the tidal potential on the Sun, and the speed, jerk force, and z axis coordinate of the Sun relative to the barycenter of the solar system. The authors found multiple evidences of spectral coherence on annual and subannual scales between TSI power spectra and theoretical planetary spectra. This suggests that TSI is modulated at specific frequencies by gravitational and/or electromagnetic forcings linked to the revolution of the planets around the Sun.

Scafetta and Willson (2013b) found a TSI signature of the 1.092 yr Earth-Jupiter conjunction cycle. The TSI oscillation was found to be particularly evident during the maximum of solar cycle 23 (1998–2004) and in phase synchronization with the Earth–Jupiter conjunction cycle that predicts an enhanced effect when the Earth crosses the Sun–Jupiter conjunction line. The cause was postulated to be that a slightly brighter side of the Sun was facing Jupiter, because that side would be the focus of enhanced planetary–solar couplings, both gravitational and electromagnetic. These forces exerted by Jupiter on the Sun are stronger than the force exerted on the Sun by any other planet. When the Earth crosses the Sun–Jupiter conjunction line it adds to Jupiter's planetary–solar coupling effects and sensors on Earth satellites should receive a stronger TSI signal. This planetary–solar coupling effect generates the ~ 1.092 yr cycle in the TSI record.

The 1.092 yr cycle signature detected by the satellite TSI observations is enhanced during solar activity maxima and attenuated during solar minima (Scafetta and Willson, 2013b), suggesting complex, nonlinear responses of solar internal dynamics to planetary forcings. Here we study the dynamical evolution of the harmonic characteristics of the TSI observations on annual and sub annual time scales. A multiscale dynamical spectral analysis technique is proposed and used to reveal non-stationary changes in dynamical patterns in a sequence. This technique is used to determine whether major background harmonics exist that correspond to basic planetary harmonics such as the spring, orbital and synodic periods among the planets.

2 Total Solar Irradiance Data

The daily average TSI measurements were collected during the last decade by three independent science teams: ACRIMSAT/ACRIM3 (Active Cavity Radiometer Irradiance Monitor Satellite/Active Cavity Radiometer Irradiance Monitor 3) (Willson and Mordvinov, 2003), SOHO/VIRGO (Solar and Heliopheric Observatory/Variability of solar Irradiance and Gravity Oscillations) (Fröhlich, 2006), and SORCE/TIM (Solar Radiation and Climate Experiment/Total Irradiance Monitor) (Kopp and Lawrence, 2005; Kopp et al., 2005). Cross-comparison of the three independent TSI records reduces interpretation errors due to measurement uncertainties. Dynamical patterns common to the three TSI records are sought out in order to increase the certainty of their physical origins.

ACRIM3 results have been adjusted using algorithm updates and corrections for scattering and diffraction found in recent testing at the LASP/TRF (Laboratory for Atmospherics and Space Physics/TSI Radiation Facility) (Willson, 2011). Similar corrections for the VIRGO results were recently found at LASP/TRF, and these results are now reported in an updated scale (Fröhlich, 2013). The updated ACRIM3, VIRGO and TIM results agree closely in scale and variability, with an average value during the 2008–2009 solar activity minimum near 1361 W m^{-2}.

The ACRIMSAT/ACRIM3, SOHO/VIRGO and SORCE/TIM TSI records since 2003 are shown in Fig. 1. For comparison, Fig. 1 also depicts the daily sunspot number record from the Solar Influences Data Analysis Center (SIDC).

Note that Fig. 1 shows the most recent SOHO/VIRGO record available that does not yet include the LASP/TRF scaling corrections. Thus, it is more significant to compare

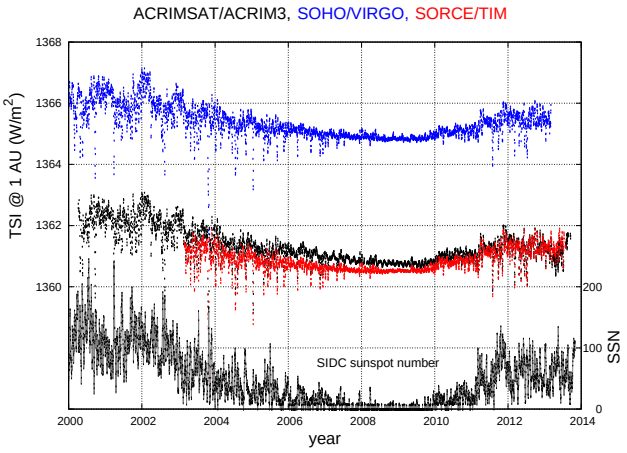

Figure 1. Comparison of ACRIMSAT/ACRIM3 (black), SOHO/VIRGO (blue) and SORCE/TIM (red) total solar irradiance records versus the SIDC daily sunspot number (gray) record. ACRIM3 is recalibrated with updated sensor degradation and algorithm LAPS/TRF corrections for scattering, diffraction and TSI scale. VIRGO does not include yet the LASP/TRF scaling corrections.

the three TSI records as percentage variation during successive two-year periods as depicted in Figs. 2 and 3.

Figure 2 uses a constant scale for each two-year period to demonstrate the progressive divergence of TIM relative to ACRIM3 and VIRGO results. The three records are scaled during the initial common two-week period (2003.15–2003.19). The close agreement of all three satellite experiments' results in 2003 was followed by continuous divergence of TIM results from those of ACRIM3 and VIRGO through 2013, when the difference reached ~ 200 ppm.

Based on previous satellite TSI observational experience, the most likely cause of the divergence is in-flight sensor degradation calibration error. The close agreement of ACRIM3 and VIRGO results, which is more evident in Figs. 2–3, indicates that an over-correction of TIM sensor degradation is the most likely explanation. However, the cause could also be a combination of degradation uncertainty by all three sensors; or it may be within the uncertainty of the self-degradation calibration capabilities of these instruments. The long-term traceability of TSI satellite results, achieved through in-flight self-calibration of degradation, is an important area of continuing research for the climate TSI database.

Figure 3 uses a variable scale on each two-year segment to provide maximum visibility of the TSI variations for each sensor. It can be clearly seen that ACRIM3, VIRGO and TIM detect nearly all the same variations. TIM appears to detect them as having slightly lower amplitudes. During the part of the solar minimum period with the quietest magnetic activity (2008.7–2009.3) there is a near absence of variations in the TIM record, while VIRGO records some of the variability detected by ACRIM3 during this time, but at lower amplitudes. Lower sensitivities of VIRGO and TIM sensors is likely responsible for these differences.

Table 1. List of the major theoretically expected harmonics associated with planetary orbits within 1.6 year period. P is the period. Mercury: (Me), Venus: (Ve), Earth: (Ea), Jupiter: (Ju). If P_1 and P_2 are the periods, the synodic period is $P_{12} = 1/|1/P_1 - 1/P_2|$, and the spring period is half of it. The variability is based on ephemeris calculations. From Scafetta and Willson (2013b).

Cycle	Type	P (day)	P (year)	min. (year)	max. (year)
Me	1/2 orbital	44 ± 0	0.1205 ± 0.000	0.1205	0.1205
Me–Ju	spring	45 ± 9	0.123 ± 0.024	0.090	0.156
Me–Ea	spring	58 ± 10	0.159 ± 0.027	0.117	0.189
Me–Ve	spring	72 ± 8	0.198 ± 0.021	0.156	0.219
Me	orbital	88 ± 0	0.241 ± 0.000	0.241	0.241
Me–Ju	synodic	90 ± 1	0.246 ± 0.002	0.243	0.250
Ea	1/4 orbital	91 ± 3	0.25 ± 0.000	0.250	0.250
Ve	1/2 orbital	112.5 ± 0	0.3075 ± 0.000	0.3075	0.3075
Me–Ea	synodic	116 ± 9	0.317 ± 0.024	0.290	0.354
Ve–Ju	spring	118 ± 1	0.324 ± 0.003	0.319	0.328
Ea	1/3 orbital	121 ± 7	0.333 ± 0.000	0.333	0.333
Me–Ve	synodic	145 ± 12	0.396 ± 0.033	0.342	0.433
Ea	1/2 orbital	182 ± 0	0.500 ± 0.000	0.5	0.5
Ea–Ju	spring	199 ± 3	0.546 ± 0.010	0.531	0.562
Ve	orbital	225 ± 0	0.615 ± 0.000	0.241	0.241
Ve–Ju	synodic	237 ± 1	0.649 ± 0.004	0.642	0.654
Ve–Ea	spring	292 ± 3	0.799 ± 0.008	0.786	0.810
Ea	orbital	365.25 ± 0	1.000 ± 0.000	1.000	1.000
Ea–Ju	synodic	399 ± 3	1.092 ± 0.009	1.082	1.104
Ea–Ve	synodic	584 ± 6	1.599 ± 0.016	1.572	1.620

3 TSI power spectrum comparison

Power spectrum evaluations of the TSI records are shown as Figs. 4, 5 and 6. In the following two subsections we analyze the multi-month scale (0.1–1.1 yr) and the solar differential rotation scale (22–40 days).

3.1 Analysis of the 0.1–1.1 yr period range

Figure 4 shows the maximum entropy method (MEM) power spectrum evaluation (Press et al., 1997) of the ACRIM3, VIRGO and TIM TSI records during the 10 yr period from 2003.15 to 2013.16. The power spectra are plotted as a function of the period ($T = 1/f$) up to 1 yr. The figure shows that the three records produce nearly all the same spectral peaks, indicating that the observed variations in TSI are definitively solar in origin. The spectral amplitude of the peaks in the ACRIM3 record is nearly always higher than that observed by VIRGO and TIM, indicating a higher sensitivity of ACRIM3 instrumentation to TSI variability. This sensitivity difference is also supported by the fact that the TIM and VIRGO records present slightly smoothed and attenuated patterns relative to those of ACRIM3. The major spectral peaks are highlighted in the figure, and occur at the following approximate periods: ~ 0.070 yr, ~ 0.095 yr, 0.20 yr,

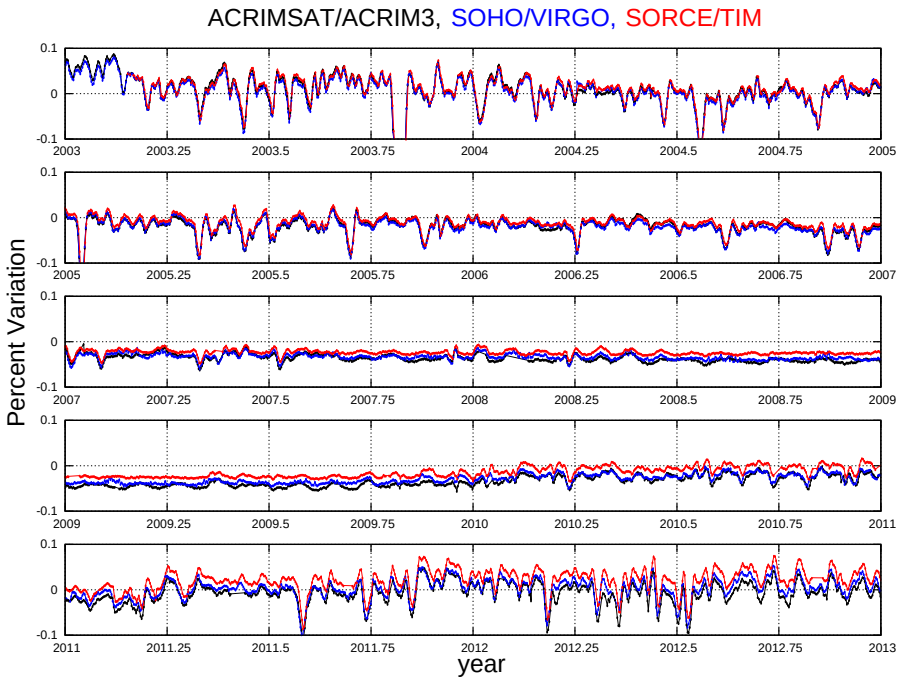

Figure 2. Percent variation comparison of ACRIMSAT/ACRIM3 (black), SOHO/VIRGO (blue) and SORCE/TIM (red) total solar irradiance records. The scale of the two-year segments is constant to highlight the divergent trend of the TIM results relative to those of the ACRIM3 and VIRGO experiments. The records are cross-scaled during the initial two-week period 2003.15–2003.19.

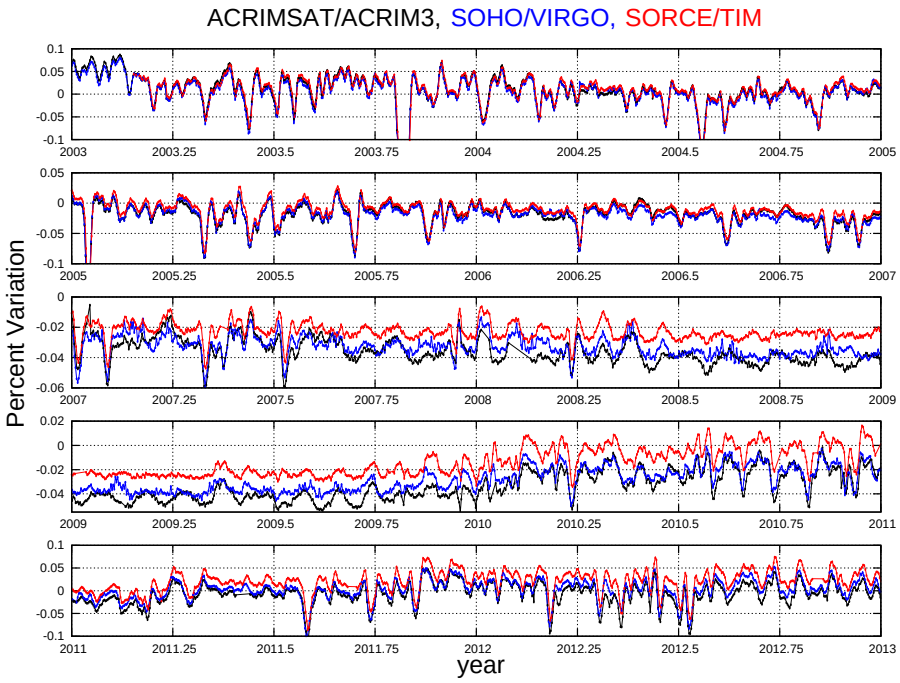

Figure 3. Percent variation comparison of ACRIMSAT/ACRIM3 (black), SOHO/VIRGO (blue) and SORCE/TIM (red) total solar irradiance records. The scale of the two-year segments is varied to highlight the detailed similarity of the variability of all three TSI records. The records are cross-scaled during the initial two-week period 2003.15–2003.19.

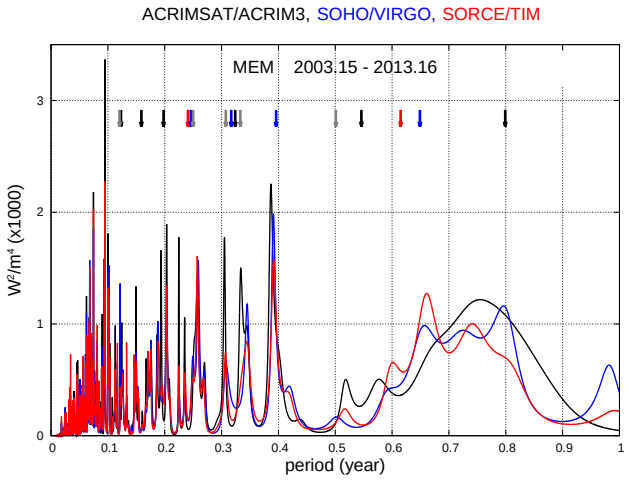

Figure 4. Maximum entropy method (MEM) power spectrum comparison of ACRIMSAT/ACRIM3 (black), SOHO/VIRGO (blue) and SORCE/TIM (red) total solar irradiance records using the data from 2003.15 to 2013.16. The colored arrows at the top of the figure indicate the major theoretically expected planetary frequencies from Mercury, Venus, Earth and Jupiter, which are reported in Table 1. Red indicates the orbital periods, black indicates the spring periods, blue indicates the synodic periods, and gray indicates the harmonics of the orbital periods listed in Table 1.

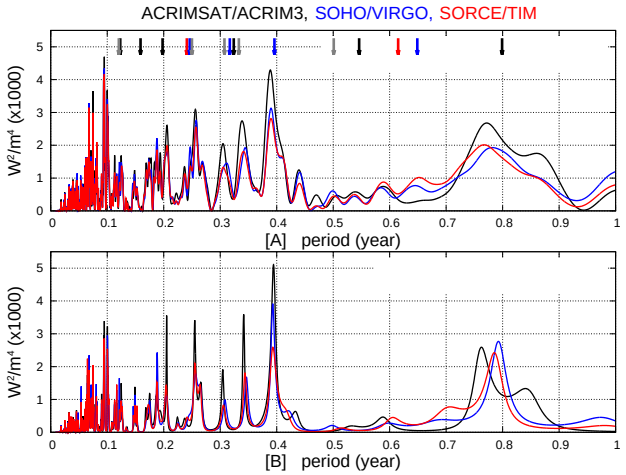

Figure 5. Power spectrum comparison of ACRIMSAT/ACRIM3 (black), SOHO/VIRGO (blue) and SORCE/TIM (red) total solar irradiance records, using the data from 2003.15 to 2011.00. **(A)** The periodogram is used; **(B)** the maximum entropy method (MEM) is used. The colored arrows at the top of the figure indicate the major theoretically expected planetary frequencies from Mercury, Venus, Earth and Jupiter, which are reported in Table 1. Red indicates the orbital periods, black indicates the spring periods, blue indicates the synodic periods, and gray indicates the harmonics of the orbital periods listed in Table 1.

0.25 yr, 0.30–0.34 yr, 0.39 yr and 0.75–0.85 yr; more uncertain peaks occur at about 0.60–0.65 yr.

The above-mentioned periods are found among the major planetary harmonics related to the orbital, synodic and spring periods for the planets. Table 1 reports these periods and their uncertainty and range during 2003–2013 for the four major tide-causing planets (Mercury, Venus, Earth and Jupiter) (Scafetta, 2012d). Table 2 shows theoretically expected periods related to the other planets as well. The major orbital, synodic and spring periods listed in Table 1 are indicated with colored arrows at the top of Fig. 4; red indicates orbital periods, black indicates spring periods, blue indicates the synodic periods, and gray indicates the harmonics of the orbital periods listed in Table 1. The additional planetary frequencies listed in Table 2 likely have only minor TSI effects and are not explicitly delineated in Fig. 4; we report these additional frequencies for completeness. Although there is currently a deficit of specific physical mechanisms to explain planet–Sun interactions, these minor frequencies may also be found in solar records.

Scafetta and Willson (2013b) found similar frequencies using theoretical equations deduced from the ephemerides of the planets, such as the tidal potential on the Sun and the speed, jerk force, and z axis coordinate of the Sun relative to the barycenter of the solar system. Statistical tests based on Monte Carlo simulations using red-noise generators for TSI synthetic records established that the probability of randomly finding a dynamical sequence manifesting a spectral coherence with the (orbital, spring and synodic) planetary theoretical harmonics equal to or larger than that found among the TSI satellite frequencies and the planetary harmonics is less than 0.05 % (Scafetta and Willson, 2013b).

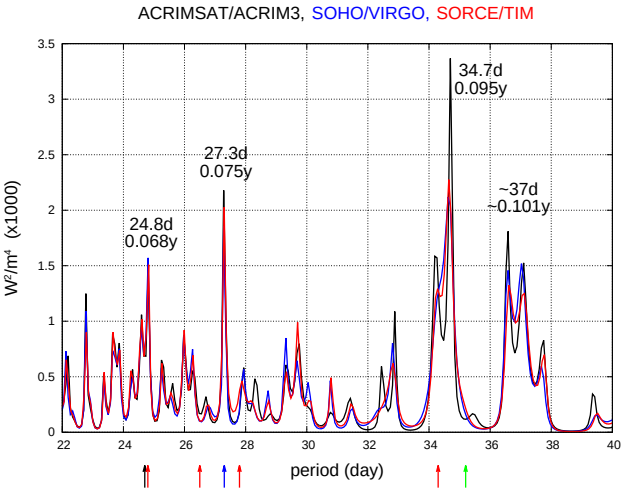

Figure 6. Magnification of the period range between 22 and 40 days depicted in Fig. 4, which is associated with the solar differential rotation scale. The arrows at the bottom depict the solar rotation cycles reported in Table 3.

A comparison between the spectral peaks shown in Fig. 4 and the colored arrows indicating the major expected

planetary frequency peaks shows a clear coherence among the TSI and the planetary harmonics on multiple scales, in particular for the periods from 0.1 to 0.5 yr and for the 0.8 yr periodicity. The three planetary periods at about 0.55 yr and between 0.6 and 0.65 yr are not equally evident in the TSI results.

As discussed in the Introduction, the response of the Sun to external planetary forcing may be nonlinear with some frequencies enhanced by internal solar dynamics during specific periods (e.g., solar maxima) and attenuated during others (e.g., solar minima). Indeed, changing the analyzed period as done in Fig. 5 (we used the data from 2003.15 to 2011) produces some differences relative to the results depicted in Fig. 4. For example, the amplitudes of the peaks are different, although their frequency position is fairly unchanged. This demonstrates that nonlinear mechanisms are regulating the phenomenon. Section 4 addresses the nonlinear dynamical evolution of the TSI patterns more systematically.

3.2 Analysis of the 22–40 day period range associated with the solar differential rotation

Figure 6 magnifies the period between 22 and 40 days depicted in Fig. 4. This range corresponds to the differential solar rotation period band. Figure 6 clearly shows a spectral peak at ~ 27.3 days (0.075 yr) (Willson and Mordvinov, 1999). This corresponds to the synodic period between the well-known Carrington solar rotation (~ 25.38 days) and the Earth's orbital period (~ 365.25 days). The Carrington period roughly corresponds to the solar rotation period at a latitude of 26° from the Sun's equatorial plane, which is the average latitude of sunspots and corresponding magnetic solar activity (Bartels, 1934), as seen from the Earth.

Figure 6 also reveals spectral peaks at ~ 24.8 days (~ 0.068 yr), at ~ 34–35 days (~ 0.093–0.096 yr) and ~ 36–38 days (~ 0.099–0.104 yr), suggesting that the sidereal equatorial and polar solar rotation cycles would also be reported in TSI records. However, the presence of these cycles in the TSI records could imply that the solar orientation relative to space also modulates solar activity. An explanation of these spectral peaks could involve a planetary influence on the Sun.

Assuming that the side of the Sun facing Jupiter is the focus of higher solar activity (Scafetta and Willson, 2013b), it is possible to interpret the ~ 24.8 days (~ 0.0679 yr) cycle as the synodic period between Jupiter's sidereal orbital period (~ 4332.6 days = ~ 11.862 yr) and the solar equatorial rotation period. The latter is estimated to be ~ 24.7 days (~ 0.0675 yr) during the period analyzed here (from 2003 to 2013). Using this estimate, additional planetary synodic cycles with the solar rotation are calculated at: ~ 26.5 days (~ 0.0725 yr), the synodic solar equatorial rotation period relative to Earth; ~ 27.75 days (~ 0.0760 yr), the synodic solar equatorial rotation period relative to Venus; and ~ 34.3 days (~ 0.0940 yr), the synodic solar equatorial rotation period relative to Mercury. See Table 3.

The ~ 34.3-day Mercury–Sun synodic period fits the TSI spectral peak at ~ 34–35 days, a period that also corresponds to the high latitude solar differential rotation rate. However, the theoretical synodic spectral peaks at ~ 26.5 days and ~ 27.75 days do not appear in Fig. 5. This would suggest that solar asymmetry causes a TSI enhancement as the Sun's more sensitive region orientates only toward Jupiter and Mercury.

Table 2. List of additional average theoretically expected harmonics associated with planetary orbits: Mercury (Me), Venus (Ve), Earth (Ea), Mars (Ma), Jupiter (Ju), Saturn (Sa), Uranus (Ur), Neptune (Ne). If P_1 and P_2 are the periods, the synodic period is $P_{12} = 1/|1/P_1 - 1/P_2|$, and the spring period is half of that (Scafetta and Willson, 2013b). The last five rows report additional spring and synodic periods of Mercury, Venus and Earth relative to the synodic periods of Jupiter and Saturn, and Earth and Jupiter. The latter periods are calculated using using the three-synodic-period equation: $P_{1(23)} = 1/|1/P_1 - |1/P_2 - 1/P_3||$.

Cycle	Type	P (year)	Type	P (year)
Me–Ne	spring	0.1206	synodic	0.2413
Me–Ur	spring	0.1208	synodic	0.2416
Me–Sa	spring	0.1215	synodic	0.2429
Me–Ma	spring	0.1382	synodic	0.2763
Ve–Ne	spring	0.3088	synodic	0.6175
Ve–Ur	spring	0.3099	synodic	0.6197
Ve–Sa	spring	0.3142	synodic	0.6283
Ve–Ma	spring	0.4571	synodic	0.9142
Ea–Ne	spring	0.5031	synodic	1.006
Ea–Ur	spring	0.5060	synodic	1.0121
Ea–Sa	spring	0.5176	synodic	1.0352
Ea–Ma	spring	1.0676	synodic	2.1352
Ma	1/2 orbital	0.9405	orbital	1.8809
Ma–Ne	spring	0.9514	synodic	1.9028
Ma–Ur	spring	0.9621	synodic	1.9241
Ma–Sa	spring	1.0047	synodic	2.0094
Ma–Ju	spring	1.1178	synodic	2.2355
Ju	1/2 orbital	5.9289	orbital	11.858
Ju–Ne	spring	6.3917	synodic	12.783
Ju–Ur	spring	6.9067	synodic	13.813
Ju–Sa	spring	9.9310	synodic	19.862
Sa	1/2 orbital	14.712	orbital	29.424
Sa–Ne	spring	17.935	synodic	35.870
Sa–Ur	spring	22.680	synodic	45.360
Ur	1/2 orbital	41.874	orbital	83.748
Ur–Ne	spring	85.723	synodic	171.45
Ne	1/2 orbital	81.862	orbital	163.72
Me–(Ju–Sa)	spring	0.122	synodic	0.244
Me–(Ea–Ju)	spring	0.155	synodic	0.309
Ve–(Ju–Sa)	spring	0.317	synodic	0.635
Ea–(Ju–Sa)	spring	0.527	synodic	1.053
Ve–(Ea–Ju)	spring	0.704	synodic	1.408

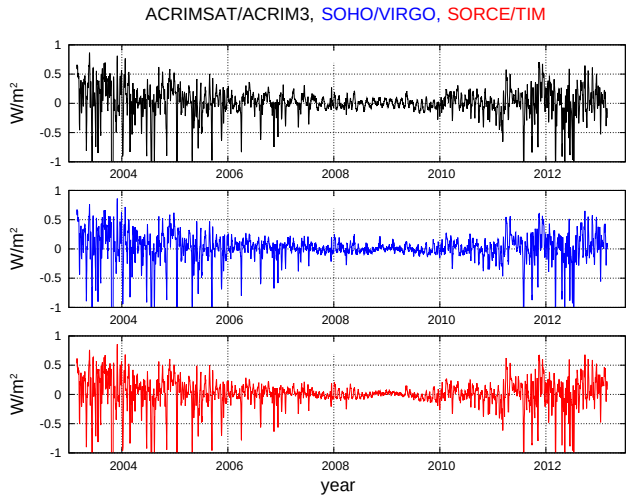

Figure 7. FFT 2 yr high-pass filtered component of the ACRIMSAT/ACRIM3 (black), SOHO/VIRGO (blue) and SORCE/TIM (red) total solar irradiance records.

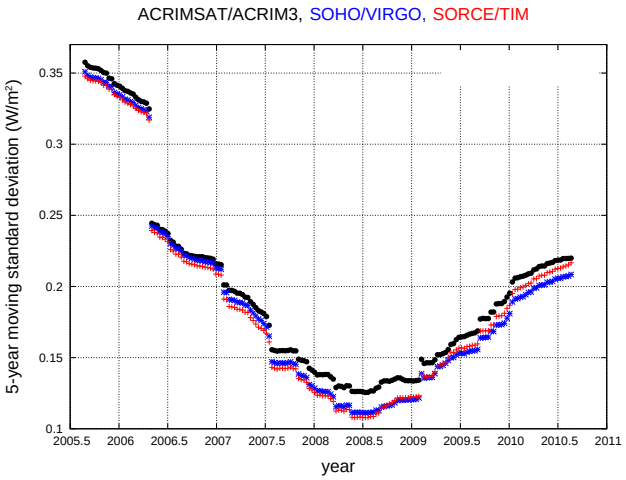

Figure 8. 5 yr moving standard deviation function $\sigma_5(t)$ of the high-pass filtered ACRIMSAT/ACRIM3 (black), SOHO/VIRGO (blue) and SORCE/TIM (red) total solar irradiance records depicted in Fig. 6.

Mercury may have a strong effect because Mercury is the closest planet to the Sun. After Jupiter, Mercury induces on the Sun the second largest tidal amplitude cycle related to a planetary orbit due to its large eccentricity ($e = 0.206$) and low inclination to the Sun's equator (3.38°) (Scafetta, 2012d, Figure 8). Moreover, the theoretical ~ 34.3 day Mercury–Sun synodic period has an almost 2/5 resonance with Mercury's orbital period (~ 88 days) or ~ 35.2 days (~ 0.096 yr). This close resonance may favor dynamical synchronization and amplification in solar dynamics and explain the wide, strong TSI spectral peak around ~ 34–35 days that appears bounded by Mercury's two theoretical frequencies, as Fig. 6 shows.

Thus, empirical evidence suggests that the differential solar rotation may be synchronized to the synodic cycles between the solar equatorial rotation and the two theoretically most relevant tidal planets: Jupiter and Mercury. Further investigation of the solar rotation period band requires a dedicated examination that is left to another work.

4 Multiscale comparative spectral analysis

Multiscale dynamical spectral analysis diagrams for the three TSI records were constructed as follows. We consecutively calculated normalized power spectrum functions using MEM, which produces sharp peaks and is less affected by leakage artifacts. We processed the TSI records after high-pass filtering to eliminate time scale variations longer than 2 yr. Figure 7 depicts the Fast Fourier Transform (FFT) 2 yr high-pass filtered components of the three TSI records. We analyzed consecutive 5 yr moving centered windows of the data (for example, the results centered in 2006 refer to the 5 yr period from 2003.5 to 2008.5).

Table 3. Solar equatorial (equ-) and Carrington (Car-) rotation cycles relative to the fixed stars and to the four major tidal planets calculated using the synodic period equation: $P_{12} = 1/|1/P_2 - 1/P_2|$, where $P_1 = 24.7$ days is the sidereal equatorial solar rotation and P_2 the orbital period of a planet. The last row reports the 2/5 Mercury's orbital resonance. The last column reports the color of the arrows shown in Fig. 6.

Cycle	Type	P (day)	P (year)	color
Sun	equ-rot	24.7	0.0676	black
Sun–Ju	equ-rot	24.8	0.0679	red
Sun–Ea	equ-rot	26.5	0.0726	red
Sun–Ea	Car-rot	27.3	0.0747	blue
Sun–Ve	equ-rot	27.8	0.0761	red
Sun–Me	equ-rot	34.3	0.0940	red
2/5 Me	resonance	35.2	0.0964	green

Figure 8 shows the 5 yr moving standard deviation functions, $\sigma_5(t)$, of the high-pass filtered TSI records that were used for local normalization of the MEM functions. During the solar minimum, $\sigma_5(t)$ is attenuated relative to the solar cycle 23 and 24 maxima in all three TSI records.

The multiscale comparative spectral analysis diagrams are depicted in Fig. 9 within the period range 0 to 1.1 yr. Figure 10 magnifies the period range from 0.10 to 0.45 yr. The diagrams were obtained by calculating MEM curves for a 5 yr moving centered window and plotting it in a column using colors to represent the strength of the spectral function. For example, the colored column above the year 2006 corresponds to the MEM power spectrum of the data covering the 5 yr period from 2003.5 to 2008.5. The presence of harmonics even when attenuated during solar minimum is emphasized by the colored column in Figs. 9 and 10, which shows

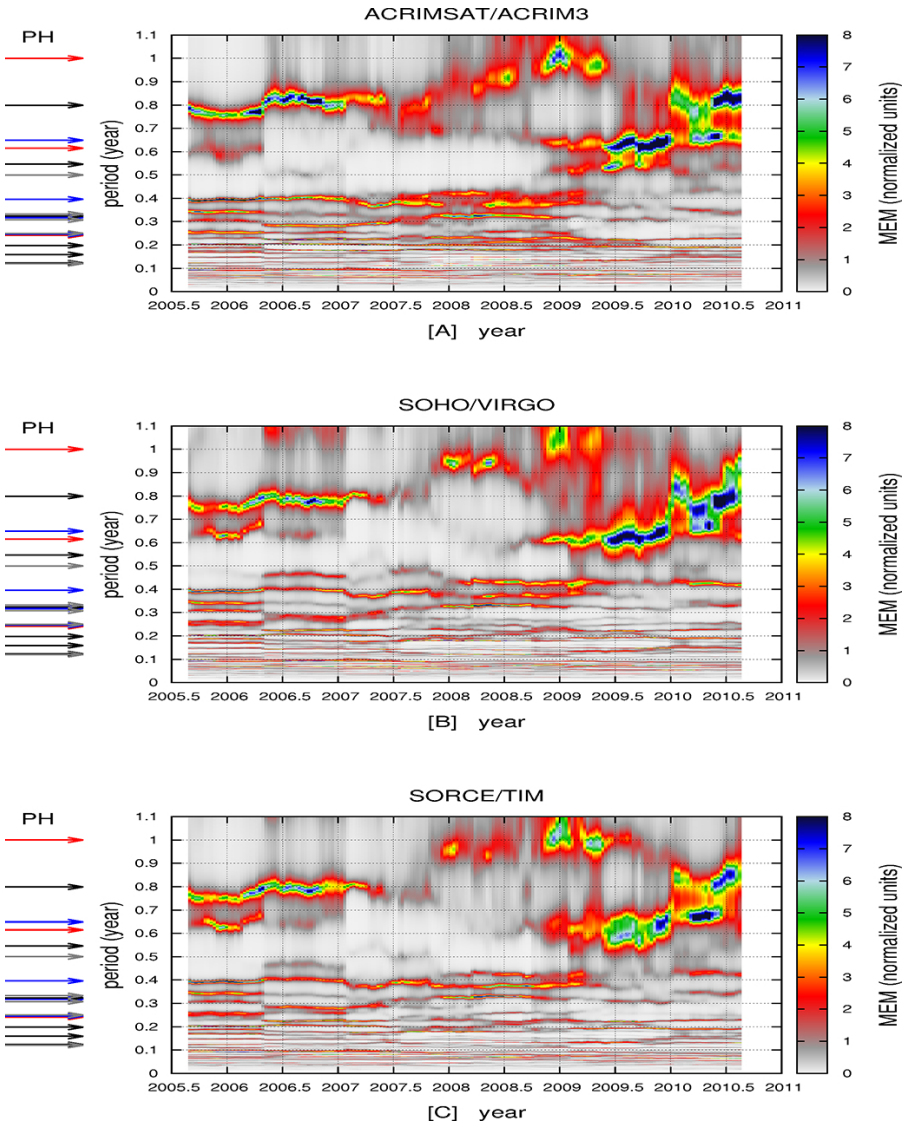

Figure 9. Moving window power spectrum comparison of **(A)** ACRIMSAT/ACRIM3; **(B)** SOHO/VIRGO; **(C)** SORCE/TIM total solar irradiance records. The maximum entropy method (MEM) is used. The colors represent the spectral strength in variance normalized units (×100), with the blue-black regions representing the strongest spectral peaks. The colored arrows at the left of the diagrams indicate the theoretically expected frequencies of the most significant planetary harmonics (PH) obtained from Mercury, Venus, Earth and Jupiter, which are reported in Table 1. Red indicates the orbital periods, black indicates the spring periods, the blue indicates the synodic periods, and gray indicates the harmonics of the orbital periods listed in Table 1.

a spectrum normalized by the variance $\sigma_5(t)$ of the data during the analyzed 5 yr interval.

Figure 9 shows that even after normalization the amplitude of some frequencies depends strongly on the strength of solar cycle activity. TSI oscillation variability is seen to be larger during solar maxima and smaller during solar minima. Major peaks (blue-black) are observed for the same periodicities seen in Figs. 4 and 5, indicated by arrows on the left. The spectral peaks are relatively stable as the 5 yr window moves in time. The stationarity of these spectral lines increases for periods below 0.5 yr. The peaks near 0.6–0.7 and 0.8 yr are attenuated or disappear during solar cycle 23–24 minimum (~ 2006.75 to 2008.75). The strong periodicities near 0.8 yr are attenuated or disappear during 2008–2009.25. In particular the peak at 0.6–0.65 yr is clearly visible before 2006.5 and after 2008.75 in all three diagrams.

Some differences can also be seen in the three panels of Figs. 9 and 10. The ACRIM3 panel is the most colorful, indicating the highest detection of variability, and TIM is the least colorful (corresponding to the standard deviation variability depicted in Fig. 8). Because the calculations are the same for all three TSI records, this implies that the spectral

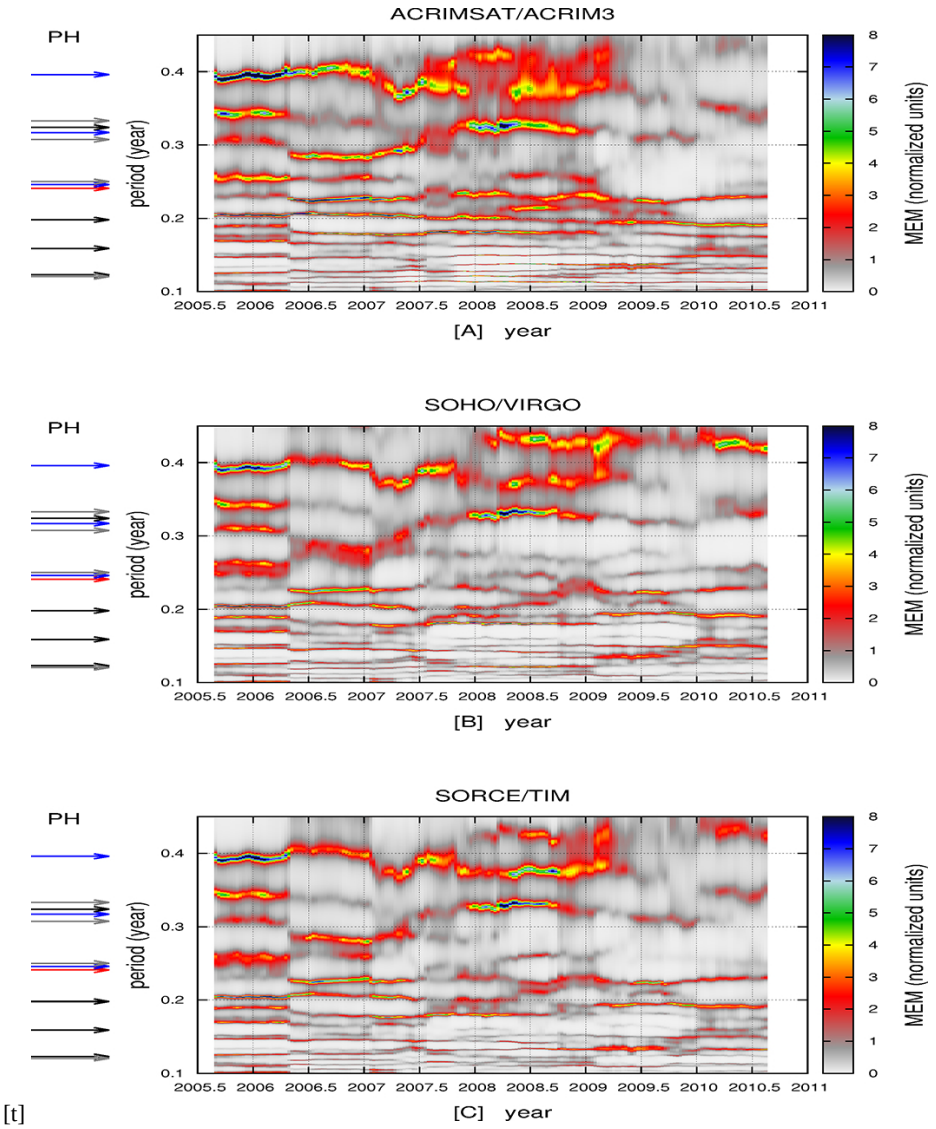

Figure 10. Magnification of Fig. 9 within the frequency period range from 0.10 to 0.45 yr.

peaks detected by ACRIM3 are generally stronger that those detected by the other two instruments, providing another confirmation that ACRIM3 sensors are more sensitive than those of VIRGO and TIM, recording stronger signals on multiple scales.

5 Discussion and conclusions

ACRIMSAT/ACRIM3, SOHO/VIRGO and SORCE/TIM TSI records overlap since 2003.15 and are found to be closely correlated with each other. Including the LASP/TRF calibration corrections for both ACRIM3 and VIRGO, all three records present a similar TSI average at about 1361 W m^{-2}. Figure 1 still depicts the SOHO/VIRGO record on an uncorrected scale (at about 1365 W m^{-2}) since the updated VIRGO record is not currently available.

Power spectrum and multiscale dynamical spectral analysis techniques have been used to study the physical properties of these data. We found that TSI is modulated by major harmonics at: ~ 0.070 yr, ~ 0.097 yr, ~ 0.20 yr, ~ 0.25 yr, ~ 0.30–0.34 yr, ~ 0.39 yr; the peaks occurring at ~ 0.55 yr, ~ 0.60–0.65 yr and ~ 0.7–0.9 yr appear to be amplified during solar activity cycle maxima and attenuated during the minima.

Other researchers have studied the fast oscillations of alternative solar indices and found results compatible with ours. Rieger et al. (1984) found that an index of energetic solar flare events presents a major variable oscillation with a period of about 154 days (0.42 yr). Similarly,

Verma et al. (1992) found a 152–158 day (0.41–0.43 yr) periodicity in records of solar nuclear gamma ray flares and sunspots. This period approximately corresponds to the Mercury–Venus synodic cycle (~ 0.4 yr), which is quite evident in Figs. 4 and 5, and may slightly vary in time as shown in Figs. 9 and 10. Pap et al. (1990) analyzed a number of solar indices (ACRIM1 TSI, 10.7 cm radio flux, Ca-K plage index, sunspot-blocking function, and UV flux at $L\alpha$, and MgII core-to-wing ratio) and found major spectral peaks at about 51 days (~ 0.14 yr), 113–117 days (0.30–0.32 yr), 150–157 days (0.41–0.43 yr), 227 days (~ 0.62 yr) and 240–330 days (0.65–0.90 yr). Caballero and Valdés-Galicia (2003) analyzed the fluctuations detected in high-altitude neutron monitor, solar and interplanetary parameters. Kilcik et al. (2010) analyzed periodicities in solar flare index for solar cycles 21–23. Tan and Cheng (2012) analyzed the solar microwave emission flux at a frequency of 2.80 GHz (F10.7) and the daily relative sunspot number (RSN) from 1 January 1965 to 31 December 2011. These three studies revealed major periodicities within the following period ranges: 53–54 days (0.14–0.15 yr); 85–90 days (0.23–0.25 yr); 115–120 days (0.31–0.33 yr); 140–150 days (0.38–0.41 yr); 230–240 days (0.62–0.66 yr); 360–370 days (0.98–1.02 yr); 395–400 days (1.08–1.10 yr). The periodicity ranges found above correspond well to those found in the TSI satellite records as shown in Figs. 4, 5, 9 and 10, and correspond to major (orbital, spring and synodic) planetary harmonics as reported in Tables 1 and 2.

Four main high-frequency periods at ~ 24.8 days (~ 0.068 yr), ~ 27.3 days (~ 0.075 yr), at ~ 34–35 days (~ 0.093–0.096 yr) and ~ 36–38 days (~ 0.099–0.104 yr) characterize the differential solar rotation. The ~ 27.3 days (~ 0.075 yr) period is the well known Earth's synodic period with the Carrington solar rotation period (~ 25.38 days). The interpretation of the other cycles is uncertain. Perhaps the ~ 24.8 days (~ 0.068 yr) and ~ 34–35 days (~ 0.093–0.096 yr) cycles are the synodic cycles between the equatorial solar rotation cycle and the orbit of Jupiter and Mercury, respectively. The latter could also be synchronized to the 2/5 resonance of the Mercury orbital period of ~ 35.2 days (~ 0.096 yr). The ~ 36–38 days (~ 0.099–0.104 yr) may be the upper bound of the polar differential solar rotation as seen from the Earth.

In conclusion, solar activity appears to be characterized by the specific major theoretical harmonics, which would be expected if the planets are modulating it. Mercury, Venus, Earth and Jupiter would provide the most modulation within the studied time scales (Scafetta, 2012c, d; Tan and Cheng, 2012). If these planets are modulating solar activity via gravitational and/or electromagnetic forces – although the physical mechanisms are still unknown – the harmonics referring to the spring, orbital and synodic periods among the planets should be present in the TSI records as well. The planetary harmonics reported in Tables 1 and 3, computed using the orbital periods of four theoretically most relevant planets (Mercury, Venus, Earth and Jupiter) correspond very closely to the harmonics observed in the TSI records (see Figs. 4, 5, 6, 9 and 10).

Our findings support the hypothesis that planetary forces are modulating solar activity and TSI on multiple time scales. Scafetta proposed a physical mechanism that may explain how the small energy dissipated by the gravitational tides may be significantly amplified up to a 4-million factor by activating a modulation of the solar nuclear fusion rate (Scafetta, 2012d). However, the additional presence of theoretical synodic cycles and an 11 yr solar cycle modulation of the subannual TSI variability also suggest electromagnetic planet–Sun interactions that could more directly drive the solar outer regions. Thus, if the planets are modulating solar activity as our analysis suggests, the solar response to planetary forcing would be complex and would nonlinearly depend on the 11 yr solar cycle. Further research is required to investigate the physical mechanisms of planetary–solar interactions and construct models capable of simulating and predicting solar activity and TSI variability.

Appendix A

The data were downloaded from the following websites:

- ACRIMSAT/ACRIM3: http://acrim.com/RESULTS/data/acrim3/daya2sddeg_ts4_Nov_2013_hdr.txt
- SOHO/VIRGO: ftp://ftp.pmodwrc.ch/pub/data/irradiance/virgo/TSI/virgo_tsi_d_v6_002_1302.dat
- SORCE/TIM: http://lasp.colorado.edu/data/sorce/tsi_data/daily/sorce_tsi_L3_c24h_latest.txt
- SSN: http://sidc.oma.be/silso/DATA/dayssn_import.dat

Acknowledgements. The National Aeronautics and Space Administration supported R. C. Willson under contract NNG004HZ42C at Columbia University, and subcontracts 1345042 and 1405003 at the Jet Propulsion Laboratory.

Edited by: N.-A. Mörner
Reviewed by: two anonymous referees

References

Abreu, J. A., Beer, J., Ferriz-Mas, A., McCracken, K. G., and Steinhilber, F.: Is there a planetary influence on solar activity?, Astron. Astrophys., 548, A88, doi:10.1051/0004-6361/201219997, 2012.

Bartels, J.: Twenty-seven day recurrences in terrestrial-magnetic and solar activity, 1923–1933, J. Geophys. Res., 39, 201–202a, doi:10.1029/TE039i003p00201, 1934.

Brown, E. W.: A Possible Explanation of the Sun-spot Period, Mon. Not. R. Astron. Soc., 60, 599–606, 1900.

Caballero, R. and Valdés-Galicia, J. F.: Statistical Analysis of the Fluctuations Detected in High-Altitude Neutron Monitor, Solar and Interplanetary Parameters, Sol. Phys., 213, 413–426, 2003.

Callebaut, D. K., de Jager, C., and Duhau, S.: The influence of planetary attractions on the solar tachocline, J. Atmos. Sol.-Terr. Phy., 80, 73–78, 2012.

Charbonneau, P.: Solar physics: The planetary hypothesis revived, Nature, 493, 613–614, 2013.

Charvátová, I.: Long-term predictive assessments of solar and geomagnetic activities made on the basis of the close similarity between the solar inertial motions in the intervals 1840–1905 and 1980–2045, New Astron., 14, 25–30, 2009.

Doodson, A. T.: The harmonic development of the tide-generating potential, P. Roy. Soc. Lond. A, 100, 305–329, 1921.

Fairbridge, R. W. and Shirley, J. H.: Prolonged minima and the 179-year cycle of the solar inertial motion, Sol. Phys., 10, 191–210, 1987.

Fröhlich, C.: Solar irradiance variability since 1978: revision of the PMOD composite during solar cycle 21, Space Sci. Rev., 125, 53–65, 2006.

Fröhlich, C.: Revised characterization of the PMO6V radiometers, ISSI, Bern, Switzerland, 14 May 2013.

Hung, C.-C.: Apparent Relations Between Solar Activity and Solar Tides Caused by the Planets, NASA/TM-2007-214817, 2007.

Jose, P. D.: Sun's motion and sunspots, Astron. J., 70, 193–200, 1965.

Kelvin (Lord, Thomson, W.): The tide gauge, tidal harmonic analyzer, and tide predictor, P. I. Civil Eng., 65, 3–24, 1881.

Kilcik, A., Özgüc, A., Rozelot, J. P., and Atas, T.: Periodicities in solar flare index for cycles 21–23 revisited, Solar Phys., 264, 255–268, 2010.

Kopp, G. and Lawrence, G.: The Total Irradiance Monitor (TIM): Instrument, Design, Sol. Phys., 230, 91–109, 2005.

Kopp, G., Heuerman, K., and Lawrence, G.: The Total Irradiance Monitor; (TIM): Instrument Calibration, Sol. Phys., 230, 111–127, 2005.

Pap, J., Tobiska, W. K., and Bouwer, S. D.: Periodicities of solar irradiance and solar activity indices, I., Sol. Phys., 129, 165–189, 1990.

Press, W. H., Teukolsky, S. A., Vetterling, W. T., and Flannery, B. P.: Numerical Recipes in C, 2nd Edn., Cambridge University Press, 1997.

Rieger, E., Kanbach, G., Reppin, C., Share, G. H., Forrest, D. J., and Chupp, E. L.: A 154-day periodicity in the occurrence of hard solar flares?, Nature, 312, 623–625, 1984.

Scafetta, N.: Empirical evidence for a celestial origin of the climate oscillations and its implications, J. Atmos. Sol.-Terr. Phy., 72, 951–970, doi:10.1016/j.jastp.2010.04.015, 2010a.

Scafetta, N.: Spectral analysis of the TSI satellite records, their comparison and interpretation. Abstract #GC21B-0868 (presented at 2010 Fall Meeting, AGU, San Francisco, Calif., 13–17 December 2010), 2010b.

Scafetta, N.: A shared frequency set between the historical mid-latitude aurora records and the global surface temperature, J. Atmos. Sol.-Terr. Phy., 74, 145–163, doi:10.1016/j.jastp.2011.10.013, 2012a.

Scafetta, N.: Testing an astronomically based decadal-scale empirical harmonic climate model versus the IPCC (2007) general circulation climate models, J. Atmos. Sol.-Terr. Phy., 80, 124–137, doi:10.1016/j.jastp.2011.12.005, 2012b.

Scafetta, N.: Multi-scale harmonic model for solar and climate cyclical variation throughout the Holocene based on Jupiter-Saturn tidal frequencies plus the 11-year solar dynamo cycle, J. Atmos. Sol.-Terr. Phy., 80, 296–311, doi:10.1016/j.jastp.2012.02.016, 2012c.

Scafetta, N.: Does the Sun work as a nuclear fusion amplifier of planetary tidal forcing? A proposal for a physical mechanism based on the mass-luminosity relation, J. Atmos. Sol.-Terr. Phy., 81–82, 27–40, doi:10.1016/j.jastp.2012.04.002, 2012d.

Scafetta, N. and Willson, R. C.: Planetary harmonics in the historical Hungarian aurora record (1523–1960), Planet. Space Sci., 78, 38–44, doi:10.1016/j.pss.2013.01.005, 2013a.

Scafetta, N. and Willson, R. C.: Empirical evidences for a planetary modulation of total solar irradiance and the TSI signature of the 1.09-year Earth-Jupiter conjunction cycle, Astrophys. Space Sci., doi:10.1007/s10509-013-1558-3, in press, 2013b.

Scafetta, N., Humlum, O., Solheim, J.-E., and Stordahl, K.: Comment on "The influence of planetary attractions on the solar tachocline" by Callebaut, de Jager and Duhau, J. Atmos. Sol.-Terr. Phy., 102, 368–371, doi:10.1016/j.jastp.2013.03.007, 2013.

Sharp, G. J.: Are Uranus & Neptune Responsible for Solar Grand Minima and Solar Cycle Modulation?, Int. J. Astron. Astrophys., 3, 260–273, 2013.

Smythe, C. M. and Eddy, J. A.: Planetary tides during Maunder sunspot minimum, Nature, 266, 434–435, 1977.

Tan, B. and Cheng, Z.: The mid-term and long-term solar quasi-periodic cycles and the possible relationship with planetary motions, Astrophys. Space Sci., 343, 511–521, 2013.

Tobias, S. M.: The Solar Dynamo, Phil. Trans. A, 360, 2741–2756, 2002.

Verma, V. K., Joshi, G. C., and Paliwal, D. C.: Study of periodicities of solar nuclear gamma ray flares and sunspots, Sol. Phys., 138, 205–208, 1992.

Willson, R. C.: Revision of ACRIMSAT/ACRIM3 TSI results based on LASP/TRF diagnostic test results for the effects of scattering, diffraction and basic SI scale traceability, (Poster GC21C-04), 2011 AGU Fall Meeting, 2011.

Willson, R. C. and Hudson, H. S.: The Sun's Luminosity Over a Complete Solar Cycle, Nature, 351, 42–44, 1991.

Willson, R. C. and Mordvinov, V.: Time-Frequency Analysis of Total Solar Irradiance Variations, Geophys. Res. Lett., 26, 3613–3616, doi:10.1029/1999GL010700, 1999.

Willson, R. C. and Mordvinov, V.: Secular total solar irradiance trend during solar cycles 21–23, Geophys. Res. Lett., 30, 1199, doi:10.1029/2002GL016038, 2003.

Wilson, I. R. G., Carter, B. D., and Waite, I. A.: Does a Spin-Orbit Coupling Between the Sun and the Jovian Planets Govern the Solar Cycle?, Publ. Astron. Soc. Aust., 25, 85–93, 2008.

Wolf, R.: Extract of a letter to Mr. Carrington, Mon. Not. R. Astron. Soc., 19, 85–86, 1859.

Wolff, C. L. and Patrone, P. N.: A new way that planets can affect the Sun, Sol. Phys., 266, 227–246, 2010.

Part XII

The sunspot cycle length – modulated by planets? Solheim, J.-E.: Pattern Recogn. Phys., 1, 159-164, doi:10.5194/prp-1-159-2013, 2013.

Pattern Recogn. Phys., 1, 159–164, 2013
www.pattern-recogn-phys.net/1/159/2013/
doi:10.5194/prp-1-159-2013

Pattern Recognition in Physics
Open Access

The sunspot cycle length – modulated by planets?

J.-E. Solheim

formerly at: Department of Physics and Technology, Universtity of Tromsø, Norway

Correspondence to: J.-E. Solheim (janesol@online.no)

Received: 1 October 2013 – Revised: 8 November 2013 – Accepted: 12 November 2013 – Published: 4 December 2013

Abstract. The Schwabe frequency band of the sunspot record since 1700 has an average period of 11.06 yr and contains four major cycles, with periods of 9.97, 10.66, 11.01 and 11.83 yr. Analysis of the O–C residuals of the timing of solar cycle minima reveals that the solar cycle length is modulated by a secular period of about 190 yr and the Gleissberg period of about 86 yr.

Based on a simple harmonic model with these periods, we predict that the solar cycle length will in average be longer during the 21st century. Cycle 24 may be about 12 yr long, while cycles 25 and 26 are estimated to be about 9 and 11 yr long. The following cycle is estimated to be 14 yr long. In all periods during the last 1000 yr, when the solar cycle length has increased due to the 190 yr cycle, a deep minimum of solar activity has occurred. This is expected to re-occur in the first part of this century.

The coherent modulation of the solar cycle length over a period of 400 yr is a strong argument for an external tidal forcing by the planets Venus, Earth, Jupiter and Saturn, as expressed in a spin-orbit coupling model.

1 Introduction

A possible relation between solar activity as manifested by sunspots and the Earth's climate has been discussed many times since William Herschel (1801) speculated on a possible connection. In recent times Reid (1987) showed, based on data on globally averaged sea surface temperature (SST), that the solar irradiance may have varied in phase with the 80–90 yr cycle represented by an envelope of the 11 yr solar activity cycle, called the Gleissberg cycle.

Friis-Christensen and Lassen (1991) investigated the relation between the sunspot numbers and Northern Hemisphere land temperature, and found similar variations, but with the temperature variations leading the sunspot numbers. They then discovered that using the solar cycle length (SCL) as an indicator of solar activity in the sense that a shorter cycle means higher activity, they could much better correlate with the NH land temperature variations. It was also demonstrated (Friis-Christensen and Lassen, 1991; Hoyt and Schatten, 1993; Larssen and Friis-Christensen, 1995) that the correlation between SCL and climate has probably been in operation for centuries. A statistical study of 69 tree ring sets, covering more than 594 yr, demonstrated that wider tree rings (better growth conditions) were associated with shorter sunspot cycles (Zhou and Butler, 1998).

In their study, Friis-Christensen and Lassen (1991) used a smoothed mean value for the SCL with the length of five solar cycles weighted 1-2-2-2-1. In a follow-up paper, Reichel et al. (2001) concluded that the right cause-and-effect ordering, in the sense of Granger causality, is present between the smoothed SCL and the cycle mean temperature anomaly for the Northern Hemisphere land air temperature in the 20th century at the 99 % significance level. This suggests that there may exist a physical mechanism linking solar activity to climate variations. However, at the turn of the century, a discrepancy between the SCL and NH land series developed (Thejll and Lassen, 2000; Thejll, 2009), because the short cycle 22 was followed by a much longer cycle 23, without sign of cooling.

Recognizing that averaged temperature series from different meteorological stations of variable quality and changing locations may contain errors and partially unknown phenomena derived from the averaging procedure, Butler (1994) proposed instead to use long series of high quality from single stations. He showed that this improved the correlation when used for temperature series for Armagh, which correlates strongly with the NH land temperature.

Archibald (2008) was the first to realize that the length of the previous sunspot cycle (PSCL) has a predictive power

for the temperature in the next sunspot cycle for certain locations, if the raw (unsmoothed) value for the SCL is used. Based on the estimated longer SC23 than SC22, he predicted cooling during SC24 for some selected locations. A systematic study of the correlation for locations around the North Atlantic was published by Solheim et al. (2012). They found that maximum correlation was obtained with an 8–12 yr lag for locations around and in the North Atlantic, and found that a correlation with a lag of one solar cycle could explain 25 to 72 per cent of the temperature variance in that region. This one cycle lag could therefore be used for forecasting the temperature in the next solar cycle. Based on SC23 being considerably longer than SC22, they forecast a temperature decline during SC24 for the sites investigated.

In order to forecast the development of SCL for longer periods, it is necessary to investigate the long-term variability of the SCLs. This was done for the first time by Fairbridge and Hameed (1983), who found that the phase differences repeated after 16 sunspot cycles, or 178 yr, if they used minima as the start time for a cycle.

This was followed up by Richards et al. (2009), who used median trace analyses of the SCL and power spectrum analysis of the O–C residuals (as explained in Eq. 1). They found that the solar cycle length is controlled by periods of 188 and 87 yr. They concluded that the length of the solar cycle should increase gradually the next ≈ 75 yr. They did not discuss the origin of their determined periods.

Regarding the 11 yr sunspot period, many scientists have noticed the bimodal structure of the distribution of solar cycle length. According to analysis by Scafetta (2012), the sunspot length probability distribution consists of three periods of about 9.98, 10.9 and 11.86 yr. The side periods appear to be closely related to the spring period of Jupiter and Saturn, which has a range between 9.5 and 10.5 yr with a median length of 9.93 yr, and the sidereal period of Jupiter (about 11.86 yr). Scafetta (2012) proposed that the central cycle period is associated with a quasi 11 yr solar dynamo cycle, which is forced by the two cyclical side attractors with periods of 9.93 and 11.86 yr. He also suggested that the secular variations of the solar cycle amplitude and length are beat periods of the three solar cycle periods, and that it is possible to describe the secular variations of the sunspot cycle with these beat periods.

Scafetta's analysis covered the period 1755–2008 (solar cycles 1–23). In the following we will investigate the solar cycles for the longer period 1700–2010, and we will also investigate the O–C residuals all the way back to 1610 to search for period combinations or harmonics. Based on a simple harmonic model we will estimate the length of the next solar cycles. Finally we will discuss if the modulation of the SCL may be controlled by the planets, as proposed by Scafetta (2012) and Wilson et al. (2008).

2 Data and methods

Yearly average sunspot numbers were downloaded from the Solar Influences Data Center (SIDC). The length and time of solar cycles were downloaded from http://www.ngdc.noaa.gov/stp/space-weather/solar-data/solar-indices/sunspot-numbers/cycle-data/table_cycle-dates_maximum-minimum.txt.

For the analysis of the sunspot number time series I have used the Period04 analysis package (Lenz and Breger, 2005), downloaded from the Period04 website at http://www.astro.univie.ac.at/dsn/dsn/Period04/. This program performs least square fitting of a number of frequencies, where initial frequencies may be determined by Fourier transform (FT) or given as input. Error analysis is done by an analytical formula (Breger et al., 1999) assuming an ideal case, or with a least square error calculation. The largest of the obtained errors is used.

The O–C technique for investigation of secular modulation of the SCL is described in detail in Richards et al. (2009). We follow their description and use the downloaded set of SCLs determined between the minima, and construct the O–C residuals cycle by cycle using the formula:

$$(\mathrm{O}-\mathrm{C})_i = (t_i - t_0) - (N_i \times P_0), \quad (1)$$

where t_i is the end time of cycle no. N_i, P_0 is the reference period investigated, and $C_i = t_0 + N_i \times P_0$.

3 Results

3.1 The 11 yr cycle

The solar cycle length variation with time since 1610 is shown in Fig. 1. We notice large variations in the 17th and 18th centuries, but with a generally shorter length from about 1850. The data set covers a total of 36 cycles, and the mean length is 11.06 ± 1.5 yr. In Fig. 2 we show the distribution of the SCL between solar minima. The median value is between 10.7 and 11.0 yr, but there are no observations in this range. This clearly indicates a double or multiple bell distribution.

The resulting periodogram of the sunspot numbers from 1700–2010 is shown in Fig. 3. We find, as did Scafetta (2012), a dominating band with periods 10–12 yr, where we identify four peaks: $P_1 = 9.97 \pm 0.02$, $P_2 = 10.66 \pm 0.02$, $P_3 = 11.010 \pm 0.001$ and $P_4 = 11.83 \pm 0.02$ yr. The errors are determined by an analytical formula (Breger et al., 1999). There is also a triplet of periods in an 8.5 yr band, and a triplet around 5.5 yr. The latter is most likely higher harmonics of three peaks in the 11 yr band.

The long period of 53 ± 0.6 yr is best explained as a 4th subharmonics of P_2 ($5 \times 10.66 = 53.3$), and the long period of 100 ± 15 yr may be related to the known Gleissberg period of 87 yr.

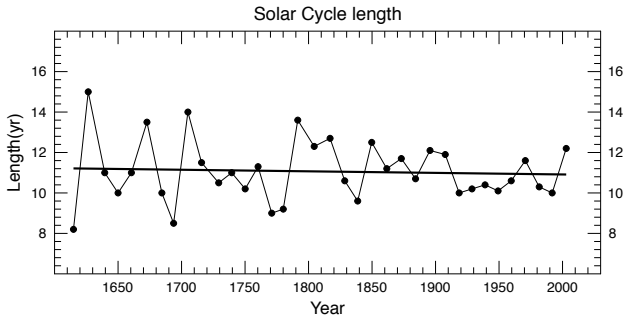

Figure 1. The solar cycle length (SCL) from 1610 as downloaded from the National Geophysical Data Center (NGDC). We observe that the SCL was longer than the mean of 11.06 yr in most of the 19th century and shorter than the mean in most in the 20th century.

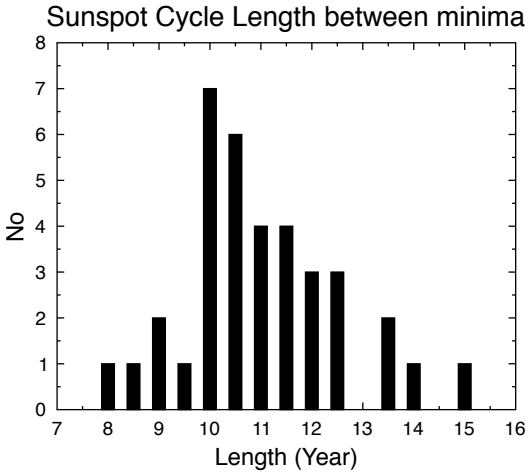

Figure 2. The distribution of the solar cycle lengths in bins of 0.5 yr width. The distribution covers 36 cycles from 1610 to 2008.

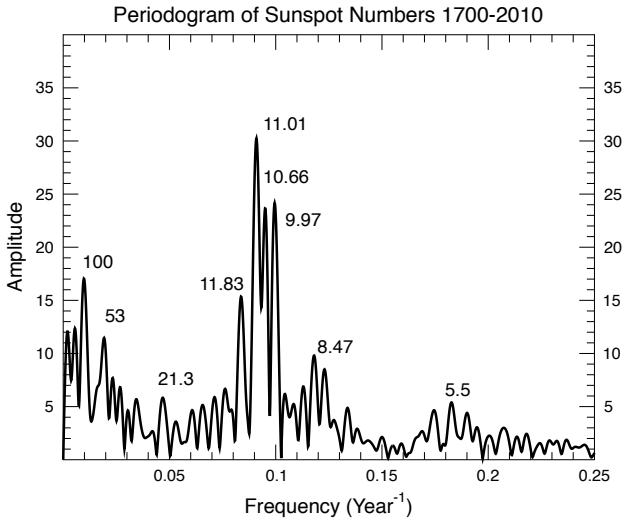

Figure 3. Amplitude spectrum of the yearly average sunspot numbers 1700–2010.

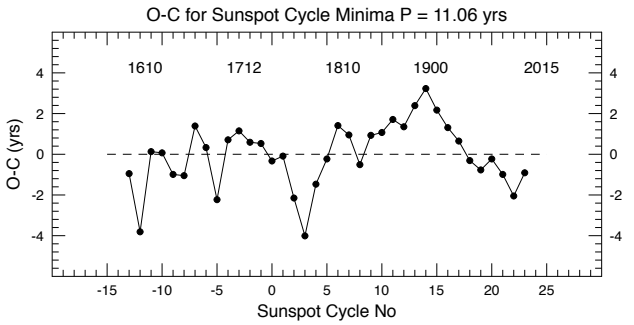

Figure 4. O–C residuals for the length of the solar cycle compared with the average period of 11.06 yr. The curve is increasing for SCL > 11.06 yr.

3.2 Long-term modulation of the length of the solar cycle

We use the average period $P = 11.06$ yr as our reference period and obtain the O–C residuals as shown in Fig. 4, where the O–C residuals are given as a function of the cycle no. As the starting point for cycle −13 we use 1610.8 with an O–C = −0.95. The residuals give us a picture of the long-term trends in SCL. We observe that the residuals increase most of the time between SC4 and SC14 (1775–1900), because the SCL is then nearly always longer than 11 yr (see also Fig. 1). Then we enter a period with shorter periods, and a warming Earth. The question is now if that will continue.

To investigate what controls the length of the solar cycle, we calculate a periodogram of the residual O–C data string, and get the amplitude spectrum shown in Fig. 5.

The spectrum consists of two dominating periods: 190 ± 9 and 85.6 ± 2 yr. Periods shorter than 50 years are harmonics of the two main periods. There is also a period of the order 440 yr, which explains why the peak around 1900 is higher than the peak around 1700. A similar result was obtained by Richards et al. (2009), who identified a Gleissberg period of 86.5 ± 12.5 yr and a secular period of 188 ± 38 yr. In their analysis they use SCLs based on both solar maxima and minima.

In Fig. 6 we show the O–C residuals with the strongest controlling period ≈ 190 yr and its subharmonic at ≈ 440 yr. This dominant cycle is the reason for an increasing period length in the 19th century and a decreasing length in the 20th century. We can therefore expect increasing SCLs in the 21st century.

Adding the Gleissberg cycle and three of the harmonics gives the fit shown in Fig. 7, where we may also obtain an estimate of near future SCLs. Times of minima can be estimated from the following equation:

$$t_{\min} = 1755.5 + 11.06 \times N_i + (\mathrm{O{-}C})_{\mathrm{est}}, \quad (2)$$

where $(\mathrm{O{-}C})_{\mathrm{est}}$ is the estimated O–C value determined with the harmonic model as shown in Fig. 7 (red curve). For the

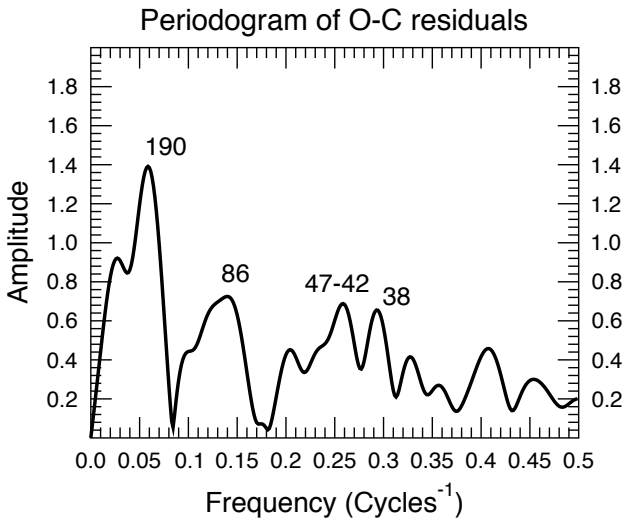

Figure 5. Amplitude spectrum of O–C residuals of the SCL measured between minima.

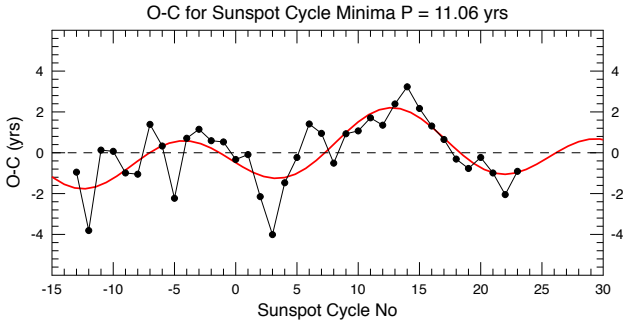

Figure 6. O–C residuals for SCL minima, with a simulation based on the dominating periods of 190 and 440 yr.

next minimum after SC24, Eq. (2) gives 2020.9, since the $(O–C)_{est}$ then is close to zero.

4 Discussion

We have shown that the solar cycle length since 1600 is controlled by stable oscillations, which provide an average cycle length of 11.06 yr. The cycle length is modulated by 3 long periods of ≈ 440, ≈ 190 and ≈ 86 yr, and some of their harmonics. If the dominating period of ≈ 190 yr is followed back in time, it is found (Richards et al., 2009) that all known solar deep minima during the last 1000 yr (the Oort, Wolf, Spörer, Maunder and Dalton minima) are close to the minimum or on the rising branch of this oscillation. We can therefore expect another grand minimum during the first part of this century.

Looking more closely at the model simulations in Fig. 7, we estimate the length of SC24 ≈ 12 yr, SCL25 ≈ 9 yr, SCL26 ≈ 11 yr and SCL27 ≈ 14 yr. The forecast for the time of the next minimum (2020.9) can be compared with the forecast

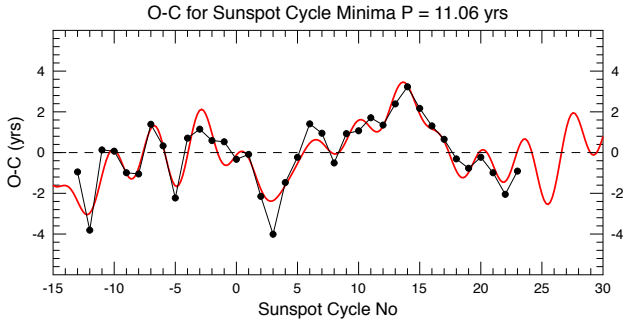

Figure 7. O–C residuals for SCL minima, with a simulation based on 6 harmonics with periods 440, 190, 86, 48, 43, and 38 yr.

based on a mathematical model (Salvador, 2013), which estimates the end of solar cycle 24 in 2018.

It has for some time been discussed if the solar cycle length is controlled by an internal or external clock. Dicke (1978) argued that the phase of the solar cycle appears to be coupled to an internal clock, because shorter cycles are usually followed by longer cycles, as if the Sun remembers the correct phase. Another view (Huyong, 1996) is that the memory effect can be explained by mean field theory, which predicts coherent changes in frequency and amplitude of a dynamo wave. However, it is admitted by solar physicists that present solar dynamo theories, although able to describe the periodicities and the polarity reversal of solar activity well, are not yet able to quantitatively explain the 11 and 22 yr cycles, nor the other observed quasi-cycles (de Jager and Versteegh, 2005). The remarkable resemblance between planetary tidal forcing periods and observed solar quasi-periods is a strong argument for a planetary tidal forcing on the solar activity.

Regarding the splitting of the 11 yr solar cycle band into 4 distinct peaks, the most remarkable is the strongest peak $P = 11.010 \pm 0.001$ yr. A period so close to 11 Earth years has a great chance to be related to the Earth's orbit. Wilson (2013) explains that the Venus–Earth–Sun periodic alignments create a tidal bulge, which for a period of 11.07 yr is speeded up by Jupiter's movement, and the next 11.07 yr are slowed down by the same. This is called the VEJ tidal-torque coupling model, and explains both the average Schwabe and Hales cycles. These tidal forces work to increase or decrease the solar rotation rate in the convective layers where the solar dynamo is situated (Wilson, 2013).

Among the other three periods in the 11 yr band, 9.97 yr is close to the Jupiter–Saturn spring tide period of 9.93 yr, which is half of the Jupiter–Saturn heliocentric conjunction period of 19.86 yr. It should be noticed that the spring tide period of Jupiter/Saturn varies between 9.5 and 10.5 yr (Scafetta, 2012). The period of 11.83 yr is close to Jupiter's orbital period of 11.86 yr. Scafetta (2012) proposes that the solar cycle period ≈ 11.0 yr is generated by the two side attractors controlled by the two giant planets. We have found another sunspot period at 10.66 yr, which also may be a

dynamo period. Both these periods are strongly forced, since they have higher harmonics of 5.5 and 5.25 yr, and one subharmonic of 21.3 yr.

By our O–C analysis we find, as did Richards et al. (2009), that the SCL is modulated by a secular period of 190 ± 9 yr in addition to a period of 86 ± 2 yr, which most likely is the Gleissberg period. The long period is close to the Jose cycle of 178.7 yr, which is the period of recurrent pattern of the movement of the Sun around the barycenter of the solar system (Jose, 1965). Fairbridge and Hameed (1985) found phase coherence of solar cycle minima over two 176 yr cycles, or 16 Schwabe periods. Our 190 yr period is also close to a period of 208 yr, which is found in cosmic ray observations and in cosmogenic isotopes, and explained by tidal torque on the Sun by the planets (Abreu et al., 2012).

However, a far better match with the 190 yr period is found by introducing a so-called Gear Effect, which modulates the tangential torque applied by the alignments of Venus and Earth to the Jupiter–Sun–Saturn system as explained by Wilson (2013). He shows that prograde and retrograde torque oscillate in a quasi bidecadal period controlled by the 19.859 yr synodic period of Jupiter and Saturn. Figure 13 in Wilson (2013) shows the angel between the center of mass of the Jupiter, Sun and Saturn system and Venus/Earth from 1013 to 2015. If we compare this with our Fig. 6, we find an excellent match between periods and phases, indicating a strong link between the modulation of the solar cycle length and the torque effect proposed by Wilson (2013). The modulation period can be calculated as the beat period between the Hale-like period of 22.137 yr and the Jupiter–Saturn synodic period of 19.859 yr. The result is a beat period of 192.98 yr or 193 ± 2 yr, when the orbital variations are included (Wilson, 2013). By also introducing the Gear Effect to the VEJ-tidal torque model, he can also explain an 88.1 yr Gleissberg cycle.

Finally, it may be instructive to compare our predictions of the next solar cycle lengths with a prediction made by de Jager and Duhau (2009), based on the dynamo model that is constructed from the relationship between the polodial and torodial magnetic cycles. They conclude that the polar cycle 24 will be similar to polar cycle 12, which means that the maxima of sunspot cycles 23 and 24 will be quite similar to those of the cycle pair 11 and 12. They further conclude that a short Dalton minimum will occur, lasting a maximum of 3 cycles (SC24-26), whereafter a grand minimum will follow, starting with cycle 27. They predict the maximum sunspots of SC24 to be 68 ± 17 with a maximum at 2014.5 ± 0.5, but do not predict the length.

At the moment we are close to the solar maximum of SC24, but have 7 more years to the next minimum, according to our forecast. During that period we will observe if the cooling forecast for the North Atlantic region will take place, and if this will also keep the global temperature in hiatus, as it has been since the start of SC23.

5 Conclusions

We have shown that the Schwabe frequency band of the sunspot record since 1700 has an average period of 11.06 yr and contains four major cycles, with periods of 9.97, 10.66, 11.01 and 11.83 yr. Analysis of the O–C residuals of the timing of solar cycle minima reveals that the solar cycle length is modulated by a secular period of about 190 yr and a Gleissberg period of about 86 yr. Our result is a confirmation of earlier phase studies by Fairbridge and Hameed (1983) and Richards et al. (2009).

Based on a simple harmonic model with these periods, we predict that the solar cycle length will increase during the 21st century. Cycle 24 may be about 12 yr long, while cycles 25 and 26 are estimated to be about 9 and 11 yr long. The following cycle 27 will be much longer. In all periods when the solar cycle length has increased due to the 190 yr cycle during the last 1000 yr, a deep minimum of solar activity has occurred. This is also to be expected in the early part of this.

The coherent modulation of the solar cycle length over a period of 400 yr is a strong argument for an external forcing by the planets Venus, Earth, Jupiter and Saturn, expressed in the spin-orbit coupling model as proposed by Wilson (2013).

Excellent phase coherence with this model is a strong added argument for this interpretation.

Acknowledgements. The author acknowledges the use of sunspot numbers and times of minima from the National Geophysical Data Center. He also thanks the Vienna astroseismological group for the excellent Period04 program package, and two referees with helpful advice for improving this publication.

Edited by: N.-A. Mörner
Reviewed by: H. Yndestad and H. Jelbring

References

Abreau, J. A., Beer, J., Ferriz-Mas, A., McCracken, K. G., and Steinhilber, F.: Is there a planetary influence on solar activity? Astron. Astrophys., 548, 9 pp., 2012.

Archibald, D.: Solar cycle 24: Implications for the United States, in: International Conference on Climate Change (www.davidarchibald.info), 2008.

Breger, M., Handler, G., Garrido, R, Audard, N., Zima, W., Paparó, M., Beichbuchner, F., Li, Zhi-ping, Jiang, Shi-yang, Liu, Zongli, Zhou, Ai-ying, Pikall, H., Stankov, A., Guzik, J. A., Sperl, M., Krzesinski, J., Ogloza, W., Pajdosz, G., Zola, S., Thomassen, T., Solheim, J.-E., Serkowitsch, E., Reegen, P., Rumpf, T., Schmalwieser, A., and Montgomery, M. H.: 30+ frequencies for the delta Scuti variable 4 Canum Venaticorum: results of the 1996 multisite campaign, Astron. Astrophys., 349, 225–235, 1999.

Butler, C. J.: Maximum and minimum temperatures at Armagh Observatory, 1844–1992, and the length of the sunspot cycle, Sol. Phys., 152, 35–42, 1994.

de Jager, C. and Versteegh, J. M.: Do planetary motions drive solar variability?, Sol. Phys., 229, 175–179, 2005.

de Jager, C. and Duhau, S.: Forecasting the parameters of sunspot cycle 24 and beyond, J. Atmos. Sol.-Terr. Phy., 71, 239–245, 2009.

Dicke, R. H.: Is there a chronometer hidden deep in the Sun?, Nature, 276, 676–680, 1978.

Fairbridge, R. W. and Hameed, S.: Phase coherence of solar cycle minima over two 178-year periods, Astron. J., 88, 867–869, 1983.

Friis-Chrisetensen, E. and Lassen, K.: Length of the solar cycle: an indicator of the solar activity closely associated with climate, Science, 254, 698–700, 1991.

Herschel, W.: Observations tending to investigate the nature of the Sun, in order to find the causes or symptoms of its variable emission of light and heat: With remarks on the use that may possibly be drawn from solar observations, Philos. T. R. Soc. Lond., 91, 265–318, 1801.

Hoyng, P.: Is the solar cycle timed by a clock?, Sol. Phys., 169, 253–264, 1996.

Hoyt, D. V. and Schatten, H. K.: A discussion of plausible solar irrandiance variations, 1700–1992, J. Geophys. Res., 98, 18895–18906, 1993.

Jose, P. D.: Sun's Motion and Sunspots, Astron. J., 70, 193–200, 1965.

Larssen, K. and Friis-Christensen, E.: Variability of the solar cycle length during the past five centuries and the apparent association with terrestrial climate, J. Atmos. Sol.-Terr. Phy., 57, 835–845, 1995.

Lenz, P. and Breger, M.: Period04 User Guide, Communications in Asteroseismology, 146, 53–136, 2005.

Reichel, R., Thejll, P., and Lassen, K.: The cause-and-effect relationship of solar cycle length and the Northern Hemisphere air surface temperature, J. Geophys. Res., 106, 15635–15641, 2001.

Reid, G. C.: Influence of solar variability on global sea surface temperatures, Nature 329, 142–143, 1987.

Richards, M. T., Rogers, M. L., and Richard, D. St. P.: Long-Term variability in the Length of the Solar Cycle, Publ. Astron. Soc. Pac., 121, 797–809, 2009.

Salvador, R. J.: A mathematical model of the sunspot cycle for the past 1000 yr, Pattern Recogn. Phys., in preparation, 2013.

Scafetta, N.: Multi-scale harmonic model for solar and climate cyclical variation throughout the Holocene based on Jupiter-Saturn tidal frequencies plus the 11.year solar dynamo cycle, J. Atmos. Sol.-Terr. Phy., 80, 296–311, 2012.

Solheim, J.-E., Stordahl, K., and Humlum, O.: The long sunspot cycle 23 predicts a significant temperature decrease in cycle 24, J. Atmos. Sol.-Terr. Phy., 80, 267–284, 2012.

Thejll, P. and Lassen, K.: Solar forcing of the Northern Hemisphere land air temperature: new data, J. Atmos. Sol.-Terr. Phy., 62, 1207–1213, 2000.

Thejll, P.: Update of the Solar Cycle Length Curve, and the Relationship to the Global Mean Temperature, Danish Climate Centre Report 09-01, 2009.

Wilson, I. R. G., Carter, B. D., and Waite, I. A.: Does a Spin-Orbit Coupling Between the Sun and the Jovian Planets Govern the Solar Cycle?, Publ. Astron. Soc. Aust., 25, 8–95, 2008.

Wilson I. R. G.: The Venus-Earth-Jupiter Spin-Orbit Coupling Model, Pattern Recogn. Phys., in preparation, 2013.

Zhou, K. and Butler, C. J.: A statistical study of the relationship between the solar cycle length and tree-ring index values, J. Atmos. Sol.-Terr. Phy., 60, 1711–1718, 1998.

Part XIII

A mathematical model of the sunspot cycle for the past 1000 yr.

Salvador, R. J.: Pattern Recogn. Phys., 1, 117-122, doi:10.5194/prp-1-117-2013, 2013.

Pattern Recogn. Phys., 1, 117–122, 2013
www.pattern-recogn-phys.net/1/117/2013/
doi:10.5194/prp-1-117-2013

Pattern Recognition in Physics
Open Access

A mathematical model of the sunspot cycle for the past 1000 yr

R. J. Salvador

Vancouver, Canada

Correspondence to: R. J. Salvador (rj_salvador@hotmail.com)

Received: 8 October 2013 – Revised: 27 October 2013 – Accepted: 30 October 2013 – Published: 15 November 2013

Abstract. Using many features of Ian Wilson's Tidal Torque theory, a mathematical model of the sunspot cycle has been created that reproduces changing sunspot cycle lengths and has an 85 % correlation with the sunspot numbers from 1749 to 2013. The model makes a reasonable representation of the sunspot cycle for the past 1000 yr, placing all the solar minimums in their right time periods. More importantly, I believe the model can be used to forecast future solar cycles quantitatively for 30 yr and directionally for 100 yr. The forecast is for a solar minimum and quiet Sun for the next 30 to 100 yr. The model is a slowly changing chaotic system with patterns that are never repeated in exactly the same way. Inferences as to the causes of the sunspot cycle patterns can be made by looking at the model's terms and relating them to aspects of the Tidal Torque theory and, possibly, Jovian magnetic field interactions.

1 Introduction

Considerable evidence now exists that the Earth's climate is heavily dependent on the solar cycle. The forecasting of solar cycles has mainly concentrated on predicting the future course of the present or the next cycle. Longer range and accurate predictions of the solar cycle pattern are necessary for understanding the future course of the Earth's climate. A useful model of the solar cycle should be able to reconstruct or recast historical solar cycles from proxy reconstructions as well as the modern record to have any credibility. Models based on theories of the dynamics of the solar dynamo are unable to do this. However, theories based on perturbations to the solar dynamo based on planetary interactions with the sun show more promise. In a recent publication, Scafetta (2012) discusses the state of solar forecasting and proposes a simplified solar cycle model based on three harmonics found in the power spectrum of the sunspot number record. Scafetta suggests that the solar cycle can be characterized by constructive and destructive interference patterns. His model successfully reconstructs the timing and pattern of past solar minimums in generic units and forecasts a solar minimum in the 2020–2045 time frame.

The model presented here is an attempt to produce a more quantitative prediction of monthly sunspot number forecasts and increase the granularity of the shape of future solar cycles. The model is based primarily on a Tidal Torque theory proposed by Wilson (2011) and two Jovian harmonics that account for the positioning of three Jovian planets.

Wilson's theory proposes that periodic alignments of Venus and the Earth on the same or opposite sides of the Sun produce temporary solar tidal bulges. Jupiter's gravitational force acts on these bulges and either speeds up or slows down the rotation of the Sun's plasma, leading to changes in solar activity. The frequency of these alignments on the same side of the Sun is 22.14 yr. Wilson also shows that the strength of the tidal force depends on the heliocentric latitude of Venus and the mean distance of Jupiter from the Sun, and that when these forces are weakest, solar minimums occur. This happens approximately every 165.5 yr. The frequency to produce a 165.5 yr beat with 22.14 yr is 19.528 yr. These two frequencies of Venus–Earth–Jupiter (VEJ) interactions are a principle basis for the model.

Wilson et al. (2008) have also shown the connection between the Hale cycle (22.1 ± 1.9 yr) and the synodic period of Jupiter and Saturn (19.859) such that their beat frequency is 178.8 yr, which is the Jose cycle. The Jupiter–Saturn synodic and the Jose cycle frequency are used in the model.

Published by Copernicus Publications.

Sharp (2013) has proposed a connection between the Uranus and Neptune synodic and grand solar minimums. Sharp (http://thetempestspark, 2013) has also produced a very instructive animation of the odd polar orientation and orbital pattern of Uranus and graphics showing how the planet's polar orientation aligns with individual solar cycle minimums. The one-quarter Uranus orbital frequency of 21.005 is used in the model.

Another well-known oscillation found in solar records is the de Vries cycle of 208 yr (see McCracken et al., 2013). The frequency of 1253 yr, together with the Jose frequency of 178.8 yr, produces a beat of 208 yr and is used in the model.

2 The model

This model is simply four interacting waves, but they are modulated to create an infinite possibility for sunspot formation.

The basic frequencies in years are:

- a VEJ frequency of 22.14 (varying),
- a VEJ frequency of 19.528 (varying and forming a beat frequency of 165.5 with 22.14),
- Jupiter–Saturn synodic frequency of 19.858,
- one-quarter Uranus orbital frequency equal to 21.005,
- two modulating frequencies of 178.8 and 1253 (forming a beat frequency of 208 yr).

Individual sunspot cycles have varying cycle lengths and this is an impediment to obtaining a continuous mathematical model for correlation. The monthly sunspot data imply that frequencies and/or phasing of the basic cycles are slowly changing over time.

It should be noted that the 178.8 frequency is also the time of rotation of the Sun around the barycenter. The perturbations described by the VEJ and Jovian frequencies are in the Sun, and therefore it is plausible that solar acceleration reasons could cause modulations to these frequencies (see Cionco and Campagnucci, 2012). This provided the idea that perhaps the Jovian 19.858 and 21.005 and the VEJ 22.14 frequencies and phases are changing over time to the barycenter rotation of 178.8.

During this work it was also found that the 19.528 VEJ frequency is changing to the slower 1253 frequency. Likewise there is a possible explanation for this in the time it takes for the orbital realignment of Venus, the Earth and Jupiter to return to the same position against the stars. See Wilson (2013 Hallstatt).

These frequency- and phase-changing capabilities are built into the model and for the most part solve the cycle length problem for correlation.

The model does not reproduce the skewed Gaussian shape of the sunspot cycles, as the model attempts to simulate the forces activating the cycle, and not the process of actual sunspot formation and disappearance. Since the time length of the formation of sunspots is unstated, the phasing in the model is left open and determined by correlation.

The following is the mathematical construction of the model.

The sunspot data was transformed into positive and negative oscillations by multiplying the monthly sunspot number (SN) by the sunspot cycle's polarity of plus or minus one.

$$\mathrm{SNC} = \mathrm{SN} \times \mathrm{POLARITY}$$

The data was then correlated to the following equation, where the Fs and Ns are scalars and the Ls and Ps are phasing parameters, and all are determined by a non-linear least squares optimization:

$$\begin{aligned}\mathrm{SNC} = {} & (F1 \times \cos(w1 \times (t + \mathrm{ph1})) + F2 \times \cos(w2 \times (t + \mathrm{ph2})) \\ & + F3 \times \cos(w3 \times (t + \mathrm{ph3})) + F4 \times \cos(w4 \times (t + \mathrm{ph4}))\end{aligned}$$

SNC is the polarity-adjusted sunspot number and T is the time in calendar years.

Ws are the modulated frequencies and are changed by either 178.8 or 1253.

$$w1 = 2 \times pi/(19.528 \times (1 + N1 \times \cos(2 \times pi/1253 \times (t + L1))))$$

$$w2 = 2 \times pi/(22.14 \times (1 + N3 \times \sin(2 \times pi/178.8 \times (t + L2))))$$

$$w3 = 2 \times pi/(19.858 \times (1 + N5 \times \cos(2 \times pi/178.8 \times (t + L3))))$$

$$w4 = 2 \times pi/(21.005 \times (1 + N7 \times \sin(2 \times pi/178.8 \times (t + L4))))$$

Phs are the modulated phases of each component of the model and are changed by the frequency of 178.8 or 1253.

$$\mathrm{ph1} = P1 \times (1 + N2 \times \cos(2 \times pi/1253 \times (t + L1)))$$

$$\mathrm{ph2} = P2 \times (1 + N4 \times \sin(2 \times pi/178.8 \times (t + L2)))$$

$$\mathrm{ph3} = P3 \times (1 + N6 \times \cos(2 \times pi/178.8 \times (t + L3)))$$

$$\mathrm{ph4} = P4 \times (1 + N8 \times \sin(2 \times pi/178.8 \times (t + L4)))$$

A model with frequencies of 1253 and 178.8 cannot be properly calibrated with only 300 yr of monthly sunspot data, as this covers only 20 % of the 1253 cycle and only one and a half cycles of the 178.8 frequency. To overcome this difficulty, sunspot data over a much longer time period are needed. Solanki et al. (2004) have reconstructed ten year average sunspot numbers for the past 11 000 yr from available ^{14}C records. Since the model requires monthly data (not 10 yr averages) and the polarity of the cycle, the Solanki data (2005) cannot be used in total. However, the Solanki data does quantify three time periods in the past 1000 yr when the sunspot number was zero, viz, the Maunder, Spörer and Wolfe minima. These monthly time periods, as defined by Solanki, can be used with the sunspot number set to zero, and then the polarity becomes a non-issue. Figure 1 shows the Solanki data (Solanki et al., 2004; Solanki, 2005) from

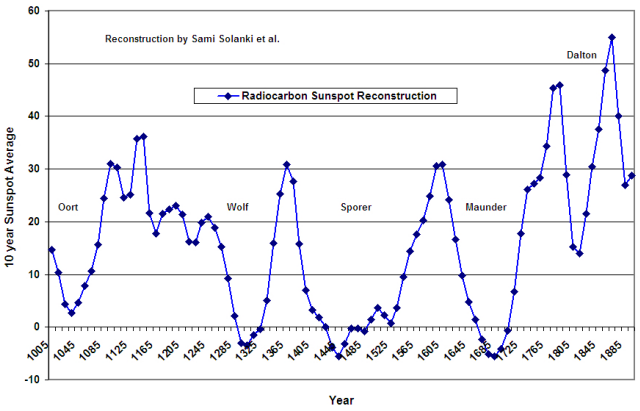

Figure 1. Solanki et al. (2004) reconstruction data from the years 1000 to 1895 of 10 yr average sunspot numbers from radio carbon 14 data, showing time periods when the average sunspot number was at or near zero.

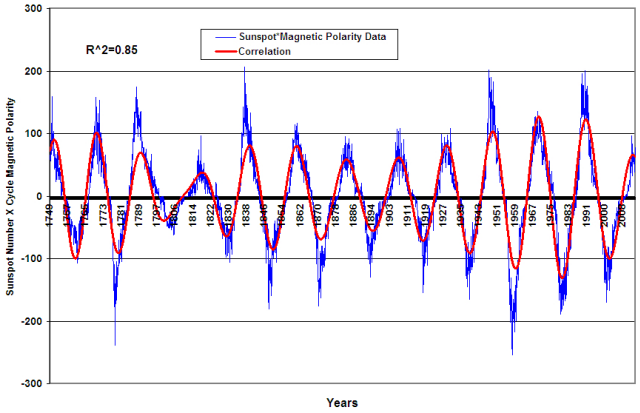

Figure 2. A comparison of the cyclical oscillation of the monthly sunspot number multiplied by a cycle polarity of plus 1 for even cycles and −1 for odd cycles from 1749 to 2013 (in blue) with the correlation model (in red).

the years 1000 to 1895, where it stops due to interferences by activities of modern society.

Using this additional data, the model has a strong correlation of $R^2 = 0.85$ for the data between 1749 and 2013, and produces a very interesting and reasonable reproduction of sunspot cycles for the past 1000 yr. Figure 2 illustrates the 1749–2013 correlation as a cyclical oscillation and Fig. 3 shows the same result in the more usual absolute value form.

3 Sunspot reconstruction for the last 1000 yr

In Fig. 4, the model is used to reconstruct the sunspot cycles from the year 1000 to the present and compared to the sunspot average data set of Solanki et al. (2004), to which the number 40 has been added to each data point to better illustrate the correspondence of the Solanki averages to the

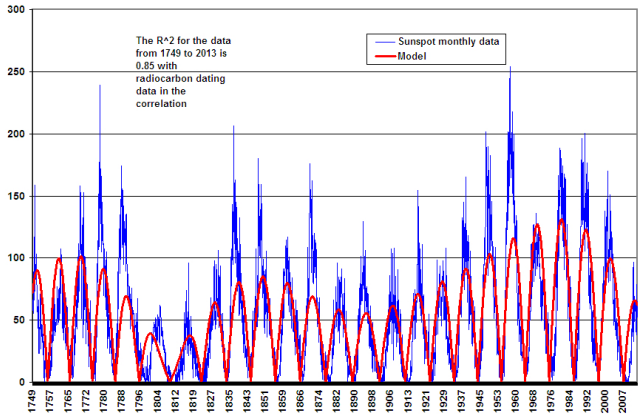

Figure 3. A comparison of monthly sunspot numbers from 1749 to 2013 (in blue) with the absolute value of the correlation model (in red), derived using the observational data from 1749 to 2013 and the additional data from Solanki et al.

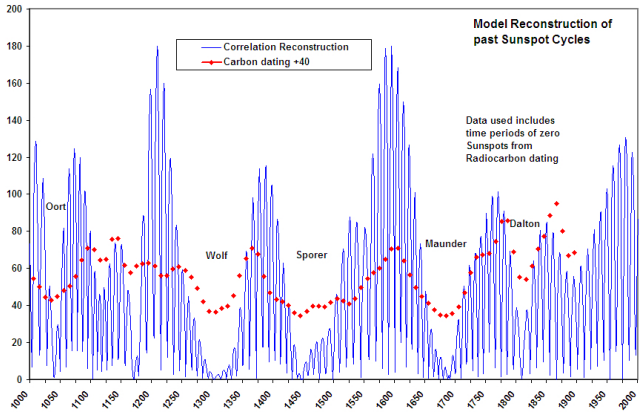

Figure 4. A comparison of monthly sunspot numbers from 1000 to 2013 (in blue), calculated from the absolute value of the correlation model, with the Solanki et al. (2004) average-derived sunspot numbers. 40 units are added to the Solanki data for illustrative purposes.

model's monthly sunspot number. This 1000 yr correlation model constitutes the basis for forecasting.

4 Forecasting

To test if the model has forecasting ability, we can redo the correlation with data only up to the years 1950 and 1900 and determine the forecast for the next 50 and 100 yr to see if the model can predict the sunspot data we have already experienced.

Figure 5 gives a forecast for the period 1950 to 2050 made from the correlation of the model with data up to 1950. The model forecasts a peaking sunspot cycle and a significant decline in sunspots around the turn of the century, and an ongoing solar minimum. The model is a little early, but directionally correct 50 yr out.

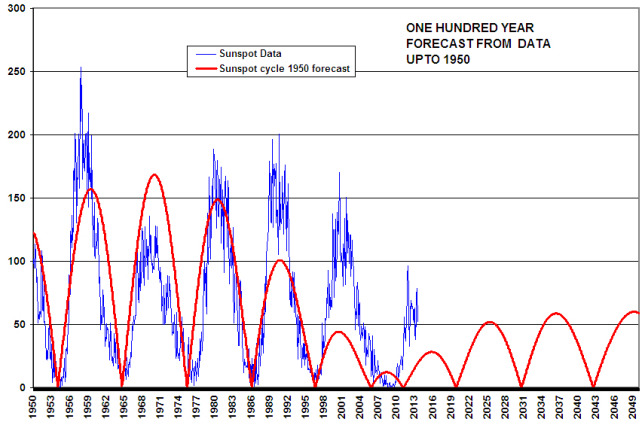

Figure 5. A comparison of monthly sunspot numbers from 1950 to 2013 (in blue) with the absolute value of the correlation model (in red), derived using data only up to 1950 and the extended forecast to 2050.

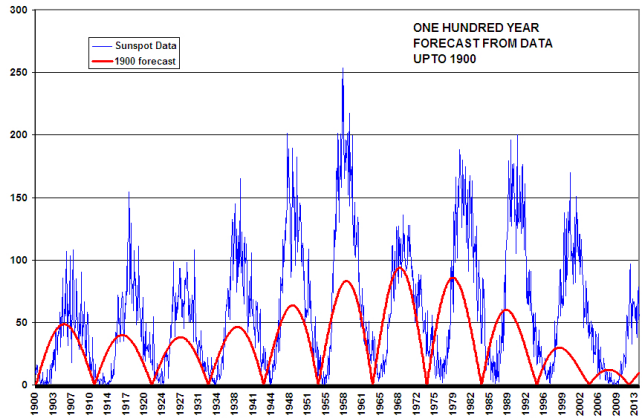

Figure 6. A comparison of monthly sunspot numbers from 1900 to 2000 (in blue) with the absolute value of the correlation model (in red), derived using data only up to 1900 and the extended forecast to 2000.

Figure 6 gives a similar forecast made with data up to 1900.

Although the model did not predict the magnitude of the increase in spot activity 50 yr past 1900, it did forecast increasing and then decreasing sunspot activity, with a minimum around the turn of the century.

I believe this shows the model has credibility in forecasting two to three sunspot cycles out and directionally for one hundred years.

Figure 7 gives a forecast made with data up to 2013. The forecast predicts a very quiet Sun for the next 100 yr. The model forecasts that the sunspot cycle will not produce sunspot values over 100 again until the cycle that starts around 2160; however, that is beyond the usable time horizon of this model.

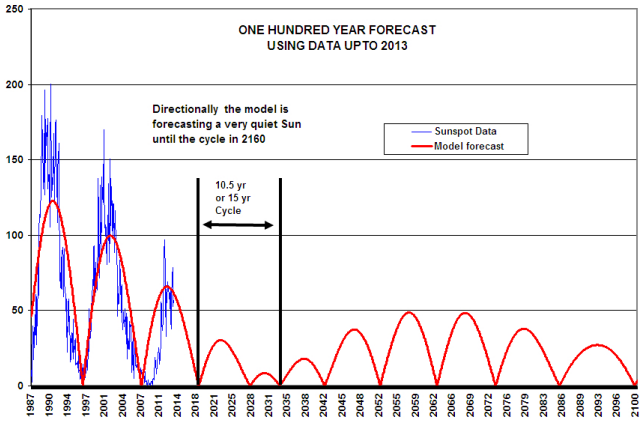

Figure 7. A comparison of monthly sunspot numbers from 1987 to 2013 (in blue) with the absolute value of the correlation model (in red), derived using data up to 2013 and the extended forecast to 2100.

The model forecasts that the existing cycle, 24, will end in 2018. The next cycle, 25, could prove to be very interesting, as the model predicts it will be difficult to tell when it ends and the next one begins. The duration of cycle 25 will be either 10.5 or 15 yr long. The model forecasts that a pronounced grand solar minimum will persist from the start of cycle 25 in 2018 out to 2060. The 100 yr, multi-cycle prediction, which shows a small rise then a further decline in cycle magnitude, suggests the minimum may extend beyond 2060. The forecast for a grand minimum in this time period is consistent with the predictions of Mörner (2011), Scafetta (2012), (2013) and Cionco and Compagnucci (2012).

5 Sunspot activation

It is instructive to examine the model for the destructive and constructive wave interactions that produce a Maunder minimum (Fig. 8) or a modern maximum, to determine if there are some implications as to how the solar system may be affecting sunspot cycles.

Figure 9 gives the sum of the two terms of the VEJ cycle (19.528 and 22.14) and the two terms of the Jovian cycles (19.585 and 21.005) from the years 1600 to 2200. The model gives equal weight in magnitude to the VEJ and Jovian cycles. These cycles can hide, and interfere both constructively and destructively with each other.

The model's two interference patterns, in turn, interfere with each other to produce the minima and maxima of the solar cycles. For example, the Dalton minimum occurred at a minimum in both the VEJ and Jovian cycles. Yet the Maunder minimum resulted from destructive wave interference when both cycles were near maxima. The Modern maximum is a result of constructive interference from a maximum in both cycles. The coming solar minimum is the result of wave pattern destructive interference between the VEJ and Jovian

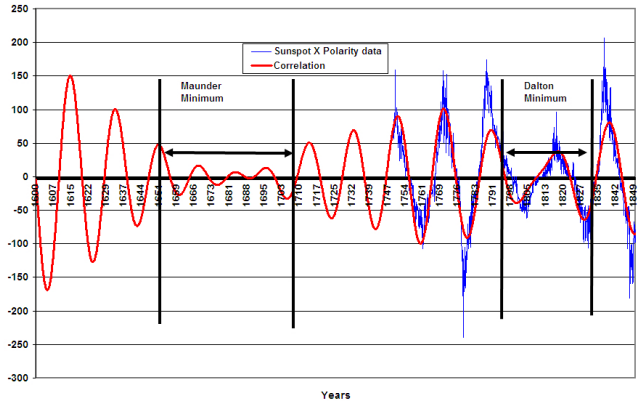

Figure 8. The red line is the model's reconstruction of the cyclical oscillation of the monthly sunspot number multiplied by a cycle polarity of plus 1 for even cycles and −1 for odd cycles from 1600 to 1850, which include the Maunder and Dalton solar minimums. The actual sunspot data multiplied by the cycle polarity for the monthly time periods from 1749 to 1850 is in blue.

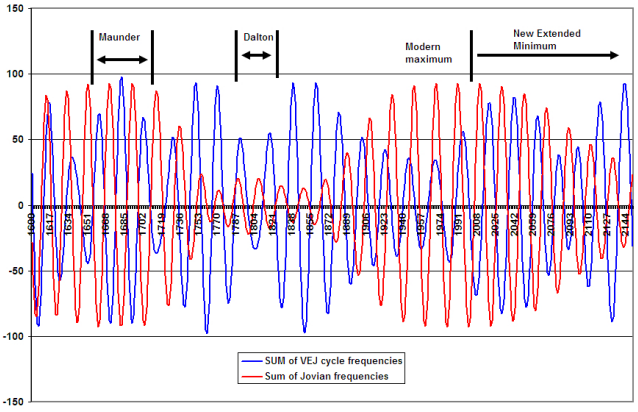

Figure 9. The blue line is the interference contribution pattern for the sum of the two VEJ frequencies (19.528, 22.14), and the red line is the interference contribution for the sum of two Jovian frequencies (19.585, 21.005) to the polarity-adjusted sunspot model for the years 1600 to 2100. The periods of destructive interference during solar minimums and constructive interference during the solar maximum can be seen by inspection of these two interference patterns. At times either the VEJ or Jovian cycles can dominate.

cycles and is extended by minimized VEJ and Jovian internal destructive interference.

This model will not work without the influence of the Uranus one-quarter orbital frequency of 21.005. The unusual orbital rotation of Uranus around its equator, I believe, is a possible indication of a magnetic to magnetic field interaction.

The VEJ and Jovian oscillations change through time, so that the same precise pattern never repeats itself. At present the VEJ cycle has an oscillation of 165.5 yr and the Jovian cycle 363.6 yr, but these change as the base frequencies and phasing are modulated.

6 Conclusions

The model predicts that the sun is entering a grand minimum, and the general shape of the model's future multi-cycle projections suggests that this minimum may persist for an extended period of time.

I believe this model captures a fundamental relationship between a gravitational disturbance in the Sun's magnetic field through the Tidal Torque process and a magnetic disturbance in the Sun's magnetic field through the Jovian planets.

I also believe this model describes a chaotic process where small changes in frequency and/or phase modulation parameters over time lead to large variations in individual solar cycle outcomes. Fortunately because the changes to the base frequencies and phasing occur slowly in terms of human life spans, we can make forecasts that may be useful.

7 Model constants

The model can be constructed in an Excel spreadsheet using the equations in this article and the values can be provided by the author through contact at this e-mail address: (rj_salvador@hotmail.com).

Acknowledgements. The author wants to express his thanks to Ian Wilson for the Tidal Torque theory and frequencies, Paul Vaughan for laying out in detail the relationship between frequencies, Tim Channon for a very timely comment, and Roger Tattersall for pointing out the Uranus one-quarter frequency and helpful articles.

Edited by: N.-A. Mörner
Reviewed by: H. Jelbring and one anonymous referee

References

Cionco, R. G. and Compagnucci, R. H.: Dynamical characterization of the last prolonged solar minima, Adv. Space Res., 50, 1434–1444, 2012.

McCracken, K. G., Beer, J., Steinhilber, F., and Abreu, J.: A phenomenological study of the cosmic ray variations over the past 9400 years, and their implications regarding solar activity and the solar dynamo, Sol. Phys., 286, 609–627, 2013.

Mörner, N-A.: Arctic environment by the middle of this century, Energy & Environment, 22, 207–218, 2011.

NASA, Sunspot Monthly Data, http://solarscience.msfc.nasa.gov/greenwch/spot_num.txt, 2012.

Scafetta, N.: Multi-scale harmonic model for solar and climate cyclical variation throughout the Holocene based on

Jupiter–Saturn tidal frequencies plus the 11-year solar dynamo cycle, J. Atmos. Sol.-Terr. Phy., 80, 296–311, 2012.

Scafetta, N.: Solar and planetary oscillation control on climate change: hindcast, forecast and a comparison with the CMIP5 GCMs, Energy & Environment, 24, 455–496, 2013.

Sharp, G. J.: Are Uranus & Neptune Responsible for Solar Grand Minima and Solar Cycle Modulation?, International Journal of Astronomy and Astrophysics, 3, 260–273, 2013.

Sharp, G. J.: http://thetempestspark.files.wordpress.com/2013/06/3-0.gif, last access: 12 November 2013.

Sharp, G. J.: http://thetempestspark.files.wordpress.com/2013/09/uranus-solar-4-rbg2.gif, last access: 12 November 2013.

Solanki, S. K.: 11,000 year sunspot reconstruction, NOAA Paleoclimatology Program and World Data Centre for Paleoclimatology, ftp://ftp.ncdc.noaa.gov/pub/data/paleo/climate_forcing/solar_variability/solanki2004-ssn.txt, 2005.

Solanki, S. K., Usoskin, I. G., Kromer, B., Schüssler, M., and Beer, J.: An unusually active Sun during recent decades compared to the previous 11,000 years, Nature, 431, 1084–1087, 2004.

Wilson, I.: Tidal-Torque model of Solar-Planetary interaction, posted 12 November, http://tallbloke.wordpress.com, 2012.

Wilson, I. R. G.: Do periodic peaks in the planetary tidal forces acting upon the Sun influence the sunspot cycle?, The General Science Journal, Dec 2011, 3812, 2011.

Wilson, I. R. G.: The VEJ Tidal Torquing model can explain many of the long-term changes in the level of solar activity, II. The 2300 year Hallstatt Cycle, posted 12 August, http://astroclimateconnection.blogspot.com.au/2013/08/the-vej-tidal-torquing-model-can.html, 2013.

Wilson, I. R. G., Carter, B. D., and Waite, I. A.: Does a spin-orbit coupling between the Sun and the Jovian Planets govern the solar cycle?, Publ. Astron. Soc. Aust., 25, 85–93, 2008.

Part XIV

General conclusions regarding the planetary–solar–terrestrial interaction.

Mörner, N.-A., Tattersall, R., Solheim, J.-E., Charvatova, I., Scafetta, N., Jelbring, H., Wilson, I. R., Salvador, R., Willson, R. C., Hejda, P., Soon, W., Velasco Herrera, V. M., Humlum, O., Archibald, D., Yndestad, H., Easterbrook, D., Casey, J., Gregori, G., and Henriksson, G.: Pattern Recogn. Phys., 1, 205-206, doi:10.5194/prp-1-205-2013, 2013.

Pattern Recogn. Phys., 1, 205–206, 2013
www.pattern-recogn-phys.net/1/205/2013/
doi:10.5194/prp-1-205-2013

Pattern Recognition in Physics
Open Access

General conclusions regarding the planetary–solar–terrestrial interaction

N.-A. Mörner[1], R. Tattersall[2], J.-E. Solheim[3], I. Charvatova[4], N. Scafetta[5], H. Jelbring[6], I. R. Wilson[7], R. Salvador[8], R. C. Willson[9], P. Hejda[10], W. Soon[11], V. M. Velasco Herrera[12], O. Humlum[13], D. Archibald[14], H. Yndestad[15], D. Easterbrook[16], J. Casey[17], G. Gregori[18], and G. Henriksson[19]

[1]Paleogeophysics & Geodynamics, Stockholm, Sweden
[2]Tallbloke, Leeds, UK
[3]Department of Physics & Technology, Tromsø, Norway
[4]Geophysical Institute, AS CR, Praha, Czech Republic
[5]Duke University, Durham, NC, USA
[6]Tellus, Stockholm, Sweden
[7]Gunnedah, Australia
[8]Vancouver, Canada
[9]ACRIM, Coronado, CA, USA
[10]Institute of Geophysics of the ASCR, Praha, Czech Republic
[11]Harvard-Smithsonian Center for Astrophysics, Cambridge, MA, USA
[12]Geophysics UNAM, Cambridge, MA, Mexico
[13]Department of Geosciences, Oslo, Norway
[14]Summa Development Ltd, Perth, Australia
[15]Aalesund University, Aalesund, Norway
[16]Department of Geology, Bellingham, WA, USA
[17]Space Sci. Res. Co. (SSRC), Orlando, FL, USA
[18]Instituto di Acustica e Sensoristica (CNR), Rome, Italy
[19]Astronomy, Uppsala, Sweden

Correspondence to: N.-A. Mörner (morner@pog.nu)

Abstract. In a collection of research papers devoted to the problem of solar variability and its origin in planetary beat, it is demonstrated that the forcing function originates from gravitational and inertial effects on the Sun from the planets and their satellites. This conclusion is shared by nineteen co-authors.

1 Introduction

The Sun is in the centre of our solar–planetary system but it has to constantly adjust its position with respect to the centre of mass in response to the planetary motions. This is because our solar–planetary system acts as a multi-body system of mutual interaction and transfer of gravity and momentum impulses.

The solar activity – i.e. the emission of heat, electromagnetic waves and particles – is known to change with time in a cyclic manner ranging from days and years to decades, centuries and millennia. The most commonly known cycle is the 11 yr cycle, which also forms a higher rank variability between "grand maxima and grand minima". During the last three grand minima (the Spörer, Maunder and Dalton Minima), the Earth experienced "Little Ice Age" conditions. Today, we seem to be at the end of a grand maximum.

Cosmogenic radionuclides (^{14}C and ^{10}Be) may record the solar variability back in time for 9500 yr or more. These records contain a number of characteristic cycles. There are, however, also additional internal sources for the production of these radionuclides to consider.

The planetary beat in gravity and momentum on the Sun from the celestial bodies circulating around the Sun can

Published by Copernicus Publications.

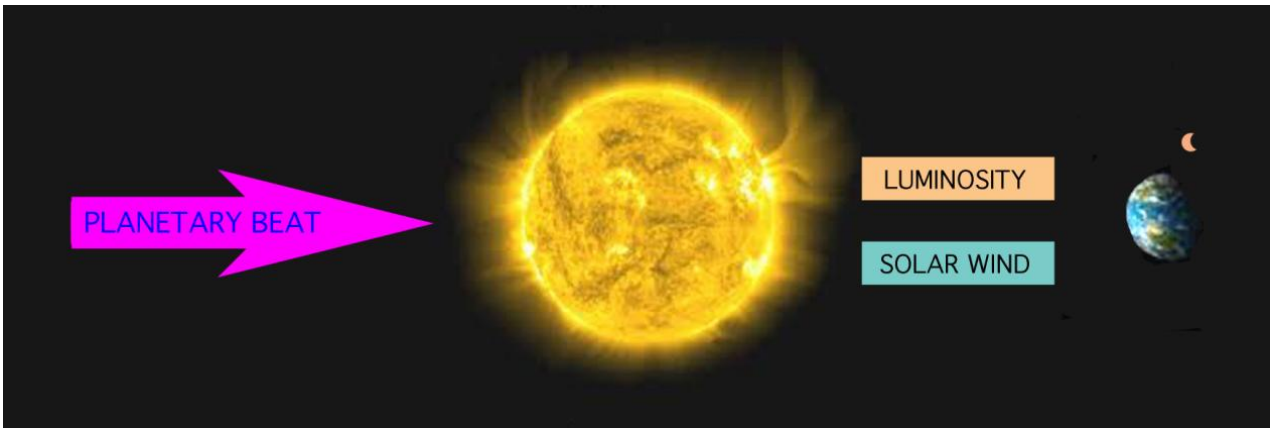

Figure 1. Illustration of the planetary–solar–terrestrial interaction here proposed.

be estimated, even calculated, and broken down into cyclic beats. Several of the papers in this volume have addressed this and presented new material.

2 Conclusions

The following conclusion and implications are formulated and agreed upon.

Conclusion 1

The solar activity varies with a number of characteristic time cycles. There are no solar theories able to explain this variability as driven and sustained by internal processes. We present (in paper after paper) a spectrum of ideas, estimates, observations and calculations to demonstrate that the driving factor of solar variability must emerge from gravitational and inertial effects on the Sun from the planets and their satellites (Fig. 1; References).

Implication 1

We hope that by the arguments and facts presented in this volume we have lifted "the planetary hypothesis" to the level of a "planetary theory", and we even foresee that it will lead to a new paradigm on planetary–solar–terrestrial interaction (Fig. 1).

We are well aware of the fact that there is much more to learn and improve, but we trust the theory is here to stay.

Implication 2

Several papers have addressed the question about the evolution of climate during the 21st century. Obviously, we are on our way into a new grand solar minimum. This sheds serious doubts on the issue of a continued, even accelerated, warming as claimed by the IPCC project.

References

All papers to be included in special issue no. 1 of PRP.

Charvatova, I. and Hejda, P.: Responses of the basic cycle of 178.7 and 2402 yr in solar-terrestrial phenomena during Holocene, Pattern Recogn. Phys., in press, 2013.

Jelbring, H.: Energy transfer in the solar system, Pattern Recogn. Phys., 1, 165–176, doi:10.5194/prp-1-165-2013, 2013.

Jelbring, H.: Celestial commensurabilities: some special cases, Pattern Recogn. Phys., 1, 143–146, doi:10.5194/prp-1-143-2013, 2013.

Mörner, N.-A.: Planetary beat and solar–terrestrial responses, Pattern Recogn. Phys., 1, 107–116, doi:10.5194/prp-1-107-2013, 2013.

Salvador, R. J.: A mathematical model of the sunspot cycle for the past 1000 yr, Pattern Recogn. Phys., 1, 117–122, doi:10.5194/prp-1-117-2013, 2013.

Scafetta, N.: The complex planetary synchronization structure of the solar system, Pattern Recogn. Phys., in press, 2013.

Scafetta, N. and Willson, R. C.: Multiscale comparative spectral analysis of satellite total solar irradiance measurements from 2003 to 2013 reveals a planetary modulation of solar activity and its nonlinear dependence on the 11 yr solar cycle, Pattern Recogn. Phys., 1, 123–133, doi:10.5194/prp-1-123-2013, 2013.

Solheim, J.-E.: Signals from the planets, via the Sun to the Earth, Pattern Recogn. Phys., 1, 177–184, doi:10.5194/prp-1-177-2013, 2013.

Solheim, J.-E.: The sunspot cycle length – modulated by planets?, Pattern Recogn. Phys., 1, 159–164, doi:10.5194/prp-1-159-2013, 2013.

Tattersall, R.: The Hum: log-normal distribution and planetary–solar resonance, Pattern Recogn. Phys., 1, 185–198, doi:10.5194/prp-1-185-2013, 2013.

Tattersall, R.: Apparent relations between planetary spin, orbit, and solar differential rotation, Pattern Recogn. Phys., 1, 199–202, doi:10.5194/prp-1-199-2013, 2013.

Wilson, I. R. G.: The Venus–Earth–Jupiter spin–orbit coupling model, Pattern Recogn. Phys., 1, 147–158, doi:10.5194/prp-1-147-2013, 2013.

Part XV

Epilogue: An Unbelievable Decision.

Mörner, N.-A., 25/Jan/2014.

Epilogue:
An Unbelievable Decision

Nils-Axel MÖRNER
Handling editor of the Special Issue of PRP; morner@pog.nu

The idea that the planetary motions affect and control the solar variability is old, but in the stage of an unproven hypothesis. In recent years major advancements have occurred and in 2013, it seemed that time was ripe for a major, multi-authored, reinvestigation. Therefore, a Special Issue of Pattern Recognition in Physics was devoted to: *"Pattern in solar variability, their planetary origin and terrestrial impacts"*. The volume includes 12 separate research papers and General Conclusions, co-authored by 19 prominent scientists. Indeed, they agreed that the driving factor of solar variability must emerge from the planetary beat on the Sun, and by that its emission of luminosity and Solar Wind both factors of which affect the Earth-Moon system. This may be held as a benchmark event in our understanding of the planetary-solar-terrestrial interaction.

Furthermore, they noted two implications of this: partly that the old hypothesis was now lifted to a firm theory, maybe even a new paradigm, and partly that we are on our way into a new grand solar minimum which *"sheds serious doubts on the issue of a continued, even accelerated, warming as claimed by the IPCC".*

"*We were alarmed by the second implication*", Martin Rasmussen, VD of Copernicus, stated, and took the unbelievable decision immediately to close down the entire journal. This happened on January 17 without any discussion with the editors (and with two papers in the process of being printed).

By this decision, **we were suddenly thrown back in the evolution of humanism and culture to the stage of inquisition and books burning**.

Still, the notion that we, from a planetary-solar-terrestrial interaction point of view, are on our way down into a grand solar minimum is vital in order to understand our near future: cooling, moderate warming or accelerated warming as claimed by the IPCC, despite no temperature rise in the last 15 years.

To debate is a vital part of science. To forbid and even close down a journal because of an inevitable conclusion which *"sheds serious doubts on the issue of a continued, even accelerated, warming as claimed by the IPCC"* is most unscientific and unethical.

Copernicus has disgraced itself in this desperate act of trying to cover up for IPCC.